Online ISSN: 1920-3853

Vol. 7, No. 1, Feb. 2013
Print ISSN : 1715-9997

Canadian Journal of pure & applied sciences

an International Journal

SENRA
Academic Publishers
British Columbia

Print ISSN 1715-9997
Online ISSN 1920-3853

Volume 7, Number 1
Feb. 2013

CANADIAN JOURNAL OF PURE AND APPLIED SCIENCES

The Canadian Journal of Pure and Applied Sciences (CJPAS-ISSN 1715-9997) is a peer reviewed multi-disciplinary specialist journal aimed at promoting research worldwide in Agricultural Sciences, Biological Sciences, Chemical Sciences, Computer and Mathematical Sciences, Engineering, Environmental Sciences, Medicine and Physics (all subjects).

CJPAS is Abstracted/Indexed in:
EBSCO, Ulrich's Periodicals Directory, Scirus, CiteSeerX, Index Copernicus, Directory of Open Access Journals, Google Scholar, CABI, Chemical Abstracts, Zoological Records, Biblioteca Central, The Intute Consortium, WorldCat. CJPAS has received Index Copernicus Journals Evaluation for 2011 = 4.63

Frequency:
3 times a year (Feb, June and Oct.)

Editorial Office
E-mail: editor@cjpas.ca
: editor@cjpas.net

SENRA Academic Publishers
5919 129 B Street Surrey
British Columbia V3X 0C5 Canada
www.cjpas.net
E-mail: senra@cjpas.ca

Board of Editorial Advisors

Member
CANADIAN ASSOCIATION OF LEARNED JOURNALS

Canadian Journal of pure&applied sciences

Volume 7, Number 1
February 2013

CONTENTS

SENRA Academic Publishers, British Columbia
Vol. 7, No. 1, pp. 2195-2201, Feb 2013
Online ISSN: 1920-3853; Print ISSN: 1715-9997

Canadian Journal of pure & applied sciences

POPULATION DYNAMICS OF *TOR MACROLEPIS* (TELEOSTEI: CYPRINIDAE) AND OTHER FISHES OF ATTOCK REGION, PAKISTAN

*Zafar Iqbal[1], Khalid Pervaiz[1] and Muhammad Naeem Javed[2]
[1]Department of Zoology, University of the Punjab, Quaid-E-Azam Campus, Lahore 54590
[2]Government Shalimar College, Lahore, Pakistan

ABSTRACT

A survey was conducted in Attock region, Pakistan to study the population dynamics of *Tor macrolepis* and other fish species. *Tor macrolepis* specimens were 133 of the total 2839 fishes collected. *Tor macrolepis* varied in total length and lateral line scales from 5.0 to 45.0cm and 24 to 28 respectively. Out of 60 fish species identified, 38 species comprised < 1% individually. Seventeen species were from 1.0 to 5.0%; 4 species such as; *Devario devario*, *Puntius conchonius*, *Puntius sophore* and *Cyprinus carpio* were 5-10% and one species *Crossocheilus diplochilus* comprised 16.06%. *Tor* and *Glyptothorix* are endemic genera to this area. There were 22 commercially important species. The population of 10 highly commercial indigenous fishes was very low and has fallen drastically. These species are, *Labeo rohita* (0.38%), *Cirhhinus mrigala* (0.52%), *Gibelion catla* (0.06%), *Mystus bleekeri* (2.57%); *Rita rita* (0.03%), *Sperrata sarwari* (0.24%), *Wallago attu* (0.10%), *Clupisoma naziri* (2.04%); *Channa marulius* (0.24%), and *T. macrolepis* (4.68%). The decline in population of commercial fishes is attributed to indiscriminate overfishing, habitat degradation, aquatic pollution and abundance of competitive exotic species. The IUCN status of fish fauna of Attock is also discussed. Effective conservation measures are suggested to sustain *Tor macrolepis* and the fish fauna in Attock region.

Keywords: Attock region, fish fauna, *Tor macrolepis*, decline population, economic status.

INTRODUCTION

Pakistan has large and widely spread inland water resources. The rivers and their tributaries, network of irrigation canals, dams and lakes constitute these aquatic resources. The Indus drainage system is the biggest river system of Pakistan and it consists of the mighty Indus River and its associated rivers and streams. Pakistan has a very rich and diversified freshwater fish fauna. The variation in fish fauna may be attributed to the fact that the area of Pakistan constitutes a transitional zone between Oriental, Palearctic and Ethiopian zoogeographical regions. Hence, these geographical entities also influenced the fish fauna of Pakistan (Mirza, 1994). Number of comprehensive studies have been done on the freshwater fish fauna of Pakistan from various natural waters bodies; (Mirza, 1975, 1980, 1994, 2003, 2004; Qurashi *et al*., 1998; Rafique, 2000, 2001; Ahmad and Mirza, 2002; Rafique *et al*., 2003; Javed *et al*., 2005; Pervaiz, 2011). Khan *et al*. (2011) and Mirza (2003) reported 183 freshwater fishes in Pakistan and Kashmir which belongs to 11 orders, 26 families and 83 genera. However, freshwater fish fauna of Pakistan are represented by not less than 193 fish species (Rafique and Khan, 2012).

Family cyprinidae supersede rest of the families with regards to its number of genera and species in Pakistan (Mirza, 2003). Many species of this family are highly commercial and have significance in aquaculture too. The economically important inland fish fauna comprise 16 species (Peter, 1999). Thirty freshwater fishes of Pakistan have high economic value (Rafique and Khan, 2012). The population of commercial fishes is declining in Pakistan (Pervaiz, 2011; Rafique and Kahn, 2012). Worldwide, fishes and fisheries are in severe decline, driven in large part by economic and population growth (Limburg *et al.*, 2011). Densely populated and rapidly expanding urban areas contribute significantly to aquatic habitat change and water pollution (Brown *et al*., 2005). Agricultural runoff also degrades and continues to degrade fish habitat. Decline in population of some of the commercially important fish species of Pakistan is associated to overexploitation, pollution and habitat fragmentation (Rafique and Khan, 2012).

Most of the studies done in Pakistan mainly described species diversity and composition of freshwater fishes, but lack important characteristics of the fish fauna, such as population dynamics of economically valued species and their conservation status. Rafique and Khan (2012) have described freshwater fish fauna of special importance, with regard to endemism, IUCN status and its rarity. The aim of present study was to investigate population dynamics, economic and conservation status of fish fauna of Attock region, Pakistan and suggest steps

*Corresponding author email: dr.zafariqbal.pu@gmail.com

to conserve and enhance production of *T. macrolepis*, the Indus Golden Mahseer.

MATERIALS AND METHODS

Fish sampling was conducted from July 2008 to June 2009. Collections was made from different sites of Attock district and adjoining areas which included Indus River, Haro River and Hassan Abdaal area. For this purpose, the Haro River was divided into four sampling zones. Each part consisted of about ten kilometer area starting from upstream of the Haro River Toll Plaza at G.T road and ending at Garyala junction with the Indus River. Fish samples were also collected from Hasan Abdaal area around Nalah Kala and adjoining water streams. At main Indus River samples were collected from two different sites. Many different methods were used to collect the fishes depending upon the circumstances like pond net, cast net, scoop net, gill net drag net and cover pot with the assistance of local fishermen. Fish specimens in field were fixed in 10% formalin. Larger specimens were also given intra-peritoneal injection of formalin. The samples were packed in soaked cotton with pure formalin and were transported to laboratory and shifted in 70% ethanol for further investigation. Each specimen was numbered and tagged in the dorsal fin. Classification was followed after Mirza and Sharif (1996) and Mirza (2004).

RESULTS

Sampling site Haro River

The Attock district is located along the main Indus River. The land of this district is sub-mountainous and with typical barani features. The Haro is the main river in this district, which originate from Murree hills (foot hills of Himalayas) flow meandering downhill and reaches Khan Pur Dam (35km from Islamabad). From Khan Pur Dam downstream, this River covers about 40km area in district Attock, and finally confluence with main Indus River at Garyala Junction near Ghazi-Brotha hydropower electric generation station. The main Haro River from Ghazi to Gariala represents transition from snow carp region to mahseer region (Mirza, 1994). There is a great diversity in water depth, width and current in different regions and different seasons in River Haro. During rainy season the river is flooded. But in other seasons, it is quite shallow and water has slow velocity. The river bed varies from sandy and gravel to sandy and rocky. The substratum of the Haro River consists of gravel covered with sand, silt and detritus, which form an excellent substrate for Mahseer breeding (Pervaiz, 2011).

Fish fauna of Attock region

A total of 2839 fish specimens were collected in six batches. The whole collection included 14 families, 39 genera and 60 species (Table 4). There were 133

Table 1. *Tor macroelpis* and other fish species from Attock Region.

Batch No.	Total fish Collected	No. of *Tor macrolepis*	% *Tor macrolepis*	% of other species
1	562	25	4.44	95.56
2	587	24	4.08	95.92
3	583	27	4.63	95.37
4	432	20	4.62	95.38
5	470	22	4.68	95.32
6	205	15	7.31	92.69
Total	2839	133	4.68	95.32

Table 2. Length wise Six *Tor macrolepis* sampling groups from Attock Region.

Length group (Cm)	Group-1	Group-1I	Group-1II	Group-1V	Group-V	Group-V1	Total
5-10	-	2	2	2	2	-	8
11-15	22	7	18	9	18	-	74
16-20	2	13	7	9	2	7	40
21-25	1	1	-	-	-	-	2
26-30	-	1	-	-	-	3	4
31-35	-	-	-	-	-	3	3
36-40	-	-	-	-	-	1	1
41-45	-	-	-	-	-	1	1
Total	25	24	27	20	22	15	133

specimens of *Tor macrolepis*, which comprised 4.68% of the entire catch. The total length of *T. macrolepis* was from 5.0 to 45.0cm. The fish of length from 5.0 to 20cm dominated the sample (122 specimens) (91.24%) and fishes from 21-45cm total length were 8.27%. The lateral line scales varied from 24 to 28 in this fish (Tables 1-3).

From 60 fish species identified in this study, thirty eight species comprised < 1% individually. Seventeen species were from 1.0 to 5.0%. Four species such as *Devario devario, Puntius conchonius, Puntius sophore* and *Cyprinus carpio* were 5-10%. Only one species *Crossocheilus diplochilus* was most abundant comprising 16.06%. Family Cyprinidae dominated the present collection with 21 genera and 35 species. The family Bagridae with 3 genera and 4 species, family Siluridae, Chandidae, and Schilbeidae with 2 genera and 2 species each, family Sisoridae with two genera and 4 species, Channidae one genus and 3 species, family Cichlidae with one genus 2 species, families Notopteridae, Nemacheilidae, Heteropneustidae, Belontidae, Gobiidae and Mastacembelidae are represented by only one species each (Table 4).

Table 3. Lateral line scales in six groups of *Tor macrolepis* from Attock Region.

Lateral line scales	Group-1	Group-1I	Group-1II	Group-1V	Group-V	Group-V1
24	2	1	-	-	-	-
25	22	20	-	-	4	-
26	-	2	3	6	8	2
27	-	1	7	8	9	13
28	-	-	17	6	1	
Total	24	24	27	20	22	15

Table 4. Population dynamics, Economic and IUCN status of fishes of Attock Region (E. S; Economic status; *** very good;**good; *Fair; - None): (Heck: Heckle)

S. No.	Family and species	Common name	No. / % of fish	E.S	IUCN Status
I	**Family Cyprinidae**				
1	*Labeo rohita* (Hamilton)	Rahu	11(0.38)	***	Least concerned
2	*Labeo calbasu* (Hamilton)	Kalbas	03(0.10)	**	Least concerned
3	*Labeo boga* (Hamilton)	Bhangan	03(0.10)	-	Least concerned
4	*Labeo diplostomus* (Heckel)	Mountain rahu	95(3.34)	-	Least concerned
5	*Labeo dyocheilus pakistanicus* Mirza &Awan	Thick lip labeo	11(0.38)	**	Least concerned
6	*Labeo angra* (Hamilton)	Buttar	06(0.20)	-	Least concerned
7	*Cirrhinus reba* (Hamilton)	Sunni	07(0.24)	**	Least concerned
8	*Cirrhinus mrigala* (Ham.)	Mori	15(0.52)	***	Least concerned
9	*Gibelion catla* (Hamilton)	Thaila	02(0.06)	***	Least concerned
10	*Tor macrolepis* (Heckel)	Indus golden mahseer	133(4.48)	***	Not evaluated
11	*Crossocheilus diplocheils* (Heck.)	Dogra	456(16.06)	*	Least concerned
12	*Cyprinus carpio* L.	Gulform	150(5.28)	**	Vulnerable
13	*Chela cachius* (Hamilton)	Bidda	03(0.10)	-	Least concerned
14	*Chela laubuca* (Hamilton)	Bidda	07(0.24)	-	Least concerned
15	*Salmophasia bacailia* (Ham.)	Small chal	40(1.40)	-	Least concerned
16	*Salmophasia punjabensis* (Day)	Punjab razor belly minnow	25(0.88)	-	Not evaluated
17	*Securicula gora* (Hamilton)	Big chal	02(0.06)	-	Least concerned
18	*Aspidoparia morar* (Hamilton)	common chilwa	140(4.93)	-	Least concerned
19	*Barilius modestus* Day	Lahori chilwa	58(2.04)	-	Not evaluated
20	*Barilius pakistanicus* Mirza & Sadiq	Pakistani chilwa	22(0.77)	-	Not evaluated

Continued…

Table 4 continued

S. No.	Family and species	Common name	No. / % of fish	E.S	IUCN Status
21	*Barilius vagra* (Hamilton)	Lahori chilwa	73(2.57)	-	Least concerned
22	*Devario devario* (Hamilton)	Patha makhni	190(6.69)	-	Least concerned
23	*Esomus danricus* (Hamilton)	Soomare	11(0.38)	-	Least concerned
24	*Rasbora daniconius* (Hamilton)	Charl	12(0.42)	-	Least concerned
25	*Systomus sarana* (Hamilton)	Kharni	14(0.49)	-	Least concerned
26	*Osteobrama cotio* (Hamilton)	Palero	07(0.24)	-	Least concerned
27	*Puntius chola* (Hamilton)	Chola popra	99(3.48)	-	Least concerned
28	*Puntius conchonius* (Hamilton)	Rosy barb	168(5.91)	-	Least concerned
29	*Puntius sophore* (Hamilton)	Sophara popra	264(9.29)	-	Least concerned
30	*Puntiu ticto* (Hamilton)	Ticto popra	18(0.63)	-	Least concerned
31	*Garra gotyla* (Gray)	Pathar chat	03(0.09)	-	Least concerned
32	*Racoma labiata* McClelland & Griffith	Kunar snow trout/chun	21(0.73)	-	Not evaluated
33	*Racoma fedtschenkoi* Kessler)	Chunni	01(0.01)	-	Not evaluated
34	*Schizothorax plagiostomus* Heckel	Swati	62(2.18)	**	Not evaluated
35	*Carassius auratus* L.	Goldfish	110(3.87)	**	Not evaluate
II	**Family Notopteridae**				
36	*Notopterus notopterus* Pallas	Pari	08(0.28)	**	Least concerned
III	**Nemacheilidae**			-	
37	*Triplophysa microps* (Steindachner)	Singhat	02(0.06)	-	Least concerned
IV	**Family Bagaridae**			-	
38	*Mystus bleekeri* (Day)	Bleekri Tingara	73(2.57)	***	Least concerned
39	*Mystus vittatus* (Bloch)	Kingar	01(0.03)	-	Least concerned
40	*Rita rita* (Hamilton)	Khagga	01(0.03)	***	Least concerned
41	*Sperrata sarwari* (Mirza *et al*)	Singhari	07(0.24)	***	Least concerned
V	**Family Sisoridae**				
42	*Gagata pakistanica* Mirza, *et al*,	Sanglai	77(2.71)	-	Not evaluated
43	*Glyptothorax naziri* Mirza & Naik	Sulemani khagga	21(0.73)	-	Not evaluated
44	*Glyptothorax punjabensis* Mirza & Kashmiri	Sulemani khagga	03(0.10)	-	Not evaluated
45	*Glyptothorax stocki* Mirza & Nijssen	Sulemani khagga	22(0.77)	-	Not evaluated
VI	**Family Siluridae**				
46	*Ompok padba* (Hamilton)	Mountain Pafta	44(1.44)	-	Near threatened
47	*Wallago autto* Bloch & Schneider	Mullee	03(0.10)	***	Near threatened
VII	**Family Heteropneustidae**				
48	*Heteropneustes fossilis* (Bloch)	Singhi	04(0.14)	**	Least concerned
VIII	**Schilbeidae**				
49	*Ailia coila* (Hamilton)	Patari	03(0.10)	-	Near threatened
50	*Clupisoma naziri* (Hamilton)	Naziri bachcha	58(2.04)	***	Not evaluated
IX	**Family Belontidae**				
51	*Xenentodon cancila* (Hamilton)	Kaan	03(0.10)	-	Least concerned

Continued…

Twenty three commercially important fish species were recorded in this collection. Ten species have “very good’ and 13 species have “good” economic value. The indigenous commercially “very good” fishes were *L. rohita* (0.38%), *C. mriagla* (0.52%), *G. catla* (0.06%), *M. bleekeri* (2.57%); *R. rita* (0.03%), *S. sarwari* (0.24%), *W. attu* (0.10%), *C. naziri* (2.04); *C. marulius* (0.24%), and *T. macrolepis* (4.68%). The four introduced species; *C. carpio* (5.28%), *C. auratus* (3.87%), *O aureus* (0.88%) and *O. mossambicus* (1.93%) are well establishes in this

Table 4 continued

S. No.	Family and species	Common name	No. / % of fish	E.S	IUCN Status
X	**Family Channidae**				
52	*Channa punctata* (Bloch)	Daula	16(0.56)	**	Least concerned
53	*Channa marulia* (Hamilton)	Soul	07(0.24)	***	Not evaluated
54	*Chana striata* (Bloch)	Soul	15(0.52)	-	Least concerned
XI	**Family Chandidae**				
55	*Chanda nana* (Hamilton)	Sheesha	48(1.49)	-	Least concern
56	*Paramabassis ranga* (Hamilton)	Sheesha	44(1.54)	-	Least concern
XII	**Family Gobiidae**				
57	*Glossogobius giuris* (Hamilton)	Guleo	11(0.38)	-	Not evaluated
XIII	**Family Cichlidae**				
58	*Oreochromis aureus* (Steindachner)	Blue tilapia	25(0.88)	**	Not evaluated
59	*Oreochromis mossambicus* (Peters)	Mozambique tilapia	55(1.93)	**	Near threatened
XIV	**Family Mastacenbelidae**				
60	*Mastacembulus armatus* (Lecepede)	Zig-zag eel/ Bam	54(1.90)	**	Least concerned

area. In spite of stocking of Chinese carps in public waters of Attock district (Nawaz personal communication) none of the three Chinese carps, grass carp *Ctenopharyngodon idella* (Valenciennes), silver carp *Hypopthylmichythus molitrix* (Valenciennes) and big head carp, *Aristichthys nobilis* (Valenciennes) was not recorded in this collection. There is much probability that these species have not been able to establish in the area. The chances of their missing from the catch seem very little. The main component of present collection is of non commercial fishes which comprised 63.33%.

The IUCN status of important fishes *T. macrolepis, S. plagiostomus, C. naziri, O. aureus, R. labiata, C. auratus* and four species of *Glyptothorax*, are not evaluated yet. Whereas, *O. pabda, W. attu* are near threatened and *C. carpio* is vulnerable. But the important fishes *L. rohita, C. mrigala, G. catla, M. bleekeri, S. sarwari, R. rita, C. marulius* are mentioned least concerned in IUCN list.

DISCUSSION

Freshwater fish fauna of Pakistan is dominated by family cyprinidae. Mirza (2003) listed 74 species from family Cyprinidae in Pakistan. The same trend is exhibited in fish fauna of Attock region, as 58.33% of the fish species belonged to family cyprinidae. The Golden Mahseer of Indus system had been assigned to *Tor putitora* (Hamilton), *Tor tor* (Hamilton) and *Tor mosal* (Hamilton) by various authors. Actually the Mahseer studied in this collection is different from all these three species. According to Mirza (2003) the name used by Heckel (1838) for Indus Mahseer appears to be correct name. Hence, the same name *Tor macrolepis* for the Indus Golden Mahseer after Mirza (2003) has been used. Pervaiz (2012a,b) has done very detailed work on the taxonomic and morphmetric analysis of this fish and has shown that *T. macrolepis* of Indus drainage system is different from the Mahseer present in Ganges Brahmaputra drainage system.

The Attock region is characterized by presence of some endemic species like Golden Mahseer of Indus, *Tor macrolepis*, *Gagata pakistanica, Glyptothorix naziri, Glyptothorix punjabensis*, and *Glyptothorix stocki* (Javed *et al.*, 2005). Three cold water species *Schizothorax plagiostomus, Racoma labiata* and *Racoma fedtschenkoi* are also represented in the present collection. The occurrence of some endemic species like genus *Glyptothorix* in this area corresponds to the typical topography of the fast flowing streams and rivers, which are shallow, clear and with rocky beds. The members of genus *Glyptothoraix* have evolved special adhesive suckers on their abdomen to adhere to substrate in fast flowing water. This character of attachment at the river bed was a prime factor in survival of these fishes in high velocity rivers and streams (Jayarm, 1982).

The presence of carnivore species like *W. attu* and *R. rita* and other carnivore fishes are probable hazard to co-habiting fishes. These fishes are pisicivorous and feed on fry, fingerlings and even big fishes. Hence, this is constant threat to other fishes. The missing Chinese Carps might have escaped during the sampling process. The exotic species *O. aureus* and *O. mossambicus, C. carpio, C. auratus* are omnivores that feed on plankton and aquatic vegetation. These species are fast breeder and compete for food and space to native species especially commercial fishes, the major carps, both in rearing facilities and wild. These four species seems well

established in Attock region. Khan *et al*. (2011) have pointed out that exotic species are becoming invasive in freshwaters of Punjab and other provinces of the country and are competing with local fauna. This adverse situation is one of the probable reasons of decline of commercially important fishes, which showed the lowest composition (0.03 to 0.24%) in the present collection. Even the majority of non-commercial fishes are also flourishing at the cost of the most valued and important fishes. The indiscriminate over exploitation of fisheries resources, habitat degradation due to flooding and illegal digging from river banks have contributed to decline of important and commercial fishes from Attock region. The majority of fishes are categorized as least concerned in IUCN Red List (IUCN, 2012). *Tor macrolepis* is not evaluated by IUCN. Only three species, *O. pabda*, *W. attu* and *O. mossambicus* are near threatened (IUCN, 2012).

The following steps are suggested concisely, not only for conservation and preservation of *T. macrolepis* but also for its sustainable production in the country. Enforcement of ban on illegal fishing methods such as; dynamiting, electrocuting and poisoning may be implemented. Save Mahseer campaign may be launched for public awareness at government level and private sector. Healthy brood stocks should be collected from suitable sites as this is the backbone of replenishment program. Scientific studies on important biological aspects such as racial analysis, disease diagnosis and health management regarding *Tor macrolepis* are suggested along its distribution region in Pakistan. A comprehensive and unified strategy for conservation of this fish be designed and adapted at country level.

CONCLUSION

Attock region of Pakistan is rich in commercial fish fauna, but its population is low and falling drastically. Measures to conserve and enhance natural fish production may prove beneficial.

ACKNOWLEDGEMENT

We are grateful to University of the Punjab, Lahore for funding this study under, “Faculty Development Program (2008-2009)”. Many thanks to Muhammad Nawaz, Assistant Director Fisheries and Fisheries staff in District Attock for their help in field work.

REFERENCES

Ahmad, Z. and Mirza, MR. 2002. Fishes of river Ravi from Lahore to Head Balloki. Biologia Pakistan. 48(1&2):317-322.

Brown, LR., Gray, RH., Hughes, RM. and Meader, MR. 2005. Effects of urbanization on Stream ecosystem. American Fisheries Society Symposium 47, Berthasda, Maryland, USA.

Heckel, J. 1838. Fishe aus Caschmir, Wien. Journal Bombay Natural History Society. 41:272-285.

IUCN. 2012. IUCN Red List of Threatened Species. Version 2011.2. <www.iucnredlist.org>

Jayram, KC. 1982. Aid to the identification of the Siluroid Fishes of India, Burma, Sri Lanka, Pakistan and Bangladesh. 5. Ariidae and Plotosidae. Record Zoological Survey of India. Paper No. 37:41.

Javed, MN., Pervaiz, K., Mirza, MR. and Bhatti, MN. 2005. Fishes of River Indus from Ghazi to Garyala, Pakistan. Biologia. 51(1):1-13.

Khan, AM., Ali, Z., Shelly, SY. and Mirza, MR. 2011. Aliens; a catastrophe for native freshwater fish diversity in Pakistan. Journal of Animals and Plants Sciences. 21:435-440.

Limburg, KE, Hughes, RM., Jackson, DC. and Brain, CZ. 2 011. Human Population Increase, Economic Growth, and Fish Conservation Collision course or Savvy Steward ship? Fisheries. 36:27-34.

Mirza, MR. 1975. Freshwater Fishes and Zoogeography of Pakistan. Bijdr. Dierk. 45:143-180.

Mirza, MR. 1980. Systematic and Zoogeography of freshwater fishes of Pakistan and Azad Kashmir. Proceedings of First Pakistan Congress of Zoology. Part A.

Mirza, MR. 1994. Geographical Distribution of freshwater fishes in Pakistan: a review. Punjab University Journal of Zoology. 9:93-108.

Mirza, MR. 2003. Checklist of freshwater fishes of Pakistan. Pakistan Journal of Zoology. Supplement Series. No. 3:1-30.

Mirza, MR. 2004. Freshwater Fishes of Pakistan, (2nd ed.). Urdu Science Board, Lahore, Pakistan.

Mirza, MR. and Sharif, HM. 1996. A Key to the fishes of Punjab. Ilmi Katab Ghar,Urdu Bazar, Lahore.

Peter, T. 1999. Coldwater fish and fisheries in Pakistan. FAO, Rome. Fisheries Technical Paper. 385:122-137.

Pervaiz, K. 2011. Aspects of Biology of Mahseer fish species from Attack Region, Pakistan. Ph.D. Thesis, Department of Zoology, University of the Punjab, Lahore, Pakistan. pp195.

Pervaiz, K., Iqbal, Z., Mirza, MR., Javed, MN., Naeem, M. and Ishtiaq, A. 2012[a]. Length–weight, length–length relationships and feeding habits of wild Indus Mahseer, *Tor macrolepis*, from Attock, Pakistan. Journal of Applied Ichthyology. 28:673-676.

Pervaiz, K., Iqbal, Z.,. Mirza, MR., Javed, MN. and Naeem, M. 2012[b]. Meristic and Morphometric Studies on Indus Mahseer *Tor macrolepis* (Teleostei: Cyprinidae) from District Attock, Pakistan. International Journal of Agriculture and Biology. 11–239/SAE/2012/14–2–169–175.

Qurashi, NA., Rafique, M., Awan, FA. and Mirza, MR. 1998. Fishes of River Haro, Pakistan. Biologia. 34:179-191.

Rafique, M. 2000. Fish Diversity and Distribution in Indus River and its drainage system. Pakistan Journal of Zoology. 32:321-332.

Rafique, M. 2001. Fish fauna of Himalayas in Pakistan with comments on the origin and dispersal of its high Asian elements. Pakistan Journal of Zoology. 33:279-288.

Rafique, M., Akhtar, S. and Niazi, HK. 2003. Fish Fauna of Jinnah Barrage and adjoining areas. Pakistan Journal of Zoology. 35:95-98.

Rafique, M. and Khan, NUH. 2012. Distribution and status of significant freshwater fishes of Pakistan. Record of Zoological Survey of Pakistan. 21:90-95.

Received: Sept 10, 2012; Accepted: Nov 1, 2012

SENRA Academic Publishers, British Columbia
Vol. 7, No. 1, pp. 2203-2209, Feb 2013
Online ISSN: 1920-3853; Print ISSN: 1715-9997

Canadian Journal of pure&applied sciences

RAW GLYCEROL AS COSUBSTRATE ON THE PAHs BIODEGRADATION IN SOIL

*Ulrich Vasconcelos[1], Fernando Jorge Santos de Oliveira[2] and Francisca Pessoa de França[3]
[1]Universidade Federal do Rio de Janeiro, Escola de Química, Bloco E, sala 109, Ilha do Fundão, CEP- 21949-900 Rio de Janeiro
[2]Petróleo Brasileiro S A, Av. Almirante Barroso, 81, 23º andar, CEP- 20031-004 Rio de Janeiro
[3]Universidade Federal do Rio de Janeiro, Escola de Química, Bloco E, sala 109, Ilha do Fundão, CEP- 21949-900 Rio de Janeiro, Brasil

ABSTRACT

The purpose of this investigation was to evaluate the efficacy of raw glycerol obtained as a by-product from the biodiesel manufacturing industry on the bioremediation of a soil contaminated with 8.43mg/kg of the USEPA 16 priority PAHs. Experiments were carried out using raw glycerol at 0.63, 0.32 and 0.16mg/kg. The second condition resulted in the best PAH biodegradation in 60 days, 68.0±0.1%, confirming that this compound may be used as a cosubstrate and adding value to this residue. Germination Index assay on soil samples proved that bioremediation eliminated the phytotoxic effects.

Keywords: Bioremediation, polycyclic aromatic hydrocarbons, raw glycerol, cosubstrate, germination index.

INTRODUTION

Polycyclic Aromatic Hydrocarbons (PAHs) are the primary organic contaminants in nature and are mainly found in soil. The hydrophobic characteristic of these molecules allows them to strongly bind to particles present in the soil, thus hindering their bioavailability and, consequently, their biodegradation. In addition, the mutagenic and carcinogenic potential of PAHs is well known and widely reported in the literature (Sanchés-Guerra *et al.*, 2012; Gong *et al.*, 2007; Mater *et al.*, 2006). PAHs originates mainly from vegetable, geochemical, and anthropogenic sources. Chemically, PAH molecules present two or more aromatic rings and cyclopentanes that are condensed and arranged in linear form, angular form, or in groups, and they are formed from saturated hydrocarbons under oxygen-deficient conditions through pyrosynthesis or pyrolysis catalyzed by constituents present in the medium (Muckian *et al.*, 2007).

Due to the complexity of the soil as well as the diversity and nature of the contaminants, several technologies have been developed and employed for the removal of polluting chemicals. Among these methods, bioremediation has been highlighted. The use of microorganisms for the removal of petroleum hydrocarbons from soil has been widely documented in the literature. This technique is environmentally friendly and is well-accepted by the public (Jacques *et al.*, 2007; Supaphol *et al.*, 2006).

*Corresponding author email: ulvasco@gmail.com

The biodegradation of PAHs in soil is slower than other hydrocarbons. These molecules are not the preferred sources of carbon, and so the microbiological removal process occurs through cometabolic pathways. Based on this principle, the addition of cosubstrates, e.g., glycerol, to the contaminated soil can contribute to the process of biodegradation. Glycerol is one of the adjuvants most widely used as a cosubstrate in various industrial bioprocesses, and it has been successfully used in the biodegradation of raw oil and in the process of denitrification of wastewater (Bodík *et al.*, 2009; Zhang *et al.*, 2005).

Glycerol has several advantages over other cosubstrates due to its osmoregulatory properties and the fact that it can serve as the preferred source of carbon in the synthesis of biosurfactants. In addition, glycerol is widely available in the market (Batista *et al.*, 2006; Nevoigt and Stahl, 1997). In this context, raw glycerol, a byproduct of the biodiesel industry, acquires an added value because it can be reused in the oil and gas industry. Glycerol production and supply have been increasing over the past years, thus stimulating research aimed at developing functional applications for the product (Ayoub and Abdullah, 2012).

Raw glycerol is regarded as an industrial waste because of its concentration of alkali metals, soaps, and other impurities derived from the process of biodiesel production. Even the raw form of glycerol can be used as a carbon source for energy and biomass production, with similar results compared to glycerin (Liu *et al.*, 2009). Because research using glycerol is a relatively new topic,

there are no reports describing its application as a cosubstrate during bioremediation of soils contaminated with PAH.

MATERIALS AND METHODS

Soil

The soil samples used in the present study were collected from a coastal region of Brazil. The samples were subjected to physicochemical and microbiological characterization, and the results are shown in table 1.

Raw glycerol

Raw glycerol was kindly provided by the Instituto Virtual Internacional de Mudanças Globais associated with the Instituto Alberto Luiz Coimbra de Pós-graduação e Pesquisa em Engenharia da Universidade Federal do Rio de Janeiro – IVIG-COPPE/UFRJ). The raw glycerol was coproduced during the process of biodiesel production from soybean (*Glycine max*, L. Merrill) by the transesterification reaction via the ethyl route using potassium hydroxide as a catalyst. The compound had the following characteristics: density 0.0011 g/cm^3, pH 9.9, ethanol content (2.8% w/w), water content (9.3% w/w), KOH content (2% w/w), glycerol content (84.4% w/w), diglyceride content (1.0% w/w), triglyceride content (<0.5% m/m), and potassium content (50.7 mg/g).

Biodegradation experiments

The biodegradation experiments were conducted for a period of 60 days in reactors with the following dimensions: 0.22 m width, 0.22 m length, and 0.09 m depth, containing 2 kg of soil. The effect of raw glycerol addition as a cosubstrate, using 0.63, 0.32, and 0.16 mg/kg of the compound, was analyzed.

To ensure adequate oxygen supply, the soil was regularly aerated by rotating it every 72 hours with a glass rod. The concentration of heterotrophic bacteria and filamentous fungi were determined from samples collected at 0, 7, 15, 30, and 60 days by the pour plate technique using Nutrient Agar (Merck, Darmstadt, Germany) containing 50 mg/L nystatin suspension at 10.000 UI/mL (Sigma, St. Louis, USA) for heterotrophic bacteria and Sabouraud Agar containing 2% glucose (Vetec, Rio de Janeiro, Brazil) and 50 mg/L ampicillin trihydrate at 96.0 to 100.5% purity (Sigma, St. Louis, USA) for filamentous fungi. Bacteria and fungi were incubated at 28±1°C for 48 hours or 72 hours, respectively. Abiotic loss was calculated using a reactor containing the same amount of soil added with a solution of 10% silver nitrate (Vasconcelos *et al*., 2011).

Ecotoxicological assay

Seed germination and root elongation tests were performed to determine the germination index (G_I), as described by Tiquia *et al*. (1996), using the following equation:

$$G_I = [(S_1/S_2) \times (R_1/R_2)] \times 100$$

Where S1 is the number of germinated seeds in the soil extract, S2 is the number of germinated seeds in the control, R1 is the average root length in the soil extract, and R2 is the average root length of the control. Seeds of *Allium porrum*, L., *Cucumis anguria*, L. and *Cucumis melo*, L. were used in this study. Incubation was performed at 22±1°C in the dark for 5 days. The test was conducted in triplicate using ten seeds of each species. The Germination Index takes into consideration control assays carried out with distilled water.

RESULTS AND DISCUSSION

The effect of the addition of raw glycerol as a cosubstrate in the biodegradation of the 16 priority PAHs from USEPA was analyzed. Degradation of the contaminants was observed in all tested concentrations. The average pH of 7.4±0.1 and soil moisture of 17.0±0.1% ($p < 0.05$) were favorable conditions for the degradation process. The percentage of biodegradation of each PAH is shown in table 2.

The addition of 0.63 mg/kg of raw glycerol promoted an approximately 64% reduction in PAH; however, the concentration of the compound that most highly stimulated the process was 0.32 mg/kg, resulting in a 6% increase in biodegradation and a 15% increase compared to the control reactor. A significant increase in the percentage of PAH removal, attributed to reduced raw glycerol content, was also observed in previous studies using the compound as a cosubstrate during the biodegradation of toxic compounds (Easterling *et al*., 2009; Chen *et al*., 2007). Attempts to reduce the concentration of raw glycerol to 0.16 mg/kg had no significant effect, yielding a value very close to that observed in the control reactor.

There was almost 100% removal of PAHs with two or three aromatic rings in all tested conditions. This was due to the simplicity of the molecular arrangement of these compounds and their low concentrations in soil. In contrast, the presence of raw glycerol negatively influenced the biodegradation of anthracene and fluorene, which corroborates the findings of Bengtsson and Zerhouni (2003). Moreover, degradation of these PAHs were inversely proportional to the concentration of raw glycerol, as observed by Baboshin *et al*. (2003), possibly related to the preferred choice of carbon source by telluric microorganisms.

Phenanthrene had the lowest percentage of removal in all reactors, including the control. The result is supported by the findings of Viñas *et al*. (2005) who observed that incomplete degradation of phenanthrene was related to

Table. 1 Characterization of the soil samples.

Analysis	Results	Reference
Texture (%)		ABNT (1984)
Clay (<0.02mm)	9±5	
Silt (0.002-0.02mm)	33±1	
Fine sand (0.02-0.2mm)	22±2	
Medium sand (0.2-0.5mm)	19±1	
Coarse sand (0.5-1.0mm)	12±4	
Gravel (>1.0mm)	5±5	
Total Organic Carbon (mg/kg)	23,000±1,000	USEPA[a] 9060
Total N (mg/kg)	1,397±30	USEPA 315.2
Total P (g/kg)	777±11	USEPA 365.3
16 priority PAHs[b] (mg/kg)	8.43±590	USEPA 8270C, 3540C e 3630C
pH	7.8±0.1	EMBRAPA (1979)
Water-Holding-Capacity (%)	21.4±0.1	Vasconcelos *et al.* (2011)
Water content (%)	10.0±0.1	EMBRAPA (1979)
Heterotrophic bacteria (UFC/g)	$34\pm1x10^6$	Vasconcelos *et al.* (2011)
Filamentous Fungi (UFC/g)	$22\pm1x10^4$	Vasconcelos *et al.* (2011)

[a] United States Environmental Protection Agency. [b] Polycyclic Aromatic Hydrocarbons

Table 2. Percentage of the USEPA 16 priority PAHs biodegradation (abiotic loss = 10±0.1%)[a]

PAH (# rings)	Raw glycerol concentration (mg/kg)			
	0.00	0.16	0.32	0.63
Naphtalene (2)	>99.9±0.1	>99.9±0.1	>99.9±0.1	>99.9±0.1
Acenaphthene (3)	>99.9±0.1	>99.9±0.1	>99.9±0.1	>99.9±0.1
Acenaphtilene (3)	>99.9±0.1	>99.9±0.1	>99.9±0.1	>99.9±0.1
Fluorene (3)	>99.9±0.1	88.0±0.1	86.0±0.1	76.0±0.1
Anthracene (3)	>99.9±0.1	55.0±0.1	46.0±0.1	44.0±0.1
Phenanthrene (3)	18.0±0.1	30.0±0.1	43.0±0.1	38.1±0.1
Fluoranthene (4)	51.8±0.1	51.8±0.1	59.7±0.1	59.5±0.1
Pyrene (4)	60.9±0.1	33.7±0.1	69.4±0.1	54.4±0.1
Benzo[a]anthracene (4)	52.2±0.1	56.3±0.1	77.2±0.1	66.8±0.1
Chrysene (4)	45.2±0.1	46.6±0.1	70.2±0.1	56.3±0.1
Benzo[b]fluoranthene (5)	65.1±0.1	67.5±0.1	79.7±0.1	73.6±0.1
Benzo[k]fluoranthene (5)	70.5±0.1	73.0±0.1	93.0±0.1	90.5±0.1
Benzo[a]pyrene (5)	52.8±0.1	55.0±0.1	85.1±0.1	81.9±0.1
Dibenz[a,h]anthracene (5)	43.5±0.1	52.5±0.1	70.7±0.1	66.2±0.1
Benzo[g,h,i]perylene (6)	85.1±0.1	85.6±0.1	85.1±0.1	74.5±0.1
Indeno[1,2,3-c,d]pyrene (6)	85.3±0.1	90.7±0.1	84.4±0.1	84.4±0.1
Biodegradation (%)	58.1±0.1	59.4±0.1	68.0±0.1	63.9±0.1

USEPA – United States Environmental Protection Agency. PAHs –Polycyclic Aromatic Hydrocarbons. [a] initial concentration = 8.43mg/kg (sum of the USEPA 16 priority PAH)

the low bioavailability of the compound when nutrient supplementation in relation to the degradation of several PAHs was analyzed.

With regard to PAHs with four to six aromatic rings, the percentage of biodegradation was between 33.7 and 93.0±0.1%. The reduction in six of the ten PAHs of this group, benzo[a]anthracene, chrysene, benzo[b]fluoranthene, benzo[k]fluoranthene, benzo[a]pyrene and dibenzo[a,h]anthracene, was due to the raw glycerol concentration used. Successful biodegradation can possibly be attributed to higher bioavailability of these compounds in the soil, favored by the emulsifying property of raw glycerol. High values were observed in the PAHs with five and six aromatic rings; these values were significantly higher than those

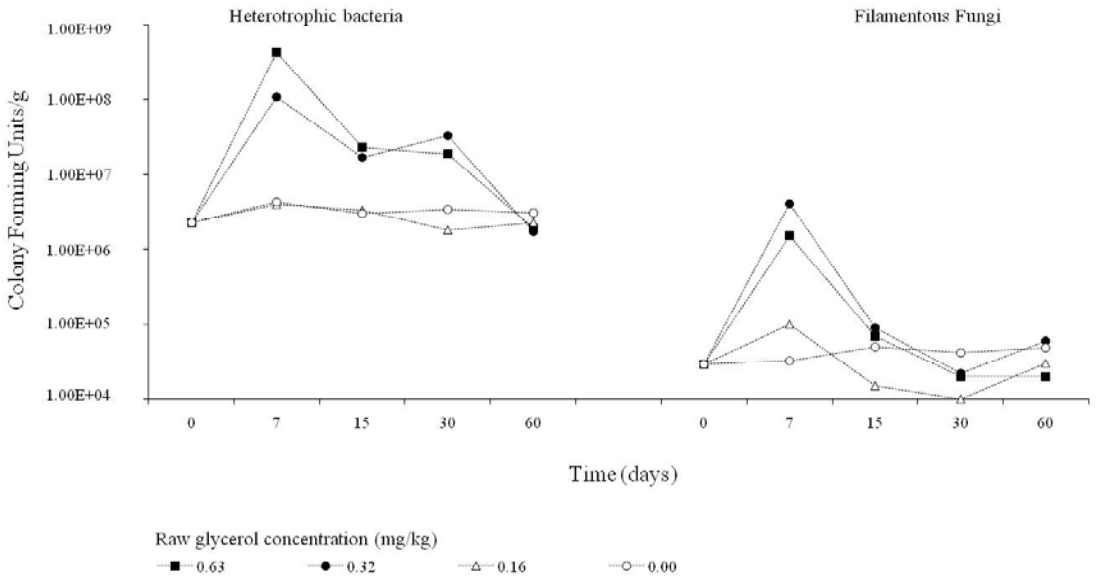

Fig. 1. Microbial concentration during PAHs biodegradation.

Table 3. Range of PHAs biodegradation (mg/kg/day) ($p \leq 0,05$)

Time (days)	Raw glycerol concentration (mg/kg)			
	0.00	0.16	0.32	0.63
0-30	0.05±0.01	0.10±0.01	0.18±0.10	0.15±0.11
30-60	0.04±0.01	0.02±0.01	0.04±0.11	0.03±0.10

PAHs – Polycyclic Aromatic Hydrocarbons

Table 4. Germination Index ($p \leq 0,05$).

Plants	Raw glycerol concentration (mg/kg)			
	0.00	0.16	0.32	0.63
Allium porrum	40.6±4.5[a]	41.9±7.4[a]	121.9±13.4[c]	108.4±15.1[c]
Cucumis anguria	50.3±5.5[a]	51.9±5.8[b]	85.1±4.9[c]	83.6±2.7[c]
Cucumis melo	73.5±6.1[b]	74.3±3.8[b]	101.9±11.2[c]	88.3±3.8[c]

[a] High phytotoxicity. [b] moderate phytotoxicity. [c] no phytotoxicity

reported in the literature (Lei *et al.*, 2005; Joner *et al*., 2004; Xu and Obbard, 2004).

In addition to raw glycerol, other PAHs may work as cosubstrates during the removal of certain PAHs with high molecular weights. This metabolic strategy has previously been investigated through kinetic studies in which removal of pyrene in the presence of fluoranthene and phenanthrene was observed (Hwang and Cutright, 2003; Dean-Ross *et al*., 2002). This observation may explain the highest percentage removal of pyrene at 69.4±0.1%, coinciding with the highest percentage removal of fluoranthene at 59.7±0.1% and phenanthrene at 43.0±0.1% in the reactor with the addition of 0.32 mg/kg raw glycerol. An important observation concerns the second highest percentage of degradation of pyrene that occurred in the reactor without the addition of raw glycerol. In this case, the microbiota used two distinct classes of cosubstrates for the removal of these PAHs.

When raw glycerol was not included in the reactor, the biodegradation percentages of PAHs with four to six aromatic rings were between 43.5 and 85.3±0.1%. The greatest reductions were observed in highly persistent molecules of benzo[g,h,i]perylene and indeno[1,2,3-c,d]pyrene. The high removal percentages can be explained by the distribution of PAHs in soil aggregates, thus favoring bioavailability.

As shown in figure 1, the presence of raw glycerol allowed for the development of a population of heterotrophic bacteria and filamentous fungi in the soil, depending on the concentration of cosubstrate employed. Furthermore, the levels of nitrogen and phosphorus ensured the necessary supply of these nutrients, which was verified by the stability of the microbial population in the reactor without raw glycerol.

The addition of 0.32 and 0.63 mg/kg of raw glycerol increased the population of heterotrophic bacteria and filamentous fungi by two orders of magnitude during the first seven days of the experiment. In the reactor containing 0.16 mg/kg of the glycerol compound, a slight increase was observed in the microbial population during the same period, possibly due to the low concentration of raw glycerol used. Over time, the microbial density decreased, and the concentration was reestablished to a similar level to that determined at the beginning of the experiment under all glycerol conditions tested.

The experimental time required for the reestablishment of heterotrophic bacteria was between 30 and 60 days. The concentration of filamentous fungi was reduced twice as fast as the bacterial concentration. Such behavior was also observed by Ballaminut and Matheus (2007) and may be attributed to the higher sensitivity of fungi to nutrient depletion. The reduction in the microbiota in this type of research is a predicted event and may also be related to the presence of toxic metabolites and the phenomenon of tolerance, in which environmental stresses, such as the petroleum hydrocarbon contamination, promote compensatory effects, causing the microbiota to balance and stabilize (Igwo-Ezikpe *et al*., 2010; Ayotamuno *et al*., 2007).

The microbial communities in soil are structured in a way that they can eliminate the xenobiotic compounds, using a mechanism involving metabolic cooperation, chemotaxis, and cometabolism. However, supplementation of the medium with a soluble carbon source at non-inhibitory concentrations directly influences the bioprocess through the induction of growth and increased metabolic rate (Pizzul *et al*., 2007; Grabowski *et al*., 2005).

Table 3 shows that the highest rates of biodegradation occurred in the first half of the experiment in systems where raw glycerol was added, coinciding with the period having higher microbial density. With the depletion of the cosubstrate, the degradation rate was significantly decreased, revealing the contribution of raw glycerol in the process, in agreement with previous studies in which glycerin was administered as a carbon source (Vasconcelos *et al*., 2011; Baboshin *et al*., 2003).

It is possible that with the depletion of raw glycerol, other molecules such as low molecular weight PAHs and light oil fractions may have been used as cosubstrates, which explains the significant decrease in the rate of daily PAH reduction in the second half of the bioprocess; however, this did not lead to the end of the bioprocess, as seen in the reactor without raw glycerol.

The raw glycerol concentration also affected the reduction of the phytotoxic effect determined by the germination index (G_I) shown in Table 4. The G_I is the result of seed germination and the rate of elongation of the root extract in contaminated soil and in control soil. For any plant, the phytotoxicity of the soil constituents is considered moderate when the G_I ranges between 50 to 80%. A G_I below 50% indicates high phytotoxicity, and a G_I above 80% indicates the lack of a phytotoxic effect (Anastasi *et al*., 2009).

An 8.43 mg/kg concentration of PAH promoted moderate (*C. anguria* and *C. melo*) to high (*A. porrum*) phytotoxicity. This result is in disagreement with the results observed by Debiane *et al*. (2008), in which a phytotoxic effect of the tested hydrocarbons was detected at concentrations above 10 mg/kg. The decrease in the inhibitory effect on plants coincided with a significant reduction in the content of the contaminant. The best condition for the PAH biodegradation test for the elimination of phytotoxicity was observed at raw glycerol concentrations of 0.63 and 0.32 mg/kg. Despite the high content of potassium and other impurities in raw glycerol, in two of the three plants tested, the G_I reached values above 100%, which indicates the presence of nutrients in the soil extract (Paradelo *et al*., 2008).

At the lowest concentration of cosubstrate tested (0.16 mg/kg), the result showed similarity to that seen in the assay with untreated soil sample, i.e., a moderate to high phytotoxicity. This result is most likely related to the cosubstrate concentration employed, which had no significant effects on the microbiota, and consequently, on the degradation of PAHs. This suggests that raw glycerol in this condition could have been used only as a preferred source of carbon and not as a cosubstrate, in agreement with the results presented by Duquenne *et al*. (1999).

The results presented in this study contribute to the understanding of raw glycerol application as a cosubstrate during the biodegradation of PAHs in soil, ensuring an efficient strategy for the removal of these contaminants as well as in reducing the toxic effects on the plants studied. In this context, the reuse of waste in the biodiesel industry can become economically viable and impart an added value to raw glycerol. Failure to remove the impurities originating during the transesterification process, due to the low volume of cosubstrate required, corroborates that assertion. In addition, future impacts to the soil due to the accumulation of potassium from the catalyst may be

avoided by employing glycerol produced by new generations of biodiesel production technologies.

CONCLUSION

Under the conditions established by the present study, the best strategy for the biological removal of PAHs was obtained by adding 0.32 mg/kg of raw glycerol, which also contributed to the elimination of phytotoxic effects in the tested plants. Most importantly, the assignment of functionality to raw glycerol reflects on the valuation of the product and contributes positively to discussions on the reuse of waste from industrial processes.

AKNOWLEDGEMENTS

The authors thank Petroleo Brasileiro S.A., CNPq, CAPES and FAPERJ for financial support.

REFERENCES

ABNT. 1984. Solo – Análise Granulométrica, Rio de Janeiro, Brasil.

Anastasi, A., Coppola, T., Prigione, V. and Varese, GC. 2009. Pyrene degradation and detoxification in soil by a consortium of basidiomycetes isolated from compost: role of laccases and peroxidases. J. Hazard Mat. 165:1229-1233.

Ayoub, M. and Abdullah, AZ. 2012. Critical review on the current scenario and significance of crude glycerol resulting from biodiesel industry towards more sustainable renewable energy industry. Renew. Sust. Energ. Rev. 16:2671-2686.

Ayotamuno, MJ., Okparanma, RN., Nweneka, EK., Ogaji, SOT. and Probert, SD. 2007. Bio-remediation of a sludge containing hydrocarbons. Appl. Energy. 84:936-943.

Baboshin, M., Finklstein, ZI. and Golovleva, LA. 2003. Fluorene cometabolism by *Rhodococcus rhodochrous* and *Pseudomonas fluorescens* cultures. Microbiology. 72: 194-198.

Ballaminut, N. and Matheus, DR. 2007. Characterization of fungal inoculum used in soil bioremediation. Braz. J. Microbiol. 38:248-252.

Batista, SB., Mouteer, AH., Amorim, FR. and Tótola, MR. 2006. Isolation and characterization of biosurfactant/bioemulsifier-producing bacteria from petroleum contaminated sites. Bioresour. Technol. 97:868-875.

Bengtsson, E. and Zerhouni, P. 2003. Effects of carbon substrate enrichment and DOC concentration on biodegradation of PAHs in soil. J. Appl. Microbiol. 94:608-617.

Bodík, I., Blšťáková, A., Sedláček, S. and Hutňan, M. 2009. Biodiesel waste as source of organic carbon for municipal WWTP denitrification. Bioresour. Technol. 100:2452-2456.

Chen, BY., Chen, WM. and Chang, JS. 2007. Optimal biostimulation strategy for phenol degradation with indigenous rhizobium *Ralstonia taiwanensis*. J. Hazard Mat. 139:232-237.

Dean-Ross, D., Moody, J. and Cerniglia, CE. 2002. Utilization of mixtures of polycyclic aromatic hydrocarbons by bacteria isolated from contaminated soils. FEMS Microbiol. Ecol. 41:1-7.

Debiane, D., Garçon, G., Verdin, A., Fontaine, J., Durand, R., Grandmougin-Ferjani, A., Shirali, P. and Lounès-Hadj Sahroui, A. 2008. *In vitro* evaluation of the oxidative stress and genotoxic potentials of anthracene on mycorrhizal chicory roots. Environ Exp Bot. 64:120-127.

Duquenne, P., Chenu, C., Richard, G. and Catroux, G. 1999. Effect of carbon source supply and its location on competition between inoculated and established bacterial strains in sterile soil microcosm. FEMS Microbiol. Ecol. 29:331-339.

Easterling, ER., French, WT., Hernandez, R. and Lichia, M. 2009. The effect of glycerol as a sole and secondary substrate on the growth and fatty acid composition of *Rhodotorula glutinis*. Bioresour. Technol. 100:356-361.

EMBRAPA. 1979. Manual de métodos de análise de solo, Rio de Janeiro.

Gong, Z., Alef, K., Wilke, BM. and Li. P. 2007. Activated carbon adsorption of PAHs from vegetable oil used in soil remediation. J. Hazard Mat. 143:372-378.

Grabowski, A., Blanchet, D. and Jeanthon, C. 2005. Characterization of long-chain fatty-acid-degrading syntrophic associations from a biodegraded oil reservoir. Res. Microbiol. 157:814-821.

Hwang, S. and Cutright, TJ. 2003. Effect of expandable clays and cometabolism on PAH biodegradation. Environ. Sci. Pollut. Res. 10:277-280.

Igwo-Ezikpe, MN., Gbenle, OG., Ilori, MO., Okpuzor, J. and Osuntoki, AA. 2010. High molecular weight polycyclic aromatic hydrocarbons biodegradation by bacteria isolated from contaminated soil in Nigeria. Res. J. Environ. Sci. 4:127-137.

Jacques, RJS., Bento, FM., Antoniolli, ZI. and Camargo, FAO. 2007. Biorremediação de solos contaminados com hidrocarbonetos aromáticos policíclicos. Ciência Rural. 37: 1192-1201.

Joner, EJ., Hirmann, D., Szolar, OHJ., Todorovic, D., Leyval, C. and Loibner, AP. 2004. Priming effects on PAH degradation and ecotoxicity during a

phytoremediation experiment. Environ. Pollut. 128:429-435.

Lei, L., Khodadoust, AP., Suidan, MT. and Tabak, HH. 2005. Biodegradation of sediment-bound PAHs in field-contaminated sediment. Wat Res. 39:349-361.

Liu, S., Rebros, M., Stephens, G. and Marr, AC. 2009. Adding value to renewables: a one pot process combining microbial cells and hydrogen transfer catalysis to utilize waste glycerol from biodiesel production. Chem. Comm. 17:2308-2310.

Mater, L., Sperb, RM., Madureira, LAS., Rosin, AP., Correa, AXR. and Radetski, CM. 2006. Proposal of a sequential treatment methodology for the safe reuse of oil-sludge contaminated soil. J. Hazard Mat. 136:967-971.

Muckian, L., Grant, R., Doyle, E. and Clipson, N. 2007. Bacterial community structures in soil contaminated by polycyclic aromatic hydrocarbons. Chemosphere. 8:1535-1541.

Nevoigt, E. and Stahl, U. 1997. Osmoregulation and glycerol metabolism in the yeast *Saccharomyces cerevisiae*. FEMS Microbiol Rev. 21:231-241.

Paradelo, R., Moldes, AB., Rodríguez, M. and Barral, MT. 2008. Relahionship between heavy metals and phytotoxicity in composts. Cy T. A. 6:143-151.

Pizzul, L., Sjögren, Å., Castillo, MP. and Stenström, J. 2007. Degradation of polycyclic aromatic hydrocarbons in soil by a two-step sequential treatment. Biodegradation. 18: 607-616.

Sanchés-Guerra, M., Pelallo-Marinéz, N., Díaz-Barriga, F., Rothenberg, S.J., Hernández-Cadena, L., Faugeron, S., Oropeza-Hernández, LF., Guaderrama-Díaz, M. and Quintanila-Veja, B. 2012. Environmental polycyclic aromatic hydroncarbon (PAH) exposure and DNA damage in Mexican children. Mut. Res./Gen. Toxicol. Environ. Mutagen. 742:66-71.

Supaphol, S., Panichsakpatana, S., Trakulnaleamsai, S., Tungkananuruk, N., Roughjanajirapa, P. and O'Donnel, AG. 2006. The selection of mixed microbial inocula in environmental biotechnology: example using petroleum contaminated tropical soils. J. Microbiol. Meth. 65:432-441.

Tiquia, SM., Tam, NFY. and Hodgkiss, IJ. 1996. Effects of composting on phytotoxicity of spent pig-manure sawdust litter. Environ. Pollut. 93:249-256.

USEPA. 1993. Method 351.2. Determination of total Kjeldahl nitrogen by semi-automatic colorimetric. Washington, DC, USA.

USEPA. 1996. Method 3540C. Soxhlet extraction. Washington, DC, USA.

USEPA. 1996. Method 3630C. Silica gel clean-up. Washington, DC, USA.

USEPA. 1996. Method 8270C. Semivolatile organic compounds by gas chromatography/mass spectrometry. Washington, DC, USA.

USEPA. 1996. Method 9060. Total Organic Carbon. Washington, DC, USA.

Vasconcelos, U., de França, FP. and Oliveira, FJS. 2011. Removal of high-molecular weight polycyclic aromatic hydrocarbons. Quím. Nova. 34:218-221.

Viñas, M., Sabaté, J., Espuny, MJ. and Solanas, AM. 2005. Bacterial community dynamics and polycyclic aromatic hydrocarbons degradation during bioremediation of heavily creosote-contaminated soil. Appl. Environ. Microbiol. 71:7008-7018.

Xu, R. and Obbard, JP. 2004. Biodegradation of polycyclic aromatic hydrocarbons in oil-contaminated beach sediments treated with nutrient amendments. J. Environ. Qual. 33:861-867.

Zhang, GL., Wu, YT., Qian, XP. and Meng, Q. 2005. Biodegradation of crude oil by *Pseudomonas aeruginosa* in the presence of rhamnolipds. J. Zhejiang Univ. Sci. 6:725-730.

Received: Oct 2, 2012; Accepted: Nov 1, 2012

SENRA Academic Publishers, British Columbia
Vol. 7, No. 1, pp. 2211-2215, Feb 2013
Online ISSN: 1920-3853; Print ISSN: 1715-9997

Canadian Journal of pure & applied sciences

DETECTION OF *SALMONELLA TYPHI* ANTIGENS ON THE SURFACE OF MOUSE PERITONEAL MACROPHAGES USING FLUORESCENT TAGGED ANTIBODIES

Deepika Sidhu, Sandeep Kumar, Gulshan Kumar and HG Bramhne
Central Research Institute, Kasauli, Himachal Pardesh-173204, India

ABSTRACT

To see the possibilities of detecting *Salmonella typhi* antigens on Macrophage surface, mouse peritoneal macrophages were infected with *S. typhi in vitro* and the macrophages were examined for morphological changes and expression of *S. typhi* surface antigens on the macrophage surfaces, using FITC tagged specific antibodies. The study showed positive results as fluorescence could be observed on the macrophage surfaces, however, the intensity of fluorescence was low.

Keywords: *S. typhi* antigen, mouse peritoneal macrophages, phagocytosis, FITC tagged antibodies.

INTRODUCTION

Globally Typhoid fever continues to be a public health problem. It is an infectious disease and is a major cause of morbidity and mortality in developing countries. Only humans are affected and most often the acquisition of *S. typhi* occurs via ingestion of food and water contaminated with excreta from carriers of bacterium (Hornick *et al*., 1970). *Salmonella* species efficiently invade the gut mucosa and servive as intracellular pathogens of macrophages (Finlay and Falkow, 1989). It is the ability to survive intracellularly that limits the effectiveness of antibody and neutrophill mediated damage and that allows the pathogens to disseminate systemically from mucosal sites. Typhoid fever is predominately a disease of school age children and young adults (Balraj *et al*., 1992)

World Health Organization (2000) estimates the annual global incidence of typhoid fever at 0.3% corresponding to about 16 million cases of which approx. 600,000 ends in death. In some developing countries of Asia and Africa the annual incidence may reach 1% with fatality rates as high as 10%. About 70% of fatalities from typhoid fever occur in Asia. Laboratory diagnosis is made by blood, bone marrow or stool cultures and with the Widal test (demonstration of *salmonella* antibodies against O-somatic and H-flagellar antigens). The Widal test is time consuming and most of the times when diagnosis is reached, it is too late to start an antibiotic regimen. Isolation of *S. typhi* is the definitive diagnosis but the bacterium is rarely isolated.

The present study was designed to see the possibilities of detecting *S. typhi* antigens on mouse macrophages by artificially infecting these with *S. typhi*. The study showed some promising initial results and the experiments need to be repeated with human circulating macrophages and then in macrophages of typhoid patients using some more sensitive tools to reach to any final conclusion about the utility of this approach.

*Corresponding author email: deepikasidhu28@yahoo.ca

MATERIALS AND METHODS

Test bacterial strains

Five strains of *Salmonella typhi*, all from invasive sites, received from NSEC (National Salmonella and Escherichia Centre, Central Research Institute, Kasauli, India) were used as test strains. The strains were revived on nutrient agar and identified as *S. typhi* on the basis of biochemical and serological characterization using standard methods.

Preparation of Fluorescent tagged antibodies

Antibodies raised against *S. typhi* "O" somatic antigen and "H" flagellar antigen were concentrated using salting out principle (Wolfson *et al*., 1948). The concentrated antibodies were then conjugated with iso-thiocyanate dye using conjugate buffer (0.5 M carbonate /bicarbonate, pH 9.5) (Johnson, 1963). The unreacted (free) dye was removed by gel filtration using a sephadex column 20 cm long and 3cm diameter. The quality of the fluorescent dye tagged antibodies was checked to ensure that the specific antibodies are tagged which react specifically with its inducer antigens. For this antigen smear was prepared on a glass slide and stained with tagged antibodies and examined under fluorescent microscope.

Collection of mouse peritoneal macrophages (Ray and Dittel, 2010)

A group of 10-13 healthy Swiss albino mice were scarified by deep ether anesthesia. Peritoneal cavity was exposed by cutting the skin of the abdominal wall as shown in figure 1. 10 ml of chilled RPMI-1640 was

Fig. 1. The peritoneal cavity of Swiss albino mouse injected with chilled RPMI.

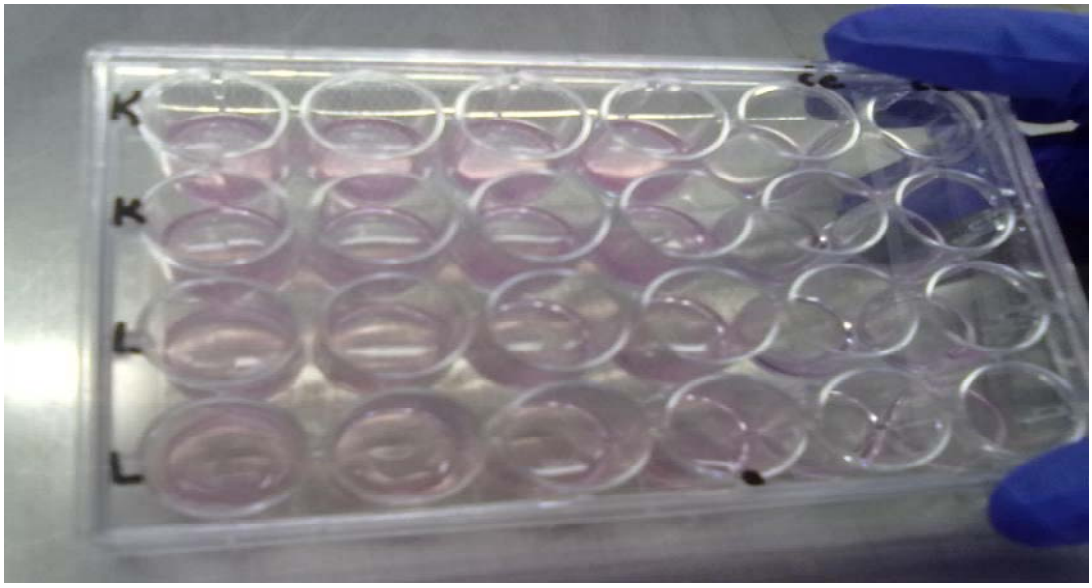

Fig. 2. The cell 24- well castor containing mouse peritoneal macrophages infected with *S. typhi.*

injected into the peritoneal cavity of each mouse. The mice were shaken vigorously to release peritoneal macrophages. The injected fluid was aspirated and collected in sterile 50 ml conical tubes.

The harvest was centrifuged at 3,000 rpm for 3 minutes at 4ºC and sediment was washed twice with RPMI. The cells thus collected were counted for validity as evaluated by trypan blue exclusion and suitably diluted in RPMI 1640 with 10% FCS to give count $1x10^6$ viable cell per ml.

1ml of cell suspension was inoculated in each well of 24 well cell castors with sterile 13mm round cover slip in each well. The cells were incubated at 37ºC for 4 hours in CO_2. After 4 hrs, cell castors were examined under the inverted microscope for the attachment of cell. The cover slips were washed with plain RPMI-1640 (without FCS) to remove non –adherent cells. Adherent macrophages on cover slips were then used for further experiment.

Infection of macrophages with S. typhi

Live and killed suspension of S. typhi was prepared. The prepared suspension of live and killed *S. typhi* were added in the wells containing adhered macrophages as shown in figure 2.

Coverslips were removed after an interval of 2, 4, 6 and 8 hours of infection with antigens and examined for

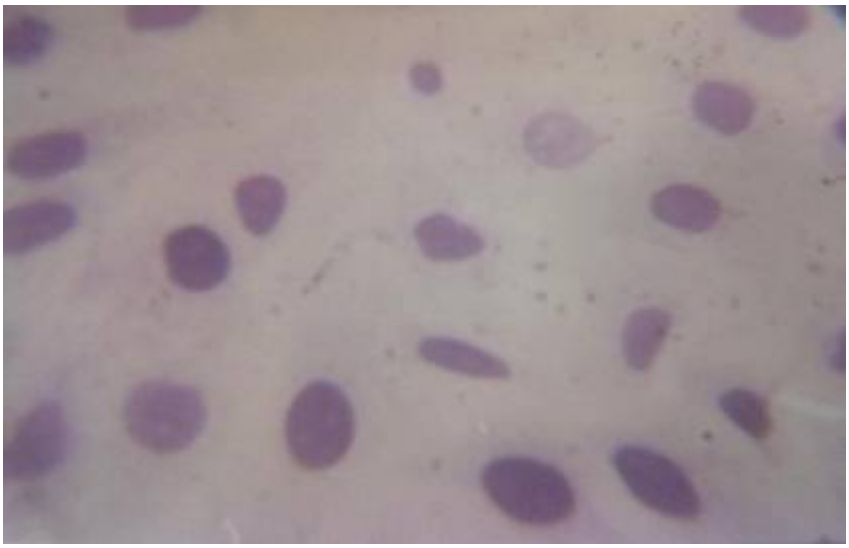

Fig. 3. Bacteria-macophage interaction after 2 hr of incubation.

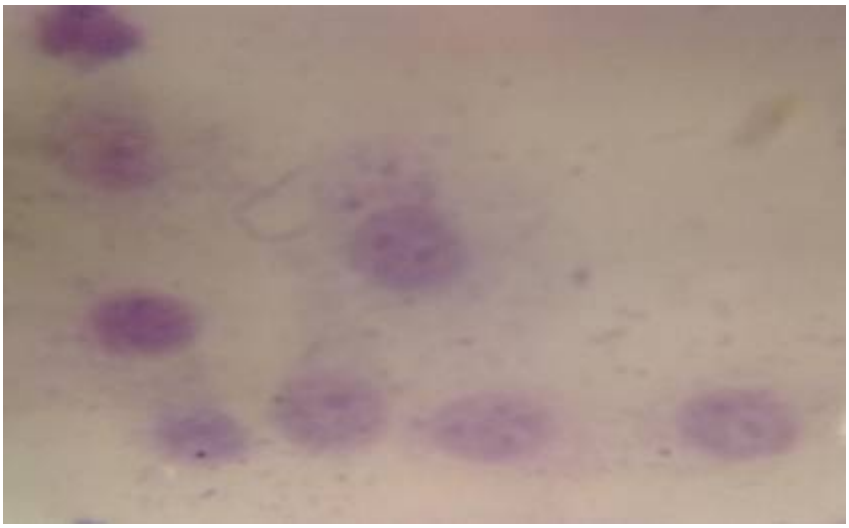

Fig. 4. Bacteria-macophage interaction after 4hr of incubation.

phagocytosis and detection of antigens on the macrophage surface.

Study of phagocytosis by macrophages (Jenkin and Benacerraf, 1960)

The cover slips were washed three times with PBS, then fixed with acetone for 30 seconds and were stained with methylene blue. Again washing with PBS was given. Coverslips were examined under inverted microscope.

Staining of activated macrophages with FITC labeled antibodies

The cover slips from the cell caster were removed after 2h, 4h, 6h, & 8h of infection and were washed 3-4 times in PBS. To check the expression of *S. typhi* O- antigen on the surface of the macrophages, the slides were stained with FITC-labeled antibodies specific to the O-antigen and observed under fluorescent microscope (10X).

RESULTS AND DISCUSSION

Bacteria –Macrophages interaction - phagocytosis

From the results it was observed that the macrophages interacted with bacteria, 2 hours after infection showing attachment and intracellular bacteria with increase in size as in figure 3. After 4 hours incubation majority of cells showed attachment as well as intracellular bacteria with enlargement in size and reversal of cytoplasm to nucleus ratio as shown in figure 4.

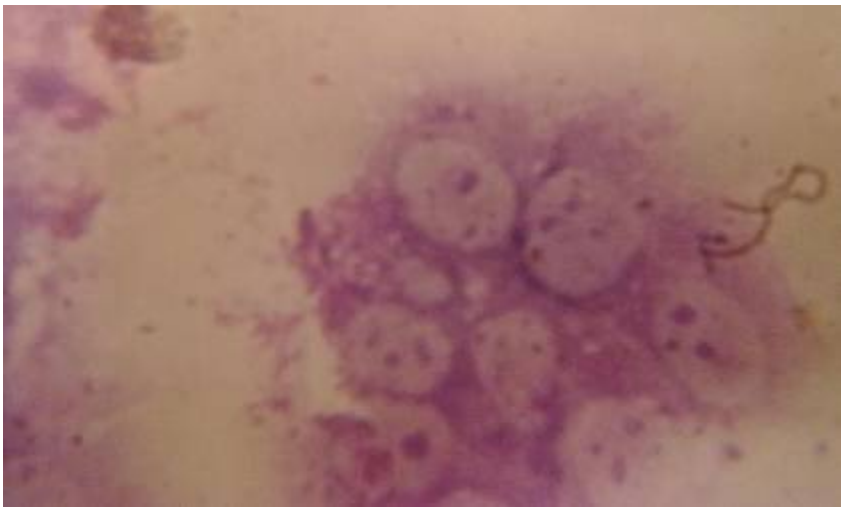

Fig. 5. Bacteria-macophage interaction after 6 hr of incubation.

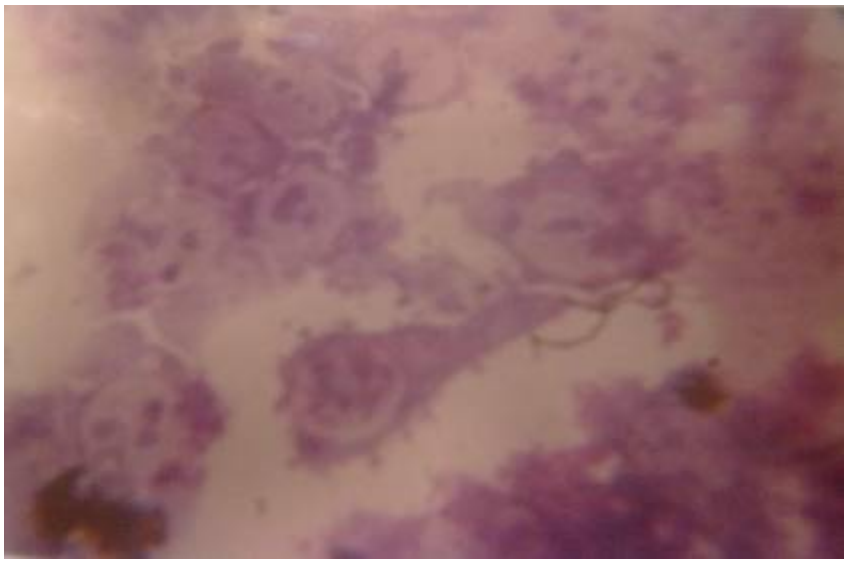

Fig. 6. Bacteria-macophage interaction after 8 hr of incubation.

After 6 hours of incubation, the activation of macrophages continued and showed a further increase in size of a cell. Granules appeared in cytoplasm and vacoulation started. At this stage bacteria were clearly visible intra-cellularly figure 5. After 8 hour few of cell ruptured while majority of cells were intact. The cells were still sticking to coverslip and enlargement was significantin as shown in figure 6.

Detection of S. typhi antigens on macrophages by staining of infected macrophages with FITC labeled antibodies.

When viewed under fluorescent microscope the infected macrophages showed flouresence on their surfaces indicating presence of *S. typhi* antigens. However, the intensity of the fluorescence was low. The results of the staining of the macrophages with fluorescent labeled antibodies have been presented in the figure 7.

Salmonellosis is recognized to be a global problem. Human salmonellosis accounts for 60-70% of all reported cases of food borne diseases (WHO, 1988). Laboratory diagnosis of the infection is made by detection of antibodies against *S. typhi* somatic O- antigen and flagellar H-antigen in the serum of the infected individual using Widal test. Early diagnosis of the disease is very important since it results in early containment of the infection and hence rapid management and treatment of the cases.

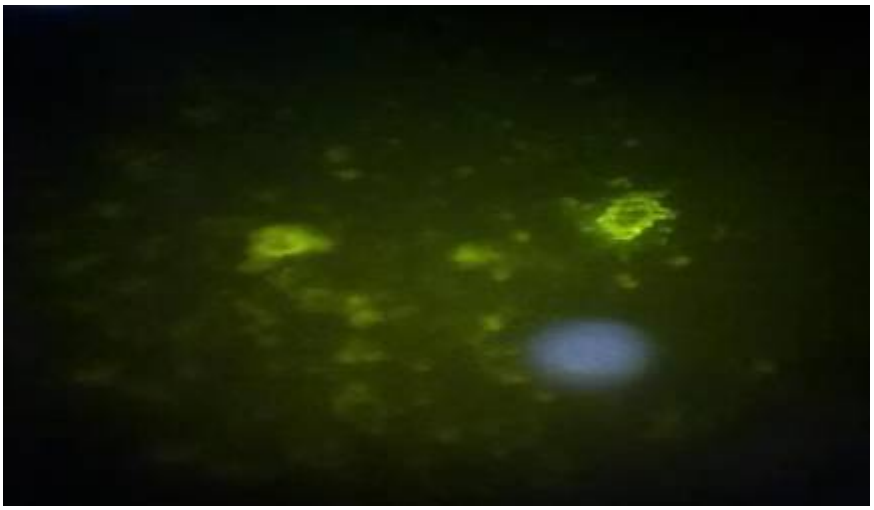

Fig. 7. Macrophages showing fluorescence under fluorescent Microscope.

As macrophages and other antigen presenting cells do carry antigenic moieties of the infecting organisms to release antibodies by the antibody producing cells hence in this study an attempt was made to see the possibility of detecting O antigens of S. typhi on mouse peritoneal macrophages and getting initial, positive results to continue the experiments with human circulating (blood) macrophages and to see the feasibility of this approach as a tool for early detection of typhoid cases. In this study, we studied the interaction between the *S. typhi* and the mouse peritoneal macrophages in-vitro. It was observed that after infection with *S. typhi*, the macrophages showed clear signs of activation like increase in size, vacoulation in the cytoplasm, irregular margins. These change were evident after 2h of infection and progressed in the same manner as is evident from the observation made after 4,6 to 8 hrs that the granulation occurred in the cytoplasm, the cell size increased considerably, the bacterial uptake by the macrophages was found to increase significantly and a few cells got ruptured while the majority of the cells were still intact. The next objective of the study was to detect the presence of the expressed O-antigens on the surface of the macrophages. For that we produced antisera against the O-antigen in rabbits. The antibodies so obtained were then labeled with FITC to stain the macrophage cells for demonstration of the surface O-antigen. To check the efficacy of the labeled antibodies we first stained the pure suspension of *S. typhi* and observed under the fluorescent microscope. The efficacy of the preparation was verified as the bacterial cells were showing fluorescence under the fluorescent microscope. FITC-labeled antibody treatment of macrophages showed fluorescence under the fluorescent microscope. The intensity of fluorescence was very small which can be due to the low quantity of expressed O-antigens on the macrophages or low sensitivity of the method used. Though fluorescent labeled antibodies treatment of the infected macrophages showed low flourscent intensity but the methylene blue stained smears revealed clear evidence of macrophage activation after infection with the *S. typhi* strains. Hence some more refined/sensitive techniques (like electron microscopy) may give better results to show the presence of antigenic moieties on the macrophage surface. Thus this approach has more scope for further studies.

REFERENCES

Balraj, V., Sridharan, G. and Jesudason, MV. 1992. Immunization against typhoid fever. Natl. Med. J. India. 5(1):12-7.

Finlay, BB. and Falkow, S. 1989. Salmonella as an intracellular parasite. Mol. Microbiol. 3:1833-1841.

Hornick, RB., Greisman, SE., Woodward, TE., DuPont, HL., Dawkins, AT. and Synder, MJ. 1970. Typhoid fever: Pathogenesis and immunological control. N. Engl. J. Med. 283:686-691.

Jenkin, C. and Benacerraf, B. 1960. In vitro studies on the interaction between mouse peritoneal macrophages and strains of *Salmonella* and *Escherichia coli*. J. Exp. Med 112(2): 403-417.

Johnson, GD. and Holborow, EJ. 1963. Nature 198:1316.

Ray, A. and Dittel, BN. 2010. Isolation of mouse peritoneal cavity cells. J. Vis. Exp. (35), e1488, DOl: 10.3791/1488.

WHO. 1988. Food poisoning by salmonella. WHO forum, 9(1)123.

WHO. 2000. WHO position paper typhoid vaccines. W.E.R.,75:257-264.

Wolfson, WQ., Cohn, C., Calvary, E. and Ichiba, F. 1948. Am. J. Clin. Pathol. 18:723.

Received: Sept 25, 2012; Accepted: Nov 29, 2012

SENRA Academic Publishers, British Columbia
Vol. 7, No. 1, pp. 2217-2222, Feb 2013
Online ISSN: 1920-3853; Print ISSN: 1715-9997

Canadian Journal of pure&applied sciences

ELECTROLYTES CHANGES INDUCED BY WEIGHT LOSS HERBAL DRUGS PHYTOLACCA AMERICANA AND PHYTOLACCA BERRY IN HYPERCHOLESTEROLEMIC RABBITS

*Ruqaiya Hasan[1], Aisha Javaid[2], Kalim R. Khan[2] and Safia Malik[2]
Department of Physiology, Faculty of Medicine, Umm Al-Qura University, Makkah, KSA
Department of Physiology, Faculty of Science, University of Karachi, Karachi-75270

ABSTRACT

Present study deals to find out the effects of two herbal weight reducing drugs Phytolacca Americana (PA) and Phytolacca Berry (PB) on plasma electrolytes in common rabbits followed by the induction of hypercholesterolemia. In PA garlic, bladder wrack and grapefruit are the additional ingredients to poke weed while PB has poke weed only. Test animals of two groups were orally administrated PA and PB in doses of 33.3 mg/day and 1.15 mg/day respectively, for 37 days. Blood samples drawn on day 0, 3, 9, 14, 21, 27 and 37 were used to measure plasma Sodium (Na^+), Potassium (K^+) and Calcium (Ca^{++}). Both herbal drugs maintained plasma Na^+ to normal levels while plasma K^+ concentration that remained low returned to normal after four weeks of treatment, significantly ($p<0.05$) depending on the duration of drug administrated. However, PA effectively returned the very high Ca^{++} concentration to normal level within one week of treatment whereas PB achieved the same normal level after three weeks of treatment. Thus it may be concluded that both weight reducing herbal drugs although maintained the plasma Na^+, K^+ and Ca^{++} concentrations to normal levels when administrated for more than five weeks, showed pronounced alterations in plasma concentrations of K^+ and Ca^{++} during early period of treatment. This effect might be attributed to the interference of drugs with Na^+-K^+ ATPase activity or blocking the Ca^{++} channels at the cellular level.

Keywords: Weight loss drugs, electrolytes, phytolacca americana, phytolacca berry, grapefruit.

INTRODUCTION

A large number of chronic and life–threatening diseases and conditions are associated with overweight and obesity (Shaw *et al*., 2007; Logue *et al*., 2011). High concentrations of cholesterol were significantly linked with overweight and obesity. (Mokdad *et al*., 2003). Dashti *et al*. (2006) found an association between ketogenic diet, obesity and high cholesterol. Other studies proved that obesity and adiposity were significantly linked with high serum cholesterol and other lipids. (Neri *et al*., 2007; Sertic *et al*., 2009; Sacheck *et al*., 2010).

Now a days herbal drugs and dietary supplements are available for the treatment of obesity and its related disorders (Shekelle *et al*., 2003; Pittler and Ernst, 2004; Feng *et al*., 2010; Bu *et al*., 2011). Weight reduction has been found in people using herbal drugs (Boozer *et al*., 2001, 2002; Feng *et al*., 2010; Bu *et al*., 2011). Poke weed is among the variety of herbs found efficacious in obesity (Willis *et al*., 2008; Ravikiran *et al*., 2011; Hasan *et al*., 2012).

There is an interlink between intake of sodium with high caloric diet intake (Lin *et al*., 1999) and various studies showed the involvement of sodium in obesity (Flodmark *et al*., 1992; Suzuki *et al*., 1996; Riazi *et al*., 2006). Mariosa *et al*. (2008) investigated the reduction of potassium in abdominal obesity. Also during the exercise testing in obese people the important role of potassium is explained by Salvadori *et al*. (2003). Although, experimentally calcium deficiency could not induce obesity (Paradis and Cabanac, 2005), however, clinical data showed the involvement of calcium in obesity. It has been found that calcium and parathormone are associated with obesity (Hultin *et al*., 2010).

In the present investigation two herbal weight reducing drugs Phytolacca Americana (PA) with a combination of herbal ingredients including Poke weed, Bladder wrack, Garlic and Grape fruit and Phytolacca Berry (PB) with single ingredient of Poke weed are administered to hypercholesterolemic rabbits to evaluate the changes in plasma electrolytes concentrations, the underlying mechanism of action of ingredients as well as their side effects (Hasan *et al*., 2011).

MATERIALS AND METHODS

Fifteen common rabbits (*Oryctolagus cuniculus*) 18 to 24 months old, ranging from 1,160 to 1,470g in weight were purchased fromlocal marketst, and were kept in well ventilated barred cages (Lab standards). They were fed on normal diet including carrots, cabbage and alfalfa.

*Corresponding author email: ruqaiya55@gmail.com

INDUCTION OF HYPERCHOLESTEROLEMIA

A modified diet containing 5g butter fat / 500g of diet was given daily for 15 days to induce hypercholesterolemia in all rabbits (Moghadasian *et al*., 1999). Blood samples were drawn on day 0 and 15.

Five rabbits were kept as controls while remaining ten were equally divided into two groups as test 1 and test 2.

DRUGS

The two experimental weight reducing herbal drugs PA and PB available in tablet form were obtained from the local chemist shop. Drugs were administered with a daily oral dose of 33.3 mg and 1.15 mg of PA and PB to test 1 and test 2 animals respectively for 37 days.

BLOOD SAMPLING

Sampling was done on day 0, 3, 9, 14, 21,27 and 37 by drawing the blood from the marginal vein of the ear with the help of 3cc disposable syringes (Moreland, 1965). Heparinized blood samples were centrifuged at 3500 rpm for 5 minutes and collected supernatants as plasma were stored at 4^{o}C to be used for analysis.

BIOCHEMICAL AND STATISTICAL ANALYSIS

Commercial biochemical kits (QCA, Spain) were used to measure plasma electrolytes Na^{+} , K^{+} and Ca^{++} . The absorbances of samples were read on Spectrophotometer (Model No. NV201, China). Statistical analyses of collecting data were performed by t-test and two - way ANOVA.

RESULTS

A consideration of table 1 indicates that, administration of modified diet to control and test rabbits for 15 days, significantly ($p<0.05$)increased the mean plasma concentrations of Na^{+} and Ca^{++} and decreased the mean plasma K^{+} concentration.

CONTROL

After 15 days, in control rabbits the exclusion of butter fat from the diet resulted in a reduction of mean plasma concentrations of Na^{+} and Ca^{++} , while K^{+} increased to the normal concentration (Figs. 1,2,3).

Table 1. Effect of butter fat (5g/kg diet) on mean plasma electrolytes concentration (mmol/l) of rabbits *Oryctolagus cuniculus*.

Days	Sodium			Potassium			Calcium		
	C	T1	T2	C	T1	T2	C	T1	T2
0	169.44 ± 8.58	155.15 ± 10.355	163.41 ± 31.99	5.16 ± 0.56	5.65 ± 0.63	5.26 ± 0.20	0.85 ± 0.44	1.67 ± 0.71	1.38 ± 0.47
15	181.85 ± 8.10	190.05 ± 45.43	208.21 ± 33.46	4.13 ± 1.09	4.65 ± 0.63	4.26 ± 0.20	2.55 ± 0.68	3.07 ± 0.34	3.38 ± 0.43

Each figure is the Mean ± SD of five values. C = Control. T1 = PA (33.3 mg/day). T2 = PB (1.15 mg/day)

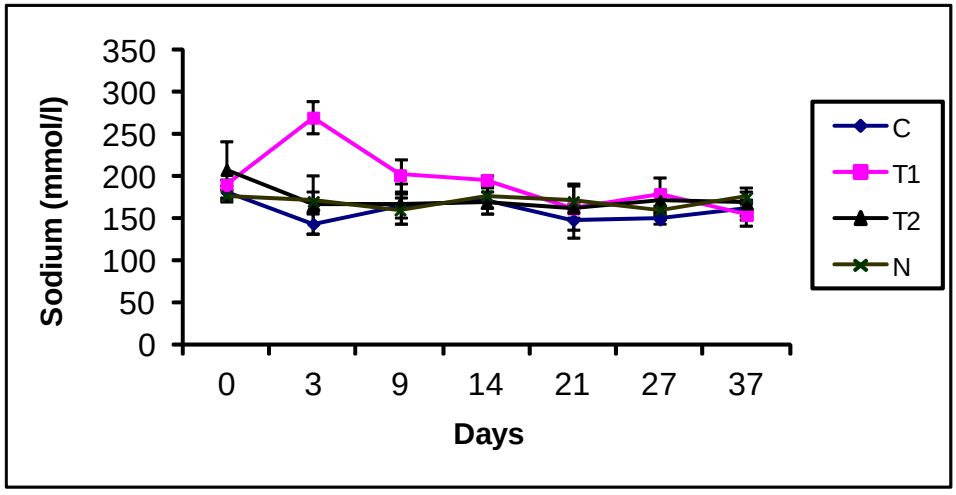

Fig. 1. Comparison of mean plasma sodium concentrations in control and test rabbits *Oryctolagus cuniculus* following the administration of weight reducing drugs.

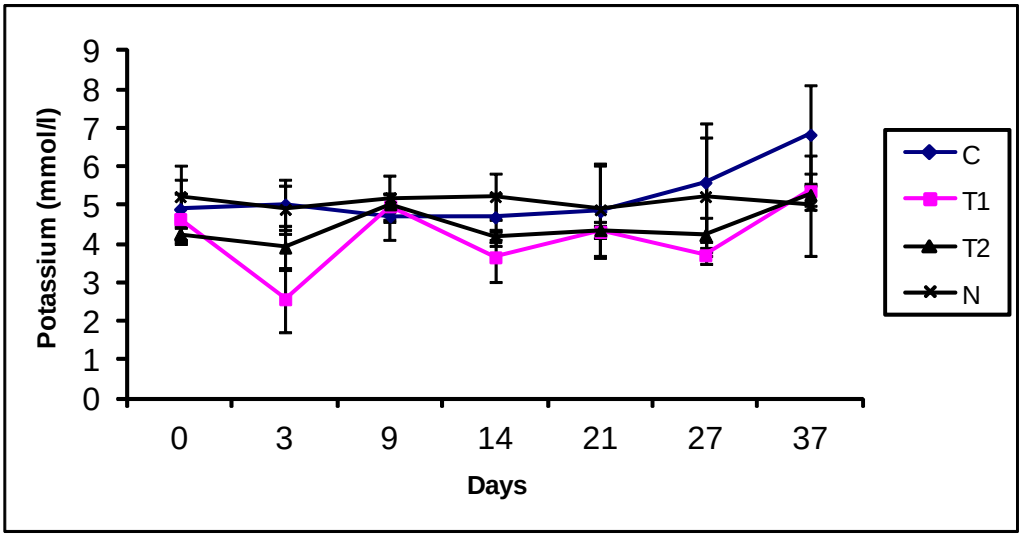

Fig. 2. Comparison of mean plasma potassium concentrations in control and test rabbits *Oryctolagus cuniculus* following the administration of weight reducing drugs.

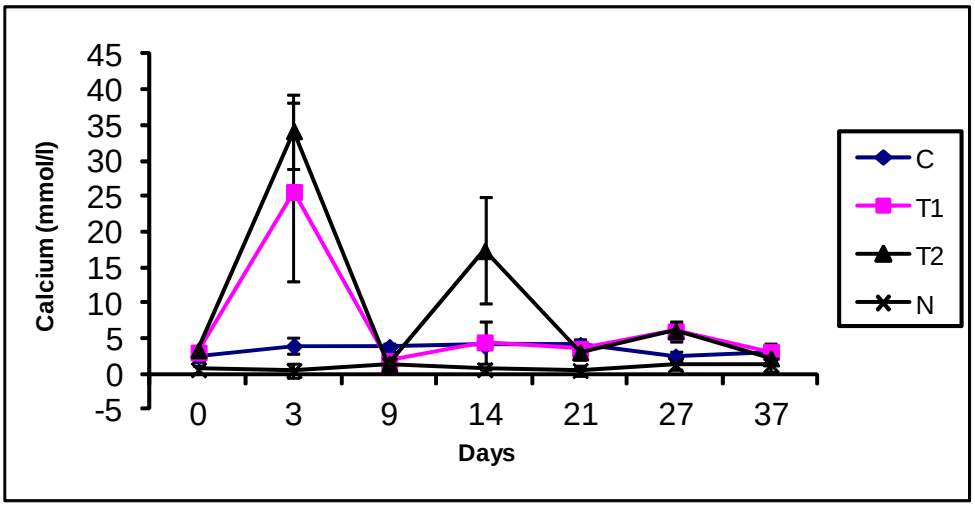

Fig. 3. Comparison of mean plasma calcium concentrations in control and test rabbits *Oryctolagus cuniculus* following the administration of weight reducing drugs.

Na^+

On day 0, test 1 rabbits with high mean plasma Na^+ concentration of 190.05 ±6.14 mmol/l, when administered with a dose of 33.3 mg/day of PA for 37 days showed a further rise in Na^+ concentration on day 3, followed by a significant ($P<0.05$) reduction up to the end of treatment. On day 37, the Na^+ concentration reached ton 154.54 ±13.34 mmol/l i.e. almost normal level (Fig. 1).

Test 2 rabbits with initial mean plasma Na^+ concentration of 208.21 ± 33.45 mmol/l, when administered with a dose of 1.15 mg/day of PB for 37 days showed a reduction in Na^+ concentration on day 3, followed by a constant, non-significant reduction till the end of the experiment (Fig. 1).

K^+

Test 1 rabbits treated with PA have a low plasma K^+ concentration with a mean value of 2.57 ± 0.83 mmol/l on day 3 which gradually raised and maintained up to the day 27, however a significant rise ($P< 0.05$) near to normal from day 9 was observed as administration of the drug continued till day 37 (Fig. 2).

The similar patterns of rise and fall in mean plasma K^+ levels were obtained in test 2 animals on day 3 and day 9 respectively treated with PB. Afterwards further significant ($P< 0.05$) reduction in mean K^+ concentration reaching to the normal values was observed (Fig. 2).

Ca^{++}

Fig. 3 shows the treatment of test 1 rabbits with PA resulted in a rapid rise of mean plasma Ca^{++} level on day 3, i.e. 25.66 ± 12.48 mmol/l that immediately declined to low levels of 1.85 ± 0.76 mmol/l on day 9 followed by a gradual rise up to day 27. Further non-significant decrease in the mean Ca++ level was evident on day 37.

Similar patterns of alterations in the mean plasma Ca++ concentration were observed following the administration of PB to test 2 rabbits on day 3 and day 9. However, a rise and fall in the mean Ca++ levels were observed on day 14 and day 21 respectively, maintained to normal levels onwards (Fig. 3).

DISCUSSION

Herbs and herbal preparations are effective in the treatment of diseases such as cancer, diabetes mellitus, obesity and cardiovascular diseases (York *et al*., 2007). In the present study an attempt is made to find out the effects of two weight reducing herbal drugs PA and PB on mean plasma Na^+, K^+ and Ca^{++} concentrations. Before the administration of drugs, hypernatremia, hypokalemia and hypercalcemia are induced in the experimental rabbits fed on a high butter fat diet. However, reversal to normal electrolyte concentrations is achieved when butter is excluded from the diet. PA, which is, a combination of different herbal constituents, administered to test 1 rabbits for five weeks returns the Na^+ to normal concentration. In contrast, PB having only poke weed maintains the normal Na^+ concentration within one week of treatment. Both the herbal drugs when administrated for longer period significantly raise the mean plasma K^+ to normal concentration. While the administration of these drugs for less than one week greatly elevate the mean plasma Ca^{++} level, followed by a reduction in the later period of the experiment however, normal concentration is not achieved.

Above observations show that the herbal weight reducing drugs without having any effects on Na^+ concentration, profoundly change the Ca^{++} concentration and K^+ concentration to a lesser extent. The laxative effect of bladder wrack and ultimate diarrhea is due to the presence of alginic acid in it which interferes with the absorption of Na^+ and K^+ (Newall *et al*., 1996).

Several studies show that bladder wrack contains vitamins and minerals like Ca^{++}, Mg^{++}, K^+, Na^+, thus increasing their blood levels (Clark *et al*., 2003). Normal mean Na^+ concentration and a significant high K^+ concentration may be attributed to the fact that herbal drugs interfere with enzyme ATPase, essential to transport these electrolytes across the membrane (Akpanabiatu *et al*., 2005).

Two constituents of grapefruit i.e. flavonoid and naringenin have an inhibitory effect on ATPase activity (Middleton and Kandaswami, 1992; Conseil *et al*., 1998) and voltage – operated Ca^{++} channels (Summanen *et al*., 2001). Further the concentration dependent vasorelaxant effect of naringenin (Saponara *et al*., 2006), greatly reduced at high concentration of K^+ (Ajay *et al*., 2003) was in agreement with present results. However, grapefruit with low Na^+ and Ca^{++} concentrations is considered a good source of K^+ (Ensminger, 1994). Another important component of PA is garlic which may be a good factor to maintain electrolyte balance by increasing serum Na^+ and K^+ levels (Oluwole, 2001). It has an inhibitory effect on Ca^{++} channels, opens the K^+-Ca^{++} channels and close L - type Ca^{++} channels promoting vasodilation (Siegel *et al*., 1992; Eskardary *et al*., 2001).

Finally it is concluded that experimental animals show a significant alteration in mean plasma K^+ and Ca^{++} concentrations in the initial period of treatment with PA and PB, that gradually return to near normal concentrations at the later part of the experiment. However, mean plasma Na^+ is maintained to a normal concentration during the treatment. Thus the persons who are obese, especially with other obesity associated complications should use the herbal weight reducing drugs with caution as data on human studies are lacking.

REFERENCES

Ajay, M., Gilani, AU. and Mustafa, RM. 2003. Effects of flavonoids on vascular smooth muscle of the isolated rat thoracic aorta. Life Sci. 74:603-612.

Akpanabiatu, MI., Umoh, IB., Udosen, EO., Udoh, AE. and Edet, EE. 2005. Rat serum electrolytes, lipid profile and cardiovascular activity on *Nauclea latifolia* leaf extract administration. Ind. J.Clin. Biochem. 20(2):29-34.

Boozer, CN., Daly, PA., Homel, P., Solomon, JL., Blanchard, D., Nasser, JA., Strauss, R. and Meredith, T. 2002. Herbal ephedra/caffeine for weight loss: A 6-month randomized safety and efficacy trial. Int. J. Obes. Relat. Metab. Disord. 26(5):593-604.

Boozer, CN., Nasser, JA., Heymsfield, SB., Wang, V., Chen, G. and Solomon, JL. 2001. An herbal supplement containing Ma Huang - Guarana for weight loss: A randomized double- blind trial. Int. J. Obes. Relat. Metab. Disord. 25:316-324.

Bu, Y., Shi, T., Meng, M., Kong, G., Tian, Y., Chen, Q., Yao, X., Feng, G., Cheng, H. and Lu, Z. 2011. A novel screening model for the molecular drug for diabetes and obesity based on tyrosine phosphatase Shp2. Bioorg. Med. Chem. Lett. 21(2):874-878.

Clark, CD., Bassett, B. and Burge, MR. 2003. Effects of kelp supplementation on thyroid function in euthyroid subjects. Endocrinol. Pract. 9(5):363-369.

Conseil, G., Baubichin, CH., Dayan, G., Jault, JM., Barron, D. and DiPietro, A. 1998. Flovonoids: A class of modulators with bifunctional interactions at vicinal ATP and steroid- binding sites on mouse P glycoprotein. Proc. Nat. Acad. Sci. 95:9831-9836.

Dashti, HM., Al-Zaid, NS., Mathew, TC., Al-Mousawi, M., Talib, H., Asfar, SK. and Behbahani, AI. 2006. Long term effects of ketogenic diet in obese subjects with high cholesterol level. Mol. Cell. Biochem. 286(1-2):1-9.

Ensminger, A. 1994. Grapefruit Foods and Nutrition Encyclopedia (2nd ed.), CRC Press Inc., Boca Raton, FL, USA. 1097-1099.

Eskandary, H., Shahabi, M. and Dabiri, S. 2001. Effects of Garlic and Nimodipine on cerebral blood flow and their neuroprotective effects after brain ischemia in rabbit. Arch. Iranian Med. 4(3):133-137.

Feng, Y., Huang, SL., Dou, W., Zhang, S., Chen, JH., Shen, Y., Shen, JH. and Leng, Y. 2010. Emodin, a natural product, selectively inhibits 11 beta-hydroxysteroid dehydrogenase type 1 and ameliorates metabolic disorder in diet-induced obese mice. Br. J. Pharmacol. 161(1):113-126.

Flodmark, CE., Henningsen, NC. and Sveger, T. 1992. Red cell sodium-potassium adenosine triphosphatase sites and intracellular sodium increased in obese school children. Miner. Electrolyte Metab. 18(1):6-8.

Hasan, R., Ahmad, M., Javaid, A. and Hussain, Z. 2011. The altered plasma electrolytes concentrations induced by weight reducing herbal drug (Mehzileen) in common rabbits. Int. J. Biol. Biotech. 8(4):575-578.

Hasan, R., Khan, KR. and Kiran, S. 2012. Role of Phytolacca Americana and Phytolacca Berry in lipid profile alteration in hypercholestrolemia induced rabbits *Oryctolagus cuniculus*. Canad Journal of Pure Applied Sciences. 6(1):1797-1802.

Hultin, H., Edfeldt, K., Sundbom, M. and Hellman, P. 2010. Left-shifted relation between calcium and parathyroid hormone in obesity. J. Clin. Endocrinol. Metab. 95(8):3973-3981.

Lin, BH., Guthrie, J. and Fraza o, E. 1999. Nutritional Quality of Home and Away - from Home Foods. In: Away - from Home Foods Increasingly Important to Quality of American Diet. USDA. Washington, DC.

Logue, J., Murray, HM., Welsh, P., Shepherd, J., Packard, C., Macfarlane, P., Cobbe, S., Ford, I. and Sattar, N. 2011. Obesity is associated with fatal coronary heart disease independently of traditional risk factors and deprivation. Heart. 97:564-568.

Mariosa, LS., Ribeiro-Filho, FF., Batista, MC., Hirota, AH., Borges, RL., Ribeiro, AB. and Zanella, MT. 2008. Abdominal obesity is associated with potassium depletion and changes in glucose homeostasis during diuretic therapy. J. Clin. Hypertens. 10(6):443-449.

Middeleton, E. and Kandaswami, C. 1992. Effect of Flavonoids on immune and inflammatory cell functions. Biochem. Pharmacol. 43:1167-1179.

Moghadasian, MH., Manus, BM., Godin, DV., Rodrigues, B. and Frohlich, JJ. 1999. Proatherogenic and antiatherogenic effect of probucol and phytosterols in apolipoprotein –E deficient mice, possible mechanisms of action. Circulation. 99:1733-1739.

Mokdad, AH., Ford, ES., Bowman, BA., Dietz., WH., Vinicor, F., Bales, VS. and Marks, JS. 2003. Prevalence of obesity, diabetes, and obesity-related health risk factors. JAMA. 289(1):76-79.

Moreland, AF. 1965. Collection and withdrawal of body fluids and infusion techniques. In: Methods of animal experimentation. Ed. Gray, WI. Vol.1, Academic Press, NY, USA. 1-42.

Neri, D., Espinoza, A., Bravo, A., Rebollo, MJ., Moraga, F., Mericq, V. and Castillo-Durán, C. 2007. Visceral adiposity and its association with serum lipids in female obese teenagers. Rev. Med. Chil. 135(3):294-300.

Newall, CA., Anderson, LA. and Phillipson, JD. 1996. Herbal Medicines: A Guide for Health Care Professionals. The Pharmaceutical Press, London. 124-126.

Oluwole, FS. 2001. Effect of Garlic on some haematological and biochemical parameters. Afr. J. Biomed. Res. 4:139-141.

Paradis, S. and Cabanac, M. 2005. Calcium deficiency cannot induce obesity in rats. Physiol. Behav. 85(3):259-264.

Pittler, MH. and Ernst, E. 2004. Dietary supplements for body-weight reduction: A systematic review. Am. J. Clin. Nutr. 79:529-536.

Ravikiran, G., Raju, AB. and Venugopal, Y. 2011. Phytolacca Americana: A review. Int. J. Res. Pharma. Biomed. Sci. 2(3):942-946.

Riazi, S., Khan, O., Hu, X. and Ecelbarger, CA. 2006. Aldosterone infusion with high-NaCl diet increases blood pressure in obese but not lean Zucker rats. Am. J. Renal Physiol. 291(3): 597-605.

Sacheck, JM., Kuder, JF. and Economos, CD. 2010. Physical fitness, adiposity, and metabolic risk factors in young college students. Med. Sci. Sports Exerc. 42(6):1039-1044.

Salvadori, A., Fanari, P., Giacomotti, E., Palmulli, P., Bolla, G., Tovaglieri, I., Luzi, L. and Longhini, E. 2003.

Kinetics of catecholamines and potassium, and heart rate during exercise testing in obese subjects. Heart rate regulation in obesity during exercise. Eur.J. Nutr. 42(4): 181-187.

Saponara, S., Testai, L., Iozzi, D., Martinotti, E., Martelli, A., Chericoni, S., Sgaragli, S., Fusi, F. and Calderone, V. 2006. (+/-) Naringenin as large conductance Ca ++ - activated K+ (BKca) channel opner in vascular smooth muscle cells. Br. J. Pharmacol. 149(8):1013-1021.

Sertic, J., Juricic, L., Ljubic, H., Bozina, T., Lovric, J., Markeljevic, J., Jelakovic, B., Merkler, M. and Reiner, Z. 2009. Variants of ESR1, APOE, LPL and IL-6 loci in young healthy subjects: association with lipid status and obesity. BMC Res Notes. 2:203. http://www.biomedcentral.com

Shaw, K., Gennat, H., O'Rourke, P. and Mar, DC. 2007. Exercise for overweight or obesity. The Cochrane Database of Systematic Reviews. Issue 2. John Wiley and Sons, Ltd.

Shekelle, PG., Hardy, ML., Morton, SC., Maglione, M., Mojica, WA., Suttorp, MJ., Rhodes, SL., Jungvig, L. and Gagne, J. 2003. Efficacy and safety of ephedra and ephedrine for weight loss and athletic performance: A meta-analysis. JAMA. 289:1537-1545.

Siegel, G., Emden, J., Wenzel, K., Mironneau, J. and Stock, G. 1992. Potassium channel activation in vascular smooth muscle. Adv. Exp. Med. Biol. 311:53-72.

Summanen, J., Vuorela, P., Rauha, JP., Tammela, P., Marjamäki, K., Pasternack, M., Törnquist, K. and Vuorela, H. 2001. Effects of simple aromatic compounds and flavonoids on Ca++ fluxes in rat pituitary GH4C1 cells. Eur. J. Pharmacol. 414(2-3):125-133.

Suzuki, H., Ikenaga, H., Hayashida, T., Otsuka, K., Kanno, Y., Ohno, Y., Ikeda, H. and Saruta, T. 1996. Sodium balance and hypertension in obese and fatty rats. Kidney Int. Suppl. 55:150-153.

Willis, WL., Goktepe, I., Isekhuemhen, OS., Reed, M., King, K. and Murray, C. 2008. The effect of mushroom and poke weed extract on salmonella, egg production and weight loss in molting hens. Poult. Sci. 87(12):2451-2457.

York, DA., Thomas, S., Greenway, FL., Liu, Z. and Rood, JC. 2007. Effect of an herbal extract Number Ten (NT) on body weight in rats. Chin. Med. 2:10, doi: 10.1186/1749-8546-2-10.

Received: Nov 2, 2012; Accepted: Dec 3, 2012

SENRA Academic Publishers, British Columbia
Vol. 7, No. 1, pp. 2223-2226, Feb 2013
Online ISSN: 1920-3853; Print ISSN: 1715-9997

Canadian Journal of pure&applied sciences

Short Communication

GLYCATED HAEMOGLOBIN, GLUCOSE AND INSULIN LEVELS IN DIABETIC TREATED RATS

*GS George[1], AA Uwakwe[2] and GO Ibeh[3]
[1] Department of Medical Biochemistry, Niger Delta University, Amassoma, Bayelsa State
[2] Department of Biochemistry, University of Port Harcourt
[3] Department of Biochemistry, University of Port Harcourt, Nigeria

ABSTRACT

In assessing the relationship between plasma glucose, insulin and glycated haemoglobin, data for these parameters were obtained after induction of Wistar albino rats with 70mg/kg body weight of streptozotocin which resulted in Type 1 model diabetes. Treatment of the rats with 10% concentration of extract of *Tapinanthus bengwensis* and *Oscimum gratissimum* was carried out for two weeks and the parameters were evaluated and compared. Rats treated with *T. benwgensis* had significant effect of reducing both plasma glucose and glycated haemoglobin (HbA1C) and increasing insulin ($P<0.05$) suggesting a higher hypoglycemic propensity.

Keywords: Glucose, glycated haemoglobin, insulin, streptozotocin, *T. bengwensis*, *O. gratissimum*

INTRODUCTION

The relative abundance of medicinal herbs in our environment and the realization that they possess active ingredients with therapeutic values has made the need for their study imperative. The World Health Organization (WHO) in 1980 released this and harped on the need to carry out scientific scrutiny of most of these herbs to elucidate their chemical constituents and pharmacological potentials by ascertaining efficiency and efficacy of the flora as a potential remedy.

Diabetes is a heterogeneous metabolic disorder characterized by chronic hyperglycemia largely due to the dynamic interactions between varying defects of insulin secretion and action. It is known that hyperglycemia itself has adverse effect on tissue insulin sensitivity and insulin secretion that make it difficult to differentiate between primary and secondary abnormalities. As identified by Ordia and Wokoma (1992) the burden of this non-communicable disease on global morbidity and mortality has gained tremendous recognition. Diabetes mellitus is now known to be a major cause of stroke, kidney failure, blindness, loss of libido etc. Arising from this knowledge, the need for the survival of diabetic patients through assessment of medication, monitoring and education has become imperative. Diabetic patients with raised plasma glucose levels have proportionally more glycation occurring both intracellularly and extracellularly. The works of Brucalla *et al*. (1992), Standing and Tailor (1992), Philips and Floege (1999) have elucidated the need to treat these complications as an integral part of the clinical stratification of diabetic patients. Several prospective studies have been carried out which showed that intensive blood glucose control is possible and could effectively control microvascular complications among diabetics. Wincor (2003), has elucidated a growing body of evidence to conclude that tight blood glucose control is possible. As shown by Buciarelli *et al*. (2002), Naka *et al*. (2004), Melpomeni *et al*. (2003) and Vlassara (2005), there is growing evidence to support that inhibition of advanced glycated end products (AGEs) formation or blockade of their downstream signaling pathway may be a promising strategy for treatment of patients with diabetic vascular complications.

Trials arongoingng on substances that may be able to prevent these processes and possibly even reverse them and the prospects are promising. Some authors have earlier reported the antidiabetic and hypoglycemic properties of African mistletoe. Obatomi *et al*. (1994) and Didem (2005) have both reported on the efficacy of mistletoe in management of diabetes. Swanson Flatt *et al*. (1989) reported a reduction in some clinical parameters associated with diabetes. As reported by Agnaniet *et al*. (2005) and Mohammed *et al*. (2007), *Oscimum gratissimum* has a dose and time dependent effect in hyperglycemic levels of streptozotocin induced diabetic rats. This study examined the response of glucose, insulin and glycated hemoglobin which are recognized as characteristic markers in diabetes mellitus following induction with streptozotocin and treatment with the herbs.

*Corresponding author email: docgeogborie@yahoo.com

MATERIALS AND METHODS

Induction of diabetes mellitus was achieved through the intraperitoneal injection of 70mg/kg body weight of streptozotocin dissolved in 1M citrate buffer, p^H 4.5 twice daily for 2 days. A total of 102 rats were used, selected among those that have exceeded glucose threshold (10.0mmol/L) 2 weeks after streptozotocin induction. Samples for fasting plasma glucose, glycated hemoglobin and insulin were collected at the tail vein. Glucose was determined by glucose oxidase method, glycated hemoglobin was determined by high performance liquid chromatography (HPLC-Esi/ms) with UV detection. Insulin was determined by radioimmunoassay. Data was analyzed by two way analysis of variance using SPSS version 6.5

RESULTS

The mean fasting plasma glucose concentration, insulin and HbA1C did not show appreciable change in the control subjects. There were however marked variation in the values of these parameters among the groups following treatment with the extracts. See tables 1,2 and 3 for glucose, HbA1c and insulin respectively.

Metabolic characteristics in control, diabetic rats, diabetic test rats and rats on Daonil following treatment with *T. bengwensis* and *O. gratissimum* are shown.

Table 1. Metabolic characteristics of glucose in control, diabetic rats, diabetic test rates and rats on Daonil following treatment with *T. bengwensis* and *O. gratissimum.*

Day	Controls	Diabetic control rats	10% *T. beng*	10% *O. grat*	DTR on Daonil	DTR on 10% *T. beng* & *O. grat*
0	4.6 ± 0.03^{e}	10.3 ± 0.03^{f}	18.3 ± 0.06^{g}	16.5 ± 0.05^{h}	18.3 ± 0.06^{i}	18.3 ± 0.41^{c}
2	4.7 ± 0.03^{j}	10.7 ± 0.03^{k}	16.3 ± 0.03^{l}	10.0 ± 0.03^{l}	16.1 ± 0.11^{l}	17.0 ± 0.32^{m}
4	4.4 ± 0.03^{n}	11.4 ± 0.00^{q}	14.2 ± 0.05^{s}	15.3 ± 0.03^{t}	14.2 ± 0.11^{u}	15.6 ± 0.33^{v}
6	4.5 ± 0.03^{w}	13.3 ± 0.08^{x}	12.1 ± 0.04^{y}	15.0 ± 0.03^{z}	12.0 ± 0.15^{g}	14.0 ± 0.51^{h}
8	4.7 ± 0.08^{i}	15.5 ± 0.05^{j}	8.8 ± 0.11^{k}	15.0 ± 0.03^{l}	10.0 ± 0.22^{m}	10.7 ± 0.41^{m}
10	5.3 ± 0.07^{k}	16.4 ± 0.11^{l}	8.0 ± 0.08^{m}	14.8 ± 0.08^{n}	9.3 ± 0.41^{v}	8.2 ± 0.25^{s}
12	4.6 ± 0.08^{t}	18.2 ± 0.08^{u}	8.5 ± 0.28^{v}	14.4 ± 0.03^{w}	7.0 ± 0.27^{x}	8.2 ± 0.25^{y}
14	4.6 ± 0.12^{z}	22.2 ± 0.08^{m}	6.3 ± 0.00^{n}	14.0 ± 0.00^{o}	5.2 ± 0.11^{p}	4.4 ± 0.14^{q}
16	4.7 ± 0.08^{r}	24.3 ± 0.93^{s}	5.6 ± 0.03^{t}	13.3 ± 0.03^{s}	4.4 ± 0.27^{v}	3.7 ± 0.15^{u}

Values are mean ± SEM of triplicate determinations. Values on the same row having the same superscript are not significantly different from each other.

Table 2. Metabolic characteristics of glycated haemoglobin in control, diabetic rats, diabetic test rats and rats on Daonil following treatment with *T. bengwensis and O. gratissimum.*

Day	Controls	Diabetic control rats	10% *T. beng*	10% *O.grat*	DTR on Daonil	DTR on 10% *T. beng* & *O. grat*
0	4.3 ± 0.03^{a}	11.6 ± 0.03^{b}	12.5 ± 0.84^{b}	12.5 ± 0.84^{b}	11.8 ± 0.71^{b}	13.3 ± 0.51^{c}
2	4.4 ± 0.06^{d}	11.0 ± 0.75^{e}	12.4 ± 0.02^{e}	12.4 ± 0.02^{e}	11.5 ± 0.82^{e}	12.0 ± 0.31^{e}
4	4.5 ± 0.05^{f}	12.2 ± 0.10^{g}	11.6 ± 0.04^{f}	11.6 ± 0.04^{f}	11.0 ± 0.77^{f}	11.0 ± 0.8^{f}
6	4.3 ± 0.03^{h}	14.3 ± 0.05^{i}	11.5 ± 0.04^{j}	11.5 ± 0.04^{j}	10.1 ± 0.82^{k}	9.3 ± 0.21^{l}
8	4.4 ± 0.04^{m}	15.6 ± 0.03^{n}	11.0 ± 0.03^{o}	11.0 ± 0.03^{o}	10.1 ± 0.82^{p}	8.0 ± 0.41^{q}
10	4.6 ± 0.03^{r}	15.9 ± 0.35^{s}	10.5 ± 0.05^{t}	10.5 ± 0.05^{t}	6.3 ± 0.84^{u}	6.2 ± 0.11^{u}
12	4.4 ± 0.04^{v}	16.3 ± 0.03^{w}	9.4 ± 0.06^{x}	9.4 ± 0.06^{x}	5.0 ± 0.88^{y}	5.1 ± 0.23^{y}
14	4.4 ± 0.03^{z}	17.4 ± 0.02^{h}	9.0 ± 0.04^{z}	9.0 ± 0.04^{m}	4.2 ± 0.86^{n}	4.6 ± 0.22^{n}
16	4.4 ± 0.57^{q}	18.3 ± 0.04^{r}	8.9 ± 0.03^{s}	8.9 ± 0.03^{s}	3.2 ± 0.42^{t}	3.0 ± 0.23^{t}

Values are mean ± SEM of triplicate determinations. Values on the same row having the same superscript are not significantly different from each other.

Table 3. Metabolic characteristics of insulin in control, diabetic rats, diabetic test rats and rats on Daonil following treatment with *T. bengwensis* and *O. gratissimum.*

Day	Controls	Diabetic control rats	10% *T. beng*	10% *O. grat*	DTR on Daonil	DTR on 10% *T. beng* & *O. grat*
0	5.3 ± 0.43^{a}	5.8 ± 0.22^{a}	0.4 ± 0.18^{b}	0.63 ± 0.13^{b}	0.5 ± 0.17^{b}	0.5 ± 0.12^{b}
2	5.4 ± 0.22^{c}	4.2 ± 0.11^{d}	0.6 ± 0.11^{e}	0.6 ± 0.15^{e}	0.8 ± 0.18^{e}	0.5 ± 0.13^{f}
4	4.8 ± 0.42^{g}	4.0 ± 0.12^{h}	0.6 ± 0.11^{r}	0.7 ± 0.16^{i}	0.9 ± 0.21^{i}	0.7 ± 0.12^{i}
6	4.2 ± 0.42^{k}	3.0 ± 0.13^{l}	1.3 ± 0.13^{m}	0.8 ± 0.27^{n}	1.2 ± 0.23^{o}	1.3 ± 0.13^{o}
8	4.8 ± 0.58^{p}	2.6 ± 0.11^{a}	1.5 ± 0.18^{r}	0.9 ± 0.12^{s}	1.6 ± 0.22^{t}	1.7 ± 0.12^{t}
10	4.8 ± 0.22^{u}	1.4 ± 0.12^{v}	2.0 ± 0.22^{w}	1.1 ± 0.11^{x}	2.3 ± 0.24^{y}	1.9 ± 0.34^{z}
12	4.5 ± 0.22^{n}	1.0 ± 0.11^{m}	2.3 ± 0.11^{q}	1.0 ± 0.12^{p}	3.2 ± 0.16^{r}	2.4 ± 0.11^{v}
14	4.8 ± 0.27^{g}	0.5 ± 0.26^{h}	3.0 ± 0.12^{l}	1.2 ± 0.15^{j}	3.5 ± 0.16^{k}	2.6 ± 0.14^{l}
16	4.7 ± 0.22^{d}	0.2 ± 0.17^{e}	3.3 ± 0.25^{f}	1.3 ± 0.16^{g}	3.8 ± 0.13^{h}	$3.6+0.16^{i}$

Values are mean ± SEM of triplicate determinations. Values on the same row having the same superscript are not significantly different from each other.
DTR;Diabetic Test Rat

DISCUSSION

The three parameters, glucose, glycated haemoglobin (HbA1c) and insulin play fundamental roles in the pathogenesis of diabetes depending on their levels in circulation. Glucose toxicity which could be direct or indirect may be as a result of direct interaction with proteins and membranes or indirect as a result of the production of reactive sugars acting on membranes and enhancing diabetic complications. Increased glucose concentration as evidenced in hyperglycemia is known to be a major predisposing factor in production of reactive glucose by-products in particular α-deoxyglycosone and glyoxal which are more than 10,000x more chemically reactive than glucose(Beisswenger and Thormally, 2003). While they could inhibit cell growth, they are also known to produce precursors for activated glycated end product formation as shown earlier by Brownlee (2001). It is now known that animals have mechanisms to control the damage caused by unavoidable non-enzymatic glycation. These protective mechanisms are determined by genetically encoded enzymes which determines the level of glycated agents (Fioretto and Mauer, 1996). In diabetes, these mechanism are important due to increased glycemic stress. Furthermore, these protective mechanisms are impaired by metabolic perturbation produced by the diabetic state. HbA1c provides an accurate and reliable method to assess the glycemic control in patients with diabetes. Measurement of glycated hemoglobin in patients with diabetes is accepted as a standard for assessment of recent glycemic control and is a critical element in clinical practice (Lester, 1989). Hyperglycemia is known to have an adverse effect on tissue insulin sensitivity and insulin secretion that makes it difficult to differentiate between primary and secondary abnormalities. In assessing the relationship between glucose, HbA1c and insulin, we observed a positive correlation in reduction of both glucose and HbA1c in animals treated with the extract. There was however a slight elevation of insulin after treatment. The results suggest a greater amount of insulin production in rats treated with 10% T. *bengwensis* accounting for the reduced glucose and HbA1c in comparison with the normal and diabetic test rats. It thus authenticates the fact that the insulin effect in accelerating peripheral glucose disposal was supported by additional mechanism. The insulin: glucose ratio is occasionally used as an index of insulin sensitivity. This ratio was similar in the groups suggesting an adequate insulin response to the treatment.

Phytochemical analysis of mistletoe as earlier reported by Obatomi (1994) and Allessi (2003) have attributed the hypoglycemic properties to the presence of some constituents notably cholins, lectins, tannins and saponins. A combination of the antinutrient behaviour and activity of secondary plant metabolites must have potentiated these actions. The effects of flavoniods, quercetin and ferrulic acid on pancreatic β-cells which leads to their proliferation and secretion of more insulin have earlier been reported by Kako *et al*. (1997), Okamoto (1970), Mesh and Menon (2004) and Sri-Balasubashini *et al*. (2004) suggesting β-cells recovery as the mechanism by which hyperglycemia caused by streptozotocin reduces glucose. As shown by Gray *et al*. (1997, 1998), aqueous extract of mistletoe enhanced insulin secretion and mimicked the effect of insulin on glucose metabolism. This dual pancreatic and extrapancreatic action would prove to be an important advance on existing therapies used to manage diabetes mellitus.

REFERENCES

Allesi, D., Beger, A., Cepko, C.,Colombet, I.,Costigan, M. and Glunezoglu, A. 2003. Mistletoe. Complementary Alternative Medicine Review.1-4.

Agnanient, H., Arguilet, J., Bessieve, JW. and Menut, C. 2005. Aromatic plant of tropical Central Africa. Part XL – VIL. Chemical and Biological Investigation of essential oil of Occimum species from Gaboni. J. ESS. Oil Res. Abstract.

Beisswenger, T. 2003. Biochem Biophys. Acta, 1637:98-106.

Brucalla, A. and Cerami, A. 1992. Advanced glycosylation: Chemistry, Biology and Implications for Diabetes and aging. Adv. Pharmacol 23:1-34.

Brownlee, M. 2001. Biochemistry and Molecular cell Biology of diabetic complications. Nature. 414:813-820.

Buciarelli, I., Wendt, T. and Qu, W. 2002. Rage Blocade Stabilize established artheriosclerosis in diabetic apolipoprotein E-Null mice. Circulation.106:2827-35.

Didem, DO., Mustata, A., Nilufers, F. and Erdem, Y. 2005. Evaluation of hypoglycemic effect and antioxidant activity of three viscum album subspecies (*European mistletoe*) in streptozotocin-diabetic rats. J. Ethnopharmacol. 98:95-102.

Fioretto, P., Mauer, Brocco E., Vellusi, M., Frigato, F., Muollo, B., Sambataro, M., Abaterusso, C., Baggio, B., Crepaldi, G. and Nosadini, R.1999. Patterns of renal injury in NIDDM Patients with microalbuminuria. Diabetologica. 39:1569-1576 .

Gray, AM. and Flatt, PR. 1997. Pancreatice and extra pancreatic effect of the traditional antidiabetic plant *medica sativa* (lucerne). The British Journal of Nutrition. 78(2):325-334.

Gray, AM. and Flatt, PR. 1998. Antihyperglycemic action of *Encalyptus globules* (Encalyptus) are associated with pancreatic and extra-pancreatic effects in mice. The Journal of Nutrition. 81(3):203-209.

Kako, M., Mirura, T., Nishiyama, Y., Ichimara, M. and Kato, A. 1997. Hypoglycemic activity of some Tritepenoid glycosides J. Nat. prod. 60:604-605.

Lester, E. 1989. The clinical value of glycated hemoglobin and plasma protein. Ann clin Biochem. 26:213-219.

Melpomeni, P. 2003. Glucose, Advanced Glycated En products, and diabetic complications: What is New and What Works. Clinical Diabetes. 21(4):148-149.

Mahesh, T. and Menon, PV. 2004. Quercetin alleviates oxidative stress in streptozotocin Induced diabetic rats. Phythe. Res.18:123-127.

Mohammed, A., Tanko,Y., Okasha, AM., Magazi, RA. and Yaro, AH. 2007. Effects of acqueous extract of *Ocimum gratissimum* on blood glucose levels of stretozotocin induced Wister rats. African Journal of Biotecnology. 6(18):2087-2090.

Naka, Y., Buciarelli, LG. and Went, T. 2004. RAGE Axis. Animal Model and Novel insights into vascular complications of Diabetes Arterioster Vasc Biol. 24:1342-1349.

Obatomi, DK., Bikomo, EO. and Victor, JT. 1994. Antidiabetic properties of the African Mistletoe in streptozotocin-induced Diabetic Rat. J. Ethnopharmacol. 81:231-237.

Odia, OJ. and Wokoma, FS. 1992. Mortality pattern in medical wards of a Nigerian Teaching Hospital. Orient. 4:96-101.

Okamoto, K. 1970. Experimental production of Diabetes in Diabetes mellitus: Theory and Practice. Eds. Ellenberge M. and Rifkin H. Blackinson Publications McGraw-Hill Book Company, New York, USA. 236-243.

Philip, A., Floeye, A. and Jansson, U.1999. Progression of Diabetic Nephropathy from cell studies and animal models. Kidney Blood Press Res. 22:81-97.

Sri-Balasubashini, M., Rukkumani, R., Vismanathan, P. and Menon, PV. 2004. Ferulic acid alleviates lipid peroxidation in Diabetic rats. Phytother Res. 18:310-314.

Standing, SJ. and Taylor, RP. 1992. Glycated an assessment of high capacity liquid chromatography and immunoassay methods. Ann clin Biochem. 29:494:505.

Swanstson-Flatt, SK., Day, C., Baily, CJ. and Flatt, PR. 1989. Evolution of traditional plant treatment for diabetics. Studies in streptozotocin diabetic mice. In Acta Diabetol Lat. 26(1):51-5.

Vlassara, H. 2005. Advanced Glycation in Health and Disease: Role of the Mordern Environment. Annals of the New York Academy of Science. 1043:452-460 doi:10 1196/annals. 1333.05

Wincor, PH. 2003. Heart Disease and Diabetes. Ed. Fisher, M. London. Martin Dienitz Ltd. 121-70.

WHO Expert Committee on Diabetes Mellitus. 1980. Second Report WHO Technical Rep. Serv. 646:1-80.

Received: Jan 7, 2012; Revised: Aug 11, 2012; Accepted: Aug 13, 2012

SENRA Academic Publishers, British Columbia
Vol. 7, No. 1, pp. 2227-2240, Feb 2013
Online ISSN: 1920-3853; Print ISSN: 1715-9997

Canadian Journal of pure&applied sciences

PIEZOELECTROMAGNETIC SH-SAWS: A REVIEW

A A Zakharenko
International Institute of Zakharenko Waves (IIZWs)
660037, Krasnoyarsk-37, 17701, Krasnoyarsk, Russia

ABSTRACT

This review has a purpose to acquaint the experimental and theoretical research society with the recent theoretical achievements in the research field of the shear-horizontal surface acoustic wave (SH-SAW) propagation in the two-phase materials. It is well-known that to know the SH-SAW characteristics can be very important for the sensor applications. Since 2007, several contributors have achieved some progress in the theory when it was theoretically demonstrated that several new SH-SAWs can propagate in novel two-phase materials called the piezoelectromagnetics (PEMs) or the magneto-electro-elastic materials. For the last half-decade, a lot of new SH-SAWs were discovered and it was also found that they can propagate in the cubic PEMs and the transversely isotropic piezoelectromagnetic materials of class 6 *mm*. For the same set of the boundary conditions, it is already known that only one SH-SAW can propagate in the cubic PEMs and at least two SH-SAWs can propagate in the hexagonal PEMs of class 6 *mm*. They can have potential applications in the SH-SAW sensors such as biosensors, physical and chemical sensors. It was also discussed that some theoretical results cannot be true.

PACS: 51.40.+p, 62.65.+k, 68.35.Gy, 68.35.Iv, 68.60.Bs, 74.25.Ld, 74.25.Ha, 75.20.En, 75.80.+q, 81.70.Cv
Keywords: hexagonal (6 *mm*) and cubic piezoelectromagnetics, magnetoelectric effect, new SH-SAWs and electromagnetic wave.

INTRODUCTION

The propagation characteristics of various acoustic waves or electromagnetic waves in new composite materials or structures have received an increasing interest in the scientific society due to their importance in the development and design of novel technical devices based on different acoustic waves and optical phenomena. Up to now, much review work (Bichurin *et al*., 2011; Srinivasan, 2010; Özgür *et al*., 2009; Zhai *et al*., 2008; Eerenstein *et al*., 2006; Fiebig, 2005; Fang *et al*., 2008; Sihvola, 2007; Hill and Spaldin, 2000; Prellier *et al*., 2005; Spaldin and Fiebig, 2005; Khomskii, 2006; Smolenskii and Chupis, 1982; Cheong and Mostovoy, 2007; Ramesh and Spaldin, 2007; Kimura, 2007; Kimura *et al*., 2003; Wang *et al*., 2009; Ramesh, 2009; Delaney *et al*., 2009; Gopinath *et al*., 2012; Fert, 2008a,b; Chappert and Kim, 2008; Bibes and Barthélémy, 2008; Bichurin *et al*., 2006; Fetisov *et al*., 2006; Srinivasan and Fetisov, 2006; Priya *et al*., 2007; Grossinger *et al*., 2008; Ahn *et al*., 2009; Petrov *et al*., 2003; Harshe *et al*., 1993; Chu *et al*., 2007; Nan *et al*., 2008; Schmid, 1994; Ryu *et al*., 2002; Chen *et al*., 2012) has been devoted to the two-phase piezoelectromagnetic (PEM) materials, also called the magneto-electro-elastic materials (MEEMs). The two-phase materials are one class of new (composite) materials that exhibit the co-existence of the piezoelectric phase and the piezomagnetic phase. Also, these materials can naturally show an evidence of sizable magnetoelectric coupling at room temperatures. It is well-known that one of the pioneer works (Astrov, 1960; Astrov, 1961; Rado and Folen, 1961; Van Suchtelen, 1972; Van den Boomgaard *et al*., 1974; Van Run *et al*., 1974; Van den Boomgaard *et al*., 1976; Wood and Austin, 1975) on the magnetoelectric effect relates to 1960 (Astrov, 1960). The relatively large magnetoelectric effect was also revealed in several piezoelectromagnetic monocrystals such as Cr_2O_3 (Fiebig, 2005), $LiCoPO_4$ (Rivera, 1994), and $TbPO_4$ (Rado *et al*., 1984). However, the review papers mentioned above did not focus on some problems of the shear-horizontal surface acoustic wave (SH-SAW) propagation in the two-phase materials.

Surface acoustic waves (Gulyaev, 1998) can be defined by the well-known classification accepted in acoustic textbooks: SAW is the wave propagating parallel to the surface of a solid when both the wavevector and the energy flux vector are parallel to the surface and the wave amplitude is quickly (in terms of wavelength) decreasing into the depth of the solid. It is thought that it is possible to supplement this definition. It is well-known that the SAW wavevector can have an imaginary part. This is a SAW feature. Therefore, it is possible to understand the SAWs by the way that there is an equilibrium exchange between the real and imaginary parts resulting in the SAW propagation. It is worth mentioning that several types of SAWs (Gulyaev, 1998) are known. However, this is not the aim of this review to mention all possible

*Corresponding author email: aazaaz@inbox.ru

SAWs in solids and discuss them. The main purpose of this review is to acquaint the reader with some recently obtained SH-SAW characteristics of the transversely isotropic piezoelectromagnetic (composite) materials of class 6 *mm* (hexagonal symmetry) and the cubic PEMs.

It is surprising that the very important SH-SAW characteristics were discovered in the two-phase materials only within the last half-decade, while the SH-SAW characteristics of the single-phase materials such as the pure piezoelectric and pure piezomagnetics are well-known already during more than forty years. Indeed, the SH-SAWs called the surface Bleustein-Gulyaev (BG) waves (Bleustein, 1968; Gulyaev, 1969) are well-accepted. In the transversely isotropic piezoelectrics there are totally two different surface BG-waves: the faster and slower waves propagating on the electrically open and electrically closed surface, respectively, when the surface is also mechanically free. The values of two BG-waves are naturally situated just below the value of the shear-horizontal bulk acoustic wave (SH-BAW). In the two-phase materials, a set of new SH-SAWs (Melkumyan, 2007; Liu *et al*., 2007; Wang *et al*., 2007; Wei *et al*., 2009; Zakharenko, 2010; Zakharenko, 2011a,b; Zakharenko, 2012a) guided by the free surface were recently discovered. The values of all the new SH-SAWs must be also situated just below the value of the PEM SH-BAW.

Melkumyan (2007) has theoretically treated the SH-SAW propagation problems when the waves are guided by the interface between two identical PEM half-spaces of the hexagonal (6 *mm*) symmetry. He has found as many as twelve new SH-SAWs and demonstrated the explicit forms for the SH-SAW velocities in the cases of different electrical and magnetic boundary conditions. In the same year, Liu, Fang, and Liu (Liu *et al*., 2007) as well as Wang *et al*. (2007) have also represented a new SH-SAW propagating along the free surface of the transversely isotropic piezoelectro-magnetics of class 6 *mm*. They also found their explicit forms for the new SH-SAWs. Wei *et al*. (2009) have considered the SH-SAW propagation in the same configuration treated in theoretical works (Liu *at al*., 2007; Wang *et al*., 2007). Using different boundary conditions, the authors of the work (Wei *et al*., 2009) have stated that they have theoretically discovered three new SH-SAWs for the hexagonal PEM half-space and demonstrated the corresponding explicit forms. To complete the list of the new SH-SAWs guided by the free surface of the hexagonal PEM, the author of the work (Zakharenko, 2010) has additionally discovered seven new SH-SAWs for the cases of different electrical and magnetic boundary conditions and also demonstrated the corresponding explicit forms for the wave velocities. Concerning the cubic PEMs, it was revealed in (Zakharenko, 2011b) that seven new SH-SAWs can also propagate and their velocities are different from those in the case of wave propagation in the hexagonal PEMs. Using works (Melkumyan, 2007; Liu *et al*., 2007; Wang *et al*., 2007; Wei *et al*., 2009; Zakharenko, 2010; Zakharenko, 2011a,b; Zakharenko, 2012a), it is thought that one can find the complete list of the SH-SAWs that can propagate along the PEM free surface. However, it is believed that some obtained solutions cannot be true due to the used theoretical method. This will be discussed below.

It is thought that the modern experimental techniques to generate surface waves in piezoelectromagnetics must exist. Indeed, SH-SAWs can be produced by electromagnetic acoustic transducers (EMATs) (Ribichini *et al*., 2010). The EMATs can offer a series of advantages in comparison with the traditional piezoelectric transducers (Thompson, 1990; Hirao and Ogi, 2003). These experimental tools of the SH-SAW (SH-BAW) propagation investigations in the piezoelectromagnetics can be used already today. Also, an optical method can be used. An improved optical method for measurements of both the phase and group velocities described in (Kolosovskii *et al*., 1998) allows one to measure the phase velocity with accuracy ~ 2 m/s. It is well-known that SH-SAWs can be used in sensors and for the non-destructive testing and evaluation of the piezoelectromagnetics. Indeed, because of the capability of energy conversion between the electrical and magnetic fields, PEMs are suitable for novel device applications such as magnetic field sensors, resonators, electric-field-tunable filters, phase shifters, and delay lines. Most of these technical devices are pertaining to the knowledge of the acoustic wave propagation. So, there has been a growing interest in the wave propagation problems in PEM monocrystals and structures within the last half-decade.

It is expected that piezoelectromagnetic (composite) materials can be widely used for sensor applications instead of piezoelectrics or together with them. It is true that SH-SAW sensors can usually have significantly higher sensitivity than that of the BAW devices. This reason is given by the fact that in the case of SAWs the acoustic energy is concentrated at the surface and hence, any perturbations of the surface can have a larger effect than in BAW devices. The piezoelectric sensors were used already for the last three decades. One of the key aims in the design of the sensor is to create the device sensitive only to one particular quantity (in the optimum case.) This is also true for microsensors. Comparing with the older sensor technologies, microsensors can have several advantages such as small size, low cost, and excellent performance (Sze, 1994; Galipeau *et al*., 1997). Development of newer microsensor technologies was caused by the high demand for low-cost and high-performance sensors to measure physical and chemical environmental parameters. Common physical parameters

include temperature, pressure, acceleration, and stress. Common chemical parameters can be also measured and include humidity, hazardous gases, and biological materials (Sze, 1994; Galipeau *et al*., 1997; Ballantine *et al*., 1997).

Microelectromechanical systems (MEMSs) can consist of microsensors which can have the mechanical and electrical components (or functions) in a single unit. SAW devices can be associated with the earliest type of MEMSs because of the utilization of electrically generated (and electrically detected) mechanical (acoustic) waves. It is thought that the earliest uses of the SAW devices as the microsensors were reported in 1978 to measure such physical property as pressure (Das *et al*., 1978) and in 1979 to measure chemical properties of thin films (Wohltjen, 1979). Temperature, stress, pressure, electric and magnetic fields (Sze, 1994) can be the external physical parameters that can affect the SAW characteristics. Film properties that can affect the SAW device are as follows: mass, density, conductivity, permittivity, stress, and viscoelasticity (Sze, 1994; Ballantine *et al*., 1997). In addition, an important feature of SAW sensors is that they can be easily used in wireless applications. These sensors can be operated in both active and passive modes, of which the second is particularly interesting because the sensor does not need a power source and can be read using a special FM radar system. The active mode example can be demonstrated with the frequency control element in an oscillator (Das *et al*., 1978). Wireless temperature (Bao *et al*., 1987) and stress (Varadan *et al*., 1996) sensors can be the passive mode examples.

The major sensor markets are military, automotive, industrial and environmental, food industry, and medical. The sensors are based on (bio)chemical and physical sensing properties. It is also necessary to mention that the application area of novel SAW sensors can be extended into micro scale. For instance, a recent paper (Yang *et al*., 2011) designs a novel SAW micro position sensor which can be fabricated with MEMS technology, see also work (Adler and Desmares, 1987). The main countries which have well-developed sensor industry are China, Japan, and the United States. For example, one company of either country mentioned above can produce several million sensors per day. Therefore, this is a very big market and number of relevant patents offering novel sensor devices for the market increases. Some recent patents are cited in (Pereira da Cunha, 2007; Zhang, 2011; Malocha, 2009; Cular, 2011; Cular *et al*., 2011). It is expected that the recent theoretical achievements discussed in this review can help the researchers to be familiar with the SH-SAW characteristics leading to the correct interpretation of experimental results. This can result in the development of a set of different SH-SAW devices and correct description in patent applications. This is true because the wave propagation in the two-phase materials has some very important peculiarities discussed below.

SH-SAWs in Hexagonal PEMs (6 *mm*)

This section acquaints the reader with the recent achievements concerning the wave propagation in the transversely isotropic piezoelectromagnetics. First of all, it is necessary to give a short theory for the SH-SAW propagation in the hexagonal piezoelectromagnetics of class 6 *mm*. The configuration is shown in figure 1. The SH-SAW can propagate only on certain cuts and in certain propagation directions. Therefore, the direction of wave propagation is perpendicular to the sixfold symmetry axis and the wave polarization (anti-plane polarization) is along the axis.

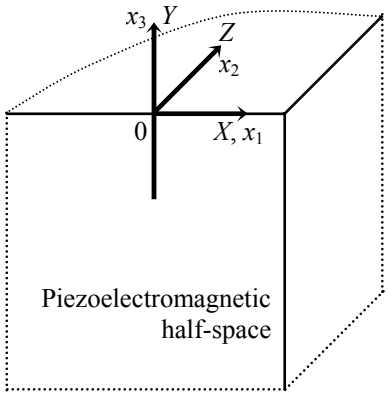

Fig. 1. The rectangular coordinate system for the transversely isotropic (6 *mm*) piezoelectromagnetic half-space. The propagation direction is along the x_1-axis and the wave damps towards the depth of the solid, namely towards the negative values of the x_3-axis. The SH-SAWs are polarized along the x_2-axis directed along the sixfold axis of symmetry. X, Y, and Z are the crystallographic axes.

For a two-phase material, it is possible to use a thermodynamic potential to describe its thermodynamic properties. The thermodynamic process can be naturally considered as adiabatic with the constant entropy. Also, it is thought that it is convenient to choose the following thermodynamic variables written in the tensor forms: stress σ_{ij}, strain η_{ij}, electrical field E_i, electrical induction D_i (electrical displacement), magnetic field H_i, magnetic flux B_i (magnetic displacement) where the indexes i and j run from 1 to 3. In this case, the well-known strain-displacement relation and the quasi-static approximations can be also applied. Using the Gibbs thermodynamic potential, the constitutive relations (Zakharenko, 2010; Zakharenko, 2011b) for a linearly piezoelectromagnetic solid can be then written. As a result, the following material constants can be thermodynamically determined:

the elastic stiffness constant C, piezoelectric constant e, piezomagnetic coefficient h, dielectric permittivity coefficient ε, magnetic permeability coefficient μ, and electromagnetic constant α. It is noted that the constants mentioned above are written already in the treated case (Zakharenko, 2010).

Exploiting the Maxwell equations such as div**B** = 0 and div**D** = 0, the governing mechanical, magnetostatic, and electrostatic equilibriums can be also used in order to write the equations of motion. It is thought that it is convenient to use the tensor form of the coupled equations of motion. Leaving only those equations of motion which relate to the SH-wave propagation, it is possible to determine all the eigenvalues and corresponding eigenvector components for a suitable phase velocity. The very important fact is that in a two-phase material, two different sets of the eigenvector components can exist. This can result in such unique situation when two solutions can be found. Therefore, it is necessary to state that SH-SAWs can propagate guided by the mechanically free surface (normal component of stress σ_{32} = 0) when different electrical and magnetic boundary conditions are also applied at the vacuum-solid interface. The realization of the boundary conditions for the two-phase materials possessing both the piezoelectric and piezomagnetic phases is perfectly described in (Al'shits *et al*., 1992). It is obvious that this peculiarity is present only in the two-phase materials and cannot be revealed in the single-phase materials for the case of the pure SH-wave propagation. Therefore, it is indispensable to review the obtained results of the SH-SAW propagation in the transversely isotropic piezoelectromagnetic materials.

The case of σ_{32} = 0, φ = 0, and ψ = 0

This is the case of the mechanically free, electrically closed (φ = 0) and magnetically open (ψ = 0) surface. This case was theoretically considered in (Melkumyan, 2007; Wei *et al*., 2009, Zakharenko, 2010). In 2007, Melkumyan was the first researcher discovered in his theoretical work (Melkumyan, 2007) that with this set of the boundary conditions, the new SH-SAW can propagate along the interface of two identical PEMs. He also found an explicit form for the new SH-SAW velocity. In 2009, the authors of the paper (Wei *et al*., 2009) have treated the case of wave propagation along the vacuum-PEM interface and received the same formula for the SH-SAW velocity. However, they did not mention work (Melkumyan, 2007) and stated that they have found the new SH-SAW. Also, their explicit form for the velocity was given in a complicated form. It is thought that a convenient explicit form for the new SH-SAW velocity discovered by Melkumyan was obtained in the book (Zakharenko, 2010). This book theoretically studied the wave propagation problems in a transversely isotropic PEM. Also, (Zakharenko, 2010) has stated that the new SH-SAW propagating in a two-phase material can be called the surface Bleustein-Gulyaev-Melkumyan (BGM) wave to have an analogy to the slower surface BG-wave propagating in a single-phase material. Indeed, in a two-phase PEM, two solutions for the SH-SAW velocity can be found. However, for this set of the boundary conditions, two solutions coincide and both can be represented in the same convenient form (Zakharenko, 2010; Zakharenko, 2011a) written below:

$$V_{BGM} = V_{tem}\left[1-\left(\frac{K_{em}^2}{1+K_{em}^2}\right)^2\right]^{1/2} \tag{1}$$

In equation (1), the velocity denoted by V_{tem} is the speed of the shear-horizontal bulk acoustic wave (SH-BAW) coupled with both the electrical potential and the magnetic potential. It reads:

$$V_{tem} = V_{t4}\left(1+K_{em}^2\right)^{1/2} \tag{2}$$

In equations (1) and (2), the very important material parameter denoted by K_{em}^2 is called the coefficient of the magnetoelectromechanical coupling or CMEMC. It couples all the material constants listed above, but the mass density ρ. It has the following form:

$$K_{em}^2 = \frac{\mu e^2 + \varepsilon h^2 - 2\alpha e h}{C\left(\varepsilon\mu - \alpha^2\right)} \tag{3}$$

Also, the velocity V_{t4} in equation (2) is written as follows:

$$V_{t4} = \sqrt{C/\rho} \tag{4}$$

In definition (4), the velocity V_{t4} represents the SH-BAW speed in the case of zero value of the CMEMC. It is obvious that the SH-BAW in equation (4) is uncoupled with both the electric and magnetic potentials and therefore, represents a purely mechanical SH-wave.

Also, the electromagnetic constant α in equation (3) can be very small. As a result, α = 0 can lead to the following natural decoupling between the characteristics of the piezoelectric and piezomagnetic phases:

$$K_{em}^2 = K_e^2 + K_m^2 \tag{5}$$

In expression (5), the CMEMC reduces to the well-known single-phase parameters defined by the following formulae:

$$K_e^2 = \frac{e^2}{\varepsilon C} \tag{6}$$

$$K_m^2 = \frac{h^2}{\mu C} \tag{7}$$

The first material parameter defined by the relation (6) is called the coefficient of the electromechanical coupling (CEMC) and characterizes a purely piezoelectric material. The second parameter defined by the relation (7) is called

the coefficient of the magnetomechanical coupling (CMMC) and represents an important characteristic for a purely piezomagnetic crystal.

It is well-known that in a single-phase piezoelectric material, the corresponding SH-SAW called the slower BG-wave can propagate along the mechanically free and electrically closed surface. In this case, the formula for the surface BG-wave can be written as follows:

$$V_{BGEC} = V_{te}\left[1-\left(\frac{K_e^2}{1+K_e^2}\right)^2\right]^{1/2} \quad (8)$$

In equation (8), the SH-BAW velocity V_{te} propagating in a pure piezoelectrics is defined by the following expression:

$$V_{te} = V_{t4}\left(1+K_e^2\right)^{1/2} \quad (9)$$

where the velocity V_{t4} is defined by relation (4).

It is worth noting that the formula (8) for the slower surface BG-wave can be obtained from equation (1) by setting $h = 0$ and $\alpha = 0$ in the definitions (2) for V_{tem} and (3) for K_{em}^2. It is obvious that formulas (1) and (8) have the same mathematical structure. However, formula (8) cannot reduce to a formula (1) and they represent different cases.

Concerning the other single-phase materials such as the pure piezomagnetics, the slower BG-wave can propagate along the mechanically free and magnetically open surface. The velocity V_{BGMO} of the surface BG-wave can be written in the following form:

$$V_{BGMO} = V_{tm}\left[1-\left(\frac{K_m^2}{1+K_m^2}\right)^2\right]^{1/2} \quad (10)$$

Formula (10) can be also obtained from equation (1) by setting $e = 0$ and $\alpha = 0$ in V_{tem} and K_{em}^2. In equation (10), the SH-BAW velocity V_{tm} propagating in a pure piezomagnetics is written as follows:

$$V_{tm} = V_{t4}\left(1+K_m^2\right)^{1/2} \quad (11)$$

where the expression for the SH-BAW velocity V_{t4} is written in the formula (4).

The case of $\sigma_{32} = 0$, $D = 0$, and $B = 0$

This is the case of the mechanically free, electrically open, and magnetically closed surface. This case of the boundary conditions was also considered in (Melkumyan, 2007; Wei *et al*., 2009; Zakharenko, 2010). These theoretical works soundly demonstrated that no SH-SAW solutions can be found. The single possibility is the propagation of the well-known SH-BAW velocity V_{tem} defined by expression (2).

The case of $\sigma_{32} = 0$, $\varphi = 0$, and $B = 0$

This is the case of the SH-wave propagation guided by the mechanically free, electrically closed, and magnetically closed surface. In this case, an explicit form for the propagation velocity of the new SH-SAW was also obtained in (Melkumyan, 2007). His theoretical work was published in 2007. In two years, Wei, Liu, and Fang (Wei *et al*., 2009) have also obtained some of the theoretical results by Melkumyan. Note that the authors of the paper (Wei *et al*., 2009) have studied the SH-wave propagation along the vacuum-solid interface and did not cite the work (Melkumyan, 2007). As a result, they have written that they have obtained the new results. This is true, but they have only confirmed the previously obtained result (Melkumyan, 2007). Therefore, the new SH-SAW was discovered in (Melkumyan, 2007) for this case of the boundary conditions. (Zakharenko, 2010) has also confirmed the results of works (Melkumyan, 2007; Wei *et al*., 2009), and (Zakharenko, 2012a) has introduced some further theoretical investigations of the new SH-SAW velocity. This new SH-SAW was then called the piezoelectric exchange surface Melkumyan wave or PEESM-wave (Zakharenko, 2012a). It is essential to state that this solution corresponds to the first set of the eigenvector components. However, it doesn't matter which set of two can be called the first. It is noted that the second SH-SAW solution will be also given in this subsection below.

It is thought that the convenient explicit form for the velocity V_{PEESM} is given in (Zakharenko, 2010, Zakharenko, 2012a) and expressed as follows:

$$V_{PEESM} = V_{tem}\left[1-\left(\frac{K_{em}^2-K_m^2}{1+K_{em}^2}\right)^2\right]^{1/2} \quad (12)$$

It is thought that the explicit form in equation (12) can be convenient for understanding of the physical sense. Indeed, the following term $K_{em}^2 - K_m^2$ in equation (12) represents a subtraction of two material parameters. The second parameter called the CMMC (K_m^2) represents the purely piezomagnetic phase defined by the presence of the piezomagnetic effect. The first parameter called the CMEMC (K_{em}^2) couples the piezoelectric and piezomagnetic effects via the magnetoelectric effect. The last can be understood as some exchange between the piezoelectric and piezomagnetic phases. So, $K_{em}^2 - K_m^2$ can represent a purely piezoelectric phase plus some exchange between these two phases. This means that for $\alpha <> 0$ one copes here with both the phases because some exchange remains.

However, the theoretical method used in excellent works (Melkumyan, 2007; Wei *et al*., 2009) was unable to reach the second SH-SAW solution. This is true because the

authors of papers (Melkumyan, 2007; Wei *et al*., 2009) did not illustrate that this problem of the SH-wave propagation in the two-phase materials is more complicated. Also, they did not demonstrate the eigenvalues and eigenvectors. Therefore, they did not find these two different sets of the eigenvector components. Book (Zakharenko, 2010) has demonstrated that the formula (12) can be obtained and it corresponds to one of the possible two sets of the eigenvector components. Using the second set and the electrical and magnetic boundary conditions of this subsection, work (Zakharenko, 2010) has naturally revealed the following explicit form for the velocity of the new SH-SAW which can also propagate in the two-phase materials:

$$V_{new} = V_{tem}\left[1-\left(\frac{\alpha^2}{\varepsilon\mu}\frac{K_{em}^2-K_\alpha^2}{1+K_{em}^2}\right)^2\right]^{1/2} \quad (13)$$

where the non-dimensional value of K_α^2 can be first met in the book (Zakharenko, 2010). This exchange coefficient, K_α^2, couples only two terms in the CMEMC, K_{em}^2, which contain the electromagnetic constant α. It is defined by the following relation:

$$K_\alpha^2 = \frac{\alpha eh}{C\alpha^2} = \frac{eh}{\alpha C} \quad (14)$$

It is clearly seen in relation (14) that the value of K_α^2 can approach infinity as soon as the value of the electromagnetic constant α vanishes. However, this undesirable situation is compensated by the factor of $(\alpha^2/\varepsilon\mu)$ in equation (13). This factor can be also introduced as the relation of two velocities. These velocities can be denoted by V_α and V_{EM} and are defined by the following formulas:

$$V_\alpha^2 = \frac{1}{\alpha^2} \quad (15)$$

$$V_{EM}^2 = \frac{1}{\varepsilon\mu} \quad (16)$$

It is noted that relation (16) represents the well-known speed of the electromagnetic wave propagating in a bulk solid. Usually, the speed V_{EM} is approximately five orders higher than the SH-BAW speed defined by expression (2).

It is crucial to discuss the new result given in the formula (13). It is apparent that as soon as the value of the constant α vanishes, the new SH-SAW velocity in expression (13) reduces to the SH-BAW velocity V_{tem}. This can mean that the propagation of this new SH-SAW is caused by the magnetoelectric effect. It was mentioned above that the electromagnetic constant α is very small. Also, this value is restricted by the following inequality (Özgür *et al*., 2009; Fiebig, 2005; Wei *et al*., 2009):

$$\alpha^2 < \varepsilon\mu \quad (17)$$

As a result, the value of this new SH-SAW can be situated too close to the SH-BAW value due to the small value of α. Also, (Zakharenko, 2012a) discusses the case when the new SH-SAW velocity in expression (13) can also reduce to the SH-BAW velocity V_{tem} for a large value of α where $\alpha > 0$. This peculiarity does not exist for $\alpha < 0$. In equation (13), it is obvious that this can happen as soon as the following condition occurs: $K_{em}^2 - K_\alpha^2 = 0$. Also, the solution (13) exists in the case of the other electrical and magnetic boundary conditions considered in the following subsection.

The case of $\sigma_{32} = 0$, $D = 0$, and $\psi = 0$

This case of the mechanically free, electrically open, and magnetically open surface also results in the possibility of propagation of two SH-SAWs with different velocities. Using the first set of the eigenvector components, book (Zakharenko, 2010) also revealed the explicit form for the new SH-SAW velocity, for which the formula is coinciding with formula (13) corresponding to the second set of the eigenvector components in the case of the previous subsection. This is a unique case when one can find for the different sets of the boundary conditions that the SH-SAW propagation velocity will be the same. Therefore, all the peculiarities discussed in the previous subsection are true in this case. However, the second set of the eigenvector components together with this set of the boundary conditions can reveal the other SH-SAW velocity.

Using the second set of the eigenvector components, work (Zakharenko, 2010) has also confirmed the theoretical result of work (Melkumyan, 2007). In 2009, theoretical work (Wei *et al*., 2009) has also found the result obtained in (Melkumyan, 2007). However, the authors of the work (Wei *et al*., 2009) did not cite the work by Melkumyan and did not compare their results with the previous discoveries. As a result, (Wei *et al*., 2009) stated that the new SH-SAWs were discovered by the authors. (Zakharenko, 2010) has stated that this new SH-SAW was discovered by Melkumyan in his theoretical work (Melkumyan, 2007). (Zakharenko, 2012a) carried out further investigations and the new SH-SAW by Melkumyan was called the piezomagnetic exchange surface Melkumyan wave or PMESM-wave, because this solution is very important similar to the others and it is already necessary to distinguish it from the other new SH-SAWs which can propagate in the PEMs. It is worth noting that works (Melkumyan, 2007; Wei *et al*., 2009) have used the theoretical method with which it is possible to reveal the only single solution of two. It is interesting that the V_{PEESM} in equation (12) corresponds to one set of the eigenvector components, while the V_{PMESM} in equation (18) written below corresponds to the other set. This can mean that this theoretical method used in (Melkumyan,

2007; Wei *et al*., 2009) can confuse these two sets of the eigenvector components. This can give incorrect results in some complicated cases. This will be also discussed in the following subsection. However, this theoretical method revealed three SH-SAWs in the correct forms written in equations (1), (12), and (18).

It is thought that the most convenient explicit form for the PMESM-wave velocity, V_{PMESM}, was given in (Zakharenko, 2010; Zakharenko, 2012a) and it reads as follows:

$$V_{PMESM} = V_{tem}\left[1-\left(\frac{K_{em}^2-K_e^2}{1+K_{em}^2}\right)^2\right]^{1/2} \quad (18)$$

In equation (18), $K_{em}^2 - K_e^2$ can mean that the remaining product of this subtraction can represent the piezomagnetic phase plus some exchange between the piezoelectric and piezomagnetic phases. It is apparent that something from the piezoelectric phase is present in the exchange form. For $\alpha <> 0$, one consequently deals with both the piezoelectric and piezomagnetic phases coupled through the magnetoelectric effect. Also, it is possible that when one has $K_{em}^2 - K_e^2 = 0$ in equation (18), the value of this SH-SAW velocity reduces to the value of the SH-BAW velocity denoted by V_{tem}. Perhaps, this can happen for a relatively large value of α when $\alpha > 0$.

The case of $\sigma_{32} = 0$, $\varphi = \varphi^f$, $D = D^f$, $\psi = \psi^f$, $B = B^f$

It is thought that this is the most complicated case for the theoretical investigations of the SH-wave propagation in the transversely isotropic PEM materials. The acoustic SH-waves are guided by the mechanically free surface. This surface is in contact with the free space, also called a vacuum. Therefore, it is necessary to account the vacuum characteristics. However, it is well-known that the elastic constant C_0 of a vacuum is approximately thirteen orders smaller than that of a solid. Its value is given in (Kiang and Tong, 2010): C_0 = 0.001 Pa. For this reason, the material parameter of a vacuum can be neglected. This is usual for many theoretical descriptions. However, the free space also possesses the electrical and magnetic material constants and they cannot be neglected. The vacuum magnetic permeability constant, μ_0, is defined by $\mu_0 = 4\pi\times10^{-7}$ [H/m] = $12.5663706144\times10^{-7}$ [H/m]. Also, the vacuum dielectric permittivity constant, ε_0, is defined by $\varepsilon_0 = 10^{-7}/(4\pi C_L^2) = 8.854187817\times10^{-12}$ [F/m] where the parameter C_L represents the speed of light in a vacuum and is expressed as follows:

$$C_L^2 = \frac{1}{\varepsilon_0\mu_0} \quad (19)$$

It is possible to use the superscript "f" for a vacuum. It is necessary to account that the electrical potential in a vacuum denoted by φ^f and the magnetic potential denoted by φ^f must vanish far from the surface. Also, the following conditions must be satisfied at the vacuum-solid interface: $\varphi = \varphi^f$, $D = D^f$, $\psi = \psi^f$, $B = B^f$. This means that the electrical characteristics such as the electrical potential and the electric displacement must continue at the interface. The same must be required for the magnetic characteristics such as the magnetic potential and the magnetic flux. These boundary conditions at the vacuum-solid interface lead to the existence of two different SH-SAWs. They correspond to two different sets of the eigenvector components. Zakharenko (2010) provides both complicated solutions written in the original convenient forms. Following work (Zakharenko, 2010), the velocity of the new SH-SAW can be given in the following explicit form:

$$V_{new} = V_{tem}\left[1-\left(\frac{K_{em}^2-K_e^2+\alpha^2C_L^2\frac{\varepsilon_0}{\varepsilon}\left(K_{em}^2-K_\alpha^2\right)}{\left(1+K_{em}^2\right)\left(1+\frac{\mu}{\mu_0}\right)}\right)^2\right]^{1/2} \quad (20)$$

In equation (20), the term $K_{em}^2 - K_e^2$ represents a subtraction of the purely piezoelectric phase from the coupled piezoelectromagnetic phase. Also, the following factor $\alpha^2C_L^2(\varepsilon_0/\varepsilon)$ demonsofates the dependence on the speed of light in a vacuum. It is obvious that this factor can be very small for a small value of α and large value of ε. They are the material parameters of the piezoelectromagnetics. It is necessary to mention that the value of α is restricted by inequality (17). This means that the value of the velocity V_α in equation (15) must be always larger than that of the velocity V_{EM} of the bulk electromagnetic wave defined by the formula (16). Therefore, it is expected that $\alpha^2C_L^2(\varepsilon_0/\varepsilon)$ < 1 or even $\alpha^2C_L^2(\varepsilon_0/\varepsilon)$ << 1. Also, the value of K_α^2 decreases when the value of α increases. It is worth noting that the value of α can have a positive or negative sign depending on the direction of the applied magnetic field. In general, the value of the electromagnetic constant α is very small. So, it is also possible to write the velocity of the new SH-SAW for the case of $\alpha = 0$ in the following simplified form:

$$V = V_{tem0}\left[1-\left(\frac{K_m^2}{\left(1+K_e^2+K_m^2\right)\left(1+\mu/\mu_0\right)}\right)^2\right]^{1/2} \quad (21)$$

where the SH-BAW velocity V_{tem0} is defined by the following expression:

$$V_{tem0} = V_{t4}\left(1+K_e^2+K_m^2\right)^{1/2} \quad (22)$$

In expression (22), the SH-BAW velocity V_{t4} is defined by formula (4). As soon as the piezoelectric constant e equals to zero in equations (21) and (22), equation (21) reduces to the velocity V_{BGpm} of the faster surface BG wave (Bleustein, 1968; Gulyaev, 1969) propagating in a pure piezomagnetics:

$$V_{BGpm} = V_{tm}\left[1-\left(\frac{K_m^2}{\left(1+K_m^2\right)\left(1+\mu/\mu_0\right)}\right)^2\right]^{1/2} \tag{23}$$

In equation (23), the SH-BAW velocity V_{tm} is defined by expression (11). It is well-known that the value of the velocity V_{BGpm} is situated slightly below the value of the velocity V_{tm}. In the case of $h = 0$ and $\alpha = 0$, equation (20) also reduces to the SH-BAW velocity V_{tm} defined by expression (11) which is the wave characteristic for a pure piezomagnetics. Indeed, it is natural that a piezoelectromagnetics can possess incorporative properties of the piezoelectric phase and the piezomagnetic phase.

For the other set of the eigenvector components, the explicit form for the velocity of the other new SH-SAW, which can propagate along the surface, was also introduced in the book (Zakharenko, 2010). It is thought that (Zakharenko, 2010, 2011a) provide the convenient form of the solution. The velocity of the new SH-SAW can be then written in the following form (Zakharenko, 2010; Zakharenko, 2011a):

$$V_{new} = V_{tem}\left[1-\left(\frac{K_{em}^2-K_m^2+\alpha^2C_L^2\frac{\mu_0}{\mu}\left(K_{em}^2-K_\alpha^2\right)}{\left(1+K_{em}^2\right)\left(1+\frac{\varepsilon}{\varepsilon_0}\right)}\right)^2\right]^{1/2} \tag{24}$$

It is thought that the term $K_{em}^2 - K_m^2$ in equation (24) can be interpreted as a subtraction of the purely piezomagnetic phase from the coupled piezoelectromagnetic phase. Also, the following factor $\alpha^2 C_L^2(\mu_0/\mu)$ can be very small due to a small value of α. However, this is not always true. For instance, when $\alpha^2 \to \varepsilon\mu$ occurs and $\varepsilon\mu$ is quite large due to $\mu/\mu_0 \sim 100$ and $\varepsilon/\varepsilon_0 \sim 100$, it is possible that the following factor $\alpha^2 C_L^2(\mu_0/\mu)$ can approach such large number as 100. On the other hand, large values of μ and ε can result in a very small value of the CMEMC, K_{em}^2. As a result, the value under the square root in expression (24) can be larger than zero. This means that this new SH-SAW can propagate in such PEM materials.

Also, in the case of a negligibly small value of the electromagnetic constant α, it is possible to write the velocity of this new SH-SAW in the following simplified form:

$$V = V_{tem0}\left[1-\left(\frac{K_e^2}{\left(1+K_e^2+K_m^2\right)\left(1+\varepsilon/\varepsilon_0\right)}\right)^2\right]^{1/2} \tag{25}$$

where the SH-BAW velocity V_{tem0} is defined by expression (22). For the zero value of the piezomagnetic coefficient h, formula (25) also reduces to the well-known velocity V_{BGpe} of the faster surface BG wave (Bleustein, 1968; Gulyaev, 1969) propagating in a pure piezoelectrics:

$$V_{BGpe} = V_{te}\left[1-\left(\frac{K_e^2}{\left(1+K_e^2\right)\left(1+\varepsilon/\varepsilon_0\right)}\right)^2\right]^{1/2} \tag{26}$$

It is worth noticing that the value of the velocity V_{BGpe} is situated slightly below the value of the velocity V_{te}. Also, one can verify that with $e = 0$ and $\alpha = 0$, equation (24) reduces to the SH-BAW velocity V_{te} defined by expression (9) which is the wave characteristic for a pure piezoelectrics.

It was demonstrated in this subsection that two solutions can always exist in this set of the electrical and magnetic boundary conditions. They were obtained following the theoretical method used in the book (Zakharenko, 2010) and they correspond to two different sets of the eigenvector components. However, the reader can find works (Liu *et al*., 2007; Wang *et al*., 2007) in which the authors have used the other theoretical method. Unfortunately, this method can give only single solution for the velocity of the new SH-SAW and this solution differs from those written above in formulae (20) and (24). The authors of theoretical works (Liu *et al*., 2007; Wang *et al*., 2007) have found the following formula in the case:

$$V_{new} = V_{tem}\left[1-\left(\frac{\frac{\varepsilon_0}{\varepsilon}\left(K_{em}^2-K_m^2\right)+\frac{\mu_0}{\mu}\left(K_{em}^2-K_e^2\right)+\frac{\varepsilon_0\mu_0}{\varepsilon\mu}K_{em}^2}{\left(1+K_{em}^2\right)\left(1-\delta+\frac{\varepsilon_0\mu_0}{\varepsilon\mu}+\frac{\varepsilon_0}{\varepsilon}+\frac{\mu_0}{\mu}\right)}\right)^2\right]^{1/2} \tag{27}$$

In expression (27), one can find that work (Wang *at al*., 2007) provides $\delta = 0$, but work (Liu *at al*., 2007) offers $\delta = \alpha^2/(\varepsilon\mu)$. It is noted that the explicit form for the new SH-SAW velocity defined by expression (27) is also given in a convenient form to compare with the results of Zakharenko (2010) given in the formulae (20) and (24). The reader can also find that (Liu *et al*., 2007; Wang *et al*., 2007) provide the new SH-SAW velocity expressed by convenient explicit form (27) in very complicated forms.

The work of Liu *et al*. (2007 and Wang *et al*. (2007) have also stated that the expression (27) represents a new result. This means that they have found the new SH-SAW

propagating in a transversely isotropic piezoelectromagnetic material. To obtain a formula (27), they probably used the theoretical method which can mix both the different sets of the eigenvector components. As a result, they have reached only single solution (27) instead of possible two solutions (20) and (24) for the two-phase materials. It is thought that their method is somewhat inaccurate because the two sets should be separately used. Therefore, the author of this review cannot agree with the result demonstrated in formula (27) by the authors of papers Liu *et al*. (2007) and Wang *et al*. (2007). Indeed, to obtain an SH-SAW velocity is not easy in the case of the two-phase materials.

It is also possible to discuss the result given in expression (27). For simplicity, it is necessary to use $\delta = 0$ (Wang *et al*., 2007). For $\alpha = 0$, expression (27) can be rewritten in the following simplified form:

$$V = V_{tem0}\left[1-\left(\frac{K_e^2}{\left(1+K_e^2+K_m^2\right)\left(1+\varepsilon/\varepsilon_0\right)}+\frac{K_m^2}{\left(1+K_e^2+K_m^2\right)\left(1+\mu/\mu_0\right)}\right)^2\right]^{1/2} \quad (28)$$

The explicit form in equation (28) is convenient for comparison with those in equations (21) and (25). It is flagrant that for $e = 0$, the SH-SAW velocity in expression (28) reduces to the velocity V_{BGpm} of the faster BG-wave (23) in a pure piezomagnetics. For $h = 0$, the velocity in expression (28) also reduces to the velocity V_{BGpe} of the faster BG-wave (26) in a pure piezoelectrics. Also, two fractions with the following factors $(1 + \varepsilon/\varepsilon_0)$ and $(1 + \mu/\mu_0)$ in the denominators are present under the square root in expression (28). However, only one corresponding fraction of two is present in the expression (21) or (25). Comparing with these two expressions, formula (28) looks like it can give a value of the SH-SAW velocity situated not closer to the value of the SH-BAW velocity, V_{tem0}. It is expected that this fact can also occur when the expression (27) is compared with expressions (20) and (24).

SH-SAWs in Cubic PEMs

It is thought that SH-SAWs can also propagate in cubic piezoelectromagnetics. There is currently the single work concerning the wave propagation in the cubic PEMs (Zakharenko, 2011b). The theory of the wave propagation in the cubic PEMs is significantly more complicated than that for the hexagonal PEMs. In the case of the cubic PEMs, two sets of the eigenvector components also exist. However, they always result in the single solution because the two solutions coincide. This is unlike the transversely isotropic PEMs and can be useful for experimentalists when the presence of the second solution is not desirable. Also, experimental evidence of any SH-SAW propagation in the transversely isotropic PEMs or cubic PEMs is still not available. Probably, this is due to the fact that the SH-SAW propagation in the hexagonal PEMs was discovered only half-decade ago.

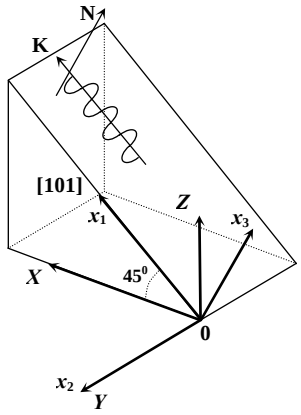

Fig. 2. The SH-SAW propagation along direction for the cubic piezoelectromagnetics. **K** is the wavevector in the direction of wave propagation and **N** is the vector of the surface normal. *X*, *Y*, and *Z* are the crystallographic axes.

Figure 2 shows the configuration for the wave propagation in the cubic PEM. The SH-SAW can propagate in the direction or relevant. The wave polarization is perpendicular to both the propagation direction and the surface normal. All the theoretical procedures sketchy described in the previous section are also used here. The forms of the eigenvalues and the eigenvectors can be very complicated. The eigenvalues are purely imaginary for $K_{em}^2 < 1/3$ and can be complex for $K_{em}^2 > 1/3$. In a cubic PEM with $K_{em}^2 < 1/3$, SH-SAW solutions can be found just below the value of the SH-BAW velocity V_{tem} defined by expression (2). However, SH-SAW solutions for the cubic PEM with $K_{em}^2 > 1/3$ are situated just below the value of some velocity V_K where $V_K < V_{tem}$. As a result, all the cubic PEMs can be divided into two groups: the first group is for the cubic PEMs with $K_{em}^2 < 1/3$ and the second is for those with $K_{em}^2 > 1/3$. For both the groups, the SH-SAW velocities cannot be represented in explicit forms. This is unlike the transversely isotropic PEMs. However, Zakharenko, (2011b) has found that the surface BGM can also propagate in the cubic PEMs for the corresponding set of the boundary conditions. It is thought that it is useful to start the review of the cubic PEMs with this case.

The case of $\sigma_{32} = 0$, $\varphi = 0$, and $\psi = 0$

For the mechanically free, electrically closed ($\varphi = 0$) and magnetically open ($\psi = 0$) surface of the cubic PEM, work (Zakharenko, 2011b) has revealed that the surface BGM-wave is solidly found when either of two sets of the eigenvector components is used. It is thought that the explicit form for the surface BGM-wave velocity defined

by expression (1) can be rewritten in the following simplified form:

$$V_{BGM} = V_{tem}\left[\frac{1+2K_{em}^2}{\left(1+K_{em}^2\right)^2}\right]^{1/2} \tag{29}$$

It is thought that this form is more convenient when a digital calculator is used for evaluation of the value of the surface BGM-wave velocity. It is thought that this is the single case when the SH-SAW solution can be represented in an explicit form. It is possible to review the other boundary conditions for the problem of SH-wave propagation in the cubic PEMs.

The case of $\sigma_{32} = 0$, $D = 0$, and $B = 0$

Zakharenko (2011b) has also theoretically verified a possibility of propagation of SH-SAWs guided by the mechanically free, electrically open, and magnetically closed surface. It was found that for both the sets of the eigenvector components, the phase velocity solution denoted by V_K can be revealed. This solution corresponds to two equal eigenvalues which naturally give equal eigenvectors. Therefore, the value of the determinant of the boundary conditions can equal to zero as soon as the equal eigenvalues are utilized. The details can be found in Zakharenko (2011b).

The velocity V_K is defined by the following explicit form:

$$V_K = a_K V_{t4} \tag{30}$$

where

$$a_K = 2\sqrt{K_{em}\left(1+K_{em}^2\right)^{1/2} - K_{em}^2} \tag{31}$$

In equation (30), the SH-BAW velocity V_{t4} is defined by the expression (4).

It is necessary to acquaint the reader with the fact that this solution is always present and does not depend on the applied boundary conditions. This is similar to the solution corresponding to the SH-BAW velocity V_{tem}. It is also expected that the SH-wave propagating with the velocity V_K can be generated in the cubic PEM. Concerning experimental measurements of SAWs, it is also thought that some elements of crystals symmetry (screw axis or glide reflection) must be broken near the surface. Thus, to experimentally distinguish different types of SAWs can be very complicated and unclear.

Other Sets of the Boundary Conditions

For the other sets of the boundary conditions, two SH-SAW solutions (Zakharenko, 2011b) are also found. However, each pair of the solutions gives the same value of the new SH-SAW velocity. This can mean that in each case only single new SH-SAW can propagate. This is unlike the problem of the SH-wave propagation in the transversely isotropic PEMs reviewed in the previous section. For the cubic piezoelectromagnetics, the value of the velocity V_{new} can be written in the following common form:

$$V_{new} = V_{tem}\sqrt{1-b^2} \tag{32}$$

where the parameter b is defined below in expression (33). Zakharenko (2011b) has also demonstrated the following compact form for the parameter b:

$$b = n_3^{(3)} n_3^{(5)} = -\frac{\mathrm{j}B\left[n_3^{(5)}\left(m^{(2)} - \gamma_K^2\right) - n_3^{(3)}\left(m^{(3)} - \gamma_K^2\right)\right]}{A\left(m^{(3)} - m^{(2)}\right)} \tag{33}$$

where j is the imaginary unity, $\mathrm{j} = (-1)^{1/2}$.

Equations (32) and (33) represent recursive formulae for the determination of the suitable phase velocity for each case of the electrical and magnetic boundary conditions. In equation (33), the material parameters A and B represent complicated functions on all the material constants and their explicit forms can be found in Zakharenko (2011b). Also, the eigenvalues in equation (33) are defined by the following formula:

$$n_3^{(3,5)} = -\mathrm{j}\sqrt{1-m^{(2,3)}} \tag{34}$$

where

$$m^{(2,3)} = \frac{B_t \pm \sqrt{B_t^2 - 16K_{em}^2\left(1+K_{em}^2\right)}}{2\left(1+K_{em}^2\right)} \tag{35}$$

$$B_t = \left(1+K_{em}^2\right)\left(\frac{V_{ph}}{V_{tem}}\right)^2 + 4K_{em}^2 \tag{36}$$

In equation (33), the non-dimensional parameter γ_K, which represents the normalized phase velocity V_{ph} of the new SH-SAW, is defined as follows:

$$\gamma_K = \frac{V_{ph}}{V_{t4}} \tag{37}$$

It is thought that it is unnecessary to give the complicated theory for each case of the boundary conditions. The reader can find the theory in Zakharenko (2011b). This all mentioned above relates to the propagation problems of different SH-SAWs for the usual cases when the values of the SH-SAW velocities are situated just below the value of the SH-BAW velocity V_{tem}. However, in cubic piezoelectromagnetics there is the case when the value of the SH-wave velocity can be slightly larger than that of V_{tem}. This case is discussed in the following subsection.

Surface Electromagnetic Wave or SH-SAW

In this problem of wave propagation, the SH-wave also propagates in the direction in the cubic piezoelectromagnetics. In this case, one of three suitable

eigenvalues is real, but not imaginary or complex. Fortunately, it does not participate in the complete displacements. For the mechanically free surface, several combinations of the following electrical and magnetic boundary conditions can be used: electrically closed, electrically open, magnetically closed, magnetically open surface. For some boundary conditions, this new SH-wave can represent a purely electromagnetic wave and some sets of the electrical and magnetic boundary conditions promise that the new SH-wave can represent really new SH-SAW (Zakharenko, 2012b). This new SH-SAW can propagate with the speed slightly larger than that of the SH-BAW V_{tem}. The existence conditions for the new SH-wave can be very complicated and depend on all the material parameters. It is also expected that these theoretical results can be applied to some problems the SH-wave propagation in the left-handed metamaterials because three-dimensional metamaterials Chen *et al*. (2011) can be created. The recent review of the sensor applications of metamaterial can be found in Chen *et al*. (2012).

Following the theoretical work (Zakharenko, 2012b), the solution for the velocity of the new SH-wave is given in the following explicit form:

$$V_{new} = V_{t4}\sqrt{2} = V_{tem}\sqrt{\frac{2}{1+K_{em}^2}} \tag{38}$$

where V_{tem} and V_{t4} are the speeds of the SH-BAWs coupled and uncoupled with both the electrical and magnetic potentials, respectively. In equation (38), it is clearly seen that $V_{tem} < V_{new}$ for $K_{em}^2 < 1$. This fact allows one to state that the velocity of the new SH-wave is positioned in the velocity range where leaky acoustic SH-waves can exist.

For the electrical and magnetic boundary conditions such as $\varphi = 0$ and $\psi = 0$ as well as $D = 0$ and $B = 0$, the new SH-wave can represent a purely electromagnetic wave propagating with the slow speed defined by expression (38). Indeed, the new SH-wave can be purely electromagnetic due to the existence condition such as $h\varepsilon = e\alpha$ (Zakharenko, 2012b) resulting in zero value of the mechanical displacement (eigenvector component): $U \rightarrow (h\varepsilon - e\alpha)K_{em}^2 = 0$ (Zakharenko, 2012b). It was also discussed in Zakharenko (2012b) that this situation can also mean that this slow wave can be truly acoustic, and the piezoelectromagnetic properties can compensate the mechanical ones resulting in zero value of the mechanical displacement during the wave propagation. Indeed, this slow electromagnetic SH-wave propagates with the speed slightly above the V_{tem}. It is well-known that acoustic wave speeds including V_{tem} and V_{new} in equation (38) are approximately five orders slower than the speed of the electromagnetic wave propagating in a bulk solid defined by the relation (16). This extreme slowness of the new SH-wave exemplifies that some connection with the mechanical displacement is conserved. Therefore, the new SH-wave can be called the surface acoustic magnetoelectric wave (Zakharenko, 2012b). This can illuminate that this SH-wave relates to an acoustic branch, but not an optic one.

This new electromagnetic wave can relate to the surface acoustic-phonon polaritons (SAPPs) and it is necessary to distinguish them from the surface optic-phonon polaritons (SOPPs.) The SOPPs (Huber *et al*., 2008) are well-known because SOPPs on crystal substrates have applications in microscopy, biosensing, and photonics. The SOPPs are defined as electromagnetic surface modes formed by the strong coupling of light and optical phonons in polar crystals. They are generally excited using IR or THz radiation. Generation and control of the SOPPs are essential for realizing novel applications in microscopy, data storage, thermal emission, or in the field of metamaterials. However, a comparatively little attention is still given to the SOPPs. They have certain advantages including their ability to be generated in a wide spectral range, from IR to THz wavelengths at the surface of a large variety of semiconductors, insulators, and ferroelectrics (Huber *et al*., 2008). Minin and Minin (2010) have also mentioned that surface electromagnetic effects can enhance the efficiency of numerous physical and chemical processes (Schatz and van Duyne, 2002), as these effects can lead to an increase of the electromagnetic fields at the surface. This can give rise to an improved experimental sensitivity.

CONCLUSION

This review work has acquainted the reader with the recent achievements in the theory of SH-SAW propagation in the two-phase cubic and transversely isotropic (class 6 *mm*) piezoelectromagnetic materials. The reader can find in this review that using the same set of the electrical and magnetic boundary conditions, two SH-SAWs can propagate in the transversely isotropic PEM materials and only single SH-SAW can propagate in the cubic PEMs. To know this fact can be useful for the case when the presence of the second SH-SAW is not desirable, or vice versa, i.e. this fact can help in design of novel technical devices. Also, in the cubic PEMs, the other solutions can exist. They were also discussed. For instance, it was discussed the case when the SH-wave solution can represent a purely electromagnetic wave or true SH-SAW. Finally, it is necessary to state that this review relates to the wave propagation guide by the PEM free surface. However, the reader can find book (Zakharenko, 2012c) which discusses the propagation problems of new interfacial SH-waves when two dissimilar PEMs are used.

REFERENCES

Adler, R. and Desmares, PJ. 1987. An economical touch panel using SAW absorption. The IEEE Transactions on Ultrasonics, Ferroelectrics, and Frequency Control. 34(2):195-201.

Ahn, CW., Maurya, D., Park, CS., Nahm, S. and Priya, S. 2009. A generalized rule for large piezoelectric response in perovskite oxide ceramics and its application for design of lead-free compositions. Journal of Applied Physics. 105(11):114108. pp6.

Al'shits, VI., Darinskii, AN. and Lothe, J. 1992. On the existence of surface waves in half-infinite anisotropic elastic media with piezoelectric and piezomagnetic properties. Wave Motion. 16(3):265-283.

Astrov, DN. 1960. The magnetoelectric effect in antiferromagnets. Soviet Physics – Journal of Experimental and Theoretical Physics (JETP). 11:708-709 [1960. Zhurnal Experientalnoi i Teoreticheskoi Fiziki (USSR). 38:984–985].

Astrov, DN. 1961. Magnetoelectric effect in antiferromagnetic Cr_2O_3. Soviet Physics – Journal of Experimental and Theoretical Physics (JETP). 13(4):729-733.

Ballantine, DS., White, RM., Martin, SJ., Ricco, AJ., Zellers, ET., Frye, GC. and Wohltjen, H. 1997. Acoustic Wave Sensors. Academic Press, San Diego, CA, USA.

Bao, XQ., Burkhard, W., Varadan, VV. and Varadan, VK. 1987. SAW temperature sensor and remote reading system. Proceedings of the IEEE Ultrasonics Symposium. Denver, CO, Piscataway, NJ, USA. 583-585.

Bibes, M. and Barthélémy, A. 2008. Multiferroics: Towards a magnetoelectric memory. Nature Materials. 7:425-426.

Bichurin, MI., Petrov, VM., Filippov, DA., Srinivasan, G. and Nan, SV. 2006. Magnetoelectric materials. Academia Estestvoznaniya Publishers, Moscow.

Bichurin, MI., Petrov, VM., Zakharov, A., Kovalenko, D., Yang, SC., Maurya, D., Bedekar, V. and Priya, SH. 2011. Magnetoelectric interactions in lead-based and lead-free composites. Materials. 2011(4):651-702.

Bleustein, JL. 1968. A new surface wave in piezoelectric materials. Applied Physics Letters. 13(12):412-413.

Chappert, C. and Kim, JV. 2008. Metal spintronics: Electronics free of charge. Nature Physics. 4:837-838.

Chen, T., Li, S. and Sun, H. 2012. Metamaterials application in sensing. MDPI Sensors. 12(3):2742-2765.

Chen, WT., Chen, ChJ., Wu, PCh., Sun, Sh., Zhou, L., Guo, G-Y., Hsiao, ChT., Yang, K-Y., Zheludev, NI. and Tsai, DP. 2011. Optical magnetic response in three-dimensional metamaterial of upright plasmonic metamolecules. Optics Express. 19(13):12837-12842.

Cheong, S-W. and Mostovoy, M. 2007. Multiferroics: A magnetic twist for ferroelectricity. Nature Materials. 6:13-20.

Chu, YH., Martin, LW., Holcomb, MB. and Ramesh, R. 2007. Controlling magnetism with multiferroics. Materials Today. 10(10):16-23.

Cular, S. 2011. Integrated thickness shear mode (TSM) sensor and surface acoustic wave (SAW) device for simultaneous sensing and removal of analytes. September 13, US Patent No. 8018121.

Cular, S., Bhethanabotla, VR. and Branch, DW. 2011. Simultaneous sample manipulation and sensing using surface acoustic waves. February 1, US Patent No. 7878063.

Das, P., Lanzl, C. and Barone, D. 1978. A surface acoustic wave transmitting hydrophone. Proceedings of the IEEE Ultrasonics Symposium. Cherry Hill, NJ, USA. 458-463.

Delaney, KT., Mostovoy, M. and Spaldin, NA. 2009. Superexchange-driven magnetoelectricity in magnetic vertices. Physical Review Letters. 102:157203. pp4.

Eerenstein, W., Mathur, ND. and Scott, JF. 2006. Multiferroic and magnetoelectric materials. Nature. 442:759-765.

Fang, D., Wan, Yo-P., Feng, X. and Soh, AK. 2008. Deformation and fracture of functional ferromagnetic. ASME Applied Mechanics Review. 61(2):020803. pp23.

Fert, A. 2008[a]. Origin, development, and future of spintronics. Nobel lectures. Reviews of Modern Physics. 80(4):1517-1530.

Fert, A. 2008[b]. Origin, development, and future of spintronics. Nobel lectures. Physics – Uspekhi. 51(12):1336-1348 [2008. Uspekhi Phizicheskikh Nauk (Moscow). 178(12):1336-1348].

Fetisov, YK., Bush, AA., Kamentsev, KE., Ostashchenko, AY. and Srinivasan, G. 2006. Ferrite-piezoelectric multilayers for magnetic field sensors. The IEEE Sensor Journal. 6(4):935-938.

Fiebig, M. 2005. Revival of the magnetoelectric effect. Journal of Physics D: Applied Physics. 38(8):R123–R152.

Galipeau, DW., Story, PR., Vetelino, KA. and Mileham, RD. 1997. Surface acoustic wave microsensors and applications. Smart Materials and Structures. 6:658-667.

Gopinath, SCB., Awazu, K. and Fujimaki, M. 2012. Waveguide-mode sensors as aptasensors. MDPI Sensors. 12:2136-2151.

Grossinger, R., Duong, GV. and Sato-Turtelli, R. 2008. The physics of magnetoelectric composites. Journal of Magnetism and Magnetic Materials. 320:1972-1977.

Gulyaev, YuV. 1969. Electroacoustic surface waves in solids. Soviet Physics Journal of Experimental and Theoretical Physics Letters. 9:37-38.

Gulyaev, YuV. 1998. Review of shear surface acoustic waves in solids. IEEE Transactions on Ultrasonics, Ferroelectrics, and Frequency Control. 45(4):935-938.

Harshe, G., Dougherty, JP. and Newnham, RE. 1993. Theoretical modelling of 3-0/0-3 magnetoelectric composites. International Journal of Applied Electromagnetics in Materials. 4(1):161-171.

Hill, NA. and Spaldin, NA. 2000. Why are there so few magnetoelectric materials? Journal of Physical Chemistry B. 104:6697-6709.

Hirao, M. and Ogi, H. 2003. EMATs for science and industry: Non-contacting ultrasonic measurements. Kluwer Academic, Boston, MA, USA.

Huber, AJ., Deutsch, B., Novotny, L. and Hillenbrand, R. 2008. Focusing on surface phonon polaritons. Applied Physics Letters. 92(20):203104. pp3.

Khomskii, DI. 2006. Multiferroics: Different ways to combine magnetism and ferroelectricity. Journal of Magnetism and Magnetic Materials. 306(1):1-8.

Kiang, J. and Tong, L. 2010. Nonlinear magneto-mechanical finite element analysis of Ni–Mn–Ga single crystals. Smart Materials and Structures. 19(1):015017.pp17.

Kimura, T. 2007. Spiral magnets as magnetoelectrics. Annual Review of Materials Research. 37:387-413.

Kimura, T., Goto, T., Shintani, H., Ishizaka, K., Arima, T. and Tokura, Y. 2003. Magnetic control of ferroelectric polarization. Nature. 426:55-58.

Kolosovskii, EA., Tsarev, AV. and Yakovkin, IB. 1998. Improved procedure for measuring SAW velocity in anisotropic structures. Acoustical Physics Reports (Moscow). 44:793-800.

Liu, JX., Fang, DN. and Liu, XL. 2007. A shear horizontal surface wave in magnetoelectric materials. IEEE Transactions on Ultrasonics, Ferroelectrics, and Frequency Control. 54(7):1287-1289.

Malocha, DC. 2009. Multi-transducer/antenna surface acoustic wave device sensor and tag. November 24, US Patent No. 7623037.

Melkumyan, A. 2007. Twelve shear surface waves guided by clamped/free boundaries in magneto-electro-elastic materials. International Journal of Solids and Structures. 44(10):3594-3599.

Minin, I. and Minin, O. 2010. 3D diffractive focusing THz of in-plane surface plasmon polariton waves. Journal of Electromagnetic Analysis & Applications. 2:116-119.

Nan, CW., Bichurin, MI., Dong, SX., Viehland, D. and Srinivasan, G. 2008. Multiferroic magnetoelectric composites: Historical perspective, status, and future directions. Journal of Applied Physics. 103(3):031101.

Özgür, Ü., Alivov, Ya. and Morkoç, H. 2009. Microwave ferrites, part 2: Passive components and electrical tuning. Journal of Materials Science: Materials in Electronics. 20(10):911-952.

Pereira da Cunha, M. 2007. Surface acoustic wave devices for high temperature applications. October 23, US Patent No. 7285894.

Petrov, VM., Bichurin, MI., Laletin, VM., Paddubnaya, N. and Srinivasan, G. 2003. Modeling of magnetoelectric effects in ferromagnetic/piezoelectric bulk composites. In: Proceedings of the 5th International Conference on Magnetoelectric Interaction Phenomena in Crystals. MEIPIC-5, 21–24 September, Sudak, Ukraine, arXiv:cond-mat/0401645.

Prellier, W., Singh, MP. and Murugavel, P. 2005. The single-phase multiferroic oxides – from bulk to thin film. Journal of Physics: Condensed Matter. 17(30):R803-R832.

Priya, S., Islam, RA., Dong, SX. and Viehland, D. 2007. Recent advancements in magnetoelectric particulate and laminate composites. Journal of Electroceramics. 19:147-164.

Rado, GT., Ferrari, JM. and Maisch, WG. 1984. Magnetoelectric susceptibility and magnetic symmetry of magnetoelectrically annealed $TbPO_4$. Physical Review B. 29(7):4041-4048.

Rado, GT. and Folen, VJ. 1961. Observation of the magnetically induced magnetoelectric effect and evidence for antiferromagnetic domains. Physical Review Letters. 7(8):310-311.

Ramesh, R. 2009. Materials science: Emerging routes to multiferroics. Nature. 461:1218-1219.

Ramesh, R. and Spaldin, NA. 2007. Multiferroics: Progress and prospects in thin films. Nature Materials. 6:21-29.

Ribichini, R., Cegla, F., Nagy, PB. and Cawley, P. 2010. Quantitative modeling of the transduction of electromagnetic acoustic transducers operating on ferromagnetic media. IEEE Transactions on Ultrasonics, Ferroelectrics, and Frequency Control. 57(12):2808-2817.

Rivera, J-P. 1994. The linear magnetoelectric effect in $LiCoPO_4$ revisited. Ferroelectrics. 161(1):147-164.

Ryu, J., Priya, Sh., Uchino, K. and Kim, HE. 2002. Magnetoelectric effect in composites of magnetostrictive and piezoelectric materials. Journal of Electroceramics. 8:107-119.

Schatz, GC. and van Duyne, RP. (Eds.) 2002. Electromagnetic mechanism of surface-enhanced spectroscopy. Wiley, New York, USA.

Schmid, H. 1994. Magnetic ferroelectric materials. Bulletin of Materials Science. 17(7):1411-1414.

Sihvola, A. 2007. Metamaterials in electromagnetics. Metamaterials. 1(1):2-11.

Smolenskii, GA. and Chupis, IE. 1982. Ferroelectromagnets. Soviet Physics Uspekhi (Uspekhi Phizicheskikh Nauk, Moscow). 25(7):475-493.

Spaldin, NA. and Fiebig, M. 2005. The renaissance of magnetoelectric multiferroics. Science. 309(5733):391-392.

Srinivasan, G. 2010. Magnetoelectric composites. Annual Review of Materials Research. 40:153-178.

Srinivasan, G. and Fetisov, YK. 2006. Microwave magnetoelectric effects and signal processing devices. Integrated Ferroelectrics. 83(1):89-98.

Sze, SM. 1994. Semiconductor Sensors. Wiley, New York, USA.

Thompson, RB. 1990. Physical principles of measurements with EMAT transducers. In: Physical Acoustics. Eds. Mason WP. and Thurston, RN. Academic Press, New York, 19:157-200.

Van den Boomgaard, J., Terrell, DR., Born, RAJ. and Giller, HFJI. 1974. *In-situ* grown eutectic magnetoelectric composite-material. 1. Composition and unidirectional solidification. Journal of Materials Science. 9(10):1705-1709.

Van den Boomgaard, J., van Run, AMJG. and van Suchtelen, J. 1976. Piezoelectric-piezomagnetic composites with magnetoelectric effect. Ferroelectrics. 14:727-728.

Van Run, AMJG., Terrell, DR. and Scholing, JH. 1974. *In-situ* grown eutectic magnetoelectric composite-material. 2. Physical properties. Journal of Materials Science. 9(10):1710-1714.

Van Suchtelen, J. 1972. Product properties: A new application of composite materials. Phillips Research Reports. 27(1):28-37.

Varadan, VK., Varadan, VV. and Bao, XQ. 1996. Integration of interdigital transducers, MEMS and antennas for smart structures. Proceedings of the SPIE. International Society of Optical Engineering, San Diego, CA, Bellingham, WA: SPIE. 95-106.

Wang, KF., Liu, J-M. and Ren, ZF. 2009. Multiferroicity: The coupling between magnetic and polarization orders. Advances in Physics. 58(4):321-448.

Wang, BL., Mai, YW. and Niraula, OP. 2007. A horizontal shear surface wave in magnetoelectroelastic materials. Philosophical Magazine Letters. 87(1):53-58.

Wei, WY., Liu, JX. and Fang, DN. 2009. Existence of shear horizontal surface waves in a magneto-electro-elastic material. Chinese Physics Letters. 26(10):104301. pp3.

Wohltjen, H. 1979. Surface acoustic wave probe for chemical analysis. Analytical Chemistry. 51(9):1458-1475.

Wood, VE. and Austin, AE. 1975. In: Magnetoelectric Interaction Phenomena in Crystals. Eds. Freeman, AJ. And Schmid, H. Gordon and Breach Science Publishers, Newark, USA. 181-194.

Yang, K., Li, Z., Shang, LW. and Yi, WD. 2011. Design and analysis of a novel surface acoustic wave micro position sensor. Journal of Electromagnetic Analysis and Applications. 3:439-442.

Zakharenko, AA. 2010. Propagation of seven new SH-SAWs in piezoelectromagnetics of class 6 *mm*. LAP LAMBERT Academic Publishing GmbH & Co. KG, Saarbruecken–Krasnoyarsk. pp84.

Zakharenko, AA. 2011[a]. Analytical investigation of surface wave characteristics of piezoelectromagnetics of class 6 *mm*. International Scholarly Research Network (ISRN) Applied Mathematics (India). 2011:408529.pp8.

Zakharenko, AA. 2011[b]. Seven new SH-SAWs in cubic piezoelectromagnetics. LAP LAMBERT Academic Publishing GmbH & Co. KG, Saarbruecken–Krasnoyarsk. pp172.

Zakharenko, AA. 2012[a]. On wave characteristics of piezoelectromagnetics. Pramana – Journal of Physics. Indian Academy of Science. 79(2): in press.

Zakharenko, AA. 2012[b]. On propagation problems of new surface wave in cubic piezoelectromagnetics. Open Journal of Acoustics. Scientific Research Publishing, California, USA. 2(3): in press.

Zakharenko, AA. 2012[c]. Twenty two new interfacial SH-waves in dissimilar PEMs. LAP LAMBERT Academic Publishing GmbH & Co. KG, Saarbruecken–Krasnoyarsk. pp148.

Zhai, J., Xing, ZP., Dong, ShX., Li, JF. and Viehland, D. 2008. Magnetoelectric laminate composites: an overview. Journal of the American Ceramic Society. 91(2):351-358.

Zhang, WW. 2011. Surface acoustic wave based humidity sensor apparatus with integrated signal conditioning. September 13, US Patent No. 8015872.

Received: July 22, 2012; Accepted: Oct 29, 2012

SENRA Academic Publishers, British Columbia
Vol. 7, No. 1, pp. 2241-2250, Feb 2013
Online ISSN: 1920-3853; Print ISSN: 1715-9997

Canadian Journal of pure & applied sciences

ANALYSIS OF NITRIC ACID ACTIVATED UKPOR KAOLIN: STRUCTURAL TRANSFORMATIONS AND ADSORPTIVE PROPERTIES

*RO Ajemba, V I Ugonabo, PK Igbokwe and OD Onukwuli
Department of Chemical Engineering, Nnamdi Azikiwe University, PMB 5025, Awka, Anambra, Nigeria

ABSTRACT

This study analyzed the structural transformations and adsorption properties of Ukpor clay after nitric acid activation. The clay samples were mined, sun-dried, sized, and reacted with different concentrations of nitric acid ranging from 2 to 16mol/L at various times of 0.5 to 3 hours. The untreated and treated samples were characterized using X-ray Fluorescence and Fourier Transform Infrared (FTIR) Spectroscopy. The adsorptive capacities of the treated samples were investigated by using them to adsorb color pigments from palm oil. The analyses showed that nitric acid leaching caused an exchange of the octahedral cations; Al^{3+}, Fe^{3+}, and Mg^{2+} with H^{+} ions and this exchange increased with increase in acid concentration and period of activation. The surface area of the activated samples was observed to increase with increase in concentration and time to about four times that of the raw sample. The adsorption results showed that the adsorptive performance of the modified samples was improved from 27.6% to 85.4%. The equilibrium results fitted Freundlich isotherm model. This study has shown that acid activation led to some structural transformations of Ukpor clay which enhanced the adsorption performance of the clay thereby making it an effective adsorbent for palm oil bleaching.

Keywords: Adsorption, bleaching, surface area, color pigment, isotherm, equilibrium

INTRODUCTION

High cost of mostly used adsorbents such as activated carbons, in the purification and refining of edible and non edible oils, has necessitated for a substitute for them by low cost adsorbents such as clay minerals. Clay minerals, enormously abundant in nature, have been considered as a potential source of adsorbent for removing color pigments from edible oils. Nonetheless, the effective application of these materials in this area is limited due to small surface area and presence of net negative surface charge, leading to low adsorption capacity. All these factors have led to the need for research and development in the field of modification of clay surfaces to enhance their adsorptive properties. Surface modified clays have high potential to provide an alternative to most widely used activated carbon. Therefore, in order to ameliorate the adsorption properties and range of applicability, a number of physical and chemical methods have been investigated to modify the clays, including heat treatment (Al-Asheh *et al*., 2003; Chaisena and Rangsriwatananon, 2004), acid activation (Zorica *et al*., 2011; Motlagh *et al*., 2008 and 2011; Taha *et al*., 2011; Eze *et al*., 2012; Folatto *et al*., 2011), treating the cationic surfactants (Wang and Wang, 2008), and polymer modification (Chen *et al*., 2008; Liu, 2007).

Acid activation of clay minerals involves treating the clay with inorganic acids such as H_2SO_4, HCl, or HNO_3 (Diaz and de SouzaSantozs, 2001). The acid activation of clays alters the structural properties, such as, surface area and average pore volume (Doulia *et al*., 2009), and also changes some chemical properties such as cation exchange capacity and surface acidity of the clays, thus, generating the desired characteristics required for an effective adsorbent (Lian *et al*., 2009).

Nigeria is endowed with vast deposits of clay minerals that are unharnessed. The deposit located at Ukpor has not been employed industrially, but, it is only used for local pottery work by the rural inhabitants. This clay mineral can be harnessed and modified to increase its usability in the purification and bleaching of palm oil. Palm oil is a major source of dietary food for people in the western part of Africa and this oil has some storage and use difficulties. Palm oil congeals on storage at ambient temperature and has a very low smoke point, which makes it unsuitable for frying. These difficulties can be reduced if the oil can be bleached to remove the impurities. Impurities present in palm oil can be reduced appreciably by adsorption process or bleaching by using clay mineral adsorbents. Christidis *et al*. (1997) examined the bleaching capacity and acid activation of bentonite from Aegean, Greece, observing a five-fold increase of the surface area of raw materials. The activated samples were rendered suitable for bleaching of rapeseed oil. It was determined that the optimum bleaching capacity is not associated with maximum surface area and the optimum conditions for activation are obtained by using a variety of combinations of acid strength and residence

*Corresponding author email: ginaajemba@rocketmail.com

time. The preparation of acid-activated clay materials must be controlled in order to obtain maximum bleaching capacity (Kirali and Lacin, 2006; Rozic *et al*., 2010). Usman *et al*., (2012) investigated the applicability of clay from Ibeshe in bleaching palm oil. They observed that the clay after acid activation only increased the color reduction from 9.1 % to 27.3%, a poor performance as an adsorbent.

MATERIALS AND METHODS

Materials

Ash-colored clay material from Ukpor (N: 5° 54' 27.5"; E: 6° 56' 3.7"; A: 137m) in Nnewi South, Anambra state, Nigeria was used as the primary raw material. Refined palm oil was obtained at oil mill located at Isuofia (N: 6° 1' 60"; E: 7° 2' 60"; A: 361m). All chemicals used were analytical grade, bought from Conraws Company Ltd, Enugu.

Experimental Methods

Acid activation of the clay sample

The clay material was prepared for activation by air-drying and grinding to a particle size of 0.212 mm. 10 g of the prepared sample was weighed into flask (250ml capacity) and 100 ml of sulphuric acid solution was added. The resulting suspension was heated on a magnetically stirred hot plate at temperature of 90^{o}C for 2 hours 30 minutes. At the end of the experimental duration, the resulting slurry was poured into a Buchner funnel to separate the acid and clay. The residual clay was washed severally with distilled water until neutral point was obtained with pH indicator. The clay residue was dried in an oven at 80^{o}C for 4 hours. The dried samples were crushed and sieved again to 0.212 mm particle size. The activation process was repeated with varying acid concentrations of 2 – 16 mol/L of HNO_3, varying time of 0.5 – 3 hours, and varying temperatures of 70 – 120^{o}C. The clay samples thus prepared were labeled UK0, UK2, UK4, UK8, UK12, UK14, and UK16, where the numbers indicate the acid concentrations used in the activation step.

Characterization

The chemical and mineralogical compositions of the natural and activated clay samples were determined. The chemical composition was determined using X-ray fluorescence (XRF), Philips PW 2400 XRF spectrometer; while the mineralogical composition was determined using Fourier transform infrared (FTIR), Shimadzu S8400 spectrophotometer, with samples prepared by the conventional KBr disc method.

Specific surface area

The surface area was determined using ethylene glycol mono-ethyl-ether (EGME) described by Carter *et al.*, (1964 and 1965). Clay samples were sun-dried and grinded to pass No. 40 sieve. A small amount of the sample was then placed in an oven at a temperature of 105 ^{0}C overnight to remove water and then dried with P_2O_5. One gram of the dried sample was spread into the bottom of aluminium tare and weighed (W_a) using an analytical balance with an accuracy of 0.001 g. Approximately 3.0 ml of laboratory grade EGME was added to the sample using a pipette and mixed together with a gentle swirling motion to create uniform slurry. All clay samples were covered with the EGME in order to obtain an accurate surface area measurement. The aluminium tare was then placed inside a standard laboratory glass sealed vacuum desiccator and allowed to equilibrate for 20 min. The desiccator was then evacuated using vacuum pump. The aluminium tare was removed from the desiccator and weighed (W_s) after a period of 12, 16, and 24 hours. When the mass of the sample varied by more than 0.001 grams between two measurements, the sample was placed back in the desiccator and evacuated again for an additional 2 hours. The process was continued until the sample mass did not vary by more than 0.001 g. The surface area was expressed as follows:

$$A = \frac{Wa}{0.000286Ws} \quad (1)$$

A = surface area, W_a = weight of EGME retained by the sample, W_s = weight of P_2O_5-dried sample, 0.000286 is the weight of EGME required to form uni-molecular layer on a square meter of the surface (Chiou *et al.*, 1993).

Cation Exchange Capacity (CEC) (Ingelthorpe *et al*., 1993)

5 g of the clay sample was weighed into the 250 ml polythene bottle with a magnetic stirrer. The bottle and its contents were weighed (M_1). 100 ml of buffered barium chloride solution was added to the bottle and was placed on a magnetic stirring plate and agitated for 1 hour. At the end of the period, the bottle was centrifuged at 1500 rpm for 15 minutes and the supernatant was discarded. Further 200 ml of the buffered barium chloride solution was added and the mixture was agitated on a magnetic stirring plate for another 1 hour. The bottle and its contents were left overnight. The following day, the bottle and its contents were centrifuged at 1500 rpm for 15 minutes and the supernatant discarded. 200 ml of distilled water was added and agitated for a few minutes on the magnetic stirring plate. It was centrifuged for further 15 minutes and the supernatant discarded. The bottle and its contents were weighed (M_2). 100 ml of $MgSO_4$ solution was pipette into the bottle and stirred well and was left to stand for 2 hours with occasional agitation on the magnetic stirring plate. After 2 hours the contents were centrifuged at 1500 rpm for 15 minutes and the supernatant decanted into the stopper bottle. 5 ml aliquot of this solution was pipette into a 100 ml conical beaker and 5 ml of ammonia buffer and 6 drops of indicator were added to it. This mixture was titrated with standard EDTA (titer A_1 ml). Another titration was done with a 5 ml of

aliquot of 0.05 M $MgSO_4$ solution (titer *B* ml). The end point was indicated by a blue to pink color change. The Cation Exchange Capacity was calculated as follows:

$$CEC = 8\left\{B - \frac{(A_1 \times (100 + M_2 - M_1))}{100}\right\} meg/100g \quad (2)$$

Where M_1 = weight of bottle plus dry content (g), M_2 = weight of bottle plus wet content (g), A_1 = titration end-point of sample (ml), and B = titration end-point of $MgSO_4$ solution (ml)

Bleaching experiment

The bleaching experiments were carried out in a batch process. 50 g of the refined palm oil was charged into a 250 ml beaker and 2 g of the activated clay samples were also added. The mixture of clay and oil were placed in a water bath and heated to a temperature of 80 ^{0}C for 30 minutes under continuous stirring. At the end of the reaction, the slurry formed was filtered through a dry filter paper. The bleaching capacity of the acid activated clays was then determined by measuring the color of the bleached oils using a UV-Vis spectrophotometer (Shimadzu UV mini 1240) at a wavelength of 450 nm. The bleaching efficiency of the acid activated clay was calculated in this study using the following equation:

$$\%\ Bleaching\ Efficiency = \frac{(A_{unbleached} - A_{bleached})}{A_{unbleached}} x\ 100 \quad (3)$$

Where $A_{unbleached}$ and $A_{bleached}$ are the absorbencies of the unbleached and bleached oils, respectively.

RESULTS AND DISCUSSION

Characterization

The changes in the chemical composition of the natural and acid activated Ukpor clay at different acid concentrations are shown in table 1. The content of SiO_2 was observed to increase as the acid concentration increased up to 14mol/L and decreased with further increase in concentration (Fig. 1) and this could be due to the formation of mullite which protects the clay layers from further acid attack. The contents of the octahedral cations (Al_2O_3, Fe_2O_3, and MgO) decreased intensely as the acid concentration increased and increased with further attack after 14 mol/L concentration (Fig. 2). The behaviour shown by the Al_2O_3, Fe_2O_3, and MgO contents with progressive acid treatment is related to the progressive dissolution of the clay mineral. The octahedral sheet destruction passes the cations into the solution, while the silica generated by the tetrahedral sheet remains in the solid phase due to its insolubility (Dias *et al*., 2003). Pesquera *et al*. (1992) suggest that this free silica generated by the initial destruction of the tetrahedral sheet, is polymerized by the effect of such high acid concentration and is deposited on the undestroyed silicate fractions, thereby protecting it from further acid attack.

Surface area analysis

It was observed from the surface area analysis of the natural and treated samples that the surface area increased as the acid concentration used in the activation step increased. The increase in surface area from natural to activated samples relates to the elimination of the exchangeable cations, de-lamination, and the generation of micro-porosity during the processes (Dias *et al*., 2003). This increase continued up to the sample activated with 14 mol/L of HNO_3 and dropped when the concentration was increased to 16mol/L (Fig. 3). This is attributed to the polymerization of the generated free silica by the effect of excess acid concentration and is deposited on the surface of the clay particle preventing it from further attack

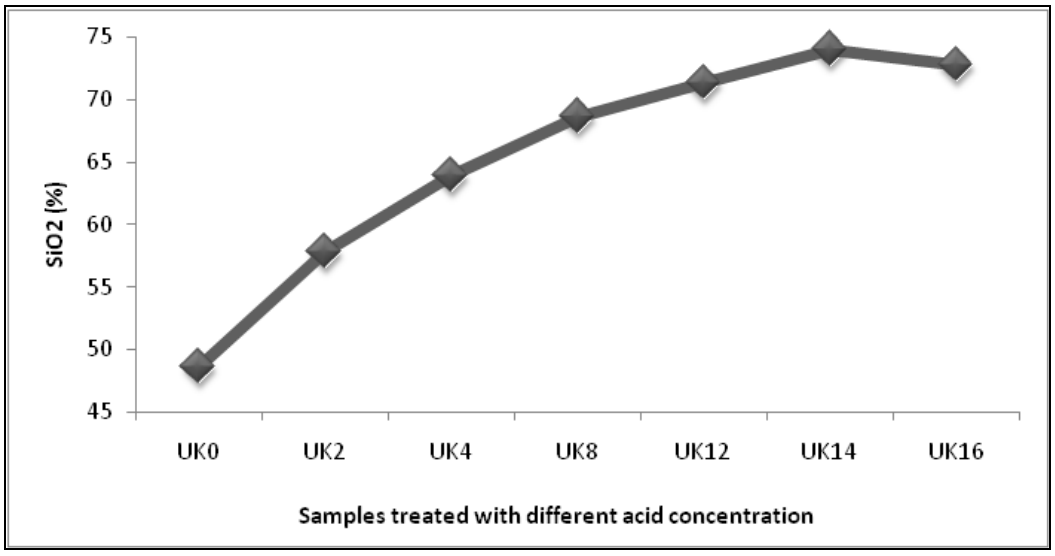

Fig. 1. SiO_2 content of the clay sample after activation with HNO_3 (time = 3 hours, temperature = 120^{o}C).

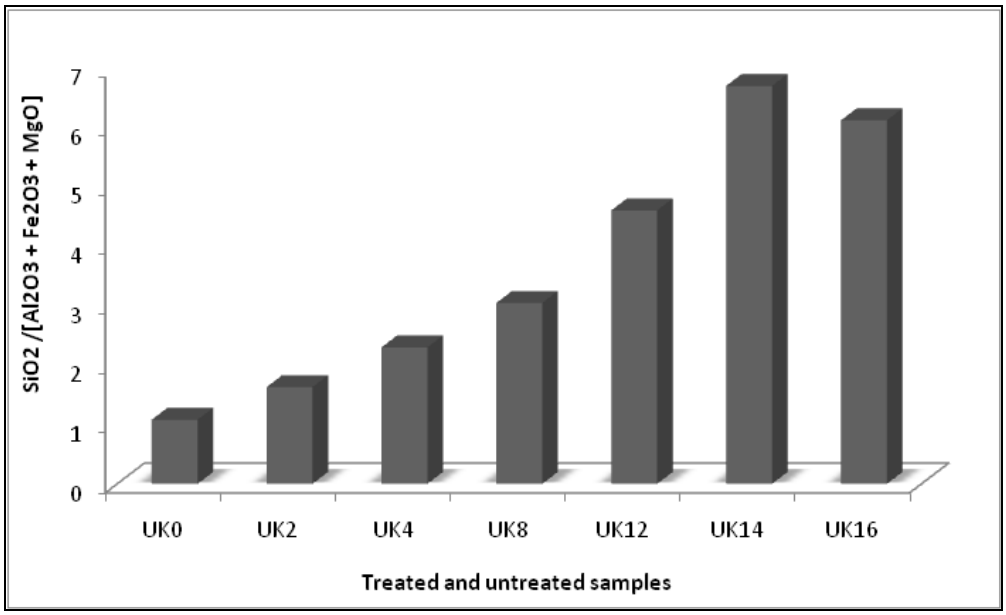

Fig. 2. Variation of SiO_2 / [Al_2O_3 + Fe_2O_3 + MgO] ratios for samples treated with different acid concentrations (time = 3 hours, temperature = 120^oC).

Table 1. Chemical analysis and cation exchange capacity (CEC) of the natural and acid activated Ukpor clay samples determined by XRF.

Chemical composition (%)	Clay samples						
	NT0	UK2	UK4	UK8	UK12	UK14	UK16
Al_2O_3	26.9	21.45	17.04	13.97	9.88	7.16	7.52
SiO_2	48.6	57.8	63.93	68.64	71.36	74.04	72.73
Fe_2O_3	16.13	12.51	9.65	7.83	4.99	3.35	3.85
CaO	0.08	0.05	0.03	0.02	0.02	0.02	0.02
MgO	1.78	1.46	1.08	0.74	0.61	0.52	0.50
K_2O	0.11	0.07	0.05	0.03	0.03	0.03	0.03
TiO_2	2.06	1.74	1.36	1.01	0.84	0.65	0.73
LOI	3.67	2.73	2.25	1.92	1.56	1.21	0.87
Total	99.33	97.81	95.39	94.16	89.29	86.98	86.25
Cation exchange capacity (CEC) (meg/100g)	97	78	63	57	50	46	48

(Pesquera *et al*., 1992). Also, the surface area increase as the acid concentration increased is attributed to the reduction in the contents of the octahedral cations of Al^{3+}, Fe^{3+}, and Mg^{2+}, and the increase in the ratio of SiO_2 / (Al_2O_3 + Fe_2O_3 + MgO) as in figure 4.

Fourier Transform Infrared (FTIR) spectroscopy analysis

The spectra of the untreated and the sample treated with 14 mol/L HNO_3 are shown in figures 5 and 6, respectively. FTIR spectra of the raw and acid-leached clay samples were carried out in the range from 400 – 4000 cm^{-1} to study the effect of acid-leaching on the clay mineral. The changes in the functional groups provide the indication of the modifications that occurred during the activation process. During the acid-leaching of the clay samples the protons from the acid medium penetrate into the clay structures attacking the OH groups thereby causing the alteration in the adsorptive bands attributed to the OH vibrations and octahedral cations. The intensities of the stretching bands observed at 3449, 1639, and 792 cm^{-1} (associated with O-H, along with Al-OH stretch) decreased after acid-activation. The increase in the severity of acid caused the disappearance of the stretching bands at 3692, 3525, and 1104 cm^{-1} assigned to the H-O-H stretching. The peak assigned to Si-O-Si stretch at 472, 685, 920 and 1037, 1037, 3626 cm^{-1} remained after acid leaching with slight increase in the intensities, similar result was reported by others (Christidis *et al*., 1997;

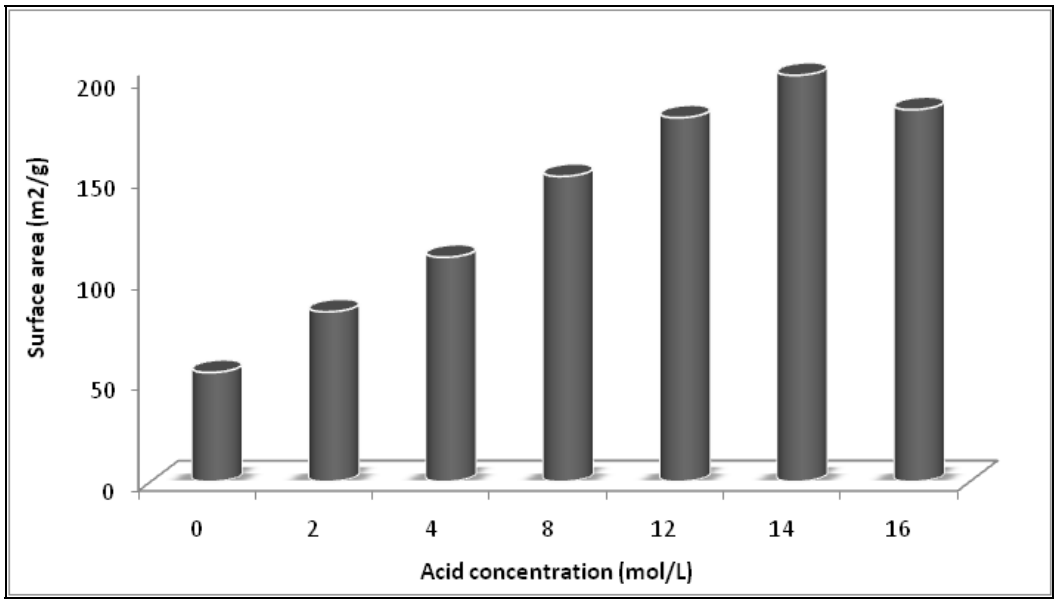

Fig. 3. Variation of the surface area with acid concentration used in activation of the samples (time = 3 hours, temperature = 120^{o}C).

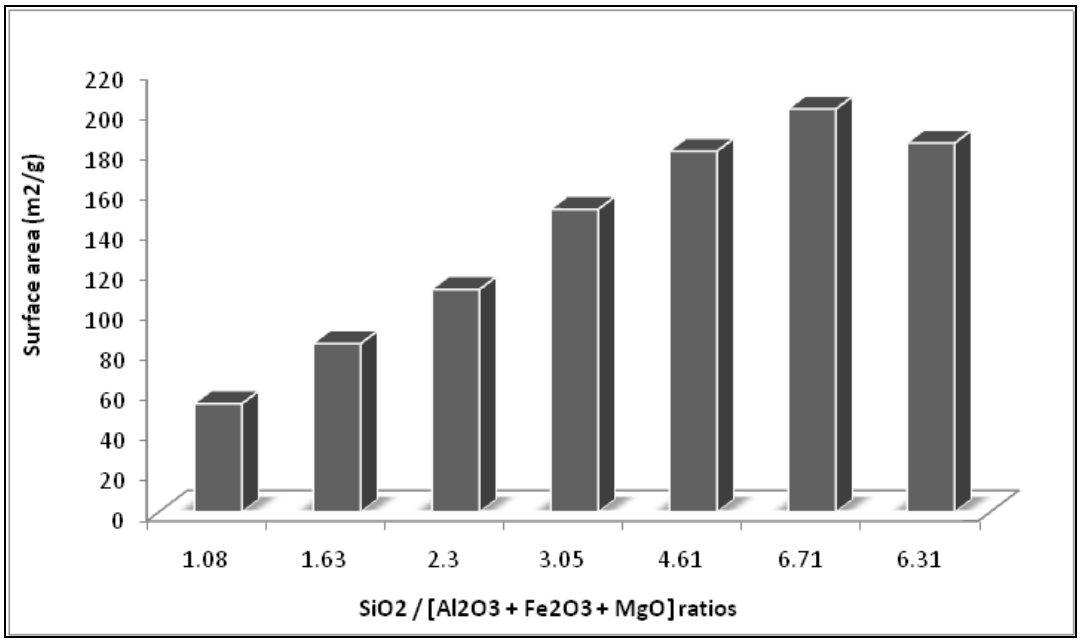

Fig. 4. Variation of surface area with change in SiO_2 / [Al_2O_3 + Fe_2O_3 + MgO] ratios.

Komadel *et al.*, 1990). The transformation of the tetrahedral occurred at 720 cm^{-1} which was increased after the acid treatment.

Effect of activation time on the clay samples

The activation experiment was performed at various times ranging from 0.5 to 3 hours. The results of the studies are depicted in figure 7. The figure shows that the surface area increased as the time of activation increased alongside the acid concentration. The prolonged period of activation allowed for maximum contact between the clay mineral and the acid molecules which aided the dissolution of the cations from the octahedral layer (aluminium, ferric, and magnesium ions). These ions then replaces the alkaline earth cations (Ca^{2+}, Na^{+}, and K^{+}) in the interlayer region, and this led to increase in surface area and porosity as a result of the inaccessible sites within the clay structure that were opened up (Taylor, 2005).

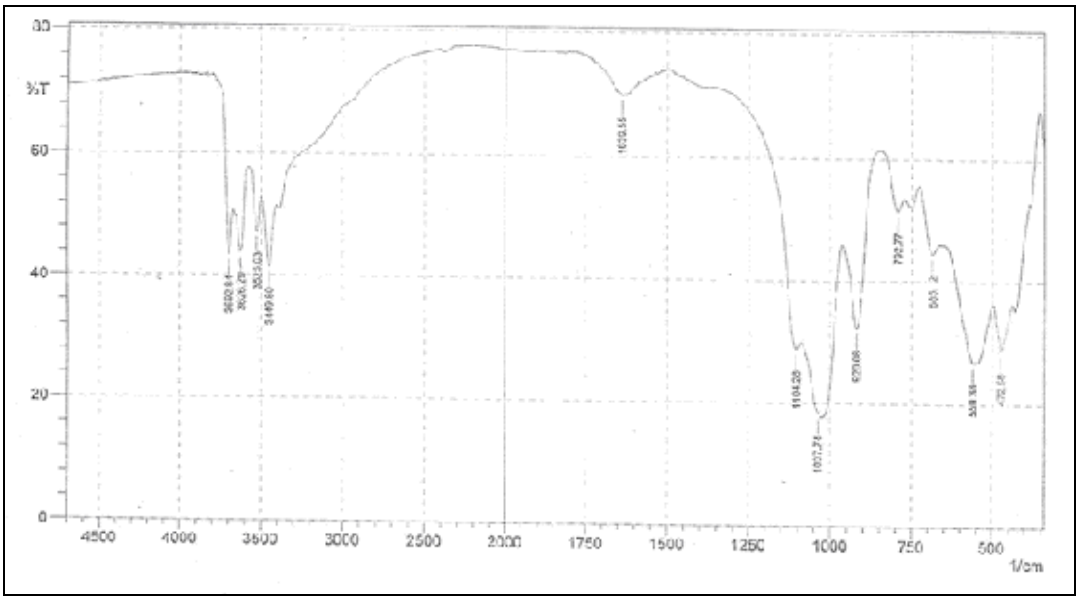

Fig. 5. FTIR spectrum of untreated Ukpor clay sample.

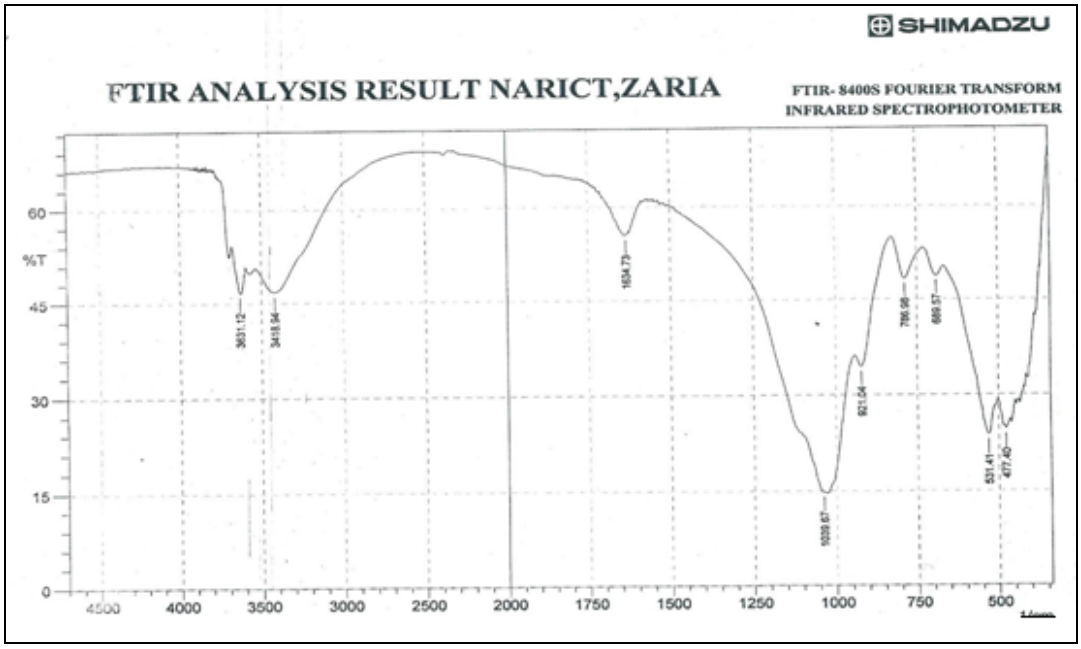

Fig. 6. FTIR spectrum of Ukpor clay sample treated with 14 mol/L of HNO_3.

Bleaching Studies

The results of the bleaching studies performed using the natural and acid activated samples are shown in figure 8. The figure shows that the bleaching efficiency increases with an increase in the acid concentration used in the activation step. The increase reached a maximum with the sample activated with 14mol/L HNO_3 and decreased thereafter with further increase in the acid concentration. This decrease in bleaching efficiency is attributed to the small surface area and high $Al_2O_3 + Fe_2O_3 + MgO$ content exhibited by the sample activated with 16mol/L of HNO_3 that led to the destruction of the clay crystalline structure as shown in figure 9.

Adsorption Isotherms

The mechanism of adsorption of the color pigments onto the acid modified Ukpor clay was determined by evaluating the equilibrium data obtained from the

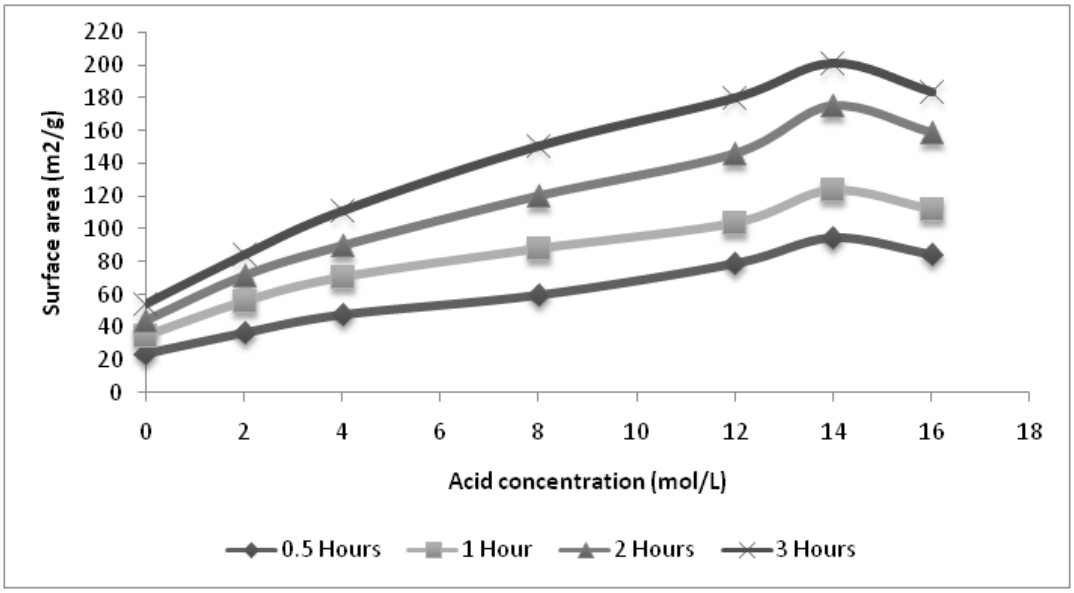

Fig. 7. Variation of surface area with time at different acid concentrations.

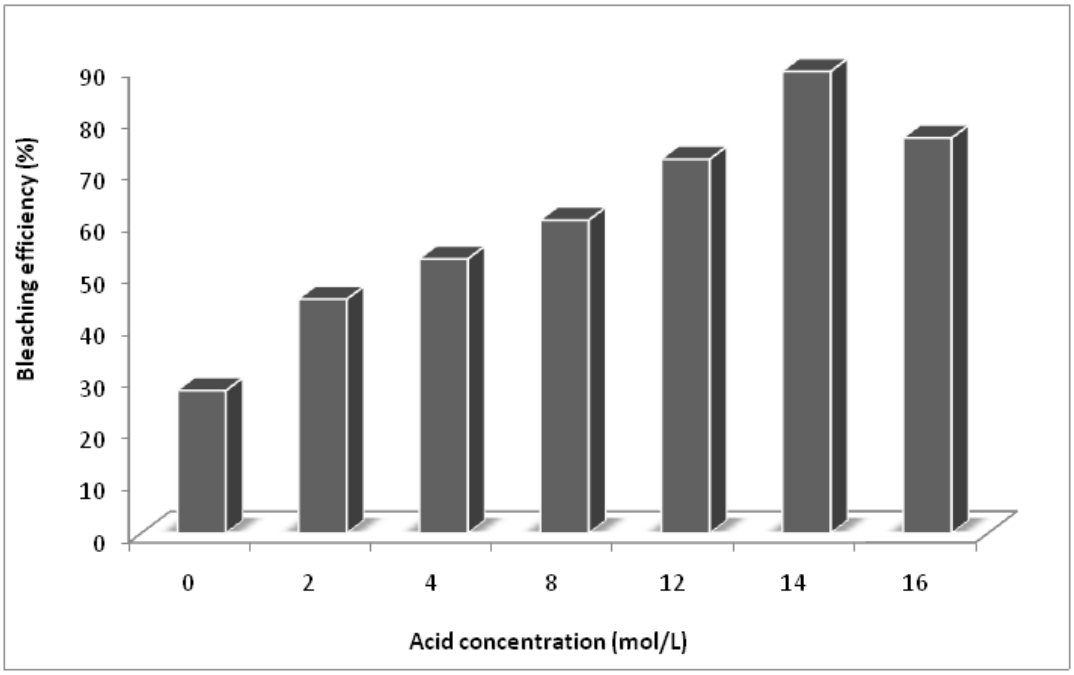

Fig. 8. Variation of the bleaching efficiency with acid concentrations used in the activation (time 3 hours, temperature 120^{o}C).

experiments. In this study, both the Langmuir and Freundlich isotherm models were used to analyze the adsorption experimental data. The basic assumption of Langmuir model is that the formation of monolayer takes place on the surface of the adsorbent indicating that only one color pigment molecule could be adsorbed on one adsorption site and the intermolecular forces decrease with the distance. The model is given by the following equation:

$$\frac{C_e}{q_e} = \frac{C_e}{q_m} + \frac{1}{K_L q_m} \quad (3)$$

Where C_e is the equilibrium concentration of the pigments (mg/l), q_e is the amount of color pigment adsorbed per unit of adsorbent (mg), q_m the Langmuir constant for adsorption capacity (mg/g) and K_L is the Langmuir constant for energy of adsorption (L/g). The values of q_m and K_L were obtained from the slopes and the intercept of

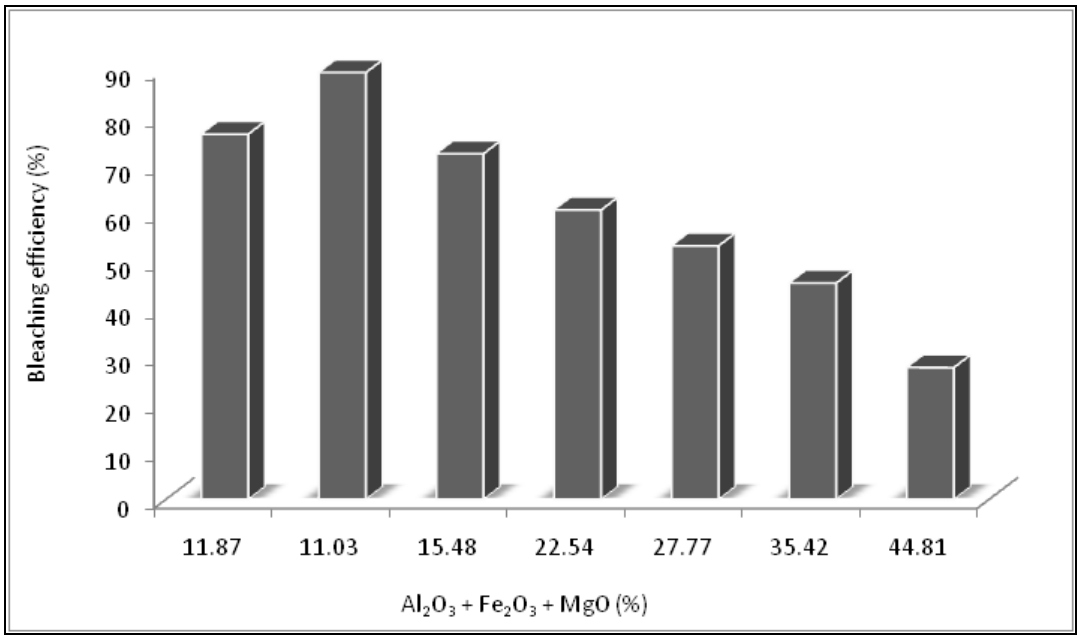

Fig. 9. Variation of the bleaching efficiency with $Al_2O_3 + Fe_2O_3 + MgO$ content.

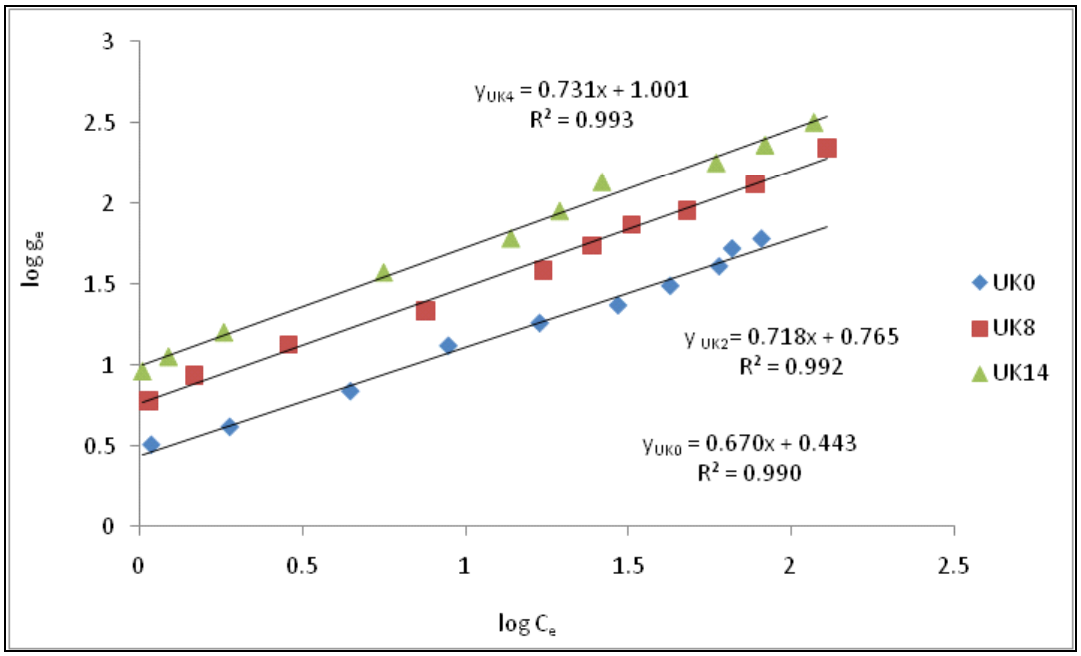

Fig. 10. Freundlich adsorption isotherm for colour pigment adsorption onto acid modified Ukpor clay.

the linear plots of C_e/q_e versus C_e (not shown) and are shown in table 2.

The Freundlich model is applicable to heterogeneous systems and it involves the formation of multi-layers. The Freundlich adsorption isotherm is given by the equation:

$$\log q_e = \log k_f + \frac{1}{n}(\log C_e) \quad (4)$$

Where k_f and n are the Freundlich constants and represent the adsorption capacity and measure of heterogeneity, respectively. The values of k_f and n were obtained from the slopes and intercepts of the linear plots of q_e versus C_e as shown in figure 10 and the values are presented also in table 2. A comparison of the values of the coefficient of determination (R^2) shown in table 2, shows that the adsorption experimental data conformed better to the Freundlich adsorption isotherm and therefore, it can be concluded that the adsorption of color pigments onto acid modified Ukpor clay occurred in multi-layer.

Table 2. Freundlich and Langmuir isotherm constants and the respective correlation coefficients.

Isotherm Model	Model Parameters	Clay Type		
		UK0	UK8	UK14
Langmuir	q_m	72.43	74.61	83.75
	K_L	0.074	0.072	0.083
	R^2	0.986	0.982	0.988
Freundlich	k_f	2.77	5.82	10.02
	n	1.49	1.39	1.37
	R^2	0.990	0.992	0.993

CONCLUSION

The analysis of the structural and adsorptive effects of nitric acid activation of Ukpor clay has been successfully investigated. The results showed that the acid activation caused physical and chemical modifications on the treated clay samples. The structural properties affected are surface area, adsorption capacity, and cation exchange capacity. The activated samples exhibited a high adsorptive capacity thereby affirming the effectiveness of the acid treatment. The surface area was observed to increase with an increase in the acid concentration and reaction time. The equilibrium study showed that the prepared adsorbent adsorbed in multi-layers in accordance with Freundlich isotherm model. It can then be concluded that acid activation of Ukpor kaolin enhances its adsorptive capacity and makes it an effective adsorbent for palm oil bleaching.

REFERENCES

Al-Asheh, S., Banat, F. and Abu-Aitah, L. 2003. Adsorption of phenol using different types of activated bentonites. Separation Purification Technology. 33:1-10.

Carter, DL., Heilman, MD. and Gonzalez, CL. 1965. Ethylene Glycol Mono-ethyl Ether for determining surface area of silicate minerals. Soil Science. 100:356-360.

Carter, DL., Mortland, MM. and Kemper, WD. 1964. Specific surface. Methods of soil analysis. Agronomy, No. 9, Part 1 (2nd ed.). American Society of Agronomy. 456-478.

Chaisena, A. and Rangsriwatananon, K. 2004. Effects of thermal and acid treatments on some Physico-chemical properties of Lampang diatomite. Suranere Journal of Science and Technology. 11:289-299.

Chen, R., Peng, F. and Su, S. 2008. Synthesis and characterization of novel swelling tunable oligomeric poly (styrene-co-acrylamide) modified clays. Journal of Applied Polymer Science. 108:2712-2717.

Chiou, CT., Rutherford, DW. and Manes, M. 1993. Sorption of N_2 and EGME vapours on some soils, clays, and mineral oxides and determination of sample surface areas by use of sorption data. Environmental Science Technology. 27:1587-1594.

Christidis, GE., Scott, PW. and Dumham, AC. 1997. Acid activation and bleaching capacity of bentonites from the islands of Milos and Chios, Aegean and Greece. Applied Clay Science. 12:329-347.

Dias, MI., Suarez, MB., Prates, S. and MartinPozas, JM. 2003. Characterization and acid activation of Portuguese special clays. Clay Minerals. 38:537-549.

Diaz, FRV. and DeSouzaSanctozs, R. 2001. Studies on the acid activation of Brazilian smectite clays, Quim. Nova. 24:343-353.

Doulia, D., Leodopoloud, C., Gimouhopoulos, K. and Rigas, F. 2009. Adsorption of humic acid on acid-activated Greek bentonite. Journal of Colloid and Interface Science. 340:131-141.

Eze, KA., Nwadiogbu, JO. and Nwamkwere, ET. 2012. Effect of acid treatment on the physicochemical properties of kaolin clay. Archives of Applied Science Research. 4:792-794.

Foletto, EL., Colazzo, GC., Volzone, C. and Porto, LM. 2011. Sunflower oil bleaching by adsorption onto acid-activated bentonite. Brazilian Journal of Chemical Engineering. 28:169-174.

Inglethorpe, SDJ., Morgan, DJ., Highley, DE. and Bloodworth, AJ. 1993. Industrial mineral laboratory manual- Bentonite. British Geological Survey Technical Report. WG/93/20.

Kirali, EG. and Lacin, O. 2006. Statistical modeling of acid activation on cotton oil bleaching by Turkish bentonite. Journal of Food Engineering. 75:137-141.

Komandel, P., Schmidt, D., Medejova, J. and Cicel, J. 1990. Alteration of smectites by treatment with hydrochloric acid and sodium carbonate solutions. Applied Clay Science. 5:113-122.

Lian, L., Guo, L. and Guo, C. 2009. Adsorption of congo red from aqueous solution on Ca-bentonite. Journal of Hazardous Materials. 161:126-131.

Liu, P. 2007. Polymer modified clay minerals: A review. Applied Clay Science. 38:64-76.

Motlagh, MK., Rigi, ZA. and Yuzbashi, AA. 2008. To evaluate an acid activated bentonite from Khorasan (Iran) for use as bleaching clay. International Journal of Engineering Science. 19:83-87.

Motlagh, MK., Youzbashi, AA. and Rigi, ZA. 2011. Effect of acid activation on structural and bleaching properties of a bentonite. Iranian Journal of Material Sciences & Engineering. 8: 50 – 56.

Pesquera, C., Gonzalez, F., Benito, I., Blanco, C., Mendioroz, S. and Pajares, J. 1992. Passivation of a montmorillonite by the silica created in acid activation. Journal of Material Chemistry. 2:907-911.

Rozic, L., Novkovic, T. and Petrovic S. 2010. Modeling and optimization process parameters of acid activation of bentonite by response surface methodology. Applied Clay Science. 48:154-158.

Taha, KK., Tagelsir, MS. and Musa, AM. 2011. Performance of Sudanese activated bentonite in bleaching cotton seed oil. Journal of Bangladesh Chemical Society. 24:191-201.

Taylor, DR. 2005. Bleaching, Bailey's Industrial Oil and Fat Products (6^{th} ed.), John Wiley & Sons, Inc.

Usman, MA., Ekwueme, VI., Alaje, TO. and Mohammed, AO. 2012. Characterization, acid activation, and bleaching performance of Ibeshe clay, Lagos, Nigeria. ISRN Ceramics. doi:10.5402/2012/658508.

Wang, L. and Wang, A. 2008. Adsorption properties of congo red from aqueous solution onto surfactant-modified montmorillonite. Journal of Hazardous Material. 160:173-180.

Zorica, PT., Mladenovic SB., Babic BM., Logar VA., Dordevic AR. and Cupac, SB. 2011. Modification of smectite structure by sulphuric acid and characteristics of the modified smectite. Journal of Agricultural Science. 56:25-35.

Received: Aug 7, 2012; Accepted: Oct 3, 2012

SENRA Academic Publishers, British Columbia
Vol. 7, No. 1, pp. 2251-2270, Feb 2013
Online ISSN: 1920-3853; Print ISSN: 1715-9997

Canadian Journal of pure&applied sciences

SCALABILITY OF WEB SERVICES SOLUTION BUILT ON ROA

*Godspower O Ekuobase and Emmanuel A Onibere
Department of Computer Science, University of Benin, Benin City, Nigeria

ABSTRACT

ROA an acronym for Replication Oriented Architecture is speculated as capable of attenuating the scalability defect of Web Services and help Application Programmers build Scalable Web Services Solution. The essence of this paper is to authenticate the scalability of Web Services solution built on ROA. We have selected a test problem that enabled the test of the architecture in its worst state scenario. We have also developed ten different Web Services solution for this problem but with different number of replicas ranging from one to ten using Java technologies. We have subjected these systems to load tests using Apache JMeter under varying load stress vis-à-vis the solutions built on conventional Web Service Java technologies, void of any solution architecture, for the same problem and platform. The data from Apache JMeter (throughput and response time) underwent mathematical transformation to realize relative scalability estimates at the varying load points. These estimates were subjected to statistical analysis and the result is that ROA can enhance the scalability of Web Service by about 32%. This scalability is guaranteed 90% of the time. We also exposed areas where we think ROA can be improved.

Keywords: ROA, scalability, web services, web services solution, apache JMeter, java EE.

INTRODUCTION

Ekuobase and Onibere (2011) asserted that the poor scalability of Web Services, if not properly addressed, may not only pose a serious threat to its survivability but may also lead the Information Technology (IT) community into shambles as Web Services has the potential of becoming the ubiquitous platform technology for next-generation computing systems, having an unprecedented number of active systems dependent on it, and hence introduced ROA and claimed that ROA can attenuate the scalability defect of Web Services and help application programmers build scalable Web Services solution. It is however imperative that the scalability claim on ROA be authenticated, for this claim to be given any consideration. This paper authenticates the scalability of Web Services solution built on ROA. We were careful to use a test (small-to-medium sized) software development project of an application with little or no computational capability because of the fears raised in Ekuobase and Onibere (2011).

The Automated Teller Machine (ATM) System is the application system of choice. The ATM system was selected because it requires less computational capability, easy to appreciate, conversational, and incorporates the use of back end system (database). Besides, the ATM system is in reality of high activity and great economic importance. Also, with the proliferation of hand held devices, emergence of ubiquitous systems and the move towards cashless society, the ATM system reflects two important domains – financial transaction (be it commerce or governance) and ubiquitous systems domains – that will be fully dependent on Web services.

MATERIALS AND METHODS

We began the software development project by first selecting an appropriate software development methodology (SDM) for it. We observed that no SDM is a failure and none is a silver bullet; they all have their strengths and weaknesses and project domain or nature of software projects they suite most (Ekuobase, 2006) as summarized in table 1. From table 1, it became obvious that the agile software development approach (Ekuobase, 2006; Agile Alliance, 2001) is most appropriate for the software development task. The tailored agile approach, depicted in figure 1, was adopted as the software development process. The software development tools used were basically software and hardware tools. These tools and the roles they played in the research are highlighted as follows:

Hardware Tools: the tools in this category were the computer and its peripherals. In particular, Dell notebook (Intel® CPU T2080 @ 1.73GHz x 2, Duo Core; 794MHz, 2.0GB RAM and 150GB Hard Disk) was used for developing the prototype system. It also served as host to the software tools used in this research.

Software Tools: we choose to discuss software tools under Operating System, Development Platform, Language, Integrated Development Environment (IDE), and Packages.

*Corresponding author email: godspower.ekuobase@gmail.com

❖ **Operating System:** We settled for Microsoft Windows XP Professional Version 2002 Service Pack 2 which work seamlessly with the other software tools used in the research and for which our institution holds a multi-user license. The Operating System enabled our applications and other software tools used interact with the machine and tap its computational and peripheral resources.

❖ **Development Platform:** The choice of Java EE (Jendrock *et al*., 2006) as our Development platform for building the Web services solution, is not only because we were biased towards the platform as a result of our priori comfortable Java programming experience but also because as it stands today, Java EE and Microsoft. NET platforms remain the most dominant application developer's platform for enterprise applications in general and Web Services solutions in particular (Birman, 2005; Williams, 2003; Vawter and Roman, 2001) but Microsoft .NET platform is proprietary.

❖ **Language:** Here, we mean programming language, modelling language and Database Management System (DBMS). Obviously, our core programming language of implementation is Java 5.0 (van der Linden, 2004; Horstmann and Cornell, 2005a, 2005b; Deitel and Deitel, 2010) since it is the only language our choice platform supports. Java was used for coding. The Structured Query Language (SQL) being the de facto language for interacting with DBMS was adopted. Our choice of Java DB as our DBMS for building and managing the databases was based on seamless compatibility with both Java and NetBeans – our Integrated Development Environment of choice. The Unified Modelling Language (UML) was used for the systems design but not without some modifications since object oriented analysis and design which UML stands for, fall short of the concept of service orientation which requires additional elements for it to be realized (Zimmermann *et al*., 2004; Arsanjani, 2004).

❖ **Integrated Development Environment (IDE):** We have several IDEs that support Java. They include JBuilder, JCreator, Eclipse, and NetBeans. We choose NetBeans (NetBeans 6.0) on the ground of familiarity though it is not in any way less powerful than the others. Normally, IDE makes programming easy, nimble and interesting.

❖ **Packages:** the following software packages were handy. Argo UML (Ramirez *et al*., 2006; Tolke and Klink, 2006) – for the UML design, Apache JMeter (http://jakarta.apache.org/) – request generation, load testing the Web Services application and capturing of useful data as response time and throughput which were vital to this research, and Microsoft Excel – for data manipulation and computation. We added Apache JMeter as plug-in to NetBeans, to ease its use with the IDE.

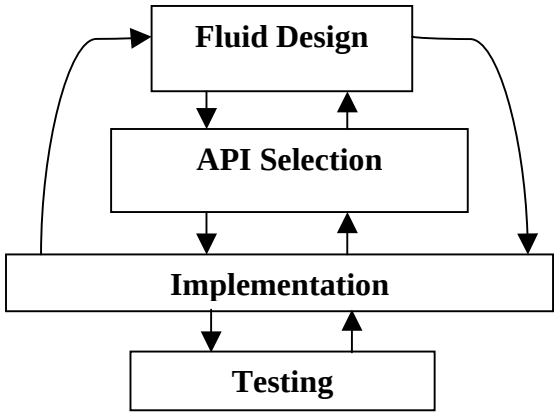

Fig. 1. An Agile Implementation Model.

Table 1. Software Projects and the basic Software Development Approaches.

Agile Software Development Approach	Traditional Software Development Approach
Visible systems	Legacy/embedded systems
Low risk projects	High risk projects
Blurred and unstable requirements	Explicit and fairly stable requirements
Small to medium sized projects	Large and complex projects
Time~to~market driven	Product quality driven

The following assumptions about the ATM system under construction were made:

a. The ATM system does not concern itself with the working and the nature of the ATM terminals (screen, card reader, keypad, cash dispenser and deposit slot).
b. The ATM system serves as a base station for several ATM terminals with the sole duty of interfacing with the user.
c. The ATM system does not include security features sufficient for real life deployment.
d. Although ATM system provides four basic services as depicted in figure 2 and 3, only the Fund Transfer service was built since it encompasses the other basic ATM services.

The service equivalent of the ATM system is modeled in figure 4. Observe that the ATM was replaced in the service model by two SOAP routers - Web Services client and Web services solution that communicate in a SOAP request-response manner. These in turn communicate with backend (logic) objects directly as in the object model and thus same internal state as its object equivalent

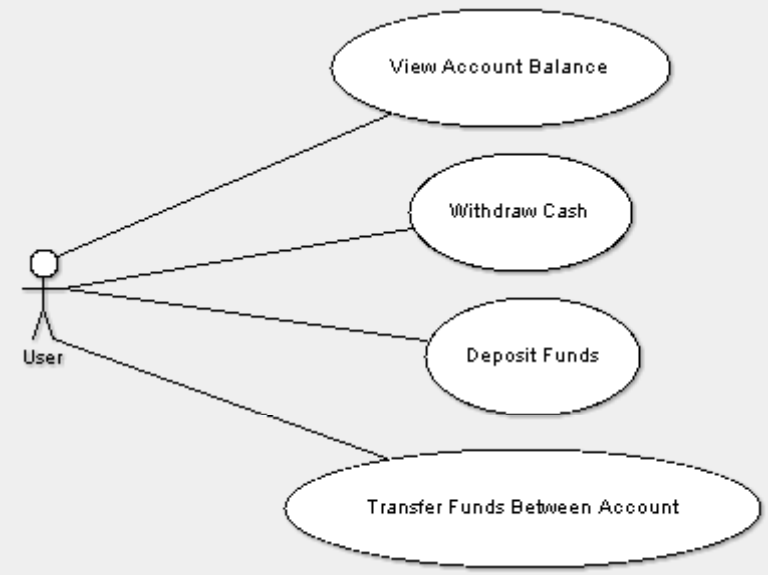

Fig. 2. Use Case Diagram for the ATM System.

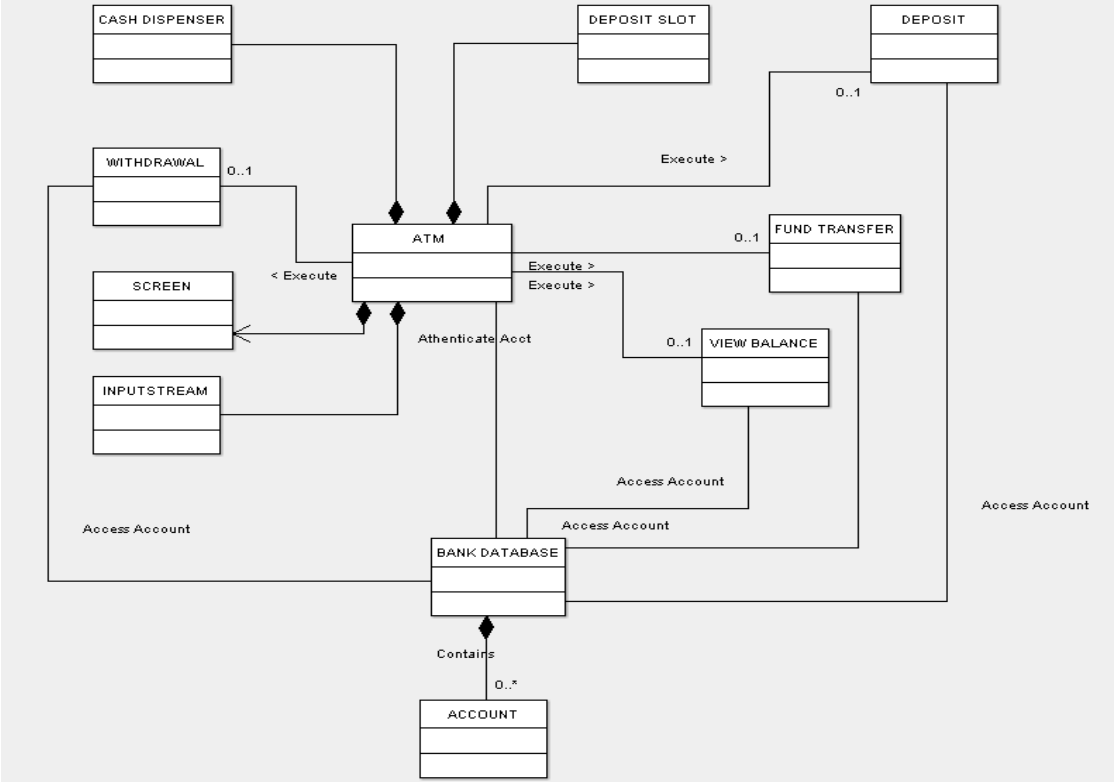

Fig. 4. Class Diagram for the ATM system.

is maintained. The implication of this is that the logic state of a Web Services solution is basically the same as that of its object counterpart and can be modeled in the same manner. A significant difference is however evident during communication with external (Web Services) systems, when it has to perform the ritual of invocation, serialization/deserialization and deployment (Hansen, 2007). At this stage UML modeling symbols proved inadequate and we had to adopt the SOAP router class symbol in Hansen (2007), which is reproduced in figure 5. This compound symbol aggregates UML symbols with the exception of the SOAP symbol which emphasizes the basic transportation mode of Web Services. The UML symbol usage is consistent with the original UML

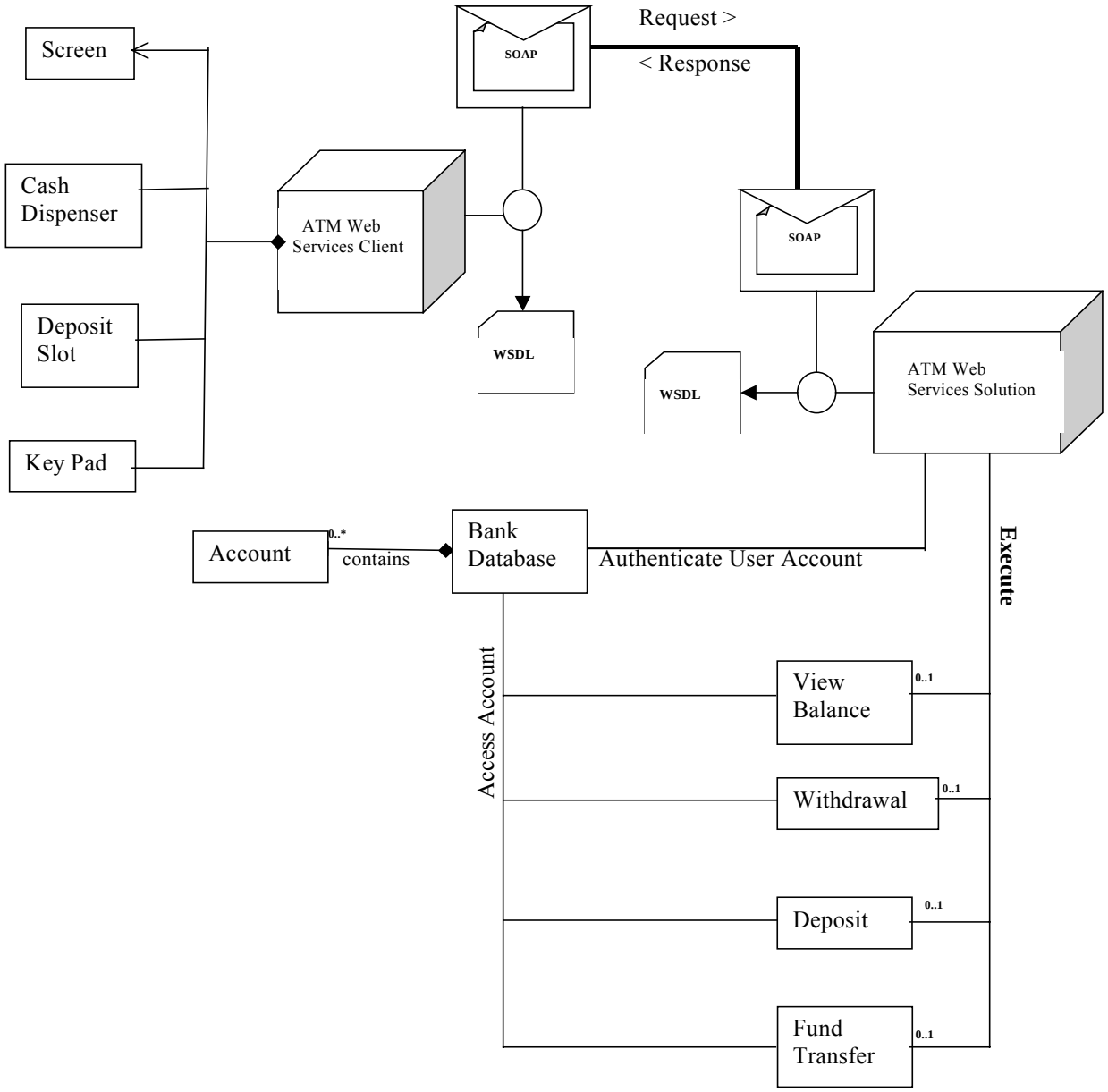

Fig. 4. Equivalent Service Model for the ATM system using Modified UML.

definitions (Rumbaugh *et al*., 1999). Figure 6 captures the sequence diagram for the Fund Transfer ATM service.

Java Application Programming Interfaces (APIs) were selected to design the implementation equivalent of ROA, depicted in figure7, for a single set of service replica. The Java EE programming models selected were Servlet, Enterprise Java Bean (EJB), Java Messaging Service (JMS) and SOAP with Attachment API for Java (SAAJ) (Crawford and Farley, 2006; Jendrock *et al*., 2006).

The EJB-endpoint is a service replica – the Web Services endpoint. As figure 7 shows, the replication logic of ROA is implemented as Java Messaging Service (JMS) on Java Servlet. Besides strength of realization, these APIs ensures portability, loose coupling, and very low overhead of WSTPRL – the virtual WS-Server (Crawford and Farley, 2006). In particular, a Servlet is persistent i.e. instead of shutting down at the end of each request the servlet can remain loaded, ready to handle subsequent requests (Crawford and Farley, 2006; Jendrock *et al*., 2006) and this guarantees a continuous active state of the WSTPRL. As depicted in figure 7, servlet accepts requests from the WS-Client and passes it (as JMS message producer) to the JMS messaging domain (Queue) from where the EJB-endpoints, which also serves as a

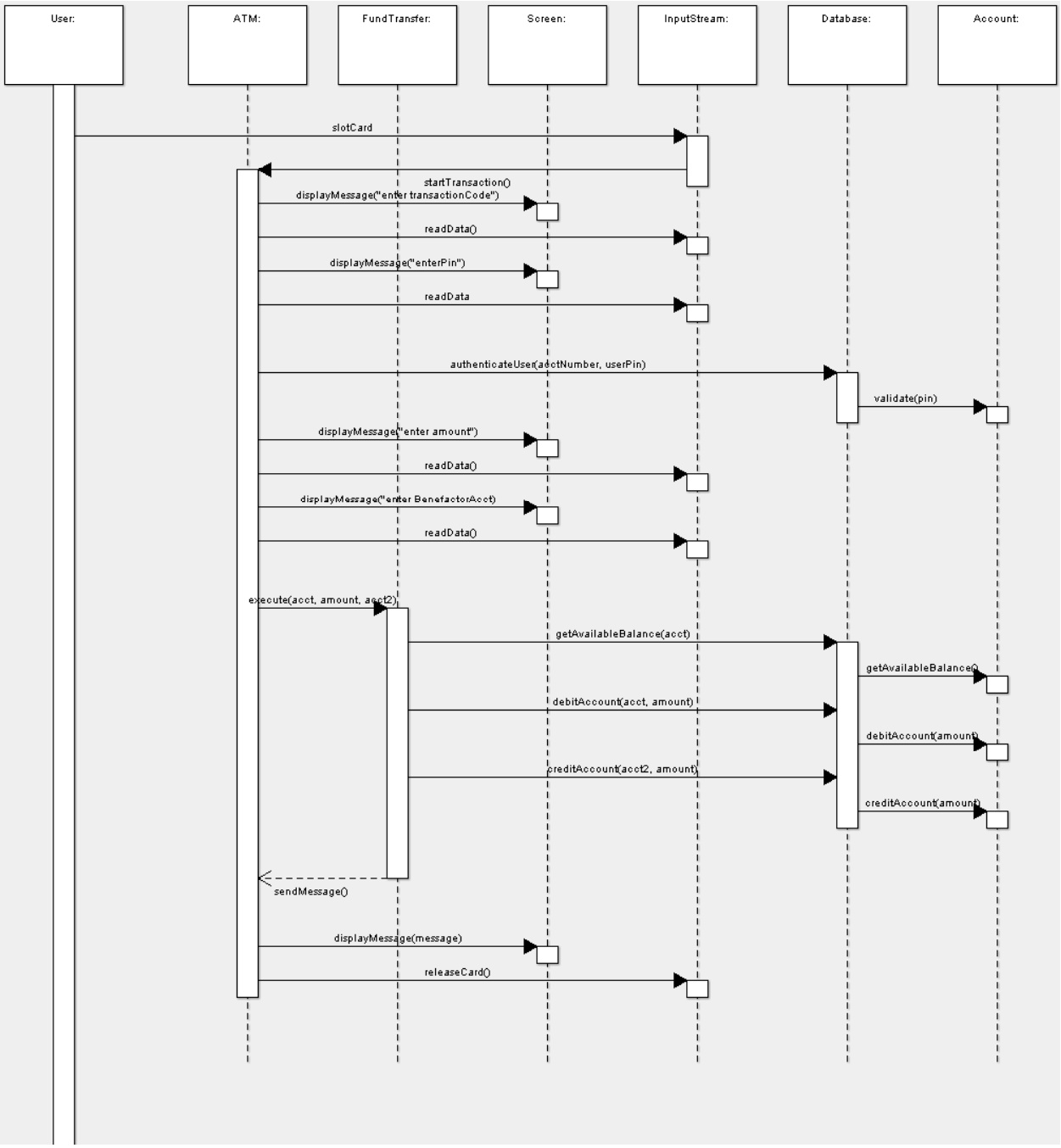

Fig. 5. Sequence Diagram for Fund Transfer ATM Service.

JMS message consumer, fetches messages asynchronously. This fetching by an EJB-endpoint is done as soon as it has no "job on hand". Clearly, the JMS provider can handle any (increasing) number of service replicas as though it is just one i.e. seamlessly accommodates replica growth.

We also made use of a small sized database built using Java DB – an open source Relational Database Management System (RDBMS) for 20 account holders with a varying fictitious amount in the accounts; as captured in figure 8. Each account has three fields: account number, account pin and available amount.

In all, eleven Web services solutions were built on the API's of the Java platform using NetBeans 6.0. Ten of these solutions were built using the Java equivalent of ROA (Fig. 7) with each differing in their number of endpoint replicas in the range of one to ten while the remaining one was not built on ROA but using JAX-WS

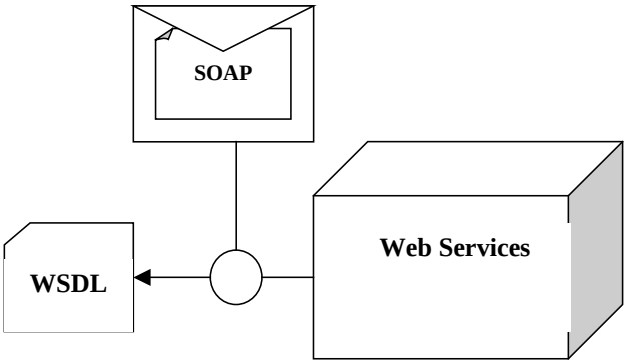

Fig. 6. Symbol for modeling SOAP Router Class.

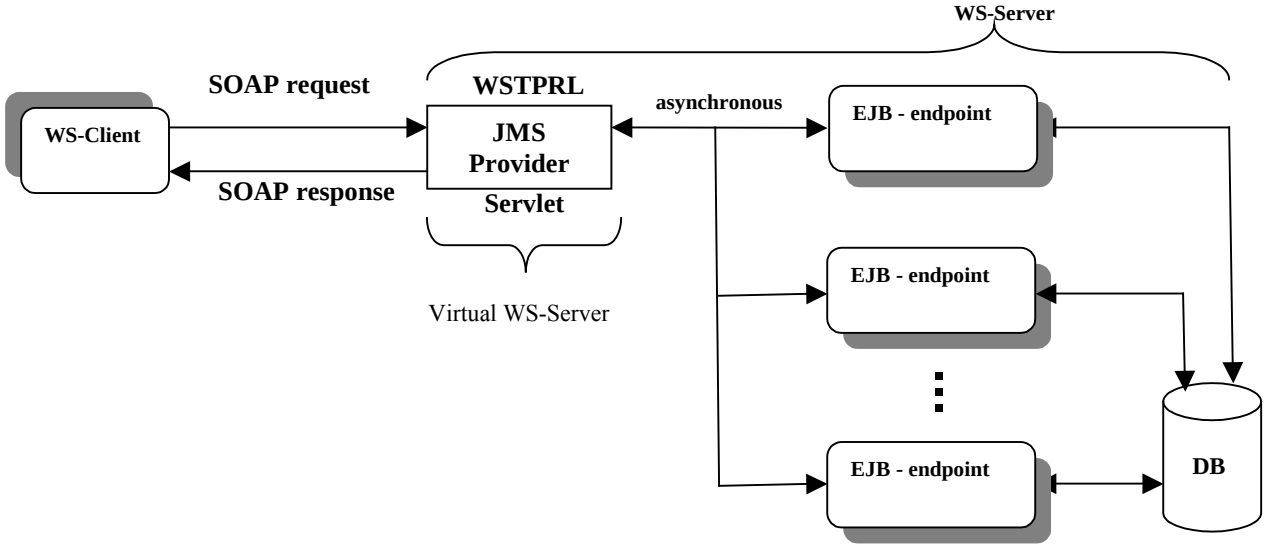

Fig. 7. ROA Implementation Equivalent using Java Technology.

API for Java (Deitel and Deitel, 2010; Crawford and Farley, 2006; Jendrock *et al*., 2006). This last solution is hereafter referred to as the conventional solution while the others will be referred to as ROA solutions.

These systems are all server side applications and we therefore need a client to consume them. Apache JMeter will play this role. Apache JMeter is not only a load generator but also load testing tool. It can handle any type of request from HTTP requests to SOAP request depending on how its test plan is prepared.

We subjected the solutions to load performance test under varying loads (sample size) ranging from one to 2000 requests per five seconds using Apache JMeter. The resultant data sample throughput and response time for each of the applications were collected. We then entered this data into Microsoft Excel for appropriate manipulation and computation of scalability. The manipulation and computation were based on the mathematical model for estimating the computational strength of applications with increasing requests (Ekuobase, 2009), given by:

$$\text{if } |S_{ij} - S_{ij+1}| < \xi \quad \text{for all j in J,} \tag{1}$$

where ξ is the user degradation tolerance, we say application i is scalable. Where S_{ij} is the computational strength of an application i for j request per square unit time and is given by:

$$S_{ij} = K * (T_{ij}/R_{ij}) \tag{2}$$

Where k is a constant denoting server and hardware strengths, T_{ij} = application throughput per unit request; T_{ij} is converted to per millisecond (ms), R_{ij} = application mid response time for a given set of request (sample) in millisecond (ms), i represents the application; in our case, i = 0(1) 10 ; where i = 0 is for the application realized by the conventional approach otherwise i denotes application realized by ROA and in particular denotes the number of endpoint replicas in the application. j = sample size per unit time; in our case, we defined j to be in the set J = {1, 5, 10, 50, 100, 150, 200, 250, 300, 350, 400, 450, 500, 550, 600, 650, 700, 750,800,850,900,950,1000, 1100,

Table 2. Scalability Data for Web Services Solution built using the Conventional Approach.

Runs Number	Number of Request (sample size)	Throughput in per minute	Per request Throughput in per minutes	Per request Throughput in per ms (T_{ij})	Mid-response of sample size (R_{ij}) in ms	Computational strength per unit request (S_{ij}) in $(ms)^{-2}$	Performance degradation in $(ms)^{-2}$
1	1	14.3301	14.3301	0.003981	4187	9.50701E-07	
2	5	37.9459	7.58918	0.002108	3969	5.31143E-07	
3	10	71.908	7.1908	0.001997	4047	4.93562E-07	3.7581E-08
4	50	335.0832	6.701664	0.001862	4110	4.52938E-07	4.06242E-08
5	100	660.9385	6.609385	0.001836	4125	4.45076E-07	7.86112E-09
6	150	971.2929	6.475286	0.001799	4016	4.47881E-07	2.80468E-09
7	200	1261.034	6.30517	0.001751	4062	4.31176E-07	1.67053E-08
8	250	1283.4774	5.13391	0.001426	4266	3.34291E-07	9.68847E-08
9	300	1178.7427	3.929142	0.001091	4187	2.60671E-07	7.36204E-08
10	350	2232.3462	6.378132	0.001772	4079	4.34347E-07	1.73677E-07
11	400	1737.4937	4.343734	0.001207	4063	2.96971E-07	1.37377E-07
12	450	1410.6583	3.134796	0.000871	4157	2.09472E-07	8.74985E-08
13	500	1330.554	2.661108	0.000739	4391	1.68344E-07	4.11288E-08
14	550	1311.7621	2.385022	0.000663	4125	1.60608E-07	7.73604E-09
15	600	1506.8436	2.511406	0.000698	4203	1.6598E-07	5.37218E-09
16	650	1381.6294	2.125584	0.00059	4297	1.37407E-07	2.85722E-08
17	700	815.1955	1.164565	0.000323	4297	7.52828E-08	6.21247E-08
18	750	1088.4288	1.451238	0.000403	10406	3.87394E-08	3.65435E-08
19	800	1344.9899	1.681237	0.000467	4203	1.11114E-07	7.23742E-08
20	850	2194.9645	2.582311	0.000717	4125	1.73893E-07	6.27794E-08
21	900	1210.1408	1.344601	0.000374	4594	8.13018E-08	9.25913E-08
22	950	1355.1102	1.426432	0.000396	4343	9.12344E-08	9.93266E-09
23	1000	1339.854	1.339854	0.000372	4421	8.4185E-08	7.04946E-09
24	1100	1335.8701	1.214427	0.000337	4344	7.76568E-08	6.5282E-09
25	1200	1400.1789	1.166816	0.000324	4578	7.07985E-08	6.85826E-09
26	1300	1239.287	0.953298	0.000265	4515	5.865E-08	1.21485E-08
27	1400	1534.4622	1.096044	0.000304	4515	6.74323E-08	8.78225E-09
28	1500	1371.1152	0.914077	0.000254	4610	5.50781E-08	1.23541E-08
29	1600	998.2115	0.623882	0.000173	11016	1.57317E-08	3.93464E-08
30	1700	1133.3726	0.66669	0.000185	5266	3.51674E-08	1.94357E-08
31	1800	1319.3418	0.732968	0.000204	6906	2.94819E-08	5.6855E-09
32	1900	1341.9184	0.706273	0.000196	6438	3.04733E-08	9.9135E-10
33	2000	1405.3003	0.70265	0.000195	5828	3.34902E-08	3.01688E-09
							$\bar{x}$ = 3.92253E-08

1200, 1300, 1400, 1500, 1600, 1700, 1800, 1900, 2000} in order. Since we will be comparing S_{ij} with each other using the same hardware and software, we let k = 1. The resultant data were then subjected to statistical analysis and interpretations.

In particular, we ascertained the scalability significance of the Web Services solution built using ROA over that built using the conventional approach. Since the two classes of Web Services solution were built on the same problem and platforms but with different development approaches, the student t-distribution for the difference of two means was found appropriate and adopted. The samples x and y are the computational strength (performance) degradation at varying but increasing request rates for the conventional and ROA solutions respectively. Let x and y be normally distributed with means μ_x and μ_y, and variance σ_x and σ_y respectively. The problem was to decide whether or not the use of ROA will improve the scalability of the Web Services solution.

Consequently, we tested the hypothesis H_0: $\mu_x = \mu_y$ (no scalability significance between conventional and ROA solutions), H_1: $\mu_x > \mu_y$ (conventional solution significantly scalable) and H_2: $\mu_x < \mu_y$ (ROA solution significantly scalable).

RESULTS AND DISCUSSION

After configuring the JMeter, we executed the package for varying number of threads (sample size) for each of the eleven applications and the valuable data: throughput and response time were collected. Table 2 to 12 contain these data and the resultant results including their S_{ij}'s, performance degradation and the mean performance degradation for each solution. Each of the table is for a solution. These data were subjected to statistical analysis.

Table 3. Scalability Data for Web Services Solution with one replica built on ROA.

Runs Number	Number of Request (sample size)	Throughput in per minute	Per request Throughput in per minutes	Per request Throughput in per ms (T_{ij})	Mid-response of sample size (R_{ij}) in ms	Computational strength per unit request (S_{ij}) in $(ms)^{-2}$	Performance degradation in $(ms)^{-2}$
1	1	14.2214	14.2214	0.00395	4219	9.36333E-07	
2	5	38.4764	7.69528	0.002138	4188	5.10405E-07	
3	10	70.3317	7.03317	0.001954	3985	4.90253E-07	2.01524E-08
4	50	338.6387	6.772774	0.001881	4078	4.61335E-07	2.89175E-08
5	100	661.1018	6.611018	0.001836	4157	4.41759E-07	1.95761E-08
6	150	897.2186	5.9814573	0.001662	4062	4.09039E-07	3.27205E-08
7	200	1284.3638	6.421819	0.001784	4063	4.39045E-07	3.00058E-08
8	250	1313.3701	5.2534804	0.001459	4391	3.32339E-07	1.06706E-07
9	300	1298.7013	4.3290043	0.001203	4218	2.85088E-07	4.72509E-08
10	350	1176.8662	3.3624749	0.000934	4328	2.15809E-07	6.92791E-08
11	400	2473.4618	6.1836545	0.001718	4079	4.21104E-07	2.05295E-07
12	450	2095.8037	4.6573416	0.001294	5031	2.57147E-07	1.63957E-07
13	500	1609.954	3.219908	0.000894	4516	1.98056E-07	5.90913E-08
14	550	1685.5654	3.0646644	0.000851	4188	2.0327E-07	5.21466E-09
15	600	2241.3149	3.7355248	0.001038	4390	2.36366E-07	3.30956E-08
16	650	1844.4898	2.8376766	0.000788	4235	1.86126E-07	5.02398E-08
17	700	1989.5784	2.8422549	0.00079	4203	1.87846E-07	1.71967E-09
18	750	1189.9592	1.5866123	0.000441	6515	6.76478E-08	1.20198E-07
19	800	1349.1484	1.6864355	0.000468	4281	1.09426E-07	4.17785E-08
20	850	1437.8753	1.691618	0.00047	4265	1.10174E-07	7.48043E-10
21	900	1573.0599	1.7478443	0.000486	4485	1.08252E-07	1.92195E-09
22	950	1126.9722	1.1862865	0.00033	4406	7.47898E-08	3.34626E-08
23	1000	1484.928	1.484928	0.000412	4250	9.70541E-08	2.22643E-08
24	1100	1211.3848	1.1012589	0.000306	16672	1.83484E-08	7.87057E-08
25	1200	1352.1711	1.1268093	0.000313	4547	6.88372E-08	5.04887E-08
26	1300	1221.0341	0.939257	0.000261	4828	5.40399E-08	1.47972E-08
27	1400	1409.9164	1.0070831	0.00028	4782	5.84996E-08	4.45973E-09
28	1500	1284.2832	0.8561888	0.000238	4859	4.89463E-08	9.55332E-09
29	1600	1360.8142	0.8505089	0.000236	6266	3.77039E-08	1.12425E-08
30	1700	1466.2967	0.8625275	0.00024	6000	3.99318E-08	2.22795E-09
31	1800	1106.1041	0.6145023	0.000171	5891	2.89756E-08	1.09563E-08
32	1900	1331.6201	0.7008527	0.000195	6437	3.02441E-08	1.26854E-09
33	2000	1253.6696	0.6268348	0.000174	4844	3.59457E-08	5.70156E-09
							$\bar{x}$=4.13869E-08

The performance degradation defined by equation (1) is stored in the S_{ij+1} row in each table. Observe that we began computing performance degradation from the 2nd run (5 request load). This is because Apache JMeter was configured to load test in 5 seconds i.e. its ramp-up time. Apache JMeter, (http://jakarta.apache.org/), demands that ramp-up time should not be too small or too large.

It will be noted that the two sets of Web services solution were built on the same platform, using the same technology except that the ROA's solutions were built on unique development architecture – ROA. It is also important to note that the performance load test and request generator was handled by the same package – Apache JMeter, and configured the same way.

The samples x and y are the performance degradation at varying but increasing request rates for the conventional and ROA solutions respectively. Let x and y be normally distributed with means μ_x and μ_y, and variance σ_x and σ_y respectively. The problem is to decide whether or not the use of ROA will improve the scalability of the Web Services solution. Consequently, we tested the hypothesis H_0: $\mu_x = \mu_y$ (no scalability significance between conventional and ROA systems), H_1: $\mu_x > \mu_y$ (conventional system significantly scalable) and H_2: $\mu_x < \mu_y$ (ROA system significantly scalable).

It is safe to assume $\sigma_x = \sigma_y$, and then apply the formula below (Hoel, 1962):

Table 4. Scalability Data for Web Services Solution with two replicas built on ROA.

Runs Number	Number of Request (sample size)	Throughput in per minute	Per request Throughput in per minutes	Per request Throughput in per ms (T_{ij})	Mid-response of sample size (R_{ij}) in ms	Computational strength per unit request (S_{ij}) in $(ms)^{-2}$	Performance degradation in $(ms)^{-2}$
1	1	14.7674	14.7674	0.004102	4063	1.00961E-06	
2	5	37.7977	7.55954	0.0021	4078	5.14927E-07	
3	10	70.0689	7.00689	0.001946	4141	4.70021E-07	4.49056E-08
4	50	335.6831	6.713662	0.001865	4156	4.48726E-07	2.12951E-08
5	100	614.4393	6.144393	0.001707	4140	4.12265E-07	3.64615E-08
6	150	972.973	6.4864867	0.001802	4031	4.46986E-07	3.47216E-08
7	200	1151.4105	5.7570525	0.001599	4032	3.96622E-07	5.0364E-08
8	250	1559.8246	6.2392984	0.001733	4218	4.10891E-07	1.42687E-08
9	300	1363.2233	4.5440777	0.001262	4172	3.02551E-07	1.0834E-07
10	350	1885.0987	5.3859963	0.001496	4078	3.66873E-07	6.43222E-08
11	400	1184.3079	2.9607698	0.000822	4141	1.98608E-07	1.68265E-07
12	450	1441.1529	3.202562	0.00089	4125	2.15661E-07	1.70527E-08
13	500	1441.4068	2.8828136	0.000801	4375	1.83036E-07	3.2625E-08
14	550	1317.7548	2.3959178	0.000666	4156	1.60138E-07	2.2898E-08
15	600	3674.4709	6.1241182	0.001701	4125	4.12399E-07	2.52261E-07
16	650	1539.7979	2.3689198	0.000658	4234	1.55416E-07	2.56982E-07
17	700	1664.421	2.3777443	0.00066	4406	1.49906E-07	5.51076E-09
18	750	1947.2933	2.5963911	0.000721	4265	1.69102E-07	1.91962E-08
19	800	1410.4787	1.7630984	0.00049	4297	1.13975E-07	5.51272E-08
20	850	1153.5024	1.3570616	0.000377	12687	2.97124E-08	8.42623E-08
21	900	1549.1216	1.7212462	0.000478	4235	1.12898E-07	8.31858E-08
22	950	1435.6598	1.5112208	0.00042	4437	9.46098E-08	1.82884E-08
23	1000	1459.4674	1.4594674	0.000405	4297	9.43467E-08	2.63111E-10
24	1100	1432.8203	1.3025639	0.000362	4610	7.84866E-08	1.586E-08
25	1200	1340.3079	1.1169233	0.00031	4406	7.04168E-08	8.06981E-09
26	1300	1435.301	1.1040777	0.000307	4781	6.41473E-08	6.26951E-09
27	1400	1195.2021	0.8537158	0.000237	4953	4.78787E-08	1.62686E-08
28	1500	1184.6938	0.7897959	0.000219	5406	4.05823E-08	7.29645E-09
29	1600	1231.7483	0.7698427	0.000214	5375	3.97852E-08	7.97116E-10
30	1700	1152.5548	0.6779734	0.000188	6485	2.90402E-08	1.07449E-08
31	1800	1282.3742	0.7124301	0.000198	5188	3.81452E-08	9.10495E-09
32	1900	1275.0822	0.6710959	0.000186	6422	2.90276E-08	9.11755E-09
33	2000	1176.2976	0.5881488	0.000163	7859	2.07882E-08	8.23942E-09
							$\bar{x}$=4.78182E-08

$$t = \frac{(\bar{x}-\bar{y})-(\mu_x-\mu_y)}{\sqrt{n_x s_x^2+n_y s_y^2}}\sqrt{\frac{n_x n_y (n_x+n_y-2)}{n_x+n_y}} \quad (3)$$

Where, t is the student's t distribution for difference of two means and every other elements of equation (3) assume their conventional statistical use.

In our case, sample sizes are equal and equal to 31 i.e. $n_x = n_y = 31$; therefore equation (3) can be rewritten as:

$$t = \frac{(\bar{x}-\bar{y})-(\mu_x-\mu_y)}{\sqrt{n_x s_x^2+n_y s_y^2}}\sqrt{930} \quad (4)$$

Adopting the null hypothesis H_o, we can rewrite equation (4) as (5) below:

$$t = \frac{(\bar{x}-\bar{y})}{\sqrt{n_x s_x^2+n_y s_y^2}}\sqrt{930} \quad (5)$$

but, $$ns^2 = \sum_{i=1}^{n}(x-\bar{x})^2 \quad (6)$$

Table 13 shows the computation of ns^2 for each solution: conventional solution followed by solutions built on ROA with their number of replica denoted by R1..R10. Rn means replica size is n while table 14 shows the calculation details of t, for each Web Services solution as associated.

From the student's t table (Hoel, 1962) the 0.005 critical value of t is 2.576. Observe that none of the calculated t

Table 5. Scalability Data for Web Services Solution with three replicas built on ROA.

Runs Number	Number of Request (sample size)	Throughput in per minute	Per request Throughput in per minutes	Per request Throughput in per ms (T_{ij})	Mid-response of sample size (R_{ij}) in ms	Computational strength per unit request (S_{ij}) in $(ms)^{-2}$	Performance degradation in $(ms)^{-2}$
1	1	13.9147	13.9147	0.003865	4312	8.96381E-07	
2	5	38.018	7.6036	0.002112	3890	5.42959E-07	
3	10	71.5052	7.15052	0.001986	4125	4.81516E-07	6.14427E-08
4	50	332.7418	6.654836	0.001849	4110	4.49773E-07	3.17439E-08
5	100	653.0968	6.530968	0.001814	4156	4.36515E-07	1.32573E-08
6	150	763.871	5.092473	0.001415	4157	3.40288E-07	9.62277E-08
7	200	1154.8455	5.774228	0.001604	4079	3.93222E-07	5.29342E-08
8	250	1602.7353	6.410941	0.001781	4203	4.23701E-07	3.04795E-08
9	300	1046.3291	3.487764	0.000969	6969	1.39019E-07	2.84682E-07
10	350	1611.5417	4.604405	0.001279	3985	3.20954E-07	1.81935E-07
11	400	1485.5162	3.713791	0.001032	4125	2.50087E-07	7.0867E-08
12	450	1114.8732	2.477496	0.000688	4156	1.6559E-07	8.44966E-08
13	500	1712.7198	3.42544	0.000952	4640	2.05067E-07	3.94767E-08
14	550	1558.6624	2.833932	0.000787	4188	1.87966E-07	1.71006E-08
15	600	1764.187	2.940312	0.000817	4250	1.92177E-07	4.21085E-09
16	650	1028.5898	1.582446	0.00044	7344	5.98541E-08	1.32323E-07
17	700	1852.587	2.646553	0.000735	4156	1.7689E-07	1.17036E-07
18	750	1535.5703	2.047427	0.000569	4375	1.29995E-07	4.68943E-08
19	800	1384.055	1.730069	0.000481	4250	1.13076E-07	1.6919E-08
20	850	2022.365	2.379253	0.000661	4250	1.55507E-07	4.24303E-08
21	900	1310.5842	1.456205	0.000405	4218	9.58988E-08	5.96079E-08
22	950	1503.2212	1.582338	0.00044	6172	7.12149E-08	2.46839E-08
23	1000	2019.0656	2.019066	0.000561	4390	1.27757E-07	5.65417E-08
24	1100	1535.4551	1.395868	0.000388	4328	8.9589E-08	3.81676E-08
25	1200	1621.7313	1.351443	0.000375	4547	8.25601E-08	7.0289E-09
26	1300	2714.2409	2.087878	0.00058	4797	1.20902E-07	3.83417E-08
27	1400	1230.7377	0.879098	0.000244	5547	4.40227E-08	7.68791E-08
28	1500	1037.0814	0.691388	0.000192	5985	3.20889E-08	1.19338E-08
29	1600	1226.5863	0.766616	0.000213	5438	3.91594E-08	7.07053E-09
30	1700	1147.4044	0.674944	0.000187	5110	3.66897E-08	2.46973E-09
31	1800	1029.1889	0.571772	0.000159	5500	2.88774E-08	7.81235E-09
32	1900	1055.712	0.555638	0.000154	5141	3.00221E-08	1.14479E-09
33	2000	1255.5191	0.62776	0.000174	7047	2.47449E-08	5.2772E-09
							$\bar{x}$ =5.35941E-08

value is greater than 2.576 that is the hypothesis H_1: $\mu_x > \mu_y$ is not valid and is hereby rejected. Thus, scalability conventional Web services solution is not significantly better than its equivalent solution built on ROA. This does not in any way mean that the scalability of Web services solutions built on the proposed ROA architecture is significantly better than its equivalent conventional solution.

To ascertain this latter assertion, we verified alternate hypothesis, H2:$\mu_x < \mu_y$ using the left tail t-test this time as against the right tail t-test. From the same student's t table the 0.45 critical value of t is 0.126 and only Web services solutions with five, six, seven and ten replicas have their computed t value greater than 0.126 and could be said to have significantly better scalability than its equivalent conventional Web services solution. That is H_2: $\mu_x < \mu_y$ is valid in these instances and H_0: $\mu_x = \mu_y$ holds in every other instances. Also, observe that the calculated t value for the replica five ROA's solution is highest.

We therefore assert that the scalability of Web Services solution built on ROA can be significantly better than its equivalent conventional solution depending on the replica size; an optimal replica size does exist.

Table 6. Scalability Data for Web Services Solution with four replicas built on ROA.

Runs Number	Number of Request (sample size)	Throughput in per minute	Per request Throughput in per minutes	Per request Throughput in per ms (T_{ij})	Mid-response of sample size (R_{ij}) in ms	Computational strength per unit request (S_{ij}) in $(ms)^{-2}$	Performance degradation in $(ms)^{-2}$
1	1	13.9114	13.9114	0.003864	4313	8.95961E-07	
2	5	37.6459	7.52918	0.002091	4031	5.18839E-07	
3	10	70.713	7.0713	0.001964	4078	4.8167E-07	3.71688E-08
4	50	338.6001	6.772002	0.001881	4125	4.56027E-07	2.56429E-08
5	100	676.0563	6.760563	0.001878	4157	4.51752E-07	4.27481E-09
6	150	986.7979	6.578653	0.001827	4125	4.43007E-07	8.74535E-09
7	200	1254.8363	6.274182	0.001743	4047	4.30647E-07	1.236E-08
8	250	1041.0959	4.164384	0.001157	4313	2.68206E-07	1.62441E-07
9	300	1237.3685	4.124562	0.001146	4063	2.81987E-07	1.37804E-08
10	350	1982.2541	5.663583	0.001573	4094	3.84274E-07	1.02287E-07
11	400	1708.6715	4.271679	0.001187	4172	2.84415E-07	9.98594E-08
12	450	1647.319	3.660709	0.001017	4047	2.51264E-07	3.3151E-08
13	500	3189.4535	6.378907	0.001772	4343	4.07994E-07	1.56731E-07
14	550	1117.0814	2.031057	0.000564	8218	6.8652E-08	3.39342E-07
15	600	2400	4	0.001111	4250	2.61438E-07	1.92786E-07
16	650	1799.557	2.768549	0.000769	4188	1.8363E-07	7.78081E-08
17	700	1409.5379	2.013626	0.000559	4172	1.3407E-07	4.95597E-08
18	750	1697.0886	2.262785	0.000629	4203	1.49548E-07	1.54782E-08
19	800	1650.7325	2.063416	0.000573	4250	1.34864E-07	1.46845E-08
20	850	1061.4607	1.248777	0.000347	4406	7.87296E-08	5.61342E-08
21	900	1538.7246	1.709694	0.000475	4313	1.10112E-07	3.13829E-08
22	950	1443.038	1.518987	0.000422	4235	9.96319E-08	1.04806E-08
23	1000	1448.7977	1.448798	0.000402	4438	9.06813E-08	8.95052E-09
24	1100	1453.0404	1.320946	0.000367	4453	8.24005E-08	8.28085E-09
25	1200	1677.4614	1.397885	0.000388	4484	8.65971E-08	4.19657E-09
26	1300	1407.3833	1.082603	0.000301	4844	6.20815E-08	2.45155E-08
27	1400	1147.7318	0.819808	0.000228	4750	4.7942E-08	1.41395E-08
28	1500	1087.7163	0.725144	0.000201	5844	3.44676E-08	1.34744E-08
29	1600	1535.6069	0.959754	0.000267	7063	3.77458E-08	3.27813E-09
30	1700	1629.499	0.958529	0.000266	5203	5.11739E-08	1.34282E-08
31	1800	1591.1602	0.883978	0.000246	4593	5.34617E-08	2.28772E-09
32	1900	1433.6918	0.754575	0.00021	5297	3.95703E-08	1.38913E-08
33	2000	1134.7518	0.567376	0.000158	5734	2.74859E-08	1.20844E-08
							=5.04072E-08

Table 7. Scalability Data for Web Services Solution with five replicas built on ROA.

Runs Number	Number of Request (sample size)	Throughput in per minute	Per request Throughput in per minutes	Per request Throughput in per ms (T_{ij})	Mid-response of sample size (R_{ij}) in ms	Computational strength per unit request (S_{ij}) in $(ms)^{-2}$	Performance degradation in $(ms)^{-2}$
1	1	14.6021	14.6021	0.004056	4109	9.87135E-07	
2	5	37.3506	7.47012	0.002075	4078	5.08836E-07	
3	10	71.1069	7.11069	0.001975	4094	4.8246E-07	2.63759E-08
4	50	335.6831	6.713662	0.001865	4094	4.55522E-07	2.69383E-08
5	100	651.9613	6.519613	0.001811	4156	4.35756E-07	1.97654E-08
6	150	981.6361	6.544241	0.001818	4062	4.47525E-07	1.17681E-08
7	200	992.2276	4.961138	0.001378	4078	3.37934E-07	1.09591E-07
8	250	1040.0777	4.160311	0.001156	4375	2.64147E-07	7.3787E-08
9	300	1333.9321	4.44644	0.001235	4141	2.98267E-07	3.412E-08
10	350	1286.1342	3.674669	0.001021	4094	2.49326E-07	4.89405E-08

Continued…

Table 7 continue…

Runs Number	Number of Request (sample size)	Throughput in per minute	Per request Throughput in per minutes	Per request Throughput in per ms (T_{ij})	Mid-response of sample size (R_{ij}) in ms	Computational strength per unit request (S_{ij}) in $(ms)^{-2}$	Performance degradation in $(ms)^{-2}$
11	400	1171.6462	2.929116	0.000814	4188	1.9428E-07	5.50465E-08
12	450	1394.6884	3.099308	0.000861	4219	2.04058E-07	9.77789E-09
13	500	1606.4214	3.212843	0.000892	4500	1.98324E-07	5.73391E-09
14	550	1909.6117	3.472021	0.000964	4204	2.29413E-07	3.10889E-08
15	600	1343.434	2.239057	0.000622	4219	1.47419E-07	8.19937E-08
16	650	1396.7568	2.148857	0.000597	4218	1.41514E-07	5.9052E-09
17	700	1451.7134	2.073876	0.000576	4265	1.35071E-07	6.44291E-09
18	750	1389.9614	1.853282	0.000515	4172	1.23394E-07	1.16766E-08
19	800	2019.777	2.524721	0.000701	4516	1.55295E-07	3.19007E-08
20	850	2101.7927	2.472697	0.000687	4250	1.61614E-07	6.31937E-09
21	900	1855.0964	2.061218	0.000573	4203	1.36227E-07	2.53876E-08
22	950	1706.2803	1.796085	0.000499	4281	1.16541E-07	1.96856E-08
23	1000	1437.1257	1.437126	0.000399	4375	9.12461E-08	2.5295E-08
24	1100	1381.3022	1.255729	0.000349	4422	7.88814E-08	1.23646E-08
25	1200	1666.5124	1.38876	0.000386	4375	8.81753E-08	9.29383E-09
26	1300	1516.8605	1.166816	0.000324	4438	7.30319E-08	1.51434E-08
27	1400	1090.4701	0.778907	0.000216	4687	4.61624E-08	2.68695E-08
28	1500	1230.4704	0.820314	0.000228	6688	3.40707E-08	1.20917E-08
29	1600	1140.0884	0.712555	0.000198	4782	4.13911E-08	7.32035E-09
30	1700	1055.2779	0.620752	0.000172	5922	2.9117E-08	1.2274E-08
31	1800	1246.9836	0.692769	0.000192	4765	4.03853E-08	1.12682E-08
32	1900	1104.7796	0.581463	0.000162	6906	2.3388E-08	1.69973E-08
33	2000	1166.4642	0.583232	0.000162	5875	2.7576E-08	4.18799E-09
							=2.56565E-08

Table 8. Scalability Data for Web Services Solution with six replicas built on ROA.

Runs Number	Number of Request (sample size)	Throughput in per minute	Per request Throughput in per minutes	Per request Throughput in per ms (T_{ij})	Mid-response of sample size (R_{ij}) in ms	Computational strength per unit request (S_{ij}) in $(ms)^{-2}$	Performance degradation in $(ms)^{-2}$
1	1	13.9147	13.9147	0.003865	4312	8.96381E-07	
2	5	36.5052	7.30104	0.002028	4125	4.91653E-07	
3	10	69.8162	6.98162	0.001939	4141	4.68326E-07	2.33263E-08
4	50	341.0253	6.820506	0.001895	4079	4.64473E-07	3.85331E-09
5	100	655.308	6.55308	0.00182	4094	4.44626E-07	1.98466E-08
6	150	976.3506	6.509004	0.001808	4047	4.46765E-07	2.1384E-09
7	200	1141.1183	5.705592	0.001585	4125	3.84215E-07	6.25498E-08
8	250	1533.5855	6.134342	0.001704	4234	4.02453E-07	1.82376E-08
9	300	1336.5013	4.455004	0.001238	4828	2.56318E-07	1.46135E-07
10	350	1437.4701	4.107057	0.001141	4031	2.83019E-07	2.67014E-08
11	400	1964.1542	4.910386	0.001364	4875	2.79794E-07	3.22488E-09
12	450	1807.5919	4.016871	0.001116	4282	2.60579E-07	1.92155E-08
13	500	1505.8729	3.011746	0.000837	4328	1.93299E-07	6.728E-08
14	550	1547.2618	2.813203	0.000781	6687	1.1686E-07	7.64382E-08
15	600	1331.9474	2.219912	0.000617	4203	1.46715E-07	2.98544E-08
16	650	1411.406	2.171394	0.000603	4219	1.42964E-07	3.75084E-09

Continued…

Table 8 continue…

Runs Number	Number of Request (sample size)	Throughput in per minute	Per request Throughput in per minutes	Per request Throughput in per ms (T_{ij})	Mid-response of sample size (R_{ij}) in ms	Computational strength per unit request (S_{ij}) in $(ms)^{-2}$	Performance degradation in $(ms)^{-2}$
17	700	1031.0544	1.472935	0.000409	4281	9.55731E-08	4.73908E-08
18	750	1991.6792	2.655572	0.000738	4313	1.71032E-07	7.54584E-08
19	800	1389.6911	1.737114	0.000483	4218	1.14398E-07	5.66333E-08
20	850	2238.6094	2.633658	0.000732	4250	1.72135E-07	5.77363E-08
21	900	1565.2174	1.73913	0.000483	4187	1.15379E-07	5.67555E-08
22	950	2162.2857	2.27609	0.000632	4140	1.52717E-07	3.73378E-08
23	1000	1212.1212	1.212121	0.000337	4359	7.72426E-08	7.54742E-08
24	1100	1192.8645	1.084422	0.000301	4390	6.86169E-08	8.62561E-09
25	1200	1302.0815	1.085068	0.000301	4313	6.98836E-08	1.2666E-09
26	1300	1222.628	0.940483	0.000261	4672	5.59172E-08	1.39663E-08
27	1400	1310.8819	0.936344	0.00026	4859	5.35286E-08	2.3886E-09
28	1500	1397.8879	0.931925	0.000259	4344	5.95921E-08	6.06348E-09
29	1600	1639.7083	1.024818	0.000285	4688	6.07235E-08	1.13135E-09
30	1700	1207.7581	0.710446	0.000197	5453	3.61904E-08	2.45331E-08
31	1800	1195.7991	0.664333	0.000185	8484	2.17512E-08	1.44392E-08
32	1900	1116.6931	0.587733	0.000163	5469	2.98518E-08	8.10058E-09
33	2000	1051.3405	0.52567	0.000146	5219	2.79784E-08	1.8733E-09
							$\bar{x}$ =3.19912E-08

Table 9. Scalability Data for Web Services Solution with seven replicas built on ROA.

Runs Number	Number of Request (sample size)	Throughput in per minute	Per request Throughput in per minutes	Per request Throughput in per ms (T_{ij})	Mid-response of sample size (R_{ij}) in ms	Computational strength per unit request (S_{ij}) in $(ms)^{-2}$	Performance degradation in $(ms)^{-2}$
1	1	14.171	14.171	0.00393639	4234	9.29709E-07	
2	5	38.0228	7.60456	0.00211238	4172	5.06323E-07	
3	10	70.2	7.02	0.00195	4047	4.81838E-07	2.44842E-08
4	50	331.6016	6.632032	0.00184223	4094	4.49983E-07	3.18552E-08
5	100	666.6667	6.666667	0.00185185	4125	4.48934E-07	1.04937E-09
6	150	963.2281	6.421521	0.00178376	4078	4.37409E-07	1.15244E-08
7	200	1036.4484	5.182242	0.00143951	4297	3.35004E-07	1.02406E-07
8	250	1538.4615	6.153846	0.0017094	4266	4.00704E-07	6.56997E-08
9	300	1932.7821	6.442607	0.00178961	4047	4.42207E-07	4.15037E-08
10	350	1404.4005	4.012573	0.0011146	4172	2.67163E-07	1.75044E-07
11	400	1526.8147	3.817037	0.00106029	4218	2.51372E-07	1.57907E-08
12	450	1648.3113	3.662914	0.00101748	4078	2.49504E-07	1.86851E-09
13	500	1259.023	2.518046	0.00069946	4453	1.57076E-07	9.24282E-08
14	550	1452.5287	2.640961	0.0007336	4172	1.75839E-07	1.87635E-08
15	600	1502.9433	2.504906	0.00069581	4875	1.4273E-07	3.31094E-08
16	650	2008.0321	3.08928	0.00085813	4110	2.08792E-07	6.60619E-08
17	700	1917.1954	2.738851	0.00076079	4750	1.60167E-07	4.86249E-08
18	750	2004.1865	2.672249	0.00074229	4265	1.74043E-07	1.38758E-08
19	800	1516.3002	1.895375	0.00052649	4375	1.20341E-07	5.37012E-08
20	850	1791.4852	2.10763	0.00058545	4343	1.34804E-07	1.44625E-08
21	900	1526.5186	1.696132	0.00047115	4375	1.07691E-07	2.71128E-08
22	950	1367.8249	1.439816	0.00039995	4375	9.14169E-08	1.6274E-08
23	1000	1289.4482	1.289448	0.00035818	4312	8.30659E-08	8.35099E-09
24	1100	1317.5231	1.197748	0.00033271	4563	7.29143E-08	1.01516E-08
25	1200	1242.0432	1.035036	0.00028751	4750	6.05284E-08	1.23859E-08

Continued…

Table 9 continue…

Runs Number	Number of Request (sample size)	Throughput in per minute	Per request Throughput in per minutes	Per request Throughput in per ms (T_{ij})	Mid-response of sample size (R_{ij}) in ms	Computational strength per unit request (S_{ij}) in $(ms)^{-2}$	Performance degradation in $(ms)^{-2}$
26	1300	1128.3928	0.867994	0.00024111	4657	5.17736E-08	8.75484E-09
27	1400	1106.6319	0.790451	0.00021957	4781	4.59255E-08	5.84808E-09
28	1500	1084.7425	0.723162	0.00020088	5515	3.6424E-08	9.50152E-09
29	1600	1237.2091	0.773256	0.00021479	4328	4.96288E-08	1.32048E-08
30	1700	956.6172	0.562716	0.00015631	5312	2.94258E-08	2.02029E-08
31	1800	1028.1034	0.571169	0.00015866	5062	3.13429E-08	1.91711E-09
32	1900	1159.5618	0.610296	0.00016953	5313	3.19079E-08	5.64948E-10
33	2000	1133.9047	0.566952	0.00015749	7250	2.17223E-08	1.01856E-08
							$\bar{x}$ = 3.0861

Table 10. Scalability Data for Web Services Solution with eight replicas built on ROA.

Runs Number	Number of Request (sample size)	Throughput in per minute	Per request Throughput in per minutes	Per request Throughput in per ms (T_{ij})	Mid-response of sample size (R_{ij}) in ms	Computational strength per unit request (S_{ij}) in $(ms)^{-2}$	Performance degradation in $(ms)^{-2}$
1	1	14.6592	14.6592	0.004072	4093	9.94869E-07	
2	5	36.8505	7.3701	0.002047	4016	5.09773E-07	
3	10	70.3235	7.03235	0.001953	4125	4.73559E-07	3.62145E-08
4	50	331.6383	6.632766	0.001842	4172	4.41619E-07	3.19398E-08
5	100	651.0907	6.510907	0.001809	4141	4.36751E-07	4.86828E-09
6	150	825.2338	5.501559	0.001528	4047	3.77616E-07	5.91352E-08
7	200	1275.7814	6.378907	0.001772	4047	4.37835E-07	6.02194E-08
8	250	1456.735	5.82694	0.001619	4312	3.7537E-07	6.24653E-08
9	300	1099.2366	3.664122	0.001018	4375	2.32643E-07	1.42727E-07
10	350	1367.1875	3.90625	0.001085	4110	2.64007E-07	3.13645E-08
11	400	1319.5514	3.298879	0.000916	4141	2.21288E-07	4.27188E-08
12	450	1848.1758	4.107057	0.001141	4172	2.73454E-07	5.21654E-08
13	500	2670.227	5.340454	0.001483	4391	3.37841E-07	6.43871E-08
14	550	1422.2299	2.585873	0.000718	4266	1.68377E-07	1.69464E-07
15	600	2249.7055	3.749509	0.001042	4203	2.47806E-07	7.9429E-08
16	650	1264.159	1.94486	0.00054	4172	1.29492E-07	1.18315E-07
17	700	1631.068	2.330097	0.000647	4141	1.56303E-07	2.6811E-08
18	750	1648.5328	2.198044	0.000611	4187	1.45825E-07	1.0478E-08
19	800	2022.4151	2.528019	0.000702	4234	1.65854E-07	2.00298E-08
20	850	1356.1578	1.59548	0.000443	4312	1.0278E-07	6.3074E-08
21	900	1463.1767	1.625752	0.000452	4406	1.02496E-07	2.84255E-10
22	950	1432.8448	1.508258	0.000419	4438	9.4403E-08	8.09309E-09
23	1000	2024.0767	2.024077	0.000562	4203	1.33772E-07	3.9369E-08
24	1100	1337.3465	1.21577	0.000338	5219	6.47085E-08	6.90634E-08
25	1200	1256.6103	1.047175	0.000291	4594	6.33178E-08	1.39071E-09
26	1300	1216.3301	0.935639	0.00026	4844	5.36539E-08	9.66389E-09
27	1400	1170.9928	0.836423	0.000232	5031	4.61816E-08	7.47228E-09
28	1500	1502.73	1.00182	0.000278	4719	5.89708E-08	1.27892E-08
29	1600	1348.2578	0.842661	0.000234	4812	4.86435E-08	1.03273E-08
30	1700	1416.3716	0.83316	0.000231	5344	4.33071E-08	5.33638E-09
31	1800	1517.7706	0.843206	0.000234	6328	3.70139E-08	6.29324E-09
32	1900	1243.1436	0.654286	0.000182	6891	2.63744E-08	1.06395E-08
33	2000	1505.8918	0.752946	0.000209	5078	4.11878E-08	1.48134E-08
							$\bar{x}$ = 4.1011E-08

Table 11. Scalability Data for Web Services Solution with nine replicas built on ROA.

Runs Number	Number of Request (sample size)	Throughput in per minute	Per request Throughput in per minutes	Per request Throughput in per ms (T_{ij})	Mid-response of sample size (R_{ij}) in ms	Computational strength per unit request (S_{ij}) in $(ms)^{-2}$	Performance degradation in $(ms)^{-2}$
1	1	14.4335	14.4335	0.004009	4157	9.64471E-07	
2	5	37.281	7.4562	0.002071	4094	5.05903E-07	
3	10	71.242	7.1242	0.001979	4078	4.85273E-07	2.06297E-08
4	50	333.3333	6.666666	0.001852	4094	4.52333E-07	3.29402E-08
5	100	651.8905	6.518905	0.001811	4125	4.38984E-07	1.33496E-08
6	150	953.3267	6.355511	0.001765	4047	4.36229E-07	2.75424E-09
7	200	1321.8771	6.609386	0.001836	4109	4.4681E-07	1.05803E-08
8	250	1130.7953	4.523181	0.001256	4407	2.85101E-07	1.61709E-07
9	300	1955.884	6.519613	0.001811	4062	4.4584E-07	1.6074E-07
10	350	1410.3425	4.02955	0.001119	4250	2.63369E-07	1.82471E-07
11	400	1699.115	4.247788	0.00118	4047	2.91559E-07	2.81901E-08
12	450	1453.3319	3.229626	0.000897	4203	2.13447E-07	7.81122E-08
13	500	2935.708	5.871416	0.001631	4328	3.76837E-07	1.63389E-07
14	550	1434.3372	2.607886	0.000724	5766	1.25635E-07	2.51201E-07
15	600	1656.3909	2.760652	0.000767	4312	1.7784E-07	5.22051E-08
16	650	2296.2789	3.532737	0.000981	4156	2.3612E-07	5.82799E-08
17	700	1326.0924	1.894418	0.000526	4141	1.27077E-07	1.09043E-07
18	750	1433.3934	1.911191	0.000531	4265	1.24475E-07	2.60218E-09
19	800	1541.0526	1.926316	0.000535	4141	1.29217E-07	4.74189E-09
20	850	1712.2689	2.014434	0.00056	4203	1.33135E-07	3.91764E-09
21	900	1317.0732	1.463415	0.000407	4734	8.5869E-08	4.72656E-08
22	950	2217.64	2.334358	0.000648	4281	1.51468E-07	6.55985E-08
23	1000	1462.8794	1.462879	0.000406	4625	8.78606E-08	6.3607E-08
24	1100	1758.5463	1.598678	0.000444	4390	1.01157E-07	1.32959E-08
25	1200	1278.2275	1.06519	0.000296	4672	6.33318E-08	3.78248E-08
26	1300	2080	1.6	0.000444	4454	9.97855E-08	3.64537E-08
27	1400	1326.0924	0.947209	0.000263	4828	5.44974E-08	4.5288E-08
28	1500	1564.782	1.043188	0.00029	4765	6.08131E-08	6.31568E-09
29	1600	1323.8458	0.827404	0.00023	6187	3.71479E-08	2.36652E-08
30	1700	1482.9387	0.872317	0.000242	177765	1.36309E-09	3.57849E-08
31	1800	1241.3793	0.689655	0.000192	6375	3.00503E-08	2.86872E-08
32	1900	1452.803	0.764633	0.000212	6109	3.47681E-08	4.71773E-09
33	2000	1713.4286	0.856714	0.000238	13859	1.71712E-08	1.75968E-08
							=5.68696E-08

Table 12. Scalability Data for Web Services Solution with ten replicas built on ROA.

Runs Number	Number of Request (sample size)	Throughput in per minute	Per request Throughput in per minutes	Per request Throughput in per ms (T_{ij})	Mid-response of sample size (R_{ij}) in ms	Computational strength per unit request (S_{ij}) in $(ms)^{-2}$	Performance degradation in $(ms)^{-2}$
1	1	14.2755	14.2755	0.003965	4203	9.43473E-07	
2	5	38.4763	7.69526	0.002138	4078	5.24172E-07	
3	10	71.242	7.1242	0.001979	4031	4.90931E-07	3.32403E-08
4	50	332.1891	6.643782	0.001845	4094	4.5078E-07	4.0151E-08
5	100	649.7726	6.497726	0.001805	4234	4.26293E-07	2.44876E-08
6	150	971.2929	6.475286	0.001799	4140	4.34466E-07	8.17348E-09
7	200	1101.8272	5.509136	0.00153	4219	3.6272E-07	7.17463E-08
8	250	1046.8281	4.187312	0.001163	4344	2.67758E-07	9.49616E-08

Table 12 continued…

Runs Number	Number of Request (sample size)	Throughput in per minute	Per request Throughput in per minutes	Per request Throughput in per ms (T_{ij})	Mid-response of sample size (R_{ij}) in ms	Computational strength per unit request (S_{ij}) in $(ms)^{-2}$	Performance degradation in $(ms)^{-2}$
9	300	1531.9149	5.106383	0.001418	4078	3.47827E-07	8.00689E-08
10	350	2021.1742	5.774783	0.001604	4109	3.90389E-07	4.25612E-08
11	400	1266.2903	3.165726	0.000879	4110	2.13958E-07	1.7643E-07
12	450	1339.5515	2.976781	0.000827	4172	1.98198E-07	1.57598E-08
13	500	1638.27	3.27654	0.00091	4375	2.08034E-07	9.83591E-09
14	550	1346.9388	2.44898	0.00068	4203	1.61854E-07	4.61803E-08
15	600	1691.6498	2.819416	0.000783	4218	1.85674E-07	2.38196E-08
16	650	1386.6667	2.133333	0.000593	4234	1.3996E-07	4.57131E-08
17	700	1559.1937	2.22742	0.000619	4235	1.46099E-07	6.13816E-09
18	750	1525.4237	2.033898	0.000565	4328	1.30539E-07	1.55599E-08
19	800	1252.8385	1.566048	0.000435	4187	1.03896E-07	2.66426E-08
20	850	1523.7981	1.792704	0.000498	4140	1.20283E-07	1.63872E-08
21	900	2002.8853	2.225428	0.000618	4219	1.46522E-07	2.62382E-08
22	950	1945.6581	2.048061	0.000569	4312	1.31936E-07	1.45861E-08
23	1000	1421.6662	1.421666	0.000395	4438	8.89832E-08	4.29523E-08
24	1100	1405.7903	1.277991	0.000355	4422	8.02799E-08	8.7033E-09
25	1200	1372.2388	1.143532	0.000318	4344	7.31234E-08	7.1565E-09
26	1300	1163.9012	0.895309	0.000249	4547	5.46947E-08	1.84287E-08
27	1400	1733.0665	1.237905	0.000344	5125	6.70951E-08	1.24004E-08
28	1500	1152	0.768	0.000213	5422	3.93459E-08	2.77492E-08
29	1600	1334.4825	0.834052	0.000232	6125	3.78255E-08	1.52041E-09
30	1700	1154.1726	0.678925	0.000189	6250	3.01744E-08	7.65102E-09
31	1800	1072.8809	0.596045	0.000166	4718	3.50928E-08	4.9184E-09
32	1900	1253.6014	0.65979	0.000183	5187	3.53335E-08	2.40693E-10
33	2000	1140.8254	0.570413	0.000158	5891	2.68966E-08	8.43692E-09
							$\bar{x}$ =3.09303E-08

It is also important we calculate the confidence limit for $\mu_x - \mu_y$ for those instances where ROA's solutions show significantly better scalability over their conventional equivalent. Here, equation (4) comes handy and in our case, the 90 per cent confidence limits are given by:

$$|t| < 0.126 \quad (7)$$

Substituting (4) in (7), reduces (7) to:

$$\alpha < \mu_x - \mu_y < \beta \quad (8)$$

Where α and β are the lower and upper limits respectively and are given by:

$$\alpha = (\bar{x} - \bar{y}) - 0.126\left(\frac{\sqrt{n_x s_x^2 + n_y s_y^2}}{\sqrt{930}}\right) \quad (9)$$

$$\beta = (\bar{x} - \bar{y}) + 0.126\left(\frac{\sqrt{n_x s_x^2 + n_y s_y^2}}{\sqrt{930}}\right) \quad (10)$$

Table 14 also shows these calculated values for the ROA's solutions.

Consequently, we can only guarantee α unit of increase i.e. $\alpha/\bar{x}$ per cent in scalability if ROA is used to build Web services solution. These results show that ROA can improve the scalability of a Web Services solution by 31.73% with 90% confidence.

We also wanted to know the impact of replication on the scalability of the ROA's solutions. Hence, we let ROA solution with just one replica (i.e. null replication) be the base solution and modified equations (5) and (8) into equations (11) and (12) respectively:

$$t = \frac{(\bar{y}_1 - \bar{y}_i)}{\sqrt{n_{y1} s_{y1}^2 + n_{yi} s_{yi}^2}}\sqrt{930}, \quad i = 2(1)10 \quad (11)$$

$$\alpha < \mu_{y1} - \mu_{yi} < \beta, \quad i = 2(1)10 \quad (12)$$

Where α and β are the lower and upper limits respectively and are given by:

Table 13. Table showing the computation of ns^2 for each web services solution.

$(x_i - \bar{x})^2$	Conventional	ROA, R1	ROA, R2	ROA, R3	ROA, R4	ROA, R5	ROA, R6	ROA, R7	ROA, R8	ROA, R9	ROA, R10
1	2.70382E-18	4.50908E-16	8.48304E-18	6.16004E-17	1.75257E-16	5.17614E-19	7.50801E-17	4.0671E-17	2.30066E-17	1.31333E-15	5.33613E-18
2	1.95691E-18	1.55486E-16	7.03474E-16	4.77432E-16	6.13274E-16	1.64318E-18	7.9174E-16	9.87381E-19	8.22869E-17	5.72616E-16	8.50209E-17
3	9.83713E-16	4.75714E-16	1.28975E-16	1.62706E-15	2.1282E-15	3.47052E-17	1.4749E-16	8.88766E-16	1.3063E-15	1.89399E-15	4.15089E-17
4	1.32646E-15	7.51067E-17	1.71521E-16	1.81762E-15	1.73571E-15	1.92886E-16	8.91188E-16	3.73927E-16	3.28485E-16	2.92847E-15	5.17873E-16
5	5.07151E-16	1.2953E-16	6.48095E-18	4.35426E-19	1.4476E-15	7.04497E-15	9.33827E-16	5.11855E-15	3.68962E-16	2.1427E-15	1.66595E-15
6	3.3246E-15	4.26655E-15	1.12557E-15	5.34282E-16	1.25515E-14	2.31655E-15	1.89161E-16	1.2137E-15	4.60288E-16	1.09912E-14	4.10001E-15
7	1.18302E-15	3.43859E-17	3.66286E-15	5.34018E-14	1.34152E-15	7.16306E-17	1.30288E-14	1.13255E-16	1.03462E-14	1.0789E-14	2.4146E-15
8	1.80772E-14	7.77974E-16	2.72383E-16	1.64714E-14	2.69154E-15	5.42145E-16	2.79822E-17	2.07887E-14	9.30551E-17	1.57757E-14	1.35279E-16
9	9.63367E-15	2.68658E-14	1.45075E-14	2.98355E-16	2.44552E-15	8.63776E-16	8.275E-16	2.27131E-16	2.91654E-18	8.22511E-16	2.11703E-14
10	2.3303E-15	1.50234E-14	9.46519E-16	9.54966E-16	2.97778E-16	2.5213E-16	1.63219E-16	8.40597E-16	1.24421E-16	4.5125E-16	2.30143E-16
11	3.62329E-18	3.13445E-16	2.30835E-16	1.993E-16	1.13047E-14	3.96908E-16	1.2453E-15	3.79045E-15	5.46442E-16	1.13465E-14	4.44974E-16
12	9.91574E-16	1.30843E-15	6.21018E-16	1.33177E-15	8.34834E-14	2.95115E-17	1.97553E-15	1.46363E-16	1.65E-14	3.77648E-14	2.32564E-16
13	1.14603E-15	6.8747E-17	4.17967E-14	2.4387E-15	2.02717E-14	3.17388E-15	4.56573E-18	5.05259E-18	1.47594E-15	2.17572E-17	5.05615E-17
14	1.13488E-16	7.83731E-17	4.37495E-14	6.19827E-15	7.50809E-16	3.90113E-16	7.97517E-16	1.23907E-15	5.97588E-15	1.98894E-18	2.18532E-16
15	5.2438E-16	1.57349E-15	1.78992E-15	4.02483E-15	7.18378E-19	3.69161E-16	2.37149E-16	3.15536E-16	2.01639E-16	2.72206E-15	6.14651E-16
16	7.19234E-18	6.21115E-15	8.19218E-16	4.48865E-17	1.22004E-15	1.95438E-16	1.8894E-15	2.88516E-16	9.32264E-16	2.94495E-15	2.36251E-16
17	1.09885E-15	1.53344E-19	5.34209E-17	1.34506E-15	1.27611E-15	3.89898E-17	6.07235E-16	5.2165E-16	4.40213E-16	2.7173E-15	1.83848E-17
18	5.54796E-16	1.65152E-15	1.32817E-15	1.24629E-16	3.27978E-17	3.73924E-16	6.62812E-16	2.6893E-16	4.86778E-16	2.80391E-15	2.11502E-16
19	2.84792E-15	1.55749E-15	1.25087E-15	3.61661E-17	3.61927E-16	7.23193E-20	6.13273E-16	1.40528E-17	1.65867E-15	9.22364E-17	2.20161E-17
20	8.5806E-16	6.27949E-17	8.72007E-16	8.35796E-16	1.59414E-15	3.56517E-17	2.85859E-17	2.12796E-16	1.08359E-15	7.61945E-17	2.67134E-16
21	1.03529E-15	3.65677E-16	2.26149E-15	8.68865E-18	1.71866E-15	1.30659E-19	1.89077E-15	5.06725E-16	2.6963E-18	4.53921E-17	1.44529E-16
22	1.0691E-15	1.39269E-15	1.02132E-15	2.37975E-16	1.77463E-15	1.76673E-16	5.4595E-16	4.28902E-16	7.86939E-16	1.89866E-15	4.9404E-16
23	1.04763E-15	8.28422E-17	1.57994E-15	2.16831E-15	2.13543E-15	2.67736E-16	9.44E-16	3.41351E-16	1.56977E-15	3.62704E-16	5.65194E-16
24	7.33156E-16	7.07012E-16	1.7263E-15	2.32634E-16	6.7038E-16	1.10525E-16	3.24896E-16	4.88707E-16	9.82642E-16	4.16809E-16	1.56291E-16
25	9.2678E-16	1.36362E-15	9.95379E-16	5.42193E-16	1.31535E-15	1.47142E-18	8.76313E-16	6.25674E-16	1.12485E-15	1.34133E-16	3.43358E-16
26	7.22059E-16	1.01338E-15	1.64201E-15	1.73558E-15	1.36404E-15	1.84004E-16	6.72246E-16	4.56251E-16	7.96471E-16	2.5557E-15	1.01193E-17
27	1.46668E-20	9.0869E-16	2.21098E-15	2.16444E-15	2.22115E-15	3.36214E-16	9.52329E-16	3.11762E-16	9.41488E-16	1.10253E-15	8.64942E-16
28	3.91629E-16	1.53343E-15	1.37443E-15	2.6137E-15	1.36745E-15	1.7909E-16	5.56231E-17	1.13606E-16	1.27268E-15	4.44566E-16	5.41925E-16
29	1.12492E-15	9.26027E-16	1.49872E-15	2.09597E-15	2.31549E-15	2.07022E-16	3.08072E-16	8.37781E-16	1.20532E-15	7.94245E-16	6.76619E-16
30	1.46184E-15	1.60949E-15	1.49774E-15	2.75093E-15	1.33341E-15	7.49819E-17	5.70761E-16	9.17884E-16	9.22431E-16	2.71982E-15	9.41852E-16
31	1.31105E-15	1.27345E-15	1.56648E-15	2.33452E-15	1.46864E-15	4.60896E-16	9.07086E-16	4.27496E-16	6.86316E-16	1.54235E-15	5.05952E-16
ns^2	5.53401E-14	7.22567E-14	1.3142E-13	1.09109E-13	1.63409E-13	1.83233E-14	3.31854E-14	4.18648E-14	5.27289E-14	1.20189E-13	3.79274E-14

Table 14. Table showing the computed t value and confidence limits for Conventional vs ROA's solutions.

Computed values	R1	R2	R3	R4	R5	R6	R7	R8	R9	R10
$\overline{x}-\overline{y}$	-2.16164E-09	-8.5929E-09	-1.43688E-08	-1.11819E-08	1.35688E-08	7.23414E-09	8.36376E-09	-1.78569E-09	-1.76443E-08	8.29501E-09
$n_x s_x^2+n_y s_y^2$	1.27597E-13	1.8676E-13	1.64449E-13	2.18749E-13	7.36635E-14	8.85255E-14	9.7205E-14	1.08069E-13	1.7553E-13	9.32675E-14
$\sqrt{n_x s_x^2+n_y s_y^2}$	3.57207E-07	4.32158E-07	4.05524E-07	4.67706E-07	2.7141E-07	2.97532E-07	3.11777E-07	3.28739E-07	4.18963E-07	3.05397E-07
$(\overline{x}-\overline{y})/\sqrt{n_x s_x^2+n_y s_y^2}$	-0.006051492	-0.019883704	-0.035432587	-0.023908024	0.049993858	0.02431377	0.026826084	-0.005431949	-0.042114219	0.027161365
t	-0.184545704	-0.606371487	-1.080548674	-0.729096752	1.524607762	0.741470345	0.818085603	-0.165652174	-1.284311071	0.828310308
$\left(\frac{\sqrt{n_x s_x^2+n_y s_y^2}}{\sqrt{930}}\right)$	1.17133E-08	1.4171E-08	1.32976E-08	1.53367E-08	8.89989E-09	9.75647E-09	1.02236E-08	1.07798E-08	1.37383E-08	1.00144E-08
$0.126\left(\frac{\sqrt{n_x s_x^2+n_y s_y^2}}{\sqrt{930}}\right)$	1.47587E-09	1.78555E-09	1.6755E-09	1.93242E-09	1.12139E-09	1.22932E-09	1.28817E-09	1.35825E-09	1.73103E-09	1.26181E-09
α	-3.63751E-09	-1.03784E-08	-1.60443E-08	-1.31143E-08	1.24475E-08	6.00482E-09	7.07559E-09	-3.14394E-09	-1.93753E-08	7.0332E-09
β	-6.85762E-10	-6.80735E-09	-1.26932E-08	-9.2495E-09	1.46902E-08	8.46345E-09	9.65193E-09	-4.27441E-10	-1.59133E-08	9.55682E-09
(α/$\overline{x}$) per cent	-9.273369391	-26.45854525	-40.90280964	-33.43338158	31.73322018	15.30853113	18.03832303	-8.015083425	-49.39491067	17.93024895

Table 15. Table showing the computed t value and confidence limits for the null replication ROA's solution vs other ROA's solutions.

Computed values	R2	R3	R4	R5	R6	R7	R8	R9	R10
$\overline{y_1}-\overline{y_i}$	-6.43126E-09	-1.22071E-08	-9.02029E-09	1.57305E-08	9.39577E-09	1.05254E-08	3.75944E-10	-1.54826E-08	1.04566E-08
$n_{y1}s_{y1}^2+n_{yi}s_{yi}^2$	2.03677E-13	1.81366E-13	2.35665E-13	9.058E-14	1.05442E-13	1.14122E-13	1.24986E-13	1.92446E-13	1.10184E-13
$\sqrt{n_{y1}s_{y1}^2+n_{yi}s_{yi}^2}$	4.51306E-07	4.25871E-07	4.85454E-07	3.00965E-07	3.24718E-07	3.37819E-07	3.53533E-07	4.38687E-07	3.3194E-07
$(\overline{y_1}-\overline{y_i})/\sqrt{n_{y1}s_{y1}^2+n_{yi}s_{yi}^2}$	-0.014250345	-0.028663894	-0.01858115	0.052266768	0.028935126	0.031156925	0.001063391	-0.035293159	0.031501619
t	-0.434577117	-0.874131271	-0.56664893	1.593922195	0.882402737	0.950158512	0.032429062	-1.076296682	0.96067027
$\left(\frac{\sqrt{n_{y1}s_{y1}^2+n_{yi}s_{yi}^2}}{\sqrt{930}}\right)$	1.47989E-08	1.39649E-08	1.59187E-08	9.86904E-09	1.06479E-08	1.10775E-08	1.15928E-08	1.43851E-08	1.08847E-08
$0.126\left(\frac{\sqrt{n_{y1}s_{y1}^2+n_{yi}s_{yi}^2}}{\sqrt{930}}\right)$	1.86466E-09	1.75957E-09	2.00575E-09	1.2435E-09	1.34164E-09	1.39577E-09	1.46069E-09	1.81252E-09	1.37148E-09
α	-8.29593E-09	-1.39667E-08	-1.1026E-08	1.4487E-08	8.05413E-09	9.12963E-09	-1.08475E-09	-1.72952E-08	9.08517E-09
β	-4.5666E-09	-1.04475E-08	-7.01454E-09	1.6974E-08	1.07374E-08	1.19212E-08	1.83664E-09	-1.36701E-08	1.18281E-08
(α/$\overline{y_1}$) per cent	-20.0447876	-33.74660175	-26.64135152	35.00373489	19.46055463	22.05919459	-2.620994733	-41.78894312	21.95176472

$$\alpha = (\overline{y_1} - \overline{y_i}) - 0.126\left(\frac{\sqrt{n_{y1}s_x^2 + n_{yi}s_{yi}^2}}{\sqrt{930}}\right), \text{ i =2(1)10} \quad (13)$$

$$\beta = (\overline{y_1} - \overline{y_i}) + 0.126\left(\frac{\sqrt{n_{y1}s_x^2 + n_{yi}s_{yi}^2}}{\sqrt{930}}\right), i = 2(1)10 \quad (14)$$

Similar calculations as in the cases of equations (5) and (8) were also carried out for equations (11) and (12) as shown in table 15.

This statistical result further establish the fact that an optimal replica size for maximum scalability of ROA solution exist i.e. the relationship between the replica size of ROA's solution and scalability is not linear.

CONCLUSION

ROA is capable of enhancing the scalability of Web Services solution by 32%, 90% of the time. With this development, there is renewed hope that Web Service will survive the unprecedented deployment its promises will attract. Implementers of ROA should note however that optimum replica size will vary from one solution to another and therefore will have to get the optimum replica for their solution by simply load testing the solution prior to deployment and analyzing the resultant data using the instruments as described in this paper.

Opportunities for further improvement of the scalability of Web Services solution exist:

- Strengthening the traffic handling capacity of WSTPRL.
- Support for dynamic service replication.
- The possibility of using the concept of group multicast, communication and membership to make Web Service support replication. Though a middleware approach, this may yield more scalable Web services solution.

Other areas of this research requiring further effort include:

- Determining user (client) degradation tolerance for various service domains.
- Deploying this novel Web Service architecture in real life situations.

REFERENCES

Agile Alliance. 2001. Manifesto for Agile Software Development. available online at URL: http:// www.agilemanifesto.org.

Arsanjani, A. 2004. Service-Oriented Modelling and Architecture. available online at URL: http://www.ibm.com/developerworks/library/ws-soa-design1/

Birman, KP. 2005. Reliable Distributed Systems: Technology, Web Services, and Applications. USA: Springer-Media. pp668.

Crawford, W. and Farley, J. 2006. Java Enterprise in a Nutshell, (3rd edi.). O'Reilly Media, USA. pp892.

Deitel, P. and Deitel, H. 2010. Java: How to Program, (8th edi.). Pearson Education, USA. pp1506.

Ekuobase, GO. 2006. Software Creative Milestones. Proceedings of International Conference on Advances in Engineering and Technology. Entebbe, Uganda. pp8.

Ekuobase, GO. 2009. Towards Scalable Web Services Solution. Ph.D. Thesis. University of Benin, Nigeria. pp126.

Ekuobase, G. and Onibere, E. 2011. Architecture for Scalable Web Services Solution. Canadian Journal of Pure and Applied Sciences. 5(1):1449-1453.

Hansen, MK. 2007. SOA Using Java Web Services. USA: Pearson Education. pp574.

Hoel, PG. 1966. Introduction to Mathematical Statistics, (3rd edi.). John Wiley & Sons, USA. pp427.

Horstmann, CS. and Cornel, G. 2005[a]. Core Java 2, (7th edi.). Sun Microsystems, USA. 1:762.

Horstmann, CS. and Cornel, G. 2005b. Core Java 2, (7th edi.). Sun Microsystems, USA. 2:1002.

Jendrock, E., Ball, J., Carson, D., Evans, I., Fordin, S. and Haase, K. 2006. The Java™ EE 5 Tutorial, (3rd edi.). Sun Microsystems, USA. pp1304.

van der Linden, P. 2004. Just Java 2, (6th edi.). Sun Microsystems, USA. pp816.

Ramirez, A., Vanpeperstraete, P., Rueckert, A., Odutola, K., Bennett, J., Tolke, L. and van der Wulp, M. 2006. ArgoUML User Manual: A tutorial and reference description. USA: Open Content. Also available online at http://www.opencontent.org/openpub/. pp386.

Rumbaugh, J., Jacobson, I. and Booch, G. 1999. The Unified Modelling Language Reference Manual. Addison Wesley Longman, USA. pp23-95.

Tolke, L. and Klink, M. 2006. Cook book for Developers of ArgoUML: An Introduction to Developing ArgoUML. University of California, USA. pp157.

Vawter, C. and Roman, E. 2001. J2EE vs. Microsoft.NET: A comparison of building XML-based web services. Sun Microsystems, USA. pp28.

Williams, J. 2003. The Web Services Debate: J2EE vs. .NET. Communications of the ACM. 46(6):59-63.

Zimmermann, O., Krogdahl, P. and Gee, C. 2004. Elements of Service-Oriented Analysis and Design. available online at URL:http://www.ibm.com/ developworks/ library/wssoad1/

Received: May 4, 2011; Accepted: Dec 24, 2012

SENRA Academic Publishers, British Columbia
Vol. 7, No. 1, pp. 2271-2275, Feb 2013
Online ISSN: 1920-3853; Print ISSN: 1715-9997

Canadian Journal of pure&applied sciences

EXPERIMENTAL DETERMINATION OF THE MOLECULAR WEIGHT OF SOME BINARY MIXTURES AND PETROLEUM LIQUIDS

*Isehunwa, SO, Adetoyi, GA and Oguamah, IA
Department of Petroleum Engineering, University of Ibadan, Nigeria

ABSTRACT

Accurate molecular weights of pure compounds are available and can be readily obtained in the literature. However, those of binary and multi-component mixtures are not readily available and are usually obtained from pure components by applying mixing rules, which may not be very accurate. The molecular weights of n-Nonane+n-Tetradecane, n-Hexane+n-Nonane, n-Hexane+Toluene, Toluene+n-Tetradecane and some petroleum liquids were experimentally determined using a cryoscope. The results were compared with estimates from Kay's mixing rule and the observed deviations used to modify Kay's equation in order to obtain an improved mixing rule for the molecular weight of binary mixtures. A simple relation was also established for predicting molecular weight of petroleum liquids from API gravity. The average absolute deviation (AAD) of 0.04 and 0.40 for the molecular weight of heavy and light petroleum liquids respectively represents an improvement over most of the existing correlations.

Keywords: Petroleum liquids, binary mixtures, molecular weight, mixing rule, freezing point depression.

INTRODUCTION

The molecular weight of hydrocarbon gases and liquids is very important in reservoir fluid characterization and compositional simulation. The accuracy of physical properties of hydrocarbon systems is known to affect the equation of state predictions and thermodynamic models (Whitson, 1984; Horstmann *et al*., 2000). While accurate estimates of the molecular weights of pure compounds are available in the literature and can be readily obtained, those of binary and multi-component mixtures are not and are usually obtained from pure components by applying appropriate mixing rules. When measured in the laboratory, the molecular weights of mixtures are known to be different from values obtained using 'equivalent fluid' principles by mixing pure components. Therefore, while the molecular weights of the pure components of a mixture are available, the estimated value for the complete fluid could be inaccurate. Similarly, a very accurate value of the molecular weight of a binary or complex fluid could be available, while those of the fractions could be unreliable because of the mixing rule.

Gabito *et al*. (2003) have noted that the problems associated with representing poly-disperse mixtures such as petroleum liquids are associated with the computation of average molecular weights. Kreglewski (1967) observed that the commonly used Kay's mixing rule is not very accurate for real fluids. Several theoretically-based mixing rules have been published in the literature (Panagiotopoulos and Reid, 1985; Wong and Sandler, 1992). However, Isehunwa and Falade (2007) proposed using experimental values by 'matching' the actual measured values with the 'equivalent fluid' obtained from the mixing of pure components. They suggested a simple modification of Kay's (1936) mixing rule using a substance-dependent adjustment factor obtained by trial and error. This study was aimed at improving modification of Kay's rule in binary and multicomponent hydrocarbon liquids without recourse to trial and error.

MATERIALS AND METHODS

Pure components and Petroleum mixtures with purity above 99% were obtained from different suppliers as shown in table 1.

Table 1. Properties of Pure components and Mixtures.

Substance	Supplier	Purity (%)
Benzene	BDH Chemicals	99+
n-Hexane	BDH Chemicals	99+
n-Nonane	Aldrich Chemicals	99+
n-Tetradecane	Aldrich Chemicals	99+
Toluene	BDH Chemicals	99+
DPK	AP, NNPC	99+
AGO	AP, NNPC	99+
Crude Oil	NPDC	99+

Calibration of the Cryette WR cryoscope model 5009 was done using 2.5 ml of pure benzene (42g) as solvent at the

*Corresponding author email: sunday.isehunwa@gmail.com

bath temperature of 1.5°C. Binary mixtures were prepared at different proportions of pure components. The specific gravity of all the pure liquids, binary mixtures, petroleum and petroleum products were determined using a hydrometer and converted to API gravity. The molecular weights of the liquids were determined from the cryoscope readings using equation (1):

$$MW = \frac{\text{Weight of solute x 1000 x } K_f}{\text{Weight of solvent x } \Delta FP} \quad (1)$$

Where, ΔFP is the meter reading (observed freezing point depression).

All readings were replicated three times and average values taken as the representative value.

The measured molecular weight of the binary mixtures and petroleum compounds were compared with estimated values using Kay's mixing rule and an equation was developed to relate the two. An equation was also developed to establish a relationship between the API gravity and molecular weight of the multi-component hydrocarbons.

RESULTS AND DISCUSSION

Tables 2-5 show the experimentally determined freezing point depressions and molecular weights of various for pure components and different binary mixtures. The values obtained for the pure components were chosen as control points and they generally agree with published results in the literature. Table 6 shows the measured API gravity and molecular weights of the petroleum and petroleum products. The API gravity ranged between 13 and 38, indicating rather 'heavy' liquids.

Table 2. Freezing Point Depressions and Molecular Weights of Nonane (1) + Tetradecane (2).

Mole fraction (1)	Mole fraction (2)	ΔFP milli-°C	Molecular Weight
0.0	1.0	546	198.49
0.1	0.9	549	197.40
0.2	0.8	600	180.62
0.3	0.7	608	178.25
0.4	0.6	576	188.15
0.5	0.5	648	167.24
0.6	0.4	709	152.85
0.7	0.3	720	150.52
0.8	0.2	758	142.97
0.9	0.1	823	131.68
1.0	0.0	845	128.25

Table 3. Freezing Point Depression and Molecular Weights of Hexane (1) + Nonane (2).

Mole fraction (1)	Mole fraction (2)	ΔFP milli-°C	Molecular Weight
0.0	1.0	845	128.25
0.2	0.8	930	116.53
0.4	0.6	905	119.75
0.6	0.4	1070	101.28
0.8	0.2	1121	96.68
1.0	0.0	1257	86.22

Table 4. Freezing Point Depression and Molecular Weight of Hexane (1) + Toluene (2).

Mole fraction (1)	Mole fraction (2)	ΔFP milli-°C	Molecular Weight
0.0	1.0	1176	92.15
0.2	0.8	1235	87.75
0.4	0.6	1126	96.25
0.6	0.4	1315	82.41
0.8	0.2	1230	88.11
1.0	0.0	1257	86.22

Table 5. Freezing Point Depression and Molecular Weight of Toluene (1) + Tetradecane (2).

Mole fraction (1)	Mole fraction (2)	ΔFP milli-°C	Molecular Weight
0.0	1.0	546	198.49
0.2	0.8	632	171.48
0.4	0.6	623	173.95
0.6	0.4	835	129.79
0.8	0.2	958	113.12
1.0	0.0	1176	92.15

Table 6. Freezing Point Depression and Molecular Weight of Some Complex Hydrocarbons.

Liquid	API Gravity	ΔFP milli-°C	Molecular Weight
AGO (NNPC)	12.89	489	221.62
AGO (AP)	14.38	484	223.91
DPK (NNPC)	23.99	711	152.42
DPK (AP)	25.72	667	162.48
Crude Oil (NPDC)	38.44	937	115.66

For the binary mixtures, the measured molecular weights were compared with estimates from Kay's mixing rule given as:

$$M = \sum y_i M_i \quad (2)$$

If we assume the molecular weight obtained using Kay's mixing rule is Meq, while the actual (measured) value is M, then the modified Kay's mixing rule can be obtained

from the deviations, using the approach of Isehunwa and Falade (2007) as:

$$M = [1 + \square\, y_i (1- y_i)]\, M_{eq}$$

Where,
M = Actual molecular weight measured.
M_{eq}= Molecular weight obtained from Kay's mixing rule
y_i = Mole fraction of component *i*.
M_i = Molecular weight of component *i*.
$\square$ = Component-dependent empirical constant.

Equation (3) represents an improvement on the Isehunwa-Falade adjustment factor that was obtained by trial-and-error. The empirical constants developed from the deviation of the Kay's equivalent fluid from the actual fluid are presented in Table 7. Given mole fractions and molecular weights of pure components, the actual molecular weights of binary mixtures can be obtained from the equation. Tables 8-11 show the comparison of measured values and estimates from equations (2) and (3). The measured molecular weight of the petroleum and petroleum products was statistically correlated to the API gravity to obtain the relationship defined by equation (4):

$$M = 256 - 3.65API \quad (3)$$

Equation (4) was validated with data from several Niger Delta reservoirs published by Isehunwa and Falade (2007) and compared with the Cragoe (1929), Standing (1977) and Isehunwa-Falade relations described by equations (5) – (7):

Cragoe's correlation:
$M_w = 6084/ (API-5.9)$ (5)

Standing's correlation:
$M_w = 239-2.2\ API$ (6)

Isehunwa and Falade's correlation:
$M_w = 9260.1\ (API)^{-1.2894}$ (7)

Table 12 shows the AAD obtained by applying the correlations to Niger Delta reservoir data published by Isehunwa and Falade (2007). This study provided very accurate predictions for heavy crude and petroleum products (API $\leq$ 32) and better predictions for light

Table 7. Mole fraction dependent empirical constants.

y_i	0.0	0.1	0.2	0.3	0.4	0.5	0.6	0.7	0.8	0.9	1.0
	0.00	0.35	-0.13	0.02	0.44	0.10	-0.09	0.04	0.03	-0.30	0.00

Table 8. Comparison of Experimental and Estimated Molecular Weights for Nonane (1) + Tetradecane (2) Mixtures.

Mole fraction (1)	Molecular weight		
	Experimental	Kay's Rule	This study
0.0	198.49	198.40	198.40
0.1	197.40	191.39	197.41
0.2	180.62	184.37	180.54
0.3	178.25	177.36	178.25
0.4	188.15	170.34	188.33
0.5	167.24	163.33	167.25
0.6	152.85	156.32	152.86
0.7	150.52	149.30	150.52
0.8	142.97	142.29	142.97
0.9	131.68	135.27	131.62
1.0	128.25	128.26	128.26

Table 9. Comparison of Experimental and Estimated Molecular Weights for Hexane (1) + Nonane (2) mixtures.

Mole fraction (1)	Molecular weight		
	Experimental	Kay's Rule	This study
0.0	128.25	128.26	128.26
0.2	116.53	119.84	117.35
0.4	119.75	111.43	123.19
0.6	101.28	103.01	100.74
0.8	96.68	94.60	95.05
1.0	86.22	86.18	86.18

Table 10. Comparison of Experimental and Estimated Molecular Weights for Hexane (1) + Toluene (2).

Mole fraction (1)	Molecular weight		
	Experimental	Kay's Rule	This study
0.0	92.15	92.14	92.14
0.2	87.75	90.95	89.06
0.4	96.25	89.76	99.23
0.6	82.41	88.56	86.61
0.8	88.11	87.37	87.79
1.0	86.22	86.18	86.18

Table 11. Comparison of Experimental and Estimated Molecular Weights for Toluene (1) + Tetradecane (2).

Mole fraction (1)	Molecular weight		
	Experimental	Kay's Rule	This study
0.0	198.49	198.40	198.40
0.2	171.48	177.15	173.46
0.4	173.95	155.90	172.36
0.6	129.79	134.64	131.67
0.8	113.12	113.39	113.94
1.0	92.15	92.14	92.14

hydrocarbon liquids (API ≥ 33) than Cragoe and Standing relations; the Isehunwa-Falade relation however proved best in such lighter hydrocarbons.

Table 12. AAD of different Correlations.

Correlations	Average Absolute Deviation (AAD)	
	15 – 32 API	33 - 55 API
Cragoe	1.53	1.35
Standing	0.12	0.95
Isehunwa-Falade	0.11	0.05
This Study	0.04	0.40

CONCLUSION

From the foregoing, it can be concluded that an improved empirical mixing rule based has been developed for determining the molecular weights of some binary mixtures. Similarly, an improved relation for predicting Molecular weight of petroleum oil and products from API gravity has been established.

NOMENCLATURE

AAD Average absolute deviation
AGO Automotive Gas Oil
AP African Petroleum
DPK Dual Purpose Kerosene
M molecular weight
NNPC Nigerian National Petroleum Corporation
NPDC Nigerian Petroleum Development Company
P pressure
T temperature
y mole fraction
P_b bubble point, kg/cm^2
P_c critical pressure, psia
T_b normal boiling point temperature, R
T_c critical temperature, R
M_a apparent molecular weight of a gas mixture
M_i molecular weight of the i^{th} component in the mixture
y_i mole fraction of component i in the mixture
M actual molecular weight measured
m mass of solute in solvent
ΔFP observed depression of freezing point (^{o}C)
K_f cryoscopic constant
ω ancentric factor

Subscripts
b boiling point
c critical
i property of component i

ACKNOWLEDGEMENT

The technical assistance provided by staff of Precision System Inc., USA and the laboratory staff of the department of Petroleum Engineering, University of Ibadan is acknowledged.

REFERENCES

Cragoe, CS. 1929. Thermodynamic Properties of Petroleum Products, Bureau of Standards, US Department of Commerce, Miscellaneous Publication 27.

Gabito, J. Barrufet M. and Byrant, R. 2003. Experimental and Theoretical Determination of Heavy Oil viscosity under Reservoir conditions. DOE Report DE-FG 26-99 FT 40615.

Horstmann, S., Fischer, K. and Gmehling, J. 2000. Experimental Determination of Critical Data of Mixtures and their relevance for the Development of thermodynamic Models. Chem. Eng. Sci. 56:6905-6913.

Isehunwa, OS. and Falade, GK. 2007. Improved Characterization of Heptanes-Plus Fractions of Light Crudes. Paper SPE 111918 presented at the 31st Nigeria Annual International Conference and Exhibition held in Abuja, Nigeria.

Kay, WB. 1936. Density of hydrocarbon gases and vapour. Ind. Eng. Chem. 28:1014-1019.

Kreglewski, A. 1967. A Semi-Empirical Treatment of Properties of Fluid Mixtures, Proceedings of the Thomas Alvin Boyd Lectures in Chemical Engineering; Bulletin 201, Engineering Experiment Station, Ohio State University, Columbus, Ohio, USA.

Panagiotopoulos, AZ. and Reid, RC. 1985. A New Mixing Rule for Cubic Equations of State for Highly Polar Asymmetric Systems. ACS Symp. Ser. 300, American Chemical Society, Washington, DC, USA. 571-582.

Standing, MB. 1977. Volumetric and Phase Behaviour of Oil Field Hydrocarbon Systems, SPE, Dallas, USA.

Whitson, CH. 1984. Effect of Physical Properties Estimation on Equations of State Predictions. SPEJ. December, 112-117.

Wong, DS. and Sandler, SI. 1992. A theoretically correct mixing rule for cubic equations of State. AIChE J. 38:671-680.

Received: Sept 24, 2012; Accepted: Dec 12, 2012

SENRA Academic Publishers, British Columbia
Vol. 7, No. 1, pp. 2277-2281, Feb 2013
Online ISSN: 1920-3853; Print ISSN: 1715-9997

Canadian Journal of pure&applied sciences

ESTIMATION OF EVAPORATION RATE IN UYO, NIGERIA USING THE MODIFIED PENMAN EQUATION

Utibe A Billy, Effiong U Utah and *Udosen E Akpan
Department of Physics, University of Uyo, Uyo, Akwa Ibom State, Nigeria

ABSTRACT

The rate of evaporation in Uyo (5°18'53.7''N, 7°59'39.3''E) has been estimated. The estimation is based on five meteorological data which include solar radiation, wind speed, relative humidity, pressure and temperature. These data were collected from the Nigeria Meteorological Agency in Uyo and covered a period of five years (2004 to 2008). The estimated rate of evaporation was obtained to be 2.75 ± 0.46mm/day which is very much close to that of the measured value of 2.78 ± 0.42mm/day. A high value of coefficient of determination $R^2 = 0.98$ was obtained by plotting a linear relation between the observed and the estimated evaporation. Seasonal effects were also observed in the rate of evaporation as different rates were recorded during the wet and dry seasons.

Keywords: Uyo, evaporation, estimation, seasonal.

INTRODUCTION

Evaporation involves the conversion of liquid water to water vapour at the evaporating surface such as water bodies, pavements, soils and wet vegetations. Allen and Smith (1994) observed that direct solar radiation and the ambient temperature of the air provide the necessary energy for evaporation. The rate of evaporation at any time and place depends on since meteorological factors such as wind, temperature, pressure, relative humidity and solar radiation (Thompson, 1988).

Several empirical models have been developed to estimate the rate of evaporation. Shuttleworth (1993) modified and adapted the foremost Penman equation by using SI unit to calculate evaporation. Iruthayaraj and Morachan (1977) developed appropriate local relationship between a sunken screen open pan evaporimeter and a can evaporimeter in order to determine the relationship between meteorological parameters and evaporation. It was observed that the sunken screen open pan evaporimeter recorded much lower values of evaporation than the can evaporimeter. Johnson and Sharma (2008) analyzing evaporation records in Australia observed that pan evaporation trends were mainly negative with a significant level of 5% while Penman evaporation trend was positive win no statistical significance. Rim (2004) in his study observed that solar radiation was the most sensitive meteorological factor affecting evaporation while wind speed was the least sensitive factor. Other studies on the estimation of the rate of evaporation include that of Surinder and Mahesh (2008) and Ahonsi (2004). The parameters used in estimating evaporation rate include average temperature, relative humidity, wind speed, sunshine hour, solar radiation and air pressure. In this study we develop models that correlate monthly daily evaporation with some meteorological parameter for Uyo in the Southern Nigeria.

*Corresponding author email: udosenakpan@yahoo.com

MATERIALES AND METHODS

Methodology

Data on daily solar radiation, relative humidity, maximum and minimum temperature, pressure and wind speed were obtained from the Nigeria Meteorological Agency in Uyo. The data covered the period of five years (2004 to 2008). Uyo is located on latitude 5°18'53.7''N, longitude 7°59'39.29''E and altitude of 180m above the sea level. It has equatorial climate season having much rain between March and October and dryness between November and February. Monthly averages of the data were computed and used for the analyses. The estimated evaporation rate obtained by using Penman equation modified by Shuttleworth (1993) was compared with the observed evaporation. The equation is given by

$$E_{mass} = \frac{m R_n + \gamma \times 6.43 (1+0.536 \times u_2) \delta_e}{\lambda_v (m+\gamma)} \quad (1)$$

where

E_{mass} = Evaporation rate (mm day^{-1})
m = Slope of the saturation vapour pressure curve (kPaK^{-1})
R_n = Net irradiance (MJ m^{-2} day^{-1})
γ = Psychrometric constant = $\frac{0.0016286 \times P}{\lambda_v}$ (kPaK^{-1})
U_2 = Wind speed at 2m height (m s^{-1})
δ_e = Vapour pressure deficit (kPa)

λ_v = Latent Heat of Vapourisation (MJ kg^{-1})

Estimation of Evaporation

The Shuttleworth (1993) equation given by Equation 2.2 was used to estimate the rate of evaporation in Uyo for the 5 year period (2004 – 2008). The slope of the saturation pressure curve (m) in ($kPaK^{-1}$) is given by the equation

$$m = \frac{4098\left[0.6108 \times e^{\frac{17.27 \times T}{T+237.3}}\right]}{(T+237.3)^2} \quad (2)$$

where T is the average maximum and minimum monthly temperature (FAO, 2008).

Also, the Net irradiance in (MJm^{-2} day^{-1}) is given by the equation (FAO, 2008)

$$R_n = \sigma\left[T_{max}\,K^4 + T_{min}\,K^4\right](0.34-0.14\sqrt{e_a})\left\{1.35\frac{R_s}{R_{so}} - 0.35\right\} \quad (3)$$

where

R_n = net outgoing longwave radiation [MJ m^{-2} day^{-1}],

σ = Stefan-Boltzmann constant [4.903 10^{-9} MJ K^{-4} m^{-2} day^{-1}],

$T_{max,}$ K = maximum absolute temperature during the 24-hour period [K = °C + 273.16],

$T_{min,}$ K = minimum absolute temperature during the 24-hour period [K = °C + 273.16],

e_a = actual vapour pressure [kPa],

R_s/R_{so} = relative shortwave radiation (limited to ≤ 1.0),

R_s = measured or calculated Solar radiation [MJ m^{-2} day^{-1}],

R_{so} = calculated clear-sky radiation [MJ m^{-2} day^{-1}]

where $R_{so} = (a_s + b_s)\,R_a$ (4)

and R_a is the extra terrestrial radiation for the location given by (FAO, 2008)

$$R_a = \frac{24}{\pi} \times I_{sc}\left[1+0.33\cos\left(\frac{360}{365}\right)\times d_n\right]\times[(w\sin\phi\sin\delta)+(\cos\phi\cos\delta\sin w)] \quad (5)$$

where I_{sc} is solar constant, d_n is the Julian day number. and

$$w = \cos^{-1}(-\tan\delta\tan\phi) \quad (6)$$

in which w is the sun set hour angle, δ is solar declination and Φ is the latitude.(Nwokoye, 2006).

Where no calibration has been carried out for improved a_s and b_s parameters, the values a_s = 0.25 and b_s = 0.50 are recommended (FAO, 2008).

For the purpose of this calculation, the coordinate system for the location of study is $5^0$18'53.7''N Latitude and for effective computations it is converted to decimals.

To convert, we use

$$5 + \left(18 \times \frac{1}{60}\right) + \left(53.7 \times \frac{1}{60} \times \frac{1}{60}\right) = 5.314917$$

Table 1 shows average d_n for the months of the year according to Nwokoye (2006).

Table 1. Average julian day number and declination for the months of the year.

Month	Average dn	Declination δ
January	17	-20.92
February	16	-12.95
March	16	-2.42
April	15	9.41
May	15	18.79
June	11	23.09
July	17	21.18
August	16	13.45
September	15	2.22
October	15	-9.60
November	14	-18.11
December	10	-23.05

Source: (Nwokoye, 2006)

An average of the maximum air temperature to the fourth power and the minimum air temperature to the fourth power is commonly used in the Stefan-Boltzmann equation for 24-hour time steps. The term $(0.34-0.14\sqrt{e_a})$ expresses the correction for air humidity, and will be smaller if the humidity increases. The effect of cloudiness is expressed by $(1.35\ R_s/R_{so} - 0.35)$. The term becomes smaller if the cloudiness increases and hence R_s decrease. The smaller the correct terms, the smaller the net outgoing flux of longwave radiation. The psychometric constant (ɣ) in SI Units of PaK^{-1}, relates the partial pressure of water in air to the air temperature.

It is given by the equation(FOA, 2008).

$$\gamma = \frac{(c_p)_{air} \times P}{\lambda_v \times Mw_{ratio}} \quad (7)$$

where

$(C_p)_{air}$ = the heat capacity of air = 1.006 x 10^3J/Kg

P = average monthly atmospheric pressure

λv = Latent heat of water vapourization = 2.45 x 10^6 J/Kg

Mw_{ratio} = the molecular weight ratio of water vapour to dry air.

Molecular weight of water vapour = 18 g/mol

Molecular weight of dry air = 28.9 g/mol

$$Mw_{ratio} = \frac{18}{2.89} = 0.622$$

The vapour pressure deficit (δ_e) is the difference between the saturation vapour pressure (e_s) and the actual vapour pressure (e_a) for a given time period

i.e. $\delta_e = e_s - e_a$

Saturation vapour pressure (e_s) is related to air temperature and can be calculated from air temperature for time period such as a month. The saturation vapour pressure is computed using the maximum and minimum temperature for such month to avoid underestimation of the vapour pressure deficit, thus leading to the underestimation of the rate of evaporation for the location under study (FAO, 2008).

$$e_s = \frac{e^0(T_{max}) + e^0(T_{min})}{2} \quad (8)$$

where

$$e^0(T) = 0.6108 \exp\left[\frac{17.27T}{T+237.3}\right] \quad (9)$$

$$e^0(T_{max}) = 0.6108 \exp\left[\frac{17.27T_{max}}{T_{max}+237.3}\right] \quad (10)$$

$$e^0(T_{min}) = 0.6108 \exp\left[\frac{17.27T_{min}}{T_{min}+237.3}\right] \quad (11)$$

The actual vapour pressure (e_a) can be calculated from relative humidity data depending on the availability of the data.

Therefore,

$$e_a = \frac{e^0\frac{RH_{max}}{(T_{min})}100 + e^0\frac{RH_{min}}{(T_{max})}100}{2} \quad (12)$$

e^0 (T_{min}) = saturation vapour pressure at daily minimum temperature (KPa).

e^0 (T_{max}) = saturation vapour pressure at daily maximum temperature (KPa).

RH_{max} = maximum relative humidity (%)

RH_{max} = minimum relative humidity (%)

In the absence of maximum and minimum relative humidity data Equation 3.12 is used.

$$e_a = \frac{RH_{mean}}{100}\left[\frac{e^0(T_{max}) + e^0(T_{min})}{2}\right] \quad (13)$$

where RHmean is the mean relative humidity defined as the average between RH_{max} and RH_{min}.

All the parameters for the Shuttleworth estimation of evaporation were computed and are shown in table 2.

Table 2. Parameters for the Shutleworth Estimation of Evaporation.

Months	R_n ($MJm^{-2}day^{-1}$)	e_s(KPa)	e_a(KPa)	δe(KPa)	($KPak^{-1}$)	m($KPaK^{-1}$)
January	10.28	3.96	2.80	1.16	1.954	0.141
Feb.	10.27	4.32	3.11	1.21	1.934	0.140
March	5.59	4.19	3.34	0.85	1.940	0.140
April	2.97	3.95	3.27	0.68	1.960	0.141
May	1.84	3.79	3.17	0.62	1.967	0.141
June	1.22	3.61	3.11	0.50	1.980	0.128
July	0.37	3.47	3.10	0.37	1.961	0.128
August	0.70	3.46	3.06	0.40	1.980	0.128
Sept.	0.62	3.55	3.07	0.48	1.980	0.128
October	1.66	3.73	3.16	0.57	1.967	0.128
Nov.	3.52	3.85	3.17	0.69	1.987	0.141
Dec.	7.03	3.95	3.19	0.76	1.994	0.141

Table 3. Monthly observed and estimated values of the evaporation with different meteorological parameters.

Month	Evaporation Observed (mm/day)	Evaporation Estimated (mm/day)	Average Temperature (^oC)	Pressure (mb)	Relative Humidity (%)	Solar radiation $MJm^{-2}day^{-1}$	Wind speed (m/s)
January	3.72	3.67	28.3	29.6	70.6	31.6	36.9
February	3.54	3.64	29.7	29.3	72	29.9	41.5
March	2.74	2.74	29.3	29.4	79.6	28.5	45.1
April	1.98	2.1	28.3	29.7	82.8	17.1	43.1
May	1.64	1.88	27.7	29.8	83.6	13.7	32.9
June	1.36	1.43	26.9	30	86.2	12	26.1
July	1.1	1.03	26.3	29.7	89.2	9.4	22.9
August	1.28	1.12	26.1	30	88.4	11.1	21.7
September	1.24	1.33	26.7	30	86.4	10.25	21.7
October	1.48	1.62	27.4	29.8	84.8	12.8	23
November	2.2	2.01	28	30.1	82.2	17.1	24.5
December	2.5	2.34	28.2	30.2	80.8	21.35	28.5

RESULTS AND DISCUSSION

The results of the monthly estimation of the evaporation with different meteorological parameters are presented in table 3.

Figure 1 shows the comparison between the observed and the calculated values of average evaporation over the five years period under the study. The correlation of these values is presented in figure 2, showing a high correlation coefficient of 0.98.

The rate ofnevaporation in Uyo over five years period using Shuttleworth model gives an estimated value of 2.08mm/day while the observed rate of evaporation is 2.07mm/day. It is observed that the estimated and the observed values are quite comparable. This is an indicator that the Shutleworth model used in estimating the rate of evaporation in Uyo is a good model given the meteorological and geographic parameter of the area. This model can therefore be used to estimate the rate of evaporation in the area with similar parameter where the observed data are not available.

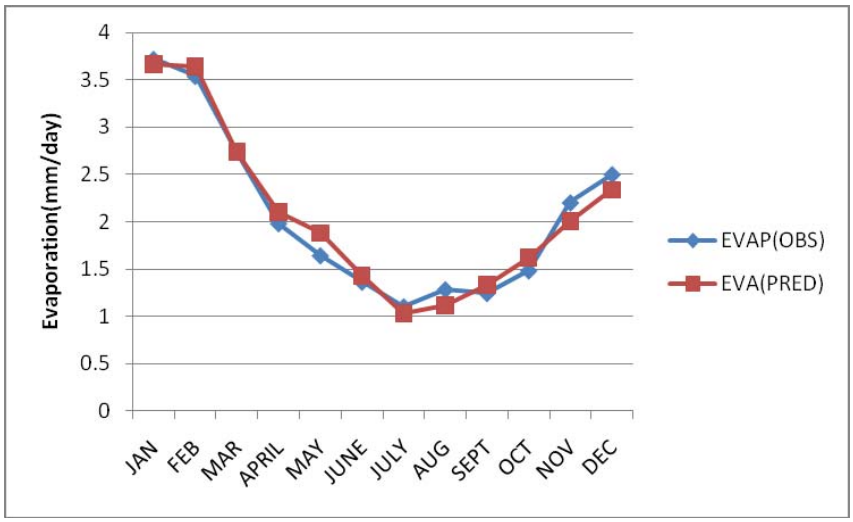

Fig. 1. Comparison of estimated and observed evaporation in Uyo.

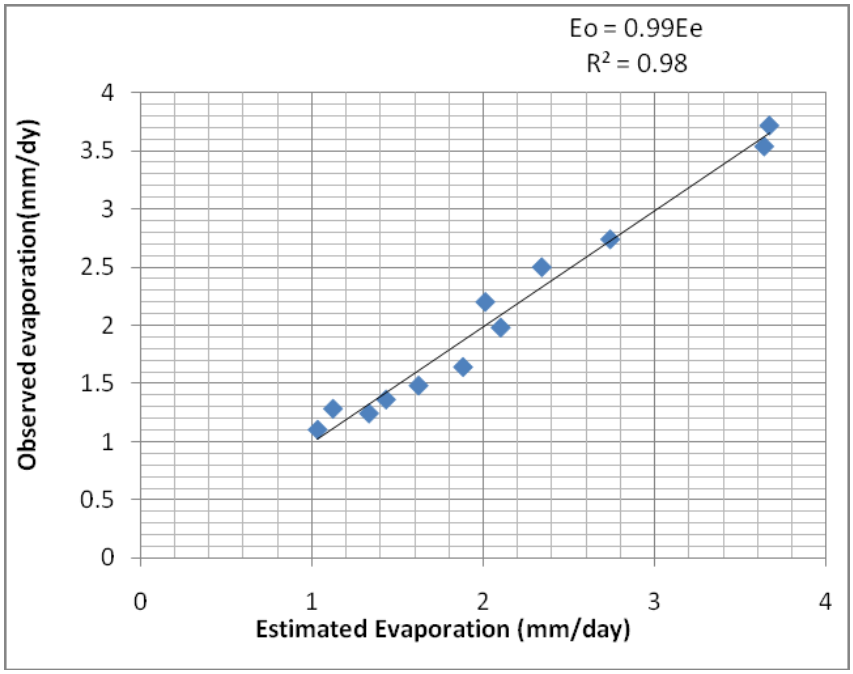

Fig. 2. Correlation between observed (Eo) and estimated (Ee) evaporation.

Comparing the results in Uyo with that of Jos in the northern part of Nigeria with evaporation rate of 5.4mm/day as observed by Ahonsi (2004), it is observed that evaporation rate in Jos is about twice higher than that of Uyo. The coefficient of determination R^2 which is a measure of how well the correlation equation fits the sample data is given in figure 2. It was observed that during the wet season which falls within the months of May and October the average rate of observed evaporation is low with the value of 1.35 ± 0.03mm/day, while that of estimated value of 1.40 ± 0.01mm/day is equally low. The low evaporation recorded during this season can be attributed to the prevailing meteorological factors of the season. These include low solar radiation, high relative humidity, and low temperature and pressure. The situation during the dry season is different. The average observed and estimated values of rate of evaporation are 2.78 ± 0.42mm/day and 2.75 ± 0.46mm/day respectively for the dry season which spands from November to April. These large values are also attributed to the prevailing meteorological factor during the period with high solar radiation, low relative humidity, and high temperature and pressure.

CONCLUSION

The rate of evaporation in Uyo has been estimated using Shuttleworth approximation with the average value of 2.75 ± 0.46 mm/day as compared with the average observed value of 2.78± 0.42 mm/day. A high value of coefficient of determination $R^2 = 0.98$ was obtained by plotting a linear relation between the observed and the estimated evaporation. Seasonal efffects are also observed on the rate of evaporation as different rates are recorded during the wet and dry seasons.

REFERENCES

Ahonsi, GE. 2004. The Effect of Solar Radiation on Evaporation at Jos, Nigeria. MSc. Thesis, University of Jos, Nigeria.

Allen, RG. and Smith, M. 1994. An update for the definition of reference Evapotranspiration. ICIO Bulletin. 43 (2):1-34.

FAO. 2008. Irrigation and drainage paper No. 24., Viale Delle Terme di Caracalla, 00100 Rome, Itally.

Iruthayaraj, MR. and Morachan, YB. 1977. Evaporation using different evaporimeters. Journal of Agriculture in the Tropics, London. 2:141-161.

Johnson, FM. and Sharma A. 2008. Estimating Evaporation – Issues and challenges, School of Civil and Environmental Journal, University of New South Wales, Australia. 3:221-237.

Nwokoye, AOC. 2006. Solar Energy Technology, other Alternative Energy Resources and Environmental Science. Rex Charles and Patrick Limited, Booksmith House, Anambra State.

Rim, CS. 2004. A Sensitivity and Error Analysis for the Penman Evapotranspiration Model. KSCE Jornal of Civil Engineering. 8(2):249-254.

Shuttleworth, WJ. 1993. Evaporation. Handbook of Hydrology. Ed. Maidment, DR. McGrew - Hill, New York, USA. 4.1-4.53.

Surinder, D. and Mahesh, P. 2008. Environmental Weather Processes. Engineering and Technology. 39:13:62-63.

Thompson, RD. 1988. Atmospheric Process and Systems. Routledge, II Fetter Lane, London. 30-65.

Received: July 14, 2012; Accepted: Nov 1, 2012

SENRA Academic Publishers, British Columbia
Vol. 7, No. 1, pp. 2283-2287, Feb 2013
Online ISSN: 1920-3853; Print ISSN: 1715-9997

Canadian Journal of pure&applied sciences

BASELINE MONITORING DATA OF VOLATILE ORGANIC COMPOUNDS (VOCs) IN TAKE LAGOS STATE, SOUTHWESTERN - NIGERIA

*Ojiodu CC[1], Okuo, JM[2] and Olumayede EG[3]
[1]Department of Chemical Sciences, Yaba College of Technology, Yaba – Lagos
[2]Department of Chemistry, University of Benin, Edo State
[3]Department of Chemical Sciences, Ondo State University of Science and Technology, Ondo State, Nigeria

ABSTRACT

The present study investigated volatile organic compounds pollution based on the principles of dilution, diffusion and dispersion in a rural fishing community of Take, Lagos state Southwestern, Nigeria. The air samples were collected by passive sampler (ORSA 5). The air samplers were exposed to a height of 1.5-2.0 m and sampling was carried out four times a month for a period of 12 months. The adsorbed VOCs were desorbed with carbondisulphide (CS_2) and the solution analysed using Gas Chromatography (GC) fitted with Flame Ionization Detector (FID). The results from analysis of the air samples collected showed that twenty (26) VOCs were captured in Take area. The VOCs were classified thus: aromatics 43%, halogenated 28%, esters 4%, ketones 13%, alcohols 6%, ethers 6%. There is a significant difference ($P_{value} < 0.05$) between the levels of VOCs in Take area. The meteorological parameters showed significant correlations with the ambient concentrations of VOCs. The principal component analysis revealed that the major sources of VOCs in Take areas are mainly Anthropogenic and three (3) factors were identified as sources of VOCs in the studied area with emissions from the waste dump dominating.

Keywords: Pollution, Baseline, gas chromatography, Sampling, anthropogenic.

INTRODUCTION

Several studies have shown that air pollution is a threat to human health (Muezzinoglu *et al*., 2001; Ho *et al*., 2002; Yamamoto, 2000; Ohura *et al.*, 2006; Simona *et al*., 2009; Zhao *et al*., 2004). VOCs are known for degrading air quality; their associated oxidants and threatening to both human health and the ecosystem (Molina *et al*., 2007; Ulman and Chilmonczyk, 2007). The short term adverse effects include conjunctive irritation, nose and throat discomfort, headache and sleeplessness, allergic skin reaction, nausea, fatique and dizziness. While the long term adverse effects include loss of coordination, leukamia, anaemia, cancer and damage to liver, kidney and central nervous system (Kim *et al*., 2001; Eljarrat and Barcelo, 2003; Environment Australia, 2001; Pohl *et al*., 2003; Kerbachi *et al*., 2006). Volatile Organic Compounds are commonly encountered by people as they go about their daily routine. Studies have shown that VOCs enter the human bloodstream through the following means inhalation, ingestion and through the skin (ATSDR, 2001). In Nigeria, air quality status of different environments has been reported (Ukepbor *et al*., 2010; Olumayede and Okuo, 2011a,b). In a previous study in Nigeria atmosphere, Olumayede *et al*. (2011a) reported that VOCs concentrations were influenced by economic activities. Similarly, Okuo *et al*. (2012) reported that ambient VOCs concentrations exhibited a significant correlation with meteorological parameters. Unfortunately, most of these studies were carried out in an urban atmosphere, while, only Okuo *et al*. (2011) reported VOC concentration in some health and financial institution Microenvironments in Benin City. In this report, VOCs levels were found to be lower than the international standards when compared.

Take is a community situated at the bank of Lagos Lagoon in Eti - osa Local Government area in Epe division of Lagos state. It is located at longitude 6.36^0 N and latitude $3.59^{0.}$. Take have a population of 108 people. The people live in make - shift stalls (houses) which are all lumped together. There are neither streets nor road network in Take. The only source of electricity is the solar power provided by the Lagos state government. Take was selected as a background study because it is an area devoid of vehicular and human activities. The only human activity in Take is fishing. Therefore, there is a need to investigate ambient air pollution by volatile organic compounds in Take areas of Lagos state. The objectives of this study are to: determine the baseline levels of Volatile Organic Compounds in Take areas of Lagos state; determine the contributions of both natural and anthropogenic sources of VOCs emitted in the areas of study.

MATERIALS AND METHODS

Sampling Locations

This study was conducted in Take areas of Lagos state. Take lies within the tropical rainforest region with two

*Corresponding author email: ojiodu1966@yahoo.com

distinct seasons: wet and dry seasons. The temperature throughout the year ranges between 21^0C and 30^0C. The humidity is relatively high while the rainfall ranges between 150mm - 200mm. The wind speed recorded during the study ranged between 3.20-6.00 ms^{-1}.

Selection of Sampling Site

The samples were collected at five sites within Take area. The sites were carefully chosen based on the following criteria: Cost of equipment, accessibility to the locations, freedom from any obstacle to the free flow of air in the vicinity and security of the sampler. The locations (sites) were chosen to reflect activities in the areas. The geo - referencing was carried out by using GARMIN GPS MAP 76S.

Table 1. Monitoring Locations, their Characteristics and Co - ordinates of Take Area.

Site	CODE	Co-ordinates	Site description
1.	TAK1	N 6^0 36' 16.7" E 3^0 58' 35.0"	A location with make - shift houses lumped together with no human activity.
2.	TAK2	N 6^0 36' 18.2" E 3^0 59' 27.9"	A location with make - shift houses lumped together with no human activity.
3.	TAK3	N 6^0 36' 40.4" E 3^0 59' 43.0"	A location with make - shift houses lumped together with no human activity.
4.	TAK4	N 6^0 36' 32.6" E 4^0 00' 07.6"	A location with make - shift houses lumped together with no human activity.
5.	TAK5	N 6^0 36' 27.4" E 3^0 59' 31.1"	A location with make - shift houses lumped together with no human activity

Sampling Device and Collection of Ambient VOCs

Ambient air samples were collected using ORSA 5 diffusion tubes from Dragger Safety, Lubeck, Germany. The Sampler comprises a glass sampling tube open at both ends and filled with activated charcoal. Each opening in sampling tube is filled with cellulose acetate diffusion barrier. Ambient air diffuses into the sampling tube in a controlled manner. The cross section, tube length and diffusion coefficient are constant and expresses the sampling rate (NIOSH, 1984).

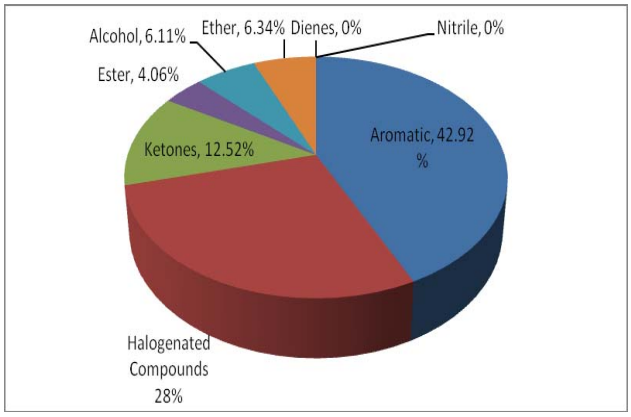

Fig. 1. Percentage Composition of each family of VOCs in Take Area.

Sampling Routine

Samplings were carried out during dry and wet seasons. The samplers were exposed at a height of 1.5 - 2.0 metres. Sampling was done 4 times a month, for a period of 12 months. The samplers were harvested after seven days and taken to the laboratory for analysis. A total of 480 samples were collected for the two seasons. During each round of ambient sampling, meterological parameters such as temperature, wind speed, wind direction and rainfall were also recorded.

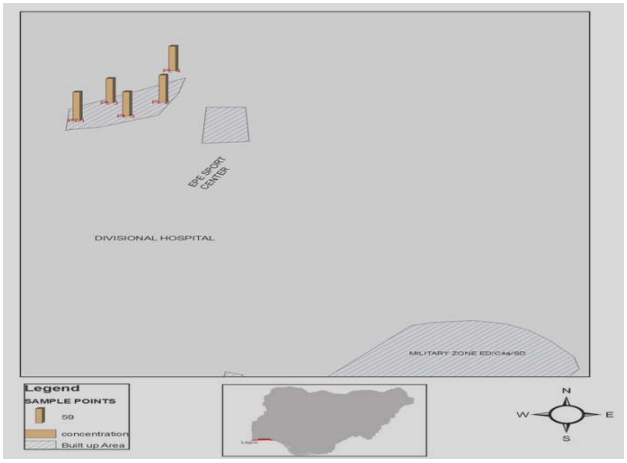

Fig. 2. GIS Map Showing the Sampling sites and in Spatial Distribution of Total VOCs Concentrations at Take Area.

ANALYTICAL METHODS

Extraction Process

After sampling, adsorption tubes were labeled and closed with special caps to avoid contamination and desorption. The samples were placed into tightly closed special plastic bags and kept in a freezer until they were processed. Before analysis, contents of both sections of the adsorbed tubes were placed into two different vials in which they were weighed, 10ml carbondisulphide (CS_2)

was added as the extraction solvent to each tube (ASTM, 1988). Samples were extracted using a magnetic stirrer (Jenweary 1103) for 30min. The extracted samples were then filtered and stored in a freezer until they were analyzed using Gas Chromatographic instrument (GC) fitted with flame ionization detector (FID). The concentrations of the analyte were read from the calibration graph, which was done with standard solution.

Chromatographic Analysis

The extracted solutions were analyzed with gas chromatograph (GC) (Perkin Elmer Clarus 500) equipped with a flame ionization detector (FID). The GC / FID was standardized and calibrated by injecting about 2µL VOC - mix into it. The GC with a capillary column (Elite - V) (40m x 0.18mm x i.d 1.0µm) was used with an initial oven temperature of 35^0C (held for 2min) increased to 60^0C at a rate of 4^0C min^{-1} (held for 0min) and finally to 225^0C at the rate of 40^0C min^{-1}(held for 5min). Helium was used as carrier gas at a constant flow rate of 45ml min^{-1}. The bake time was 8 min at 260^0C. The split ratio is 1: 40 and the injection and detection temperatures were maintained at 250^0C and 280^0C respectively.

Chemical Standards and Instrumental Calibration

External calibration was carried out with a Volatile Organic Calibration Mix containing 40 VOCs in 2000mgL^{-1} in Methanol (Supelco, Bellefonte, USA). The calibration was performed by analyzing diluted standards. The standard solution was prepared by dilution in CS_2 / methanol for gas chromatography. Seven calibration levels of concentration range of 0.1 and 3.0 mg·L^{-1} (0.1, 0.5, 1.0, 1.5, 2.0, 2.5, 3.0) with CS_2 was prepared from stock standard in a clean vial. They were freshly prepared at the moment of calibration. The instrumental calibration was performed by analyzing 2µL of the diluted standards, in order to obtain the relative response value (µv).

STATISTICAL ANALYSIS

Two - way Analysis of Variance (ANOVA) statistical test was used to evaluate significance of the differences in means, we use correlation coefficient (r^2). Sources of emission were determined using correlation coefficient ($p < 0.05$) and the factor analysis (Principal Component Analysis) (SPSS, 2007).

Factor Analysis

The Principal Component Analysis (PCA) are the primary factor analysis techniques that uses eigen value to apportion data sets to identify emission sources, chemical interaction on meterological phenomenon depending on the data sets that have been submitted to PCA. PCA is use to classify variables into groups that can then be associated with factors that contribute to pollutant levels at receptors. Three factors were extracted from Take. The first (F1), second (F2) and third (F3) factors accounted for 52.41, 32.89 and 14.70 % of the total variance.

F1: This factor is highly loaded in xylene, methylene chloride, carbontetrachloride and chloroform. The xylenes were released from waste dumpsite in the area while methylenechloride, carbontetrachloride and chloroform were released from dry cleaning processes and the use of insecticide in homes. Therefore, factor 1 is attributed to waste dumpsite and evaporative emission.

F2: Factor 2 is loaded in xylene, trichloroethane and tetrachloroethane. These solvents are released from the use of insecticides in homes and from waste dumpsite in the studied area. Hence , F2 is an indicator of emissions from evaporative sources and waste dumpsite.

F3: This factor is highly loaded in xylene, 1,2-dichloropropane and carbontetrachloride. Factor 3 is an indication of emission from waste dumpsite and evaporative sources.

Table 2. Measured Mean, Standard Deviation and Maximum values of VOCs at Take Areas (µg/m^3) n = 5.

AROMATICS VOCs	**MEAN**	**STD**	**MAX.**
Benzene	7.62	0.05	7.66
Ethylbenzene	5.26	0.13	5.48
Isopropylbenzene	3.29	0.07	3.40
Napthalene	2.37	0.06	2.46
n-Butylbenzene	2.61	0.08	2.71
n-Propylbenzene	1.97	0.05	2.03
Toluene	2.76	0.01	2.78
m+p-Xylene	18.80	0.08	18.92
o-Xylene	6.34	0.03	6.44
HALOGENATED VOCs BROMIDES			
Bromomethane	6.34	0.03	6.39
Bromoform	3.41	3.99	10.55
CHLORIDES			
Chlorobenzene	2.55	0.03	2.58
Chloroform	2.43	0.16	2.64
Carbontetrachloride	1.63	1.01	3.14
Methylenechloride	4.09	0.16	4.28
Trichloroethane	1.43	0.46	2.08
Trichlorofloromethane	2.41	0.10	2.53
1,2-dichloropropane	2.31	1.27	3.94
2,2-dichloropropane	2.66	1.27	4.05
Tetrachloroethane	2.87	1.86	4.92
KETONE VOCs			
Acetone	8.10	0.03	8.13
4-Methyl-2-Pentanone	4.98	0.06	5.05
ESTER VOC			
Isopropylacetate	4.20	0.04	4.24
ALCOHOL VOC			
Ethanol	6.31	0.09	6.43
ETHER VOC			
Tetrahydrofuran	6.62	0.01	6.62

Table 3. Total Monthly Measured VOCs Values in the Studied Areas (µg/m^3).

Months	Urban Area (Ketu-Mile 12) Mean±Sd	Rural Area (Take) Mean±Sd
January	591.53 ± 54.06	64.72 ± 6.39
February	489.87 ± 58.22	64.90 ± 6.86
March	584.56 ± 47.59	64.39 ± 8.09
April	509.18 ± 40.23	66.09 ± 5.20
May	323.28 ± 16.52	28.01 ± 6.34
June	313.12 ± 15.74	27.18 ± 4.75
July	277.97 ± 13.95	26.45 ± 2.31
August	291.99 ± 14.41	26.58 ± 2.42
September	298.75 ± 14.77	27.01 ± 5.08
October	305.62 ± 15.29	27.41 ± 5.32
November	589.02 ± 46.63	64.13 ± 5.39
December	591.73 ± 55.27	62.84 ± 7.04

RESULTS AND DISCUSSION

Twenty- Six (26) VOCs were captured in Take area (Table 1). The VOCs were classified thus: aromatics 42.92%, halogenated 28%, esters 4.06%, ketones 12.52%, alcohols 6.11% and ethers 6.34%. (Fig. 1). The most abundant compounds in Take area were BTEX and halogenated VOCs (Fig. 2). Site 5 has the most abundant BTEX (benzene 7.63, ethylbenzene 5.48, toluene 2.78 and xylenes 25.28 µg/m^3, while the lowest BTEX levels were observed at Site 2 (benzene 7.54, ethylbenzene 5.16, tuolene 2.75 and xylenes 25.09µg/m^3 (Table 2). This may be due to the principle of diffusion and dispersion of Air within and around Lagos state. The halogenated VOCs species were dominated by bromomethane, chlorobenzene, chloroform, carbon tetrachloride, trichlorofloromethane and 1,2 - dichloropropane. The mean concentrations of halogenated VOCs in the studied background area were 6.34, 2.55, 2.43, 1.63, 2.41, 2.31 µg/m^3 respectively. The halogenated VOCs not only results from the use of insecticides, cosmetics and from waste dump sites in the area. (Liu *et al*., 2008). The concentration of xylenes in Take is no doubt a reflection of the presence of dump site in the vicinity of the area. The highest Total Volatile Organic Compound was recorded in the month of April (66.09µg/m^3) while the lowest value was in July (26.45µg/m^3) (Table 3). This is because during the wet seasons, apart from dilution of the atmosphere, there is a washdown of Atmospheric Air. The Total Volatile Organic Compounds (TVOC) in Ketu - Mile 12 (urban area) is about ten (10) times the values in Take (rural area) (Table 3). Site 1 is the most polluted site in Take, apart from the presence of high human and commercial activities such as hawking of various household, consumer products and materials like footwares, cloths, plastic, detergents, inks, nail polish e.t.c in site 1, the site is located along the major roads characterized by heavy traffic (Table 4)(Olumayede *et al.*, 2012a ; Chang *et al*., 2005; Ohura *et al*., 2006; Hsieh and Tsai, 2003). There is a significant difference (P_{value} < 0.05) between VOCs in the studied background areas (Vasu *et al*., 2009; Liu *et al*., 2008; Srivastava *et al*., 2005). The level of pollution in all the sites in take is similar with site 1 having the highest level of pollution (118.42µg/m^3) (Table 4). There is a significant difference (P_{value} > 0.5) between each of meteorological factors such as temperature, relative humidity, wind speed and wind direction. The most prevailing wind direction for the year was the South - South West wind (S - SW). The Principal Component Analysis (PCA) showed that three (3) factors were identified as sources of VOCs in the studied area with emissions from waste dump dominating .

Table 4. Total Volatile Organic Compounds (TVOC), Percentage and Ranking at the Studied Areas (µg/m^3).

SITES	Ranking	Percentage %	Mean ± SD n = 10
1	1st	22.18	118.42 ± 17.86
2	2nd	21.08	112.58 ± 16.07
3	4th	18.89	100.89 ± 15.96
4	3rd	18.96	101.25 ± 20.74
5	5th	18.88	100.83 ± 18.14

CONCLUSION

Though, Take is an area devoid of pollution, the sources of pollution are basically from waste dump and evaporative sources, which occur by dilution, dispersion and diffusion of Amospheric air of Lagos-State.

ACKNOWLEDGEMENT

This study was carried out under the funding support of Nigerian Government Education Trust Fund (ETF). The authors would like to thank the Management and Staff of Vigeo Oil and Gas, Lighthouse Engineering Services and Yaba College of Technology, Lagos State, Nigerian.

REFERENCES

ASTM. 1988. Method D 3686-84: Standard practice for sampling atmospheres to collect organic compound vapours. Annual book of ASTM standard. 3(11):234-240.

ATSDR. 2001. Interaction profile of Benzene, Ethylbenzene, Toluene and Xylenes (BTEX) (draft for public comments) Atlanta: Agency for toxic Substances and diseases Registry. US Dept. of Health and Human Services.

Chang, CC., Sree, U., Lin, YS. and Lo, JG. 2005. An examination of 7.00-9.00 pm ambient air volatile organics in different seasons of Kaohsiung city, southern Taiwan. Atmos. Environ. 36:867-884.

Eljarrat, E. and Barcelo, D. 2003. Priority lists for Persistent Organic Pollutants and emerging contaminants based on their relative toxic potency in environmental samples. Trends in Analytical Chemistry. 22 :655-665.

Environmental Australia. 2001. State of Knowledge Report: Air Toxics and Indoor Air Quality in Australia, Air Toxics Section. Canberra, Australia.

Ho, KF., Lee, SC. and Chiu, GM. 2002. Characterization of selected Volatile Organic Compounds, Polycyclic aromatic hydrocarbon and Carbonyl Compounds at a roadside monitoring station: Atmos. Environ. 36:57-65.

Hsieh, CC. and Tsai, JH. 2003. VOCs concentration characteristics in Southern Taiwan. Chemosphere. 50:545-556.

Kerbachi, R., Boughedaoui, M., Bounoue, L. and Keddam, M. 2006. Ambient air pollution by aromatic hydrocarbons in Algiers. Atmos. Environ. 40:3995-4003.

Kim, YM., Harrad, S. and Harrison, RM. 2001. Concentrations and sources of VOCs in urban and public microenvironments. Environ. Sci. Tech. 35: 997-1004.

Lagos State Government LASG. 2006. Lagos State Regional plan (1980 - 2000). Ministry of Economic planning and Land Matters, Urban Regional plan Division, Ikeja, Lagos.

Liu, C., Xu, Z. and Ciuo, H. 2008. Analysis of volatile organic compounds concentration and variation trends in air of Changchum, the northeast of China. Atmospheric Environment. 34: 4459-4566.

Molina, LT., Kolb , CE., de Foy, B., Lamb, BK., Brune, WH., Jimenez, JL., Ramos - Villegas, R., Saarmiento , J., Paramo - Figueroa, VH., Cardenas , B ., Gutierrez - Avedoy, V. and Molina, MJ. 2007. Volatile Organic Compounds in Urban and industrial atmospheres: Measurement techniques and data analysis. International Journal of Environmental Analytical Chemistry. 83:199-217. doi: 10. 1080/ 6731021000050.

Muezzinoglu, A., Odabasi, M. and Onat, L. 2001. Volatile Organic Compounds in the air of Izmir, Turkey. Atmos. Environ. 35: 735- 760.

National Population Commission-NPC. 2009. Misunderstanding, Misperception and Misrepresentation of Census 2006. A rejoinder to the Publication; The Falsification of Lagos Census Figures by Lagos state.

NIOSH Publication. 1984. No 88-111. http /www .oshasic. gov./ SLT / health / guildelines.

Olumayede, EG. and Okuo, JM. 2011[a]. Variation characteristic of volatile organic compounds in the atmosphere of an urban centre. Polish Journal of Environmental studies. 21(1):177-186.

Olumayede, EG. and Okuo, JM. 2011[b]. Baseline levels of Volatile Organic Compounds in atmosphere of two urban Centre of Southwestern, Nigeria. International Journal of Chemical Science. 4(1). 45-56.

Okuo, JM., Ogbeifun, DE., Oviawe, AP. and Nwosu, EC. 2011. Air quality Status of Volatile Organic Compounds in Health and Financial Institution Microenvironments in Benin City, Nigeria. Global Journal of Pure and Applied Sciences. 17(3):299-306.

Okuo, JM., Ojiodu, CC. and Olumayede, EG. 2012. VOCs in Ketu – Mile 12 Area of Lagos, Southwestern Nigeria. Journal of Environmental Science and Engineering. A1. 766-775.

Ohura, T., Amaigai, T. and Fusaya, M. 2006. Regional assessment of ambient Volatile Organic Compounds in an industrial harbour area. Shizuoka, Japan. Atmos. Environ. 40:238-248.

Pohl, HR., Roney, N., Wilbur, S., Harrison, H., De, R. and Christopher, T. 2003. Six interaction profiles for simple mixtures: Chemosphere. 53:183-197.

Simona, N., Loris, T., Pietro, T ., Jonathan , W., Geraint. and Ovidiu, P. 2009. Determining the levels of Volatile Organic Compounds in urban Air using a Gas Chromatography - Mass Spectrometry method. 1 - 4 . J. Environ. Health.

Srivastava, A., Joseph, AE., Patil, S., More, A., Dixit, RC. and Prakash, M. 2005. Air Toxic in Ambient Air of Delhi. Atmospheric Environment. 39:59-71.

SPSS Inc. 2007. SPSS for windows, Version 15. SPSS Inc. Chicago. IIinois, USA.

Ukpebor, EE., Ukpebor, JE, Eremonene, F., Odaiase, JI. and Okoro, D. 2010. Spatial and diurnal variation of carbon dioxide pollution from motor vehicles in an urban centre. Polish Journal of Environmental studies 19 (4):817-823.

Ulman, M. and Chilmonczy, Z. 2007. Volatile Organic Compounds - Components, Sources, Determination. A review . chemia Analityczna. 52:173-200.

Vasu, T., Yoshimichi, H. and Shigeki, M. 2009. Ambient levels of volatile organic compounds in the vicinity of petrochemical industrial area of Yokohama. 1-14.

Yamamoto, N., Okayosu, HT., Muraya, S., Mori, S., Hunahashi, K. and Suzuki, K. 2000. Measurement of VOCs in the urban atmosphere of Yokohama., Japan by an automated gas around a petrochemical complex and a petroleum refinery. Sc. Total Environ. 312:103-112.

Zhao, L., Wang, X., He, Q., Wang, H., Sheng, G., Chang, LY., Fu, J. and Blake, DR. 2004. Atmos. Environ. 38:6177.

Received: Sept 18, 2012; Revised: Dec 19, 2012;
Accepted: Dec 28, 2012

SENRA Academic Publishers, British Columbia
Vol. 7, No. 1, pp. 2289-2291, Feb 2013
Online ISSN: 1920-3853; Print ISSN: 1715-9997

Canadian Journal of pure&applied sciences

Short Communication

SOME SPECIAL LAPLACE INVERSIONS

Bedier B EL-Naggar
Department of Engineering Mathematics and Physics, Cairo University, Giza, Egypt

ABSTRACT

In this paper, we establish a method for determining some special Laplace transform inversions, by forming the generating differential equations and solving by other methods. Examples of Cartesian plane methods, axially symmetric methods together with spherically symmetric cases are treated. Correspondence is made between these solutions and the solutions obtained by Laplace transform methods.

Keywords: Laplace transforms, Differential equations, Similarity solutions, Fourier transforms, Bessel functions.

INTRODUCTION

Many difficult Laplace transforms inversions can be obtained when solving initial boundary value problems. Final solutions are the results of inverting the resulting Laplace transforms. Generally speaking these inversions cannot be obtained by standard inversion methods; most powerful of which, the complex Laplace inversion method as the residues of $e^{st} f(s)$ at the poles of $f(s)$. In cases of impossibility, we search for the generating differential equation and attempt solutions by other methods, and if solutions can be obtained correspondence is to be made.

Reference is made to standard textbooks on the Laplace transform and its inversions (Gupta, 1978). Since we restrict ourselves in this paper to use similarity solutions as alternative methods we refer to (Evans, 2010).

APPLICATIONS

We start with the diffusion equation $\frac{\partial c}{\partial t} = D\,\nabla^2 c$, which reduce in one dimensional Cartesian case to:

$$\frac{\partial c}{\partial t} = D\frac{\partial^2 c}{\partial x^2} \qquad (1)$$

Together with the initial condition

$$c(x,0) = 0, \quad 0 \leq x < \infty$$

And the boundary conditions

$$c(0,t) = c_0 \quad \text{and} \quad c(\infty,t) = \frac{\partial}{\partial x}\, c(\infty,t) = 0$$

This represents diffusion in semi-infinite one dimensional slab; initially at zero concentration c (or temperature). The value of concentration or temperature at the end is a prescribed value c_0. In terms of the similarity variable (Harold, 1979) $\eta = \frac{x}{2\sqrt{Dt}}$ the solution is well known to be (DiBenedetto, 2010).

$$c(x,t) = c_0\ erfc(\eta) \qquad (2)$$

Now, let us form the solution of (1) by Laplace transform as

$$s\hat{c} = D\frac{d^2\hat{c}}{dx^2}$$

i.e. $\frac{d^2\hat{c}}{dx^2} - \frac{s}{D}\hat{c} = 0$

Which the solution

$$\hat{c}(x,s) = k\, e^{-\sqrt{\frac{s}{D}}\,x}$$

$$\hat{c}(0,s) = k = \frac{c_0}{s}$$

i.e. $\hat{c}(x,s) = \frac{c_0}{s}\, e^{-\sqrt{\frac{s}{D}}\,x}$ (3)

Obviously, comparing equations (2), (3) we can conclude

$$L^{-1}\left(\frac{1}{s}\, e^{-\sqrt{\frac{s}{D}}\,x}\right) = erfc\left(\frac{x}{2\sqrt{Dt}}\right) \qquad (4)$$

$erfc$ is the complementary error function defined by $\frac{2}{\sqrt{\pi}}\int_{\eta}^{\infty} e^{-\eta^2}\, d\eta$

Now we proceed to obtain the solution of the diffusion equation

$$\frac{\partial c}{\partial t} = D\left(\frac{\partial^2 c}{\partial r^2} + \frac{1}{r}\frac{\partial c}{\partial r}\right) \qquad (5)$$

*Corresponding author email: bbnaggar@hotmail.com

In the interior of the unit cylinder and in its exterior subject to the conditions $c(1,t) = c_0$ and $c(r,0) = 0$ for $t \geq 0$ and all radii r. Using the similarity variable $\eta = \frac{r}{2\sqrt{Dt}}$ the solution of (5) can be obtained as

$$c\left(\eta = \frac{r}{2\sqrt{Dt}}\right) = \alpha + \beta \int \frac{e^{-\eta^2}}{\eta}\, d\eta \qquad (6)$$

α , β are integration constants. For bounded solution at $r \longrightarrow \infty$

$(\eta = \infty)\ \ c(\infty,t) = 0 \ \ \therefore \ \ \alpha = 0$

Also $c(0,\infty) = c_0 \ \ (\eta = 0)$ and $c(1,t) = c_0$

Applying these boundary conditions, we obtain

$$c(r,t) = c_0 \left(1 - \frac{\int_{\frac{1}{2\sqrt{Dt}}}^{\frac{r}{2\sqrt{Dt}}} \frac{e^{-\eta^2}}{\eta} d\eta}{\int_{\frac{1}{2\sqrt{Dt}}}^{\infty} \frac{e^{-\eta^2}}{\eta} d\eta} \right) \qquad (7)$$

We now try to obtain the solution by Laplace transforms

$$s\hat{c} = D\left[\frac{d^2}{dr^2}\hat{c} + \frac{1}{r}\frac{d}{dr}\hat{c}\right]$$

i.e.

$$\frac{d^2}{dr^2}\hat{c} + \frac{1}{r}\frac{d}{dr}\hat{c} - \frac{s}{D}\hat{c} = 0$$

This is the modified Bessel equation of zero order. Bounded solution in the interior of unit circle is

$$\hat{c}\ (r,s) = \beta_1\, I_0\left(\sqrt{\frac{s}{D}}\, r\right),\ r < 1$$

I_0 is the modified Bessel function of the first kind of order zero, and bounded solutions at ∞ (Gupta, 1978b).

$$\hat{c}\ (r,s) = \beta_2\, K_0\left(\sqrt{\frac{s}{D}}\, r\right),\ \text{r} > 1$$

K_0 is the modified Bessel function of the second kind of order zero .

In both cases

$c(1,s) = \frac{1}{s} \ \ \therefore \ \ \beta_1 = \frac{1}{s}\frac{1}{I_0\sqrt{\frac{s}{D}}}$ and

$\beta_2 = \frac{1}{s}\frac{1}{K_0\sqrt{\frac{s}{D}}}$. Giving

$$c(r,t) = L^{-1}\left\{\frac{c_0}{s}\ \frac{I_0\left(\sqrt{\frac{s}{D}}\, r\right)}{I_0\left(\sqrt{\frac{s}{D}}\right)}\right\},\ r < 1 \qquad (8a)$$

And

$$c(r,t) = L^{-1}\left\{\frac{c_0}{s}\ \frac{K_0\left(\sqrt{\frac{s}{D}}\, r\right)}{K_0\left(\sqrt{\frac{s}{D}}\right)}\right\},\ r \geq 1 \qquad (8b)$$

And both two inverses are equal to

$$c(r,t) = c_0\left(1 - \frac{\int_{\frac{1}{2\sqrt{Dt}}}^{\frac{r}{2\sqrt{Dt}}} \frac{e^{-\eta^2}}{\eta} d\eta}{\int_{\frac{1}{2\sqrt{Dt}}}^{\infty} \frac{e^{-\eta^2}}{\eta} d\eta}\right)$$, for all r

For the spherically symmetric case (Beyer, 1991a).

This has the solution for $\eta = \frac{r}{2\sqrt{Dt}}$

Given by

$$c\left(\eta = \frac{r}{2\sqrt{Dt}}\right) = \gamma + \delta \int \frac{e^{-\eta^2}}{\eta^2}\, d\eta$$

γ and δ are integration constants

We can easily conclude for similar initial and boundary conditions that

$$c(r,t) = c_0\left(1 - \frac{\int_{\frac{1}{2\sqrt{Dt}}}^{\frac{r}{2\sqrt{Dt}}} \frac{e^{-\eta^2}}{\eta^2} d\eta}{\int_{\frac{1}{2\sqrt{Dt}}}^{\infty} \frac{e^{-\eta^2}}{\eta^2} d\eta}\right) \qquad (9)$$

And transform gives

$$s\hat{c} = D\left[\frac{d^2\hat{c}}{dr^2} + \frac{2}{r}\frac{d\,\hat{c}}{dr}\right]$$

i.e.

$$r^2\frac{d^2\hat{c}}{dr^2} + 2r\frac{d\,\hat{c}}{dr} - \frac{s}{D}\, r^2\, \hat{c} = 0$$

This is modified spherical Bessel equation of zero order (Beyer, 1991b) which possess a solution in terms of the spherical Bessel functions (Beyer, 1991b).

$$\hat{c}(r,s) = \delta_1\sqrt{\frac{\pi}{2}\frac{D}{s\,r}}\ J_{1/2}\left(\sqrt{\frac{s}{D}}\ r\right), \quad \text{r<1}$$

$J_{1/2}$ is the Bessel function of first kind of order $\frac{1}{2}$, and

$$\hat{c}(r,s) = \delta_2\sqrt{\frac{\pi}{2}\frac{D}{s\,r}}\ Y_{1/2}\left(\sqrt{\frac{s}{D}}\ r\right), \quad \text{r>1}$$

$Y_{1/2}$ is the Bessel function of the second kind of order $\frac{1}{2}$.

Applying conditions, we conclude that

$$L^{-1}\left\{\frac{c_0}{s}\frac{J_{1/2}\left(\sqrt{\frac{s}{D}}\,r\right)}{J_{1/2}\left(\sqrt{\frac{s}{D}}\right)}\right\}, \quad r < 1$$

$$L^{-1}\left\{\frac{c_0}{s}\frac{Y_{1/2}\left(\sqrt{\frac{s}{D}}\,r\right)}{Y_{1/2}\left(\sqrt{\frac{s}{D}}\right)}\right\}, \quad r > 1$$

Are given by the expression (9)

CONCLUSION

In this analysis we succeeded in determining some difficult inverse Laplace transforms involving special functions by employing similarity variable solutions. Other methods of solutions can be applied for comparison; such as the Fourier transform methods. If the involved integrals could be obtained; inverses can be determined explicitly. Otherwise these inversions are expressed as unevaluated integrals.

REFERENCES

Beyer, WH. 1991[a]. Standard Mathematical Tables and formulae. CRC Press, London. pp329.

Beyer, WH. 1991[b]. Standard Mathematical Tables and formulae. CRC Press, London. pp358.

DiBenedetto, E. 2010. Partial Differential Equations, (2nd edi.). Springer, NY, USA. 172-176.

Evans, LC. 2010. Partial Differential Equations, (2nd edi.). American Mathematical Society. 176-187.

Gupta, BD. 1978[a]. Mathematical Physics, Vikas publishing house, India. 856-918.

Gupta, BD. 1978[b]. Mathematical Physics. Vikas Publishing House, India. 920-921.

Harold, L. 1997. Partial Differential Equations. American Mathematical Society. 5:51-61.

Received: Dec 13, 2012; Accepted: Jan 2, 2013

SENRA Academic Publishers, British Columbia
Vol. 7, No. 1, pp. 2293-2296, Feb 2013
Online ISSN: 1920-3853; Print ISSN: 1715-9997

Canadian Journal of pure & applied sciences

Short Communication

RADIATION SAFETY STUDY OF X-RAY IRRADIATION FACILITIES AT THREE HOSPITALS IN PORT HARCOURT

*MA Briggs-Kamara[1], PC Okoye[2] and I Tamunobereton-ari[3]
[1]Department of Pure and Applied Physics, Veritas University Abuja
Obehie Campus, PMB. 7084, Aba, Abia State
[2]Department of Physics, University of Port Harcourt, PMB 5323, Port Harcourt
[3]Department of Physics, Rivers State University of Science and Technology, 500001 Port Harcourt, Nigeria

ABSTRACT

A Radiation safety study of X-ray Irradiation facilities was carried out at three Hospitals in Port Harcourt, Rivers State. This study employed the use of a specialized Geiger Muller counter, the Radalert-100, to take measurements of the levels of radiation emissions and extent of scatter radiation to the surrounding environment. A pocket dosimeter was also used to measure the absorbed doses. The background radiation in and around the radiation rooms were measured and found to range from 0.08 to 1.60μSv which are within the normal range of 0.09 to 1.70 μSv. However some technical and engineering regulations would have to be strictly followed to maintain standards.

Keywords: X-ray, irradiation, safety, absorbed dose, exposure, radiation facility.

INTRODUCTION

Radiation is one subject that is likely to cause people to become nervous and worried. Most people have undergone one form of medical X-Ray exposure/Gamma therapy or have been exposed intentionally or otherwise to one form of radiation or the other. Ionizing radiation sources can be found in a wide range of occupational settings including health care facilities, research institutions and various manufacturing facilities (Morgan and Turner, 1967). A high radiation dose given at a low rate over a period of years might have a different (probably smaller) effect from the same dose given in a short time, although the very use of a total dose summed over a long time period, of the order of a lifetime implies that the difference is unlikely to be large (Shilnikova *et al*., 1996). Children in the age group 0 – 8 yrs seem to develop leukemia naturally at a greater probability than those a little older (Stewart and Kneale, 1970). Studies (Stewart, 1970) showed that one X-ray exposure during pregnancy increased the chance of cancer in the child. Two questions of interest in this work are: how safe are the radiation emitting facilities (CT scanning inclusive), and are patients repeatedly exposed or over exposed in the course of getting good results? Although radiographers know that a smaller body mass means that lower doses can be used, the relationship of dose to image quality causes radiographers to increase the dose for higher quality (Khan, 1984). Medical patients receiving radiation treatments in Radiotherapy often experience acute effects, because they are receiving relatively high "bursts" of radiation during treatment (Rema, 2004). There is no firm basis for setting a "safe" level of exposure above background for stochastic effects. Any increase in radiation exposure is accompanied by an increased risk of stochastic effects (Kondo, 1993). The type of radiation to which the person is exposed and the pathway by which they are exposed influence health effects. Health physicists generally agree on limiting a person's exposure beyond background radiation to about 100 mrem per year from all sources. Exceptions are occupational, medical or accidental exposures. (Medical X-rays generally deliver less than 10 mrem). Regulatory Agencies generally limit exposures from specific source to the public to levels well under 100 mrem (BEIR III, 1980). This is far below the exposure levels that cause acute health effects.

MATERIALS AND METHODS

Experimental

Three Health Institutions in Port Harcourt, Nigeria were used for the study. Background radiation measurements were carried out inside the diagnostic room before and after the radiation emitting machine was put on but before use to ascertain if there were leakages. Specific radiation doses administered to patients for a number of investigations were recorded. On the average between fifteen (15) and fifty (50) patients were seen daily at the hospitals.

*Corresponding author email: briggskamara@yahoo.com

The hospitals investigated had one or more of the following radiation facilities:

1. Static Rotating Anode conventional X-ray Machines of high capacity in the range of 300 mA /600 mA, 150 kV/175 kV peak and time range of (0.06 – 4) s/ (0.001 to 5) s.
2. Mobile X-ray machines of capacities 300 mA, 120 kV and time range of .06 to 4 seconds.
3. Computerized Tomography (CT) Machine of enormous radiation emission capacity.
4. Fluoroscopic X-ray machines for real time medical imaging screening, with a considerable amount of radiation emitted each time they are in use and incidentally they are often used.
5. Magnetic Resonance Imaging [MRI] Machine of capacity 0.23Tesla.
6. Mammography machine for breast screening with a considerable though low level radiation emission.

This study employed the use of a specialized Geiger Muller counter, the Radalert-100, to take measurements of the levels of radiation emissions and extent of scatter radiation to the surrounding environment. A pocket dosimeter was used to measure the absorbed doses.

Data from radiation monitoring was taken at various points in and around the exposure rooms (as displayed on Table 1).

RESULTS AND DISCUSSION

These measurements were on single exposures. An exposure lasted between 0.06ms to 4s depending on body part under investigation. The duration of CT scanning and other high dose techniques was between five minutes to an hour depending on the investigation in progress. There was need for concern when exposures were repeated. Reasons for repeat were usually to confirm diagnosis, poor radiographic positioning, poor processing and handling, and loss. Figure1 shows the levels of radiation at various points within and outside the diagnostic rooms.

The background radiation in and around the radiation rooms were within normal range of between 0.09 and 1.70μSv (ICRP, 1992). The X-ray machines were in good shape. It was observed that the older the X-ray machine the higher the amount of radiation required to achieve a particular result. This was evident by the recording of variable doses of radiation for chest X-ray exposures and other radiological investigations. This was of concern as increasing the radiation dose increases the possibility of harm because there was always cell death at every level of radiation exposure was also a great concern exists when the radiation exposures are repeated. It was discovered that some collimators especially in older X-ray machines were ineffective as some radiation escaped even when the collimators were closed which was an anomaly. Patients' waiting area, which should be free of radiation,

Table 1. Radiation levels at selected locations and times, and within and outside diagnostic rooms.

Investigation	Hospital 1 μSv	Hospital 2 μSv	Hospital 3 μSv
Background within hospital premises	0.011	0.011	0.008
Background within the radiology diagnostic rooms	0.014	0.014	0.014
Radiation detected when the machine was put on but not in use	0.014	0.014	0.014
Radiation detected when the collimator was closed	-	0.600	0.600
Radiation detected at the entrance door when the door is open and exposure was in progress	0.940	0.940	0.890
Radiation detected during chest X-ray exposures	20.000	30.000	30.000
Radiation detected during skull X-ray exposures	160.000	170.000	170.000
Radiation absorbed by patients waiting outside the radiation room when the radiation entrance door is closed	0.800	1.600	1.600
Radiation absorbed by patients waiting outside the radiation room when the radiation room entrance door is open	9.400	9.400	9.400
Radiation exposure in adjoining offices and corridors adjacent to diagnostic rooms	0.600	0.600	0.600
Radiation exposure in adjoining offices and corridors opposite diagnostic rooms	0.340	0.342	0.342
Radiation absorbed by a patient's relation holding the patient but not wearing lead apron	60.000	60.000	60.000
Radiation absorbed by areas covered by lead apron of a patient's relation holding the patient and wearing lead apron	0.900	0.900	0.900

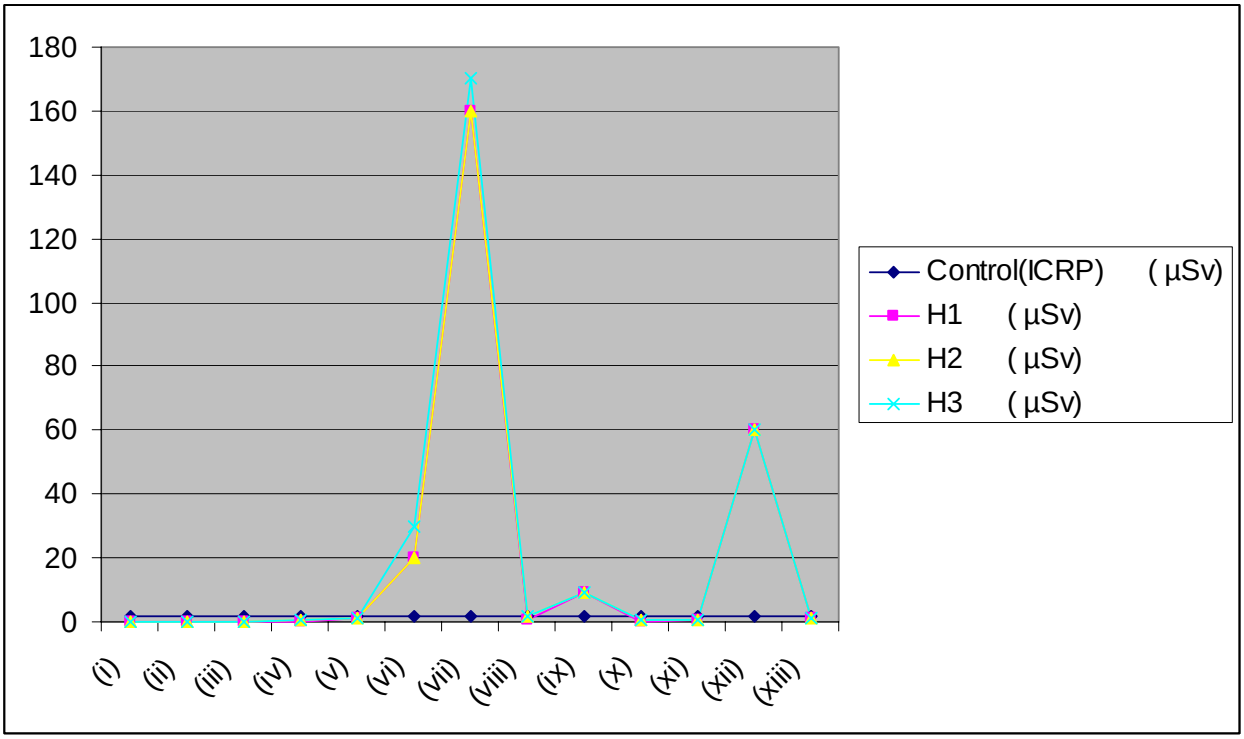

Fig. 1. Background radiation levels at the three hospitals (coded H1, H2 and H3).

Key:

within hospital premises
within the radiology diagnostic rooms
when the machine was put on but not in use
when the collimator was closed
at the entrance door when the door is open and exposure was in progress
during chest X-ray exposures
during skull X-ray exposures
by patients waiting outside the radiation room when the radiation entrance door is closed
by patients waiting outside the radiation room when the radiation room entrance door is open
in adjoining offices and corridors adjacent to diagnostic rooms
in adjoining offices and corridors opposite diagnostic rooms
by a patient's relation holding the patient but not wearing lead apron
by areas covered by lead apron of a patient's relation holding the patient and wearing lead apron

showed a significant reading of radiation. This was observed to worsen when the doors of the X- ray rooms were opened and posed a health risk for patients or staff who may stray into the diagnostic room or loiter around the corridors of the radiation room. Offices and toilets very close to the radiation rooms showed significant reading of radiation measurement.

There was also a great concern when the radiation exposures are repeated. A tangible number of repeated radiological investigations were due to technical fault and handling/packaging of the X-Ray results. Repeated radiological investigations were a sure way of increasing radiation exposures to patients and to an extent the workers. Efforts should be made to avoid/reduce repeated investigations.

Radiation workers should as a matter of routine explain every procedure to patients prior to exposures. This would help allay fears on the part of patients and get full cooperation which would help reduce repeated investigations by way of movement or failure to carry out instructions. Radiation workers should also protect every part of the patient not intended to be exposed to radiation by the application of proper coning/beam delineation and collimation. This would ensure that only areas of interest are exposed to radiation. Workers should provide lead gloves and aprons for patients to wear and protect the areas not to be exposed to radiation. Ten-day and 28-day rules should be strictly obeyed by radiation workers while attending to females of the child bearing age, pregnant or breast feeding mothers to prevent exposure of foetus or bodily contamination with radiation (Philip, 1991).

Children should be given special attention and protection as a good number of patients admitted that this was hardly the practice.

CONCLUSION

There is an urgent need for a quantitative non-destructive method for defining the extent of the field of a clinically significant radiation exposure early after its occurrence. There is also need for radiation workers to be given introductory seminars on radiation safety before they start working with radiation. The radiation workers should as a matter of practice strictly implement rules and guidelines in radiation protection. They should also ensure the calibration of their machines/ standardization of their processing chemicals. They should ensure that all accessories for X-ray machines are working properly and within safety limits. Government should as a matter of urgency overhaul all existing Health and Safety Inspection Agencies charged with regulation or accreditation of radiation workers streamlining:

1. The policies and procedures of training all Radiation workers must receive before employment.
2. Procedures for Teaching, General and Private Hospitals monitor and implement radiation safety guidelines.
3. Periodic and regular inspection and monitoring using thermo luminescence detectors, pocket dosimeters and Geiger-Mueller counters.
4. The use of film badges or their equivalents by radiation workers.

Patients/general public should on their part be self-informed and sensitized about radiation and radiation

Specific qualified persons should have the responsibility for assuring proper maintenance of the x-ray machines in line with Preventive and Corrective Maintenance Programs for X-ray machines as detailed by the International Atomic Energy Agency, IAEA. The radiation rooms should be adequately lead-lined in line with regulation. Lead-lined gloves and aprons are to be worn by staff, patients and helpers in the direct X-ray field.

ACKNOWLEDGEMENT

The authors are very grateful to staff members of the Radiologic Departments of the University of Port Harcourt Teaching Hospital (UPTH), Braithwaite Memorial Specialist Hospital (BMSH) and Rivon Clinic for their cooperation during data collection for this work.

REFERENCES

BEIR III. 1980. The effects on populations of exposure to low levels of ionizing radiation. National Academy Press, Washington DC, USA. 35-38.

ICRP. 1992. Recommendations of the International Commission on Radiological Protection, Ionizing Radiation Fact Sheet Series No. 4, ICRP Publication 40, Annals of the ICRP 60-69.

Khan, FM. 1984. The Physics of radiation therapy. Williams and Wilkins Publisher, Baltimore, USA. 475-503.

Kondo, S. 1993. Health Effects of Low-Level Radiation. Kinki University Press, Osaka, Japan. pp50.

Morgan, KZ. and Turner, JE. 1967. Principles of Radiation Protection. Wiley, New York, USA. 236.

Philip, WB. 1991. Radiographic positions and Radiologic procedures, (7th edi.). Mosby-year Book Inc., Chicago, USA. pp25.

Rema, W. 2004. Radiology casebook for medical students, (2nd edi.). Pastest Publishers limited, Sheffield, England. pp55.

Shilnikova, NS., Koshurnikova, NA. and Bolotnikova, MG. 1996. Mortality Among Workers with Chronic Radiation Sickness. Health Physics. 71(1):86-89.

Stewart, A. 1970. Radiation x-rays exposure to obstetric patients. Lancet Publishing, Toronto, Canada. 118-120.

Stewart, A. and Kneale, GW. 1970. Radiation dose effects in relation to obstetric X rays and childhood cancers. Lancet Publishing, Toronto, Canada. 1185-88.

Received: July 18, 2012; Accepted: Nov 1, 2012

SENRA Academic Publishers, British Columbia
Vol. 7, No. 1, pp. 2297-2301, Feb 2013
Online ISSN: 1920-3853; Print ISSN: 1715-9997

Canadian Journal of pure&applied sciences

Short Communication

STATISTICAL INVESTIGATION OF THE EFFECT OF SOIL COMPOST AND ROCK PHOSPHATE ON THE GROWTH CHARACTERISTICS OF OIL PALM TREE USING FACTORIAL MODEL

Mbegbu, JI[1] and *Chete FO[2]
[1]Department of Mathematics, University of Benin, Benin City
[2]Department of Computer Science, University of Benin, Benin City, Nigeria

ABSTRACT

Statistical investigation of the effect of soil composts (Factor A) and rock phosphate (Factor B) on the growth characteristics of oil palm tree was carried out at 5% level of significance. Consequently, the results showed that there are significant effects of these factors on the growth characteristics of oil palm tree. There is also a significant interaction effect of soil composts and rock phosphate on the growth characteristics.

Keywords: Factorial, experiment, model, soil compost, rock phosphate, growth, oil palm tree.

INTRODUCTION

In this work, we shall investigate the effects of Soil Compost and Rock Phosphate on the growth characteristics of Oil Palm trees. The growth characteristics considered in this work are: Number of Leaves LEF), Height (HGT), Girth (GTH), Fresh Weight Leaves (FWL), Fresh Weight Root (FWR), Fresh Weight Total (FWT), Dry Weight Leaves DWL), Dry Weight Root (DWR) and Dry Weight Total (DWT) respectively. According to Pratt and Tort (1990), Hill and Wiles (1975), the investigation shall involve the use of Factorial design experiment to achieve the desired results. Hence, the factorial design experiment becomes useful in testing the effects of two or more factors, or their interaction effects on the response variables (Box *et al*., 2005; Box, 1990; Hunter, 1994).

Now, let the soil Compost and Rock Phosphate be "Factor A" and "Factor B" at ith and jth levels of experiment respectively. Accordingly Montgomery (1991) the Factorial model for the experiment is defined as

$$\text{i= 1(1)L, j = 1(1)m, k =1(1)n}$$
$$X_{ijk} = \mu + \alpha_i + \beta_j + \phi_{ij} + \in_{ijk}, i = 1(1)4;\ j = 1(1)5, k = 1(1)3 \quad (1.1)$$

where

$X_{ijk} \equiv response\,(value)\ from\ i^{th}\ level\ of\ soil\ compost\ and\ j^{th}\ level\ of\ rock\ phosphate\ at\ k^{th}\ replication$

$\mu \equiv Overall\ mean\ value$

$\alpha_i \equiv Main\ effect\ of\ soil\ compost\ at\ i^{th}\ level$

$\beta_j \equiv Main\ effect\ of\ rock\ phosphate\ at\ j^{th}\ level$

$\phi_{ij} \equiv$ *interaction effect of soil compost and rock phosphate at* $(i, j)^{th}$ *level*

$\in_{ijk} \approx N(o, \sigma^2)$ *is the random error*

Due to cost of experimentation, we make a choice of L = 4 and m =5 levels of experiment at n = 3 replications in equation(1.1). This result to 4x5 factorial design of experiment for investigating the effects of factor A, Factor B, and their interactions on the growth characteristics of Oil Palm tree respectively.

MATERIALS AND METHODS

Under the assumption that $\in_{ijk} \approx N(o, \sigma^2)$ and exploiting model (1.1), the estimates of the parameters μ, α_i, β_j and ϕ_{ij} are (Box *et al*., 2005).

$$\hat{\mu} = \frac{1}{60}\sum_{i=1}^{4}\sum_{j=1}^{5}\sum_{k=1}^{3} X_{ijk}$$

$$\hat{\alpha}_i = \frac{1}{15}\sum_{j=1}^{5}\sum_{k=1}^{3} X_{ijk} - \hat{\mu}\ ; \qquad i = 1(1)4$$

$$\hat{\beta}_j = \frac{1}{12}\sum_{i=1}^{4}\sum_{k=1}^{3} X_{ijk} - \hat{\mu}\ ; \qquad j = 1(1)5$$

$$\hat{\phi}_{ij} = \frac{1}{3}\sum_{k=1}^{3}\left(X_{ijk} - \hat{\mu} - \hat{\alpha}_i - \hat{\beta}_j\right)\ ; \qquad i = 1(1)4,\ j = 1(1)5,\ i \neq j$$

*Corresponding author email: odichet@yahoo.com

We formulate the test hypotheses as follows:

a) H_o : $\alpha_i = 0$, for $i = 1(1)4$ (No mean effect of soil compost on the growth characteristics of oil palm tree)
Versus H_i : $\alpha_i \neq 0$, for at leasta main effectof i (There is mean effect of soil compost on the growth characteristics of oil palm tree)

b) H_o: $\beta_j = 0$, for $j = 1(1)5$ (No mean effect of rock phosphate on the growth characteristics of oil palm tree)
Versus H_i : $\beta_j \neq 0$, for at leasta main effectof j (There is mean effect of rock phosphate on the growth characteristics of oil palm tree)

c) H_o : $\phi_{ij} \neq 0$, for at least one (i, j) (There is interaction effect)

Under the null hypotheses (Cochram and Cox, 1957) in (a), (b) and (c), and for $\in_{ijk} \approx N(o, \sigma^2)$, the F-statistics for the soil compost (Factor A), rock phosphate (Factor B) and interaction (AB) are:

$$F_A = \frac{MSS_A}{MSE}, F_B = \frac{MSS_B}{MSE}, and\ F_{AB} = \frac{MSS_{AB}}{MSE} \quad (2.1)$$

respectively, where MSS_A, MSS_B, MSS_{AB} and MSE are the mean sum of squares for factor A, factor B, interaction AB and error respectively.

These statistics F_A, F_B and F_{AB} are F-distributed with degree of freedom ($v_1 = 3$, $v_2 = 40$), ($v_1 = 4$, $v_2 = 40$) and ($v_1 = 12$, $v_2 = 40$) respectively. Thus, the analysis of variance (ANOVA) table associated with the 4 x 5 factorial design is given below (Table 1):

Table 1. ANOVA table for 4 x 5 Factorial Design.

Source of variation	Degree of freedom	Sum of squares	Mean sum of squares	F-value
Soil compost (Factor A)	3	SS_A	$MSS_A = \frac{SS_A}{3}$	$F_A = \frac{MSS_A}{MSE}$
Rock phosphate (Factor B)	4	SS_B	$MSS_B = \frac{SS_B}{4}$	$F_B = \frac{MSS_B}{MSE}$
Interaction (AB)	12	SS_{AB}	$MSS_{AB} = \frac{SS_{AB}}{12}$	$F_{AB} = \frac{MSS_{AB}}{MSE}$
Error	40	SSE	$MSE = \frac{SSE}{40}$	

Data Collection

The data (Table 2) for this analysis were collected from Department of Statistics, Nigeria Institute for Oil Palm Research (NIFOR) at Benin City, Edo State, Nigeria. The data are on a factorial experiment conducted on the effect

Table 2. Presentation of Data.

Soil compost	Rock phosphate	REPLICATION 1								
		LEF	HGT	GTH	FWL	FWR	FWT	DWL	DWR	DWT
0	0	11	61	11	95.6	83	178.6	24.9	15.5	40.4
	50	11	61	11	96.1	49.4	145.3	29.7	13.1	42.8
	100	11	50	10.5	70.4	46.4	116.8	18.3	8.6	26.9
	150	13	58	11.5	96.7	69.9	166.6	26.7	14.3	41
	200	13	69	8	58.9	54	112.9	15.7	9.4	25.3
10	0	11	70	13	91.8	90.9	182.7	22.7	17.4	40.1
	50	12	71	12	86	47.1	133.1	27.9	13.6	41.5
	100	13	60	13	89.3	91.8	181.1	25.4	17.8	43.2
	150	13	62	13.5	115.3	97.5	212.8	32.2	18.2	50.4
	200	12	62	11.5	86.2	95.8	182	23.7	19.4	43.1
20	0	12	76	14	153.5	129.3	282.8	40.2	24.4	64.2
	50	12	73	13.5	135.2	96.6	231.8	37.7	21.6	59.3
	100	12	71	13	115.6	65.5	181.1	42.8	7.5	50.3
	150	12	61	10	104.1	97.7	201.8	29.2	19.8	49
	200	10	63	11.5	80.3	47.5	127.8	24.5	10.6	35.1
30	0	13	52	11	67.7	49.6	117.3	18.8	12.9	31.7
	50	12	57	11	62.1	46.8	108.9	18.1	9.9	28
	100	12	58	12	80.6	80.5	161.1	25.5	17.1	42.6
	150	12	65	10.5	68.3	56.5	124.8	**	**	**
	200	11	62	13	84.5	63.2	147.7	23.4	15.4	38.8

Continued…

Table 2 continued

Soil compost	Rock phosphate	REPLICATION 2								
		LEF	HGT	GTH	FWL	FWR	FWT	DWL	DWR	DWT
0	0	12	67	11.5	89.4	74.4	163.8	25.7	15.2	40.9
	50	11	56	9	75	57.2	132.2	21.9	15.5	37.4
	100	12	60	9.5	91.4	54.3	145.7	24.5	10.5	25
	150	12	69	10.5	88.3	69.5	157.8	24.9	13.5	38.4
	200	12	61	10	78.6	56.5	144.1	26.1	12.2	38.3
10	0	13	76	15	15.4	86.5	240.7	45.6	16.2	61.8
	50	13	61	14	107.1	65.5	172.6	33	16.1	49.1
	100	11	66	12	92.6	67.8	160.4	26.9	16.9	43.8
	150	13	64	12	101.1	72.6	173.7	26.4	16.3	42.7
	200	11	56	11	80.2	60.7	140.9	21.7	13.2	34.9
20	0	13	78	13	158.2	84.3	242.5	46.9	18.1	65
	50	13	78	11	113.3	51.1	164.4	38.4	12.6	51
	100	11	74	13	105.6	69.3	174.9	30.8	14.5	45.3
	150	12	55	14	96.6	57.7	154.3	26.3	13.4	39.7
	200	12	64	10	78.7	73.6	152.3	23.6	16	39.6
30	0	10	60	10	66.8	57.1	123.9	18	11.4	29.4
	50	11	61	12	81.6	96.1	177.7	21	24.9	45.9
	100	11	65	14	70.5	108	178.9	21.1	24.2	45.3
	150	11	53	14	76	105	181.3	21.3	21.2	42.5
	200	12	68	11	74.4	89	163.4	23.5	18.7	42.2

Soil compost	Rock phosphate	REPLICATION 3								
		LEF	HGT	GTH	FWL	FWR	FWT	DWL	DWR	DWT
0	0	12	58	11	77.5	36.8	114.3	27.2	8.8	30
	50	11	57	10.5	67.6	42.8	110.4	19.9	11.8	31.7
	100	12	70	12	71.7	44.8	116.5	19.7	11.9	31.6
	150	12	63	13.5	90.4	67	157.4	25.2	17.2	42.4
	200	12	61	13	82.3	66.2	148.5	24	16	40
10	0	13	63	11	97.3	45.8	143.5	25.8	11.8	.37.6
	50	11	70	13	112.6	66.8	179.4	41.1	16.4	57.5
	100	12	66	13.5	108.5	72.2	108.7	28	15.6	43.6
	150	11	61	11.5	101.7	79.6	181.3	30.9	18.5	49.4
	200	12	64	10	71	50.5	121.5	20.4	12.9	33.3
20	0	13	57	12	92.5	62.1	154.6	28.1	17.7	45.8
	50	13	80	14.5	169.6	95.5	265.1	60.3	24.9	85.2
	100	11	74	12	100.5	68.1	168.6	31.8	17.5	49.3
	150	13	64	11	79	54.6	133.6	23	13.6	36.6
	200	10	67	7	64.6	51.8	116.4	18.8	13.2	32
30	0	11	56	12	93.8	88.1	181.9	30	18.6	48.6
	50	11	55	10	69.3	79.1	148.4	22	21.1	43.1
	100	11	58	9.5	.87.4	82.9	170.3	26.8	20.9	47.7
	150	13	55	10	86.6	88.4	175	25.7	23.6	49.3
	200	12	59	9.5	88.4	141.1	229.5	27	30	57

of two factors namely soil compost (Factor A) at four levels and rock phosphate (Factor B) at five levels on the growth characteristics of oil palm tree which of course are the responses.

The growth characteristics measured are as follows: Number of leaves (LEF), Height (HGT), Girth (GTH), Fresh Weight leaves (FWL), Fresh weight root (FWR), Fresh weight total (FWT), Dry weight leaves (DWL), Dry weight root (DWR) and Dry weight total (DWT).

Analysis of Data

The analysis of data was done using statistical package SAS/STAT. The results are shown in the tables 3-13 below:

Table 3. ANOVA for lef.

Source of variation	Degree of freedom	Sum of squares	Mean sum of squares	F-value
Soil compost (factor A)	3	2.33	0.78	1.17
Rock phosphate (factor B)	4	4.00	1.00	1.50
Interaction (AB)	12	11.33	0.94	1.42

Table 4. ANOVA for HGT.

Source of variation	Degree of freedom	Sum of squares	Mean sum of squares	F-value
Factor A: Soil compost	3	858.00	286.00	10.15
Factor B: Rock phosphate	4	135.60	33.90	1.20
Interaction AB	12	730.00	60.83	2.16

Table 5. ANOVA for GTH.

Source of variation	Degree of freedom	Sum of squares	Mean sum of squares	F-value
Factor A: Soil compost	3	21.75	7.25	3.04
Factor B: Rock phosphate	4	20.96	5.24	2.19
Interaction AB	12	22.61	1.88	0.79

Table 6. ANOVA for FWL.

Source of variation	Degree of freedom	Sum of squares	Mean sum of squares	F-value
Factor A: Soil compost	3	10240.51	3413.50	12.88
Factor B: Rock phosphate	4	4276.99	1069.25	4.03
Interaction AB	12	7633.63	636.14	2.40

Table 7. ANOVA for FWR.

Source of variation	Degree of freedom	Sum of squares	Mean sum of squares	F-value
Factor A: Soil compost	3	4426.04	1475.35	3.63
Factor B: Rock phosphate	4	766.24	191.56	0.47
Interaction AB	12	6412.72	534.39	1.32

Table 8. ANOVA FOR FWT.

Source of variation	Degree of freedom	Sum of squares	Mean sum of squares	F-value
Factor A: Soil compost	3	16570.97	5523.66	4.94
Factor B: Rock sulphate	4	5463.76	1365.94	1.22
Interaction AB	12	23141.04	1928.42	1.72

Table 9. ANOVA for DWL.

Source of variation	Degree of freedom	Sum of squares	Mean sum of squares	F-value
Factor A: Soil compost	3	1001.10	333.70	9.65
Factor B: Rock phosphate	4	545.40	136.35	3.94
Interaction AB	12	873.17	72.76	2.10

Table 10. ANOVA for DWR.

Source of variation	Degree of freedom	Sum of squares	Mean sum of squares	F-value
Factor A: Soil compost	3	311.25	103.75	6.46
Factor B: Rock phosphate	4	45.31	11.33	0.71
Interaction AB	12	256.98	21.42	1.33

Table 11. ANOVA for DWT.

Source of variation	Degree of freedom	Sum of squares	Mean sum of squares	F-value
Factor A: Soil compost	3	1598.63	532.88	8.32
Factor B: Rock phosphate	4	609.25	152.31	2.38
Interaction AB	12	1903.16	158.60	2.48

Table 12. F-value and F-table at 5% level of significance.

		LEF	HGT	GTH	FWL	FWR	FWT	DWL	DWR	DWT
Sources of variation	F table	F-value	F-value	F-value	F-value	F-value	F-value	F-value	F-value	F-value
Factor A: Soil compost	2.84	1.17	10.15	3.04	12.88	3.63	4.94	9.65	6.46	8.32
Factor B: Rock phosphate	2.61	1.50	1.20	2.19	4.03	0.47	1.22	3.94	0.71	2.38
Interaction AB	1.92	1.42	2.16	0.79	2.40	1.32	1.72	2.10	1.33	2.48

Table 13. Statistical Decision at 5% level of significance.

	DECISIONS								
	LEF	HGT	GTH	FWL	FWR	FWT	DWL	DWR	DWT
Factor A: Soil compost	Accept H_o	Reject H_o	Reject H_o	Reject H_o	Reject H_o	Reject H_o	Reject H_o	Reject H_o	Reject H_o
Factor B: Rock phosphate	Accept H_o	Accept H_o	Accept H_o	Reject H_o	Accept H_o	Accept H_o	Reject H_o	Accept H_o	Accept H_o
Interaction AB	Accept H_o	Reject H_o	Accept H_o	Reject H_o	Accept H_o	Accept H_o	Reject H_o	Accept H_o	Reject H_o

Based on the analysis, we are 95% confident that:

i. The soil compost had a significant effect on HGT, GTH, FWR, DWR, DWT, DWL. FWT and FWL
ii. The rock phosphate had a significant effect on FWL and DWL.
iii. The soil composts had no significant effect on LEF
iv. The rock phosphate interaction effect of soil compost and rock phosphate on LEF, HGT, GTH, FWR, FWT, DWR and DWT
v. There is significant interaction effect of soil compost and rock phosphate on HGT, FWL, DWL and DWT
vi. There is no significant interaction effect of soil compost and rock phosphate on LEF, GTH, FWR, FWT and DWR.

REFERENCES

Box, GEP. 1990. Do Interactions Matter? Quality Eng. 2:365-369.

Box, GEP., Hunter. JS. and Hunter, WG. 2005. Statistics for Experimenters: Design, Innovation and Discovery (2nd ed.). John Wiley and Sons, New York, USA.

Cochran, WG. and Cox, G. 1957. Experimental Design. John Wiley and Sons Inc., New York, USA.

Hill, WJ. and Wiles, RA. 1975. Plant Experimentation (PLEX). J. Qual. Tech. 7:115-122.

Hunter, P. 1994. Interactions: Ignore them at your own risk. J. Qual. Tech. 21:174-178.

Montgomery, DC. 1984. Design and Analysis of Experiments (2nd ed.). John Wiley and Sons, New York, USA.

Pratt, A. and Tort, X. 1990. Case Study: Experimental Design in a Pet Food Manufacturing Company. Quality Eng. 3(1):59-73.

Received: May 29, 2012; Revised: Aug 28, 2012;
Accepted:Oct 31, 2012